Geoscience Frontiers 9 (2018) 789–862

HOSTED BY

ELSEVIER

Contents lists available at ScienceDirect

China University of Geosciences (Beijing)

Geoscience Frontiers

journal homepage: www.elsevier.com/locate/gsf

Focus Paper

Early Paleozoic tectonics of Asia: Towards a full-plate model

Mathew Domeier

Centre for Earth Evolution and Dynamics, University of Oslo, Norway

ARTICLE INFO

Article history:
Received 4 August 2017
Received in revised form
15 November 2017
Accepted 21 November 2017
Available online 12 December 2017
Handling Editor: M. Santosh

Keywords:
Tectonics
Asia
Early Paleozoic
Paleogeography
Paleomagnetism

ABSTRACT

Asia is key to a richer understanding of many important lithospheric processes such as crustal growth, continental evolution and orogenesis. But to properly decipher the secrets Asia holds, a first-order tectonic context is needed. This presents a challenge, however, because a great variety of alternative and often contradictory tectonic models of Asia have flourished. This plethora of models has in part arisen from efforts to explain limited observations (in space, time or discipline) without regard for the broader assemblage of established constraints. The way forward, then, is to endeavor to construct paleogeographic models that fully incorporate the diverse constraints available, namely from quantitative paleomagnetic data, the plentiful record of geologic and paleobiologic observations, and the principles of plate tectonics. This paper presents a preliminary attempt at such a synthesis concerning the early Paleozoic tectonic history of Asia. A review of salient geologic observations and paleomagnetic data from the various continental blocks and terranes of Asia is followed by the presentation of a new, full-plate tectonic model of the region from middle Cambrian to end-Silurian time (500–420 Ma). Although this work may serve as a reference point, the model itself can only be considered provisional and ideally it will evolve with time. Accordingly, all the model details are released so that they may be used to test and improve the framework as new discoveries unfold.

1. Introduction

In the simplest of terms, Asia comprises a medley of scattered Precambrian cratons and continental fragments, interwoven and bound together by an extensive network of mobile belts, like an enormous tectonic tapestry. Cast in this way, the geologic constitution of Asia sounds fundamentally no different than that of any other continent, but what sets Asia apart is time—Asia is young (largely constructed in the Paleozoic and Mesozoic)—and its sheer scale. Many of the mobile belts threading that vast tectonic patchwork are Phanerozoic in age, and they include some of the largest and longest-evolving orogens on Earth. This makes Asia a veritable treasure trove of information concerning crustal growth, continental evolution and orogenesis, and taken as a whole it embodies the world's premier tectonic menagerie. But to properly understand much of the information bound up in this immense record, we must have some understanding of the first-order tectonic context—and yet, considering its scale, complexity and relative youthfulness, the tectonic framework and history of Asia also presents one of the most intricate and colossal puzzles on our planet.

Owing to that gross complexity, in many parts of the Asian tectonic collage there has been a profusion of conceptual models of its Paleozoic–Mesozoic tectonic history, bringing to mind the common adage that '*the number of models presented approaches the number of workers there*'. To some degree, this is natural and unavoidable, as models often must be revised or rejected according to new discoveries. But to make progress, the revision of existing models or the construction of new ones must be done with reference to previously established constraints, both locally and from adjoining domains (in time and space). However, there are many examples of conceptual tectonic models erected primarily to explain only newly acquired data (e.g. new radiometric dates, the discovery of mafic-ultramafic bodies, fresh structural observations), with little regard for other previously established constraints, especially from neighboring domains of time and space. This is unfortunate because some of the best constraints that can be provided for a given tectonic model are those provided by the temporal and spatial boundary conditions. More importantly, the unremitting production of new local models to fit new local data forgoes the opportunity to test and revise our collective understanding of the

E-mail address: mathew.domeier@geo.uio.no.
Peer-review under responsibility of China University of Geosciences (Beijing).

https://doi.org/10.1016/j.gsf.2017.11.012

greater tectonic framework of a given system through tests and revisions to the best or most prominent existing models of it. A new model can always be conjured to fit new observations; the power of new observations is that they can be used to evaluate existing models to identify places where our understanding proves erroneous or incomplete.

The proliferation of conceptual models effectively made in isolation has had the effect that our understanding of the Paleozoic–Mesozoic tectonic history of Asia appears to be growing increasingly divergent and fragmented with time. But why does this trend continue? Why do we continue building isolated conceptual models instead of testing and refining larger, integrative tectonic frameworks? There are undoubtedly several reasons for this, but I suspect that one of the most significant is simply that we lack sufficient working frameworks that are widely accessible, readily testable and easy to modify and redistribute. For example, the landmark models of Zonenshain et al. (1990), Şengör et al. (1993), Windley et al. (2007) and Wilhem et al. (2012), while hugely influential to research on the Paleozoic–Mesozoic tectonics of Asia, are difficult to test, revise and re-communicate because quantitative rotation schemes (Euler poles) are not available. The purpose of this paper is to ameliorate this deficiency through the construction and documentation of a provisional early Paleozoic tectonic framework for Asia, the details of which are released so that the model may be critiqued, revised and re-distributed as new discoveries unfold.

2. From continental drift to plate tectonics

Paleogeographic models—which aim to restore the first-order arrangement of the major continental blocks of a given region at a given time—have been enormously useful stepping stones toward regional tectonic frameworks, but the conventional approach to constructing such models relies almost exclusively on paleomagnetic data and is therefore significantly limited in several ways. First, individual paleomagnetic data are discrete in time, so reconstructions based solely on them are typically made as temporally-static snapshots, with perhaps tens of millions of years between reconstructed intervals. This means that the tectonic (kinematic) feasibility of a given model is challenging to validate, if at all considered. Second, because paleomagnetic data prior to the Jurassic (before which time there is almost no in situ oceanic lithosphere) are effectively only available from the continents, paleomagnetic-based reconstructions for earlier times ignore the role of oceanic lithosphere, yielding models that, in a distinct sense, hark back to Wegener's paradigm of continental drift (Wegener, 1912). Third, because conventional paleogeographic models often neglect geologic observations and plate tectonic principles with respect to the model construction process, a great wealth of additional constraints are eschewed; this again promotes the construction of models of drifting continents rather than of tectonic plates.

Going beyond continental drift-style paleogeographic models to build plate tectonic frameworks requires a more holistic approach. Paleomagnetic data must be used in conjunction with geologic and plate tectonic data, and reconstructions must be made using 'full-plates', which include oceanic lithosphere in addition to the continental components. The incorporation of plate tectonic principles ensures that such full-plate models are spatiotemporally continuous and kinematically viable, which, at the outset, facilitates the refutation of many otherwise seemingly attractive conceptual tectonic scenarios. The integration of geologic data, in providing qualitative evidence of past relative kinematics, is perfectly complementary to the implementation of plate tectonic rules—constraining the kinematically-fluid paleogeographic model to evolve in such a way as to meet the observations borne by the rocks. In unifying these diverse constraints, full-plate models are more robust than their conceptual counterparts, but they also constitute a broad narrative of the first-order tectonic history of a region as it can presently be known, and furthermore highlight the critical questions remaining there.

Full-plate models were first introduced by the pioneering work of Stampfli and Borel (2002), but in the fifteen years since there have been a number of significant methodological advances, both in applied geodynamic concepts (Steinberger and Torsvik, 2008; Torsvik et al., 2012, 2014) and analytical tools (Boyden et al., 2011; Gurnis et al., 2012). In the last few years a new generation of full-plate models has been actively developing, and presently include global models for the late Mesozoic–Cenozoic (Seton et al., 2012) and late Paleozoic (Domeier and Torsvik, 2014), as well as a model built to link them (Matthews et al., 2016). Notably, all of these models are rooted in an absolute reference frame—where position (latitude *and* longitude) is explicitly and meaningfully defined with respect to the spin-axis and/or deep mantle—which means they can be used to study links between the surface and the deep Earth, the magnetic field or the prevailing climatic zones. Importantly, these particular models are also all open-access, meaning that the entire community can explore, utilize, evaluate and refine these models, as shared knowledge infrastructures.

With respect to the early Paleozoic, a full-plate model based on an absolute reference framework is only available for the Iapetus and Rheic ocean domains (including the landmasses of Laurentia, Baltica and northwest Gondwana) (Domeier, 2016). In a landmark contribution, Wilhem et al. (2012) presented a full-plate model of central and northern Asia for the entire Paleozoic—which has inspired and greatly facilitated the work presented here—but their model is based on a Baltica-fixed reference system and, more importantly, is now industry-owned and thus unavailable for the wider scientific community to use and test. In this paper, an early Paleozoic full-plate model of Asia is presented and the complete model details are released. The model is grounded in two absolute reference frameworks (with respect to the spin-axis and deep mantle), and constitutes part of a broader initiative to construct a global, full-plate model for the early Paleozoic. The frame of interest herein spans from the margins of Baltica in the west to the Japanese Islands in the east, and from Severnaya Zemlya in the north to the Indian subcontinent and peninsular Thailand to the south (Fig. 1).

3. Methodology

The methodology of this study follows that of Domeier and Torsvik (in press), to which I refer the inquisitive reader, as only the most indispensable points are reiterated here for the sake of brevity. Because most of the Paleozoic lithosphere has been subducted, full-plate models of the Paleozoic depend strongly on indirect inferences drawn from the records preserved on the continents, and so it is of the utmost importance that the continents be appropriately reconstructed through the time of interest. Thus, the establishment of a so-called continental reconstruction model is the first step in the construction of a full-plate model. Here, as a starting point, I adopt the existing continental reconstruction model of Torsvik et al. (2014), to which modifications and expansions have been made, as discussed later in this paper.

The continental reconstruction model of Torsvik et al. (2014) was constructed from a compilation of paleomagnetic data that record paleolatitude (Torsvik et al., 2012), large igneous provinces (LIPs) and kimberlite distributions which may constrain paleolongitude (Torsvik et al., 2008, 2010), and an array of other data that provide semi-quantitative or qualitative information about paleolatitude or relative longitudes, for example climate-sensitive

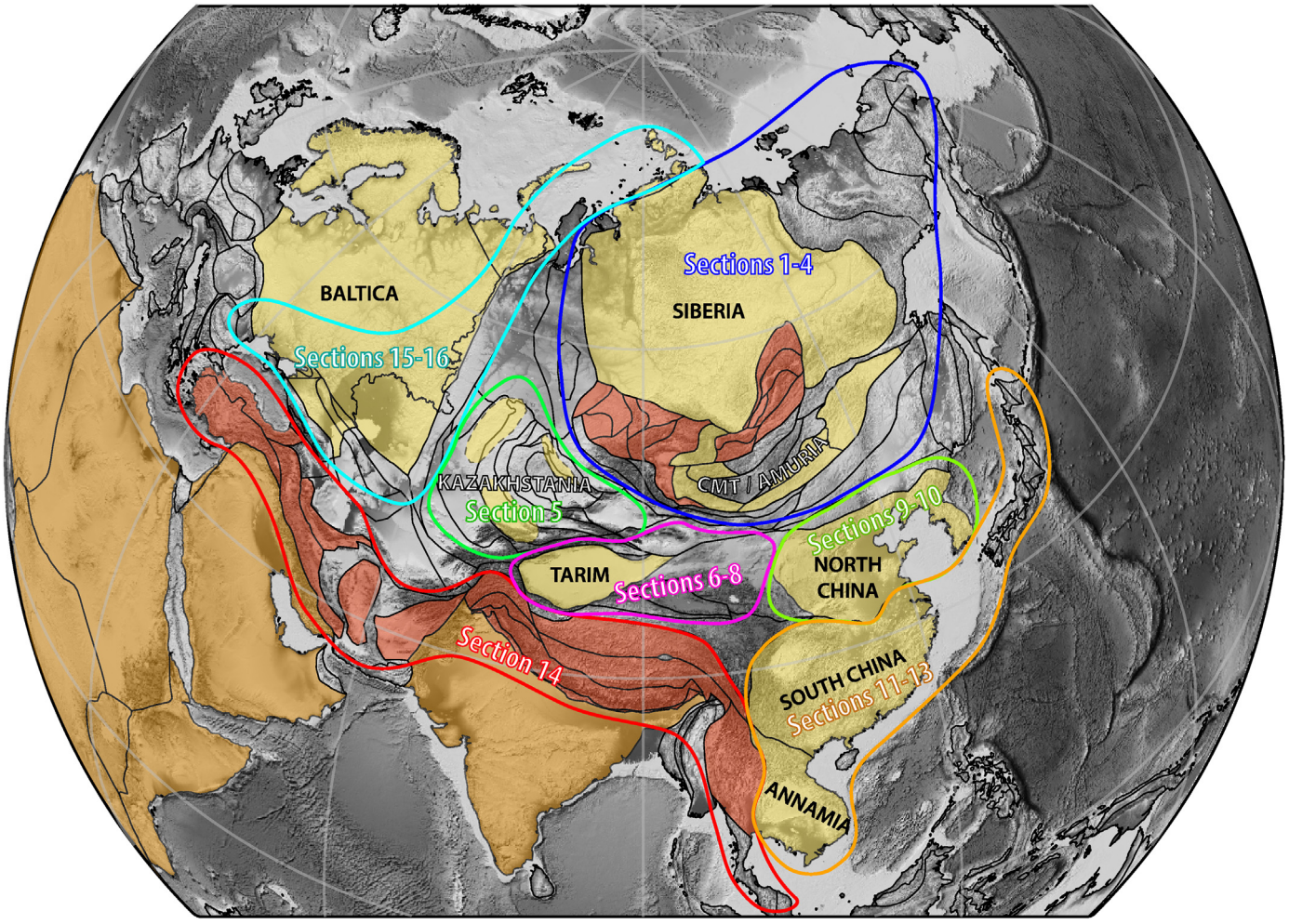

Figure 1. Overview map of regions discussed in the subsections of section 4. Colored polygons are those explicitly included in the plate model. Yellow polygons are independent cratons and continental fragments, orange polygons are cratonic blocks of Gondwana, and red polygons mantled other cratons in the early Paleozoic and therefore did not move independently.

lithofacies and provincial faunas. It is important to note that while one can be confident in the reconstruction of paleolatitude—at least where paleomagnetic data are available, demonstrably primary and of high quality—the determination of paleolongitude is a formidable problem. This is unsurprising because longitude has no meaningful celestial definition, unlike latitude, which is directly referenced to the Earth's axis of rotation. Paleozoic paleogeographic reconstructions have therefore always been erected without explicit absolute longitude control, rather relying on relative paleolongitudes that may be inferred from proximity indicators (e.g. faunal provinciality, sedimentary provenance). Nevertheless, a rather recent and altogether extraordinary observation that LIPs and kimberlites of the last 320 Ma—when restored to their original positions in a mantle reference frame—reconstruct above the present-day outline of the two large low shear velocity provinces (LLSVPs) in the lowermost mantle suggests that the LLSVPs have been relatively stable over that time, and that their margins acted as relatively-fixed plume generation zones (Torsvik et al., 2014). Following a working hypothesis that perhaps the LLSVPs have been stable for even longer, since the earliest Paleozoic, it is possible to construct Paleozoic models with provisional absolute paleolongitude, when and where LIPs and kimberlites are found. This is clearly a major assumption, and one that requires further consideration and critical testing, but as Paleozoic absolute paleolongitude is otherwise indeterminable (in so far as we yet know), the question of how to directly test the concept of long-term LLSVP stability is a vexing problem in itself. In this regard, the model presented herein importantly demonstrates that it is at least possible to construct an early Paleozoic plate model under the paradigm of long-term LLSVP stability, and may ultimately provide the input for geodynamic models designed explicitly to further investigate this hypothesis.

Once the time-dependent geography of the continents is established, the arduous task of reconstructing the ocean basins that once separated them (and which have since been subducted) can begin. Because those ocean basins and the records they held are no longer present, except as occasional ophiolitic fragments or accretionary complexes, their reconstruction is only possible through indirect inference, using both geological records preserved on the continents as well as plate tectonic clues implicitly rooted in their relative motions. The geological records from the continents, most notably those along their margins, can reveal the time-dependent nature of the former tectonic boundaries between the continents and ocean basins, thereby allowing their relative kinematics to be worked out. Such records can include arc magmatic rocks and accretionary complexes reflecting convergence, rift-successions signaling the onset of divergence, extensive strike-slip structures denoting transcurrent motion, or even stable

platform deposits that manifest a passive relationship between continent and ocean basin.

Further details of the kinematics of those lost ocean basins can be derived from the nebulous 'rules' of plate tectonics, which comprise a loose collection of tenets ranging from simple conservation laws to concepts about how idealized plate boundaries tend to behave, and common geodynamic assumptions. For example, given that the Earth is a spheroid of approximately fixed-volume and form, the total surface area of the Earth is conserved through time, meaning that the separation of two continents (ignoring deformation) would necessarily beget the production of new lithosphere between them, whereas their convergence would engender subduction of the intervening lithosphere. Importantly, such deductions drawn from plate tectonic principles are independent of the inferences gleaned from the geologic observables, and so one can be used as a check and evaluation of the other. The construction of the plate boundary network and estimation of plate kinematics from these data together is therefore necessarily an iterative process. Here I assume that plates are rigid and their boundaries are therefore discrete and divisible into segments of convergent, divergent and transcurrent motion. Transform boundaries are assumed to follow the trace of a small-circle centered on the Euler pole which describes the relative motion of its bounding plates. Along divergent boundaries, spreading is assumed to be symmetrical and orthogonal, and ridges are assumed to follow the arc of a great-circle whose plane includes the axis of the relative motion pole. No comparably general assumptions are made about the form, orientation or dynamics of subduction zones, but details about their location, duration and polarity can often be determined directly from geologic evidence. Finally, while geodynamic considerations are occasionally invoked to discriminate between otherwise equally valid kinematic solutions, they are not inherent to the construction of the model. An important avenue for future work would thus be assessment of this model against well-founded geodynamic expectations.

Modifications to the continental rotation model, and digitization and temporal management of the plate boundaries derived by the methods above were carried out using the open-source software GPlates (Boyden et al., 2011) (www.gplates.org). Following the methodology above, plate boundaries were first digitized according to the constraints imposed by the geologic record and the continental kinematics, but as the plate model must also evolve in a kinematically viable way through time, the temporal construction of the model was also necessarily iterative. This means that reconstruction choices for a given time were also informed by continental kinematics and geologic evidence from past and future time-steps. In some instances this required adjustment to the continental rotation model, which in turn affected the plate boundary determinations. Such iterations continued until the model was found to be sufficiently self-consistent with the bulk of the available evidence, although as the data themselves are mostly qualitative, this was admittedly a qualitative judgment. The solutions presented are also often non-unique; in such cases, I strove to adopt the simplest scenario that satisfied the existing constraints. Once the continental rotation model and plate boundary network were completed, the final full-plate model was built with continuously closing plate polygons, according to the method of Gurnis et al. (2012). Because the scope of this model is restricted to the domain of Asia, it is encircled by an arbitrary perimeter used to close those plates that moved partly beyond the frame of interest. It is important to note that the perimeter is geologically meaningless. Although the plate boundaries were implemented with an arbitrary time-stepping of 1 Ma, the temporal resolution of the plate model can be scaled according to the needs of the user.

4. Geological framework

The following section presents early Paleozoic geologic observations from the margins of the cratons and continental fragments that comprise present-day Asia (Fig. 1), together with succint tectonic interpretations of those data, which are presented in a highly-distilled form in Table 1. Although a vast array of observations are presented, the focus is on those geologic features which communicate information about tectonic interactions, relative kinematics and/or paleogeography. The controversial term 'terrane' is used here in an informal sense to refer to lithological units, presumed to be of the same affinity, that are demonstrated or inferred to cover fragments of continental basement. Some of these terranes comprise yet smaller, possibly distinct units that could be classified as terranes themselves. Where possible, an endeavor has been made to limit the division of terranes, but not everyone will agree with these simplifications. It is important to acknowledge that many of the names, boundaries and definitions of these terranes and geological units have been derived and adapted from earlier regional syntheses, including the colossal works of Zonenshain et al. (1990), Şengör and Natal'In (1996), Badarch et al. (2002), Cocks and Torsvik (2007), Windley et al. (2007), Xiao et al. (2010a), and Wilhem et al. (2012), among others, whose designations and interpretations have become pervasive in the literature.

In this paper, geochronological units are referenced to the timescale of Walker et al. (2013) and the informal term 'early Cambrian' refers to epochs 1 (Terreneuvian) and 2 (unnamed), 'middle Cambrian' refers to epoch 3 (unnamed), and 'late Cambrian' refers to epoch 4 (Furongian). The informal term 'early Silurian' refers to the Llandovery, 'middle Silurian' refers to the Wenlock, and 'late Silurian' refers to the Ludlow and Pridoli.

4.1. Siberia

4.1.1. Northwest Siberia

Much of the northwest margin of Siberia is blanketed by Mesozoic to Recent sedimentary rocks, notably those of the West Siberian basin, which extends from the Altai-Sayan fold belt in the southeast, north to the Arctic Ocean, and to the Uralian orogen in the west (Vyssotski et al., 2006) (Fig. 2). Nevertheless, pre-Mesozoic rocks from that margin are exposed on the Taimyr Peninsula, to the north of the Mesozoic to Recent sediments of the Yenisey-Khatanga depocenter. Taimyr is conventionally divided into three east-west trending domains: South, Central and North Taimyr. In South Taimyr, Early Ordovician to mid-Carboniferous rocks are characterized by weakly- to non-metamorphosed, carbonate-dominated, shallow marine shelf deposits (Inger et al., 1999). More distal continental slope deposits are found to the north, in Central Taimyr, where a latest Neoproterozoic to early Paleozoic succession of weakly- to non-metamorphosed marine sedimentary rocks is more black shale-rich (Inger et al., 1999; Pease and Scott, 2009). Together, South and Central Taimyr are taken to represent the latest Neoproterozoic to mid-Carboniferous northwest-facing passive margin of Siberia, which was destroyed in the late Carboniferous by the arrival of allochthonous North Taimyr (Bradley, 2008; Pease and Scott, 2009).

4.1.2. East Siberia

Following possible latest Neoproterozoic–early Cambrian rifting (Pelechaty, 1996; Khudoley et al., 2013), the eastern margin of Siberia was passive at least from the late Cambrian to Early Devonian, as evident by the typical passive margin sedimentary sequences in the southern sector of the Mesozoic Verkhoyansk fold and thrust belt. There, in the Sette-Daban Range, a near-continuous succession of carbonates extends from the latest Neoproterozoic to

Table 1
Summary interpretations for plate boundaries discussed in text.

Margin (sub-domain)	Onset (Ma)	Termination (Ma)	Type	Polarity
Siberia				
Northwest Siberia				
	Latest Neoproterozoic	320	Passive	-
East Siberia (proto-Verkhoyansk margin) and Kolyma-Omolon				
	Late Cambrian	385	Passive	-
Southwest Siberia				
Kuznetsk-Alatau and North Sayan	Late Neoproterozoic	480	Convergent	Northeast-dipping
	*Collision with Lake-Khamsara arc (Tuva-Mongolia) at 480 Ma?			
Gorny Altai-Chara	480?	Late Paleozoic	Convergent?	Northeast-dipping
Southeast Siberia				
	*Collision of Barguzin-Ikat, Olkhon and Hamar-Davaa at 500–490 Ma			
Southeast Barguzin-Ikat, Olkhon and Hamar-Davaa				
Dzhida, Uda-Vitim, Haraa	*Collision of central Mongolian ribbon terrane at 500–490 Ma?			
	450?	440?	Divergent	-
	*Opening of Mongol-Okhotsk Ocean at ~440 Ma?			
	440?	360	Passive	-
Central Mongolian ribbon terrane (CMT)/Amuria				
Northwest CMT (Tuva-Mongolia)				
	*Collision with Lake-Khamsara arc in early Cambrian			
Lake-Khamsara	Mid-Cambrian (?)	480	Convergent	Southeast-dipping
	*Collision with North Sayan arc (southwest Siberia) at 480 Ma?			
Northern margin of CMT				
	*Collision with Dzhida, Uda-Viti, Haraa (southeast Siberia) at 500–490 Ma?			
Northern margin of Amuria				
	*Opening of Mongol-Okhotsk Ocean at ~440 Ma?			
	440?	360	Passive	-
Southern margin of CMT				
Gobi Altai, Trans Altai, Xing'an, Songliao	Neoproterozoic?	Late Paleozoic	Convergent	North-dipping
Southwest CMT				
Altai-Mongolia	480	Late Paleozoic	Convergent	Northeast-dipping
The Kazakh terranes/Kazakhstania				
Krygyz North Tianshan (KNT)				
Northeast margin	Cambrian?	480	Passive	-
	*Collision with Chu-Yili at 480 Ma?			
Southwest margin	Cambrian?	480	Passive	-
	*Collision with MIT at 480 Ma?			
Krygyz Middle Tianshan (MIT)				
Northern margin	Cambrian?	480	Convergent	South-dipping
	*Collision with KNT at 480 Ma?			
Southern margin	470	Late Paleozoic	Convergent	North-dipping
	*Possible brief interruption by marginal backarc arc closure at ~450 Ma			
Chu-Yili				
Northeast margin	480	430	Convergent	Southwest-dipping
	*Collision with Aktau-Junggar at 430 Ma?			
Southwest margin	Early Cambrian	480	Convergent	Northeast-dipping
	*Collision with KNT at 480 Ma?			
Aktau-Junggar				
Northeast margin	480?	430?	Convergent	Southwest-dipping
	*Accretionary event at 430 Ma? (Related to collision with Chu-Yili?)			
Chinese Central Tianshan				
Northern margin	480	430	Convergent	South-dipping
	*Accretionary event at 430 Ma?			
Southern margin	?	420?	Passive?	-
	420?	Late Paleozoic	Convergent	North-dipping
Kokchetav + Stepnyak				
Northeast margin	Late Cambrian?	Middle Ordovician	Convergent	Southwest-dipping?
	*Accretionary event at 470? (or collision b/w Kokchetav microcontinent and Stepnyak?)			
Selety				
Margins unclear	Cambrian?	Early Ordovician?	Convergent?	?
Chingiz arc				
Southwest margin	Early Cambrian	Late Ordovician	Convergent	Northeast-dipping
	*Collision with Baidaulet-Aqbastau in Late Ordovician?			
Baidaulet-Aqbastau arc				
Northeast margin	*Collision with Chingiz arc in Late Ordovician?			
Southwest margin	Cambrian?	Middle Silurian	Convergent	Northeast-dipping
Tarim				
Northern Tarim				
	Neoproterozoic	440?	Passive?	-
	440?	400?	Convergent?	South-dipping?
Southwest Tarim				
North West Kunlun	Neoproterozoic	460?	Passive?	-
	*Collision with South West Kunlun at 460 Ma?			
Southeast Tarim				
	?	460?	Passive?	-
	*Collision with Altyn block at 460?			

(*continued on next page*)

Table 1 (*continued*)

Margin (sub-domain)	Onset (Ma)	Termination (Ma)	Type	Polarity
South West Kunlun				
Northeast margin	Cambrian	460?	Convergent	Southwest-dipping
	*Collision with North West Kunlun (SW Tarim) at 460 Ma?			
Altyn block				
Northwest margin (North Altyn belt)	Cambrian	460?	Convergent	Southeast-dipping
	*Collision with southeast Tarim at 460 Ma?			
Southeast margin (South Altyn belt)	Cambrian	460?	Convergent?	?
	*Collision at 460 Ma? (possibly an expression of collision with Tarim?)			
Beishan and Dunhuang				
Queershan unit (southwest margin of CMT?)				
Southern margin	Ordovician	Late Paleozoic	Convergent	North-dipping?
Hanshan-Mazongshan-Shuangyingshan units				
	Cambrian?	Late Paleozoic	Convergent	?
Dunhuang block + Shibanshan unit (northeast Tarim?)				
Northern margin	Cambrian?	440?	Passive?	-
	440?	Late Paleozoic	Convergent	South-dipping?
Alashan, Qilian and Qaidam				
Alashan				
Northern margin	Late Ordovician?	Late Paleozoic	Convergent?	South-dipping?
Southern margin	Cambrian?	440?	Passive?	-
	*Collision with North Qilian belt at 440 Ma?			
North Qilian belt				
Northern margin	Middle Ordovician?	440?	Convergent?	South-dipping?
	*Collision with Alashan at 440 Ma?			
Southern margin	Cambrian?	470?	Convergent	North-dipping?
	*Collision with Qilian block at 470 Ma?			
Qilian block				
Northern margin	Cambrian?	470?	Passive?	-
	*Collision with North Qilian belt at 470?			
Southern margin	?	460?	Convergent?	North-dipping?
	*Collision with North Qaidam UHP belt at 460?			
Qaidam block				
Northern margin (N. Qaidam UHP belt)	Cambrian?	460?	Passive?	-
	*Collision with Qilian block at 460?			
Southern margin (North East Kunlun)	Cambrian?	440?	Passive?	-
	*Collision with South East Kunlun at 440?			
South East Kunlun				
Northern margin	?	440?	Convergent	South-dipping?
	*Collision with Qaidam block (North East Kunlun) at 440?			
North China and North Qinling				
Northern North China				
	Cambrian	Late Paleozoic?	Convergent	South-dipping
	*Shortening between North China and Bainiamiao arc during the Silurian?			
Southern North China				
	Precambrian	440?	Passive	-
	*Collision with North Qinling at 440 Ma			
North Qinling				
	*Collision with intraoceanic subduction zones in Middle–Late Cambrian?			
Northern margin (Erlangping-Kuanping)	500	440?	Convergent	South-dipping
	*Collision with southern North China at 440 Ma			
Southern margin (Shangdan-Wuguan)	500	Mid-Carboniferous	Convergent	North-dipping
	*Collision with South Qinling in mid-Carboniferous			
South China, South Qinling and Japan				
Southeast South China				
	Neoproterozoic	Cambrian	Passive	-
	Cambrian	Silurian	?	?
	*Cambrian–Ordovician and Late Ordovician–Silurian tectonism due to marginal dynamics?			
Northern South China				
	Neoproterozoic	440?	Passive	-
	440	430	Divergent	-
	*Rifting of South Qinling at 440–430 Ma			
South Qinling				
	Neoproterozoic	440?	Passive	-
	440	430	Divergent	-
	*Rifting from northern South China block at 440–430 Ma			
Proto-Japan				
	Mid-Cambrian	Mesozoic	Convergent	West-dipping
Annamia				
Eastern Annamia	*Late Ordovician–Silurian magmatism and tectonism?			
Western Annamia	*Late Ordovician–Silurian arc magmatism and tectonism?			
Gondwana				
Turkish terranes				
Taurides	Middle Cambrian	470?	Passive?	-
	*Middle–Late Ordovician tectonism (rifting)?			
	460	Late Paleozoic	Passive?	-

Table 1 (*continued*)

Margin (sub-domain)	Onset (Ma)	Termination (Ma)	Type	Polarity
Pontides	*Early–Middle Ordovician tectonism?			
	460	430	Passive?	-
	*Siluro-Devonian tectonism?			
Iranian terranes				
	Middle Cambrian	450	Passive?	-
	*Late Ordovician–Early Silurian tectonism (rifting)?			
	430	Late Paleozoic	Passive?	-
Afghan terranes and Pamirs				
	*Cambro-Ordovician tectonism?			
	Early Ordovician	Late Paleozoic	Passive?	-
Qiangtang				
North Qiangtang	Cambrian	Silurian	Passive?	-
South Qiangtang	*Cambro-Ordovician tectonism?			
	Middle Ordovician	Devonian	Passive?	-
Lhasa				
Central Lhasa	*Cambro-Ordovician tectonism?			
	Ordovician	Devonian	Passive?	-
Himalaya				
Tethyan Himalaya	*Cambro-Ordovician tectonism?			
	Ordovician	Late Paleozoic	Passive?	-
Greater Himalaya	*Cambro-Ordovician tectonism?			
Sibumasu				
Tengchong/Baoshan	*Cambro-Ordovician tectonism?			
	Middle Ordovician	Silurian	Passive?	-
Southern Sibumasu	Middle Cambrian	Late Paleozoic	Passive?	
Baltica and North Kara terrane				
East Baltica (proto-Uralian margin)				
	Late Cambrian	480	Divergent	-
	480	380	Passive	-
Guberlya arc				
	Middle Ordovician	Late Ordovician	Convergent	?
Tagil arc				
	Late Ordovician	Devonian	Convergent	East-dipping
Southeast Baltica (Scythian platform)				
	Cambrian	Mid-Silurian	Passive	-
	*Mid-Silurian accretion of East Avalonia			
North Kara terrane				
	Neoproterozoic	Late Cambrian	Passive?	-
	*Cambro-Ordovician tectonism?			
	Middle Ordovician	Silurian	Passive?	-

*Denotes major tectonic events.

the Early Devonian, including shale-rich Cambrian and Ordovician horizons (Khudoley and Guriev, 2003). Khudoley et al. (2013) also reported the occurrence of Late Ordovician mafic intrusions in the Sette-Daban Range, but they were not accompanied by tectonism and apparently did not disrupt the passive margin. Instead, the passive margin was first interrupted in the Middle to Late Devonian by rifting and intrusion of the Yakutsk LIP, and was later further deformed in the mid-to-Late Mesozoic during development of the Verkhoyansk fold and thrust belt.

4.1.3. Southwest Siberia

To its southwest, the Siberian craton is flanked by an expansive and complex tectonic mosaic of predominantly late Neoproterozoic to early Paleozoic rocks that comprise the early Paleozoic southwest margin of greater Siberia (Figs. 2 and 3). In a reflection of its complexity (although no doubt further contributing to it), the tectonostratigraphic elements that comprise that mosaic have been demarcated, labeled, characterized and interpreted in a bewildering number of alternative ways. On the broadest scale, however, a common scheme differentiates the northwest Altai-Sayan area—thought to be comprised of only 'juvenile' (late Neoproterozoic and younger) material of island arc and oceanic derivation—from the southeast Tuva-Mongolian domain that probably contains a nucleus of Precambrian continental crust (Cocks and Torsvik, 2007; Wilhem et al., 2012).

Much of the Altai-Sayan area was formed in the late Neoproterozoic to Ordovician with the development and accretion of the Kuznetsk-Alatau and North Sayan island arc complexes, which are probably correlative (Buslov et al., 2002; Metelkin, 2013). In the Kuznetsk-Alatau island arc, subduction-related magmatism began at least by the late Ediacaran and continued into the late Cambrian (~496 Ma) (Rudnev et al., 2008; De Grave et al., 2011b). A similar late Ediacaran–Cambrian timeline is established from subduction-related magmatic rocks of the North Sayan arc (Rudnev et al., 2013). The cessation of subduction-related magmatism in those arcs coincided with the regional appearance of syn- to post-collisional granitoid magmatism, which extended into the Early Ordovician (~500–470 Ma) (De Grave et al., 2011b; Wilhem et al., 2012).

Ediacaran–late Cambrian accretionary complexes associated with the Kuznetsk-Alatau arc lie in its southwest, in the so-called Gorny-Altai, and are comprised by ophiolitic fragments and serpentinite melange, blocks of metamorphic rocks of greenschist to eclogite-facies, olistostromes and ocean island fragments including ocean-island basalts, reef-bearing carbonates and shallow-marine sediments, and volcano-sedimentary rocks (Dobretsov et al., 2004; Safonova et al., 2004). Ar–Ar dating of blueschists from those accretionary complexes has shown the youngest episode of high pressure (HP) metamorphism to be latest Cambrian (~490–485 Ma) (Volkova et al., 2011). Similarly, accretionary belts comprised by late Neoproterozoic–Cambrian ophiolitic rocks, HP metamorphic rocks and volcano-sedimentary accretionary rocks lie to the southeast of the North Sayan arc, in the West Sayan (Borus-Kurtushiba) zone. There appears to be two distinct pairs of

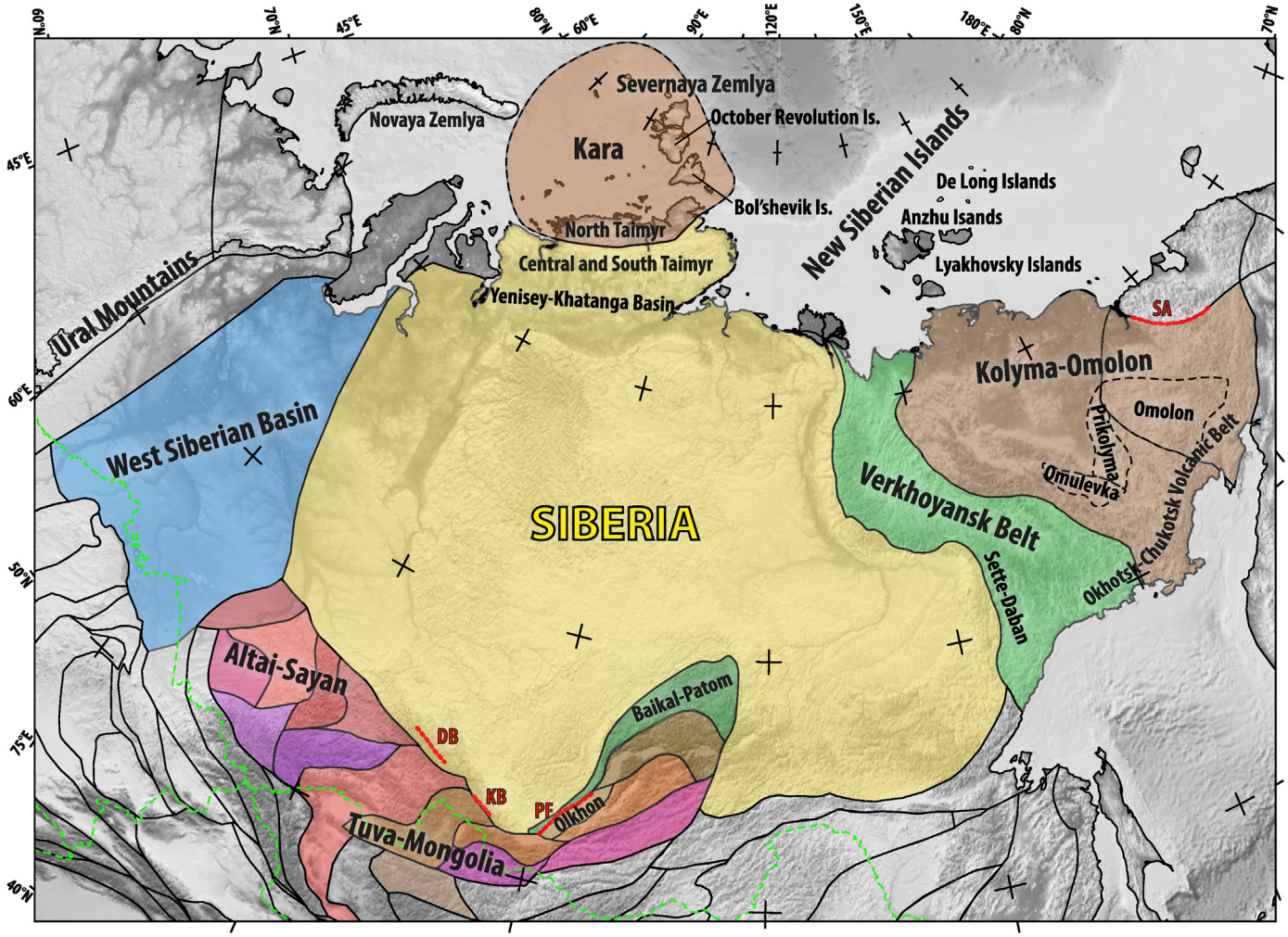

Figure 2. Overview map of Siberia and neighboring regions (section 4.1), Kolyma-Omolon (4.3), New Siberian Islands (4.4) and the North Kara terrane (4.16). Polygon colors depict generalized tectonic environment classifications: yellow, Siberian craton; brown shades, continental terranes/fragments; green shades, marginal fold-thrust belts; blue shades, sedimentary basins; red shades, continental/oceanic magmatic arcs; purple shades, oceanic/accretionary complexes. Dotted red lines denote important boundaries discussed in the text: DB, Derba belt; KB, Kitoikin belt; PF, Primorsky fault; SA, South Anyui suture. Dashed green lines show modern political boundaries for reference.

ENE–WSW trending ophiolitic and HP metamorphic belts in that zone, the northern Borus and southern Kurtushiba belts (Dobretsov and Buslov, 2004; Volkova et al., 2011). As the Kurtushiba belt is flanked to the southeast by late Neoproterozoic–Cambrian arc magmatic rocks of the Lake-Khamsara arc, it is likely that the West Sayan zone is a composite of opposed accretionary complexes that coalesced during convergence of the North Sayan and Lake-Khamsara arcs (Wilhem et al., 2012) (Fig. 4). The youngest episode of HP metamorphism in the Kurtushiba zone was early Middle Ordovician (~470–465 Ma), as determined from Ar–Ar dating of blueschists (Volkova et al., 2011). HP metamorphism possibly ended at the same time in the Borus belt, but the youngest episode of metamorphism there is only broadly constrained by Cambrian-Ordovician K–Ar dates (Dobretsov and Buslov, 2004). Together with stratigraphic observations of Ordovician molasse and Silurian shallow water shelf sediments in the West Sayan zone (Wilhem et al., 2012), the early Middle Ordovician HP metamorphic ages suggest that collision between the North Sayan and Lake-Khamsara arcs occurred in the Early Ordovician (Table 1).

Arc-related magmatism first appeared in the Lake-Khamsara arc in the latest Neoproterozoic and continued into the Early Ordovician (~480 Ma) (Kröner et al., 2014), although Rudnev et al. (2009) and Yarmolyuk et al. (2011) related the mid-Cambrian to Early Ordovician (~510–480 Ma) magmatism there to an accretionary episode. According to those workers, post-accretionary magmatism subsequently appeared in that region in the Middle Ordovician and continued until the end of that period. To the east, the Lake-Khamsara arc is juxtaposed against the Tuva-Mongolian and Dzabkhan microcontinents, which are comprised by blocks of Archean and Paleoproterozoic crystalline rocks (Gargan and Baydrag blocks) enclosed by Neoproterozoic rocks of arc- and oceanic-derivation and unconformably covered by a shared sequence of late Neoproterozoic-Cambrian shelf-carbonates (Kozakov et al., 2007; Ivanov et al., 2014). Along the suture between the Lake-Khamsara arc and the microcontinents is an accretionary melange containing the Agardagh Tes-Chem and Dariv-Khantaishir ophiolites, which are most likely correlative (Wilhem et al., 2012). Magmatic rocks from both ophiolites yield late Neoproterozoic crystallization ages (~572–570 Ma) and exhibit geochemical and petrological characteristics which suggest they developed in a supra-subduction zone environment, in association with a nascent island arc (Pfänder and Kröner, 2004; Dijkstra et al., 2006; Jian et al., 2014). Those ophiolites and the accretionary rocks they are embedded in are thus considered related to the same intraoceanic

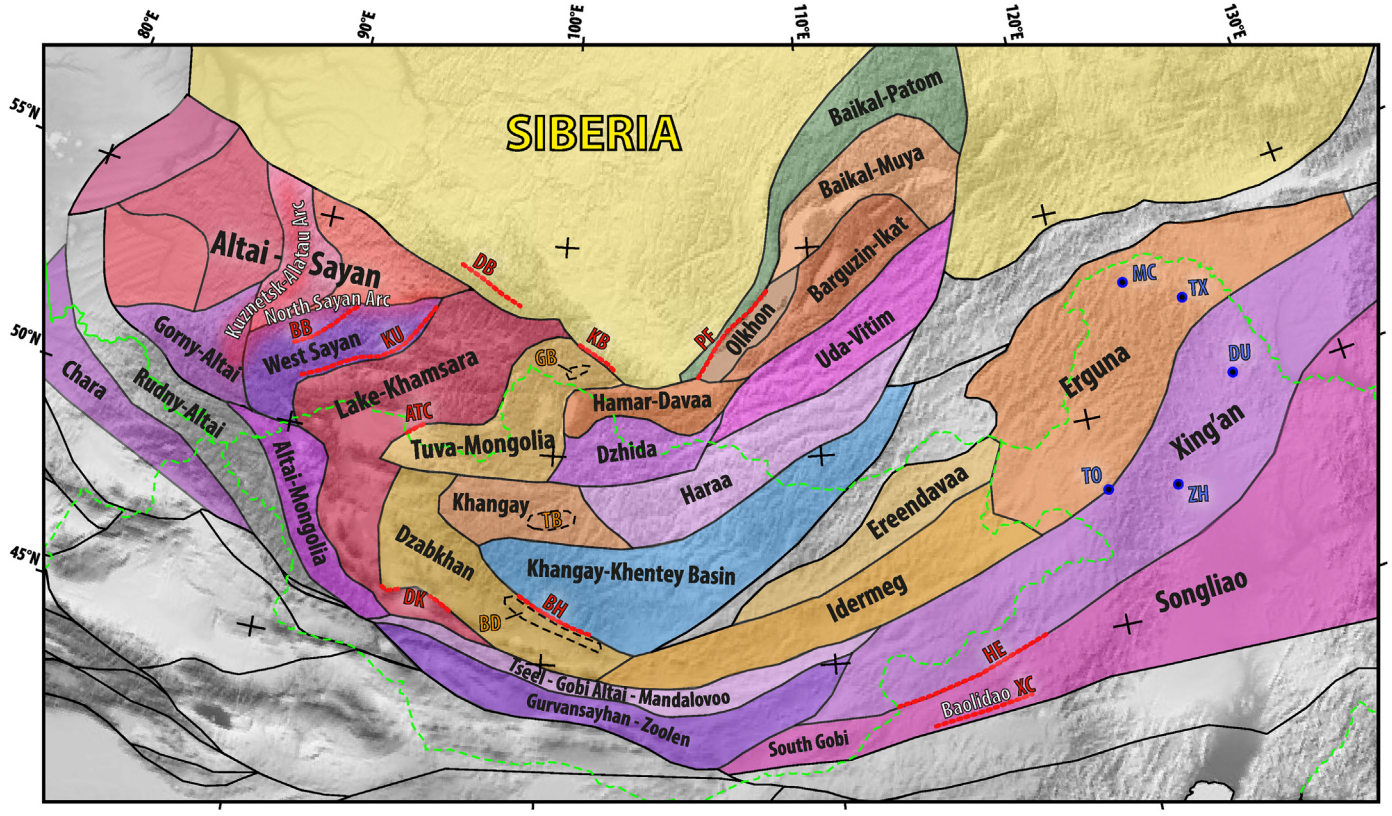

Figure 3. Overview map of southern Siberia (section 4.1) and central Mongolia (section 4.2). Polygon colors depict generalized tectonic environment classifications as in Fig. 2. Dotted red lines denote important boundaries discussed in the text: ATC, Agardagh Tes-Chem ophiolite; BB, Borus belt; BH, Bayankhongor ophiolite; DB, Derba belt; DK, Dariv-Khantaishir ophiolite; HE, Hegenshan ophiolite; KB, Kitoikin belt; KU, Kurtushiba belt; PF, Primorsky fault; XC, Xilinhot complex. Dashed black lines denote Precambrian continental blocks: BD, Baydrag; GB, Gargan; TB, Tarvagatay. Blue circles denote areas discussed in the text: DU, Duobaoshan area; MC, Mohe complex; TO, Toudaoqiao complex; TX, Tahe-Xinghuadukou area; ZH, Zhalantun area. Dashed green lines show modern political boundaries for reference.

subduction system that generated the Lake-Khamsara arc, and were ultimately obducted onto the passive margin of the Tuva-Mongolian and Dzabkhan microcontinents during later arc-continent collision. According to the occurrence of eclogites with early Cambrian (~543–537 Ma) Ar–Ar cooling ages structurally below the Dariv-Khantaishir ophiolite (Štípská et al., 2010), and mid-Cambrian (~515 Ma) post-tectonic intrusions into arc-related metamorphic rocks thrust over the Agardagh Tes-Chem ophiolite (Dijkstra et al., 2006), it is inferred that collision between the Lake-Khamsara arc and the microcontinents occurred in the early Cambrian.

According to those collected observations, by the end of the Early Ordovician (~470 Ma), most of the tectonic elements that constitute the Altai-Sayan area appear to have amalgamated with the Siberian craton. In the west of the Altai-Sayan, late Neoproterozoic to Early Ordovician forearc and accretionary rocks of the Gorny-Altai were succeeded by a thick sequence of Middle Ordovician to Early Devonian deep to shallow marine sediments that have been interpreted to represent either a passive margin (Buslov et al., 2013) or a backarc basin (Wilhem et al., 2012). The latter scenario may be supported by the occurrence of blueschists with Late Ordovician (~450 Ma) Ar–Ar cooling ages in the Chara zone to the west (Volkova et al., 2011). The serpentine melange and ophiolite-bearing Chara zone is mostly comprised by late Paleozoic rocks, but also includes blocks of Ordovician oceanic crust (Safonova et al., 2004). As pointed out by Wilhem et al. (2012), that scenario also suggests that an Ordovician-Silurian arc should be present between the Gorny-Altai and Chara zones (in the Rudny-Altai and/or Kalba-Narym zones), where there are no early Paleozoic rocks outcropping. However, further evidence of an Ordovician–Silurian active margin along the southwest of the Altai-Sayan is found in the so-called Altai-Mongolian zone, which lies to the south of the Gorny-Altai and southwest of the Lake-Khamsara arc. Previously, the Altai-Mongolian zone was considered to be floored by a Precambrian microcontinent according to the occurrence of high-grade metamorphic rocks of reportedly Precambrian age (Sun et al., 2008; Cai et al., 2011a), but subsequent geochronologic investigations of those metamorphic rocks have rather determined them to be Paleozoic (Sun et al., 2008; Cai et al., 2011a), thus casting doubt on the presence of Precambrian basement in the Altai-Mongolian zone. Moreover, the predominant age population among detrital zircons from those metamorphic rocks (~528–466 Ma) is highly similar to the detrital zircon age population in the clastic Habahe Group (~540–460 Ma)—which constitutes the oldest sedimentary sequence in the Altai-Mongolian zone—suggesting that the two are simply variably metamorphosed equivalents (Jiang et al., 2011; Cai et al., 2011a; Long et al., 2012b). The thick Habahe Group flysch was deposited in the Late Ordovician to earliest Devonian, as constrained by the youngest detrital zircon population of the flysch (~460–438 Ma), and by the age of overlying rhyolites (~445–411 Ma) (Long et al., 2010; Wang et al., 2011c). From the detrital zircon age population, composition and geochemistry of the flysch, Long et al. (2010, 2012b), and Jiang et al. (2011) concluded that the Habahe Group represents a subduction-accretion complex that received sediments from a proximal magmatic arc as well as from mafic and Precambrian rocks further to the north in the Gorny-Altai and Tuva-Mongolian regions. Fittingly, subduction-related magmatism appeared in the

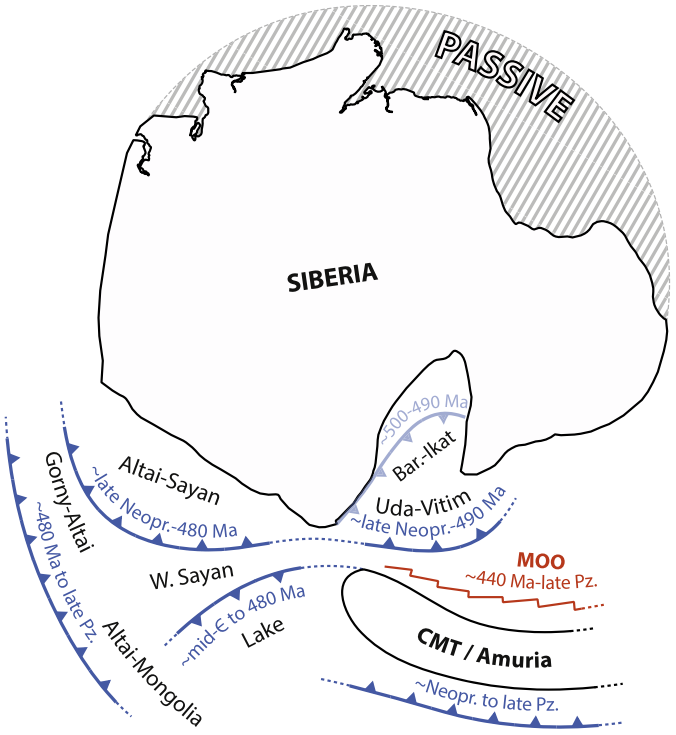

Figure 4. Schematic illustration of the principal interpretations from sections 4.1 and 4.2, concerning the early Paleozoic tectonic boundaries of Siberia and the central Mongolian ribbon terrane (CMT)/Amuria. Abbreviations: Bar.-Ikat = Barguzin-Ikat; MOO = Mongol-Okhotsk Ocean; Neopr. = Neoproterozoic; Pz. = Paleozoic; ϵ = Cambrian. Blue/red dates relate to the timing of convergent/divergent margins (Table 1).

Altai-Mongolian zone in the Early Ordovician (~478 Ma) and continued into the late Paleozoic (Glorie et al., 2011a; Cai et al., 2011b; Wang et al., 2011c), and may constitute a magmatic arc that developed along the southern active margin of the Altai-Sayan area then (Xiao and Santosh, 2014) (Fig. 4; Table 1).

4.1.4. Southeast Siberia

To the east of its juxtaposition with Tuva-Mongolia, the southern margin of the Siberian craton turns northeast and follows a prominent embayment that continues to the Baikal-Patom uplift—which comprises the Meso–Neoproterozoic passive margin of Siberia—before curving southward again (Figs. 2 and 3). In the core of that embayment, to the south of the Baikal-Patom uplift, lays the poorly-characterized Baikal-Muya and Barguzin-Ikat areas, which are furthermore variably grouped, divided and subdivided (Belichenko et al., 2006; Rytsk et al., 2011; Wilhem et al., 2012). Very generally, those areas comprise basement complexes of Precambrian and earliest Paleozoic rocks of oceanic-, island arc- and continental-derivation, most of which probably amalgamated with Siberia prior to the Early Ordovician. For example, correlatives of fossil-bearing Cambrian strata of the Siberian platform appear within latest Neoproterozoic–Cambrian cover sequences in the Baikal-Muya area, implying coherence of Baikal-Muya with the craton then (Belichenko et al., 2006; Rytsk et al., 2011). In the Barguzin-Ikat area, late Neoproterozoic to Cambrian volcanic, terrigenous and carbonate rocks cover Precambrian continental and oceanic complexes, and were variably deformed, metamorphosed and intruded by syntectonic granites at ~490–470 Ma (Gordienko et al., 2010; Rytsk et al., 2011). Subsequently, in the Ordovician and Silurian, those rocks were covered by molasse and intruded by inferred post-collisional plutons (~460–420 Ma) (Rytsk et al., 2011).

Along its western side, the embayment of the Siberian craton is nearly demarcated by Lake Baikal, and the Primorsky fault—which marks the actual craton boundary—is locally exposed along the western shore of the lake. The Primorsky fault separates early Precambrian crystalline basement and Neoproterozoic to early Cambrian platform strata of the craton from high-grade metamorphic rocks of the Olkhon belt to the southeast (Gladkochub and Donskaya, 2009). Amphibolite to granulite-facies metamorphism, deformation and syntectonic intrusion of the Olkhon rocks occurred in the late Cambrian–earliest Ordovician (~510–485 Ma), concurrent with high-grade metamorphism elsewhere along the south margin of the craton, in the Kitoikin and Derba belts (Gladkochub et al., 2008; Donskaya et al., 2013), and in the Barguzin-Ikat area to the northeast. Following the end of high-grade metamorphism, strike-slip deformation and attendant magmatism continued into the Late Ordovician (Gladkochub et al., 2008; Donskaya et al., 2013). Gladkochub et al. (2008) determined the protoliths of the high-grade Olkhon rocks to be island arc magmatic rocks and back-arc sedimentary rocks—the latter containing detrital zircons with Archean and Proterozoic ages—and assumed the belt to be an extension of the Barguzin-Ikat basement to the northeast. According to that interpretation, the high-grade metamorphic event at ~500–490 Ma could have marked the collision between a Barguzin-Ikat microcontinent and Siberia, whereas the subsequent deformation and magmatism in the Ordovician was driven by orogenic collapse and/or continuing oblique compression (Gladkochub et al., 2008). The Olkhon/Barguzin-Ikat belt may continue further to the southwest into the poorly characterized Hamar-Davaa area, where inferred late Proterozoic to Cambrian rocks were likewise subjected to intense deformation, high-grade metamorphism and plutonism in the late Cambrian (Gordienko et al., 2007; Gladkochub and Donskaya, 2009; Kovach et al., 2013).

Southeast of Hamar-Davaa, Olkhon and Barguzin-Ikat lies a complicated and expansive complex of island arcs and subduction-accretion complexes in the Dzhida and Uda-Vitim (Eravna) zones. The Dzhida subduction-accretion complex comprises inferred latest Neoproterozoic-Cambrian age volcanic, plutonic and volcano-sedimentary rocks derived from oceanic (including seamounts), island-arc, accretionary and back-arc settings (Gordienko et al., 2007, 2012). Although poorly constrained by quantitative ages, Gordienko et al. (2007) proposed that the Dzhida zone originated with the initiation of a nascent island-arc in the latest Neoproterozoic, which evolved to a mature island-arc with differentiated volcanics and carbonate shelves by the middle Cambrian. Arc magmatism ceased in the late Cambrian to Early Ordovician, possibly concurrent with the accretion of late Neoproterozoic–Cambrian seamounts, and that time was further marked by the intrusion of syn- to post-collisional granitoids (~490–477 Ma) (Gordienko et al., 2007, 2012). To the northeast of the Dzhida zone, the Uda-Vitim zone is comprised by similar latest Neoproterozoic–Cambrian arc volcanic rocks and volcano-sedimentary rocks, including carbonates (Gordienko et al., 2010; Rytsk et al., 2011).

One interpretation of the emergent regional pattern among those zones is that the Hamar-Davaa, Olkhon and Barguzin-Ikat zones are principally comprised by Neoproterozoic–Cambrian back-arc sedimentary sequences to the northwest of coeval arc-magmatic rocks in the Dzhida and Uda-Vitim zones. According to that interpretation, the Hamar-Davaa, Olkhon and Barguzin-Ikat zones together constituted a late Neoproterozoic–Cambrian back-arc system proximal to Siberia, with the active margin located to the southeast (Makrygina et al., 2007; Zorin et al., 2009). Closure of that back-arc must then have occurred in the late Cambrian–Early Ordovician, when the Hamar-Davaa, Olkhon and Barguzin-Ikat zones were subjected to regional metamorphism, with high-

grade metamorphism in the west, along the boundary with the Siberian craton, and lower-grade metamorphism occurring to the east-southeast. More speculatively, the closure of that back-arc could have been instigated by closure of an outlying ocean basin between the marginal island arcs and the inferred Precambrian terranes of the central Mongolian ribbon terrane (CMT): Tuva-Mongolia, Dzabkhan, Idermeg, Ereendavaa and Erguna (section 4.2, below) (Şengör et al., 1993; Badarch et al., 2002; Wilhem et al., 2012) (Fig. 4; Table 1). Between the CMT and the Dzhida/Uda-Vitim zones, pre-Silurian rocks are recognized in the Haraa zone, which may be a southeast continuation of the latter (Wilhem et al., 2012). There, Neoproterozoic to Early Ordovician metavolcanic and metasedimentary rocks inferred to comprise a forearc or backarc sequence are overlain and intruded by Middle-Late Ordovician to early Silurian (~460–435 Ma) felsic magmatic rocks with an arc-related geochemistry (Badarch et al., 2002; Kröner et al., 2007; Kelty et al., 2008). In considering the scarcity of contemporaneous magmatic rocks of intermediate to mafic composition, Kröner et al. (2007) concluded that the magmatic flare-up was unlikely an expression of arc magmatism, and that the arc-related geochemistry was inherited from reworked continental crust. Although the phenomenon responsible for such melting remains to be established, slab break-off has been invoked to explain comparable settings (the Choiyoi province of South America, for example (Pankhurst et al., 2006)), and could be a plausible development following an Early Ordovician collision between the CMT and greater Siberia.

Between the Haraa zone and the CMT lies the Khangay-Khentey basin, which is predominantly comprised by late Paleozoic chert, shale and sandstone. That complex is most commonly interpreted as a pair of juxtaposed accretionary margins which formed along the Mongol-Okhotsk Ocean that opened between Siberia and part of the CMT (distinguished by the designation 'Amuria') following their early Paleozoic collision, before closing again in the late Mesozoic (Van der Voo et al., 2015). The oldest dated rocks from the Khangay-Khentey basin are late Silurian radiolarian cherts that sit conformably on dolerites of ocean island-affinity (Kurihara et al., 2009). The deposition of that chert continued for ~50 Ma (into the Late Devonian) before being supplanted by siliceous shale and turbidites, displaying typical ocean plate stratigraphy (Kurihara et al., 2009; Ruppen et al., 2014). Thus, by at least the late Silurian, the Mongol-Okhotsk Ocean was open and large enough to allow for the deposition of radiolarian chert. Similarly, in the Ereendavaa zone, which flanks the Khangay-Khentey basin to the southeast, the inferred Precambrian basement is unconformably overlain by Silurian marine sediments (Bussien et al., 2011). Detrital zircon age populations from the late Paleozoic turbidites of the Khangay-Khentey basin suggest that arc-magmatism associated with MOO subduction did not initiate until the Devonian, as Cambrian to Silurian ages are rare (Kelty et al., 2008; Bussien et al., 2011).

4.2. Central Mongolian ribbon terrane and Amuria

In central Mongolia, unambiguous early Precambrian rocks are known only to the Baydrag block of the Dzabkhan microcontinent, which constitutes an Archean to Paleoproterozoic nucleus invaded by Meso-Neoproterozoic intrusions, enclosed by Neoproterozoic rocks of arc- and oceanic derivation and unconformably covered by late Neoproterozoic–Cambrian sedimentary rocks (Badarch et al., 2002; Demoux et al., 2009a; Ivanov et al., 2014). To the east of the Baydrag block and to the southeast of the Silurian to Mesozoic Khangay-Khentey basin lies the ENE–WSW trending Idermeg and Ereendavaa zones, both of which are poorly characterized but speculated to contain Precambrian basement (Badarch et al., 2002; Ruzhentsev and Nekrasov, 2009; Wilhem et al., 2012) (Fig. 3). According to the oft-referenced tectonostratigraphic scheme of Badarch et al. (2002), the Idermeg zone is a late Neoproterozoic–Cambrian passive margin floored by crystalline basement and unconformably overlain by Devonian to Mesozoic volcano-sedimentary strata. The Ereendavaa zone, accordingly, is comprised by Proterozoic basement and Neoproterozoic strata unconformably overlain by Silurian clastic rocks and late Paleozoic volcano-sedimentary strata. Granitoids intruded those zones in the late Neoproterozoic and/or early Paleozoic, but are not well-studied (Badarch et al., 2002; Ruzhentsev and Nekrasov, 2009). Despite being widely embraced in regional-scale conceptual models (Windley et al., 2007; Wilhem et al., 2012), the validity of those inferences is poorly established, or even challenged (Daoudene et al., 2009), and remains an important area for future exploration. Nonetheless, the occurrence of Precambrian rocks is well-demonstrated across the border in northeast China, in the Erguna block, which may represent the northeast-continuation of the Ereendavaa and Idermeg zones (Wilhem et al., 2012). In the center of the Erguna block, magmatic rocks previously mapped as Paleozoic or Mesozoic age are now recognized to be Neoproterozoic (~850–730 Ma) (Tang et al., 2013; Sun et al., 2014). In the Mohe complex of that block, high-grade metamorphic basement rocks that were previously assigned Archean to Paleoproterozoic ages were found to yield detrital zircons with ages as young as ~600 Ma (Zhou et al., 2011). Those rocks were metamorphosed at ~500–495 Ma, so the sedimentary protoliths must have been deposited in the late Neoproterozoic–Cambrian (Zhou et al., 2011). Neoproterozoic magmatic rocks are also recognized in the Xinghuadukou complex in the south of the block (close to the political boundary between China and Russia), where there may also be metamorphic rocks derived from Mesoproterozoic protoliths (Wu et al., 2011; Sun et al., 2014). In any case, the occurrence of middle-late Neoproterozoic intrusions and pre-Neoproterozoic detrital zircons in Neoproterozoic–Cambrian rocks implies the occurrence of still older basement there.

In the early Paleozoic, granitoid magmatism occurred in the Mohe area of the Erguna block in the mid-Cambrian (~516–504 Ma), shortly before regional metamorphism at ~500–495 Ma (Zhou et al., 2011; Wu et al., 2012; Zhou and Wilde, 2013). Subsequently, in the late Cambrian–Middle Ordovician (~500–465 Ma), granitoids (and, locally, gabbros) were emplaced in the Mohe and Tahe-Xinghuadukou areas of China (Ge et al., 2005; Wu et al., 2011) and the Amur region of Russia (Sorokin et al., 2011). In the Toudaoqiao complex in the south of the Erguna block, HP metamorphic rocks have yielded magmatic zircons of middle Cambrian age (~516–511 Ma) that are considered to date the formation of the metamorphic protoliths (Zhou et al., 2015). However, the protoliths of those blueschist-facies metamorphic rocks are inferred to be basalts of intra-oceanic origin that were accreted to the Erguna block, and therefore do not represent an episode of middle Cambrian magmatism along the block margin. The HP metamorphism of those rocks is constrained to ~511–492 Ma, according to the age of the protoliths and a ~492 Ma cross-cutting granitic dike (Zhou et al., 2015). Together with poorly-documented ophiolitic rocks in the Xinlin area to the northeast, those HP metamorphic rocks are interpreted to mark a suture between the Erguna block and the Xing'an block to its south (Wu et al., 2011; Xu et al., 2015; Zhou et al., 2015). However, the Xing'an block has been interpreted as a large subduction-accretion complex lacking a Precambrian basement (Şengör et al., 1993; Sun et al., 2014), in which case it may have been a juvenile construction on the margin of the Erguna block rather than an exotic terrane that collided with it. The Xing'an block is mostly comprised by early Paleozoic marine sediments and late Paleozoic to Cenozoic rocks, but there are Ordovician granodiorites

(~485–475 Ma) and volcanics (~450–447 Ma) in the Duobaoshan area and granitoids (~466–446 Ma) in the Zhalantun area (Wu et al., 2011, 2015; Zeng et al., 2014). From their geochemistry, Wu et al. (2015) concluded the Duobaoshan granitoids resulted from melting of an overthickened crust, whereas the volcanics were the products of a continental magmatic arc. The existence of a proximal Cambrian–Ordovician magmatic arc is further implied by a predominance of Cambrian–Ordovician detrital zircons in the early Paleozoic sedimentary rocks of the Xing'an block (Sun et al., 2014).

To the south of the Xing'an block, across the late Paleozoic Hegenshan backarc ophiolite-accretion complex (Miao et al., 2008), lies the Songliao block with a disputed Precambrian basement (Yarmolyuk et al., 2005; Li et al., 2011; Taylor et al., 2013; Pan et al., 2014; Xu et al., 2015). In the Baolidao arc of that block, prolonged arc-related magmatism occurred from the late Cambrian to the Carboniferous, although possibly with episodic hiatuses (Jian et al., 2008; Chen et al., 2009). In the southern Xing'an block to north of the Hegenshan complex, detrital zircons from Ordovician to Devonian sedimentary strata are predominantly late Cambrian to Ordovician–Silurian in age (Zhao et al., 2014a) and were probably derived both from the Baolidao arc to the south as well as from sources in the Xing'an and Erguna block to the north. Detrital zircons from strongly deformed, high-grade metamorphic rocks in the Xilinhot metamorphic complex to the southeast of the Baolidao arc are likewise comparable in age to the arc rocks and have been inferred to comprise an early Paleozoic forearc-accretionary complex associated with that arc (Chen et al., 2009). However, Precambrian zircons have also been reported from the Xilinhot metamorphic rocks and may signify that the complex is, in part, a Precambrian continental fragment that predated the onset of Cambrian-Ordovician subduction (Li et al., 2011; Xu et al., 2015).

To the west, across the China-Mongolia border, the Xilinhot arc-accretionary complex continues into the South Gobi zone where there is Ordovician–Silurian metamorphic basement covered by Silurian–Carboniferous volcano-sedimentary strata (Badarch et al., 2002; Jian et al., 2010), and disputed assertions of Precambrian basement (Yarmolyuk et al., 2005; Taylor et al., 2013). To the north of the South Gobi zone, the Gurvansayhan-Zoolen (or Trans-Altai) zone and the Tseel-Gobi Altai-Mandalovoo (or just 'Gobi Altai') zone probably represent the westward continuation of the Xing'an terrane. Within the Gobi Altai zone are exposures of undoubted Precambrian crystalline basement, locally intruded by small early Cambrian diorites and middle-late Cambrian granitoids (Demoux et al., 2009b; Jian et al., 2014). However, in the Tseel subzone, low- to high-grade metamorphic rocks that were previously speculated to be of Precambrian age are now recognized to have been deposited in the Ordovician–Silurian because they yield latest Neoproterozoic–Ordovician detrital zircons (~550–450 Ma) (Jiang et al., 2012; Burenjargal et al., 2014). From the composition and geochemistry of those metamorphic rocks, it has been inferred that their protoliths were arc-related and they most probably comprised a forearc or accretionary complex flanking latest Neoproterozoic–early Paleozoic continental arcs to the north (Lake and Tuva-Mongolia zones) (Jiang et al., 2012; Burenjargal et al., 2014). Late Ordovician sandstones from the Mandalovoo subzone also yield Neoproterozoic–Ordovician detrital zircons, reflecting a similar provenance (Kröner et al., 2010). The Gobi Altai zone also contains a dismembered early-middle Cambrian ophiolite (~523–518 Ma) embedded in a volcano-sedimentary mélange of possible Cambrian–Ordovician age, and an eclogite-bearing subduction-accretion complex of possible latest Neoproterozoic–Cambrian age (Jian et al., 2014). Following in the Ordovician to Early Devonian, the Gobi Altai zone was characterized by the deposition of clastic sediments and shallow-marine carbonates (Kröner et al., 2010). In the Trans-Altai zone, fragments of a pre-late Cambrian ophiolite and associated Cambrian forearc magmatic rocks are found in a greenschist-facies Ordovician–Silurian volcano-sedimentary mélange (Helo et al., 2006; Jian et al., 2014). The likely continuation of forearc-arc magmatism there in the Ordovician–Silurian is poorly documented, but is manifest again by the late Silurian and continues into the late Paleozoic (Badarch et al., 2002; Helo et al., 2006).

Although much about the early Paleozoic evolution of central Mongolia and northeastern China clearly remains to be discovered, a simplistic preliminary scenario consistent with most of the available data considers the Idermeg, Ereendavaa and Erguna blocks together with the Tuva Mongolia and Dzabkhan microcontinents as the nucleus of an elongate central Mongolian ribbon terrane (CMT) assemblage that collided with southern Siberia in the late Cambrian (~500–490 Ma) (Fig. 4; Table 1). Prior to that late Cambrian collision, the northern margin of the CMT may have been passive, whereas the southern margin of the CMT may already have been active since the Neoproterozoic. However, in the late Cambrian the southern margin of the CMT experienced locally intensified deformation, metamorphism and magmatism that perhaps reflected the accommodation of increased convergence following cessation of subduction to the north. Throughout the remainder of the early Paleozoic that southern margin remained active, but the prominent growth of the margin over that time, together with the occurrence of parallel accretionary systems suggests that the active margin was most likely a dynamic complex of alternately advancing and retreating marginal arcs and backarcs, the details of which are only beginning to emerge.

4.3. Kolyma-Omolon

The Kolyma-Omolon 'superterrane' (KOS) of northeastern Russia is a mosaic of small blocks comprised by Precambrian basement, Paleozoic platform rocks, basinal deposits, island arc assemblages and oceanic crustal fragments, together framed by three Mesozoic features: the Verkhoyansk fold and thrust belt to the west, the Okhotsk-Chukotsk volcanic belt to the southeast and the South Anyui suture to the northeast (Parfenov et al., 1993; Nokleberg et al., 2000) (Fig. 2). The oldest rocks of this mosaic occur as the Archean–Proterozoic crystalline basement of the Omolon massif, which represents the cratonic nucleus of the KOS. The crystalline basement of the Omolon massif is unconformably overlain by mid-to-late Neoproterozoic, Paleozoic and Mesozoic clastic and carbonate rocks, notably including a Cambrian succession of possibly rift-related continental clastic rocks and basalts and Middle-Late Devonian volcanics (Parfenov et al., 1993; Nokleberg et al., 2000). Precambrian metamorphic basement is also demonstrated or inferred to floor the Omulevka and Prikolyma terranes west of the Omolon massif, and their basements are similarly unconformably covered by latest Neoproterozoic to Paleozoic continental platform rocks. The early Paleozoic lithostratigraphy, faunas and paleomagnetically determined paleolatitudes of those Precambrian–early Paleozoic blocks are highly similar to those of the Siberian platform, and they are thought to have rifted from east Siberia in the Devonian (Parfenov et al., 1993; Nokleberg et al., 2000; Stone et al., 2003). Thus, the broad early Paleozoic platform successions of the KOS further reflect the passivity of east Siberia at that time, following possible latest Neoproterozoic to Cambrian rifting (Table 1).

4.4. New Siberian Islands

The New Siberian Islands lie to the northeast of Siberia, between the Laptev and East Siberian seas, and comprise three archipelagos, from south to northeast: the Lyakhovsky Islands, the Anzhu Islands

and the De Long Islands (Fig. 2). Due to their remoteness and ice-cover, the geology of some of those islands (notably the De Long Islands) have been scarcely studied, although recent expeditions, in part facilitated by retreating sea-ice, have contributed a wealth of novel observations. In the Anzhu Islands, early Paleozoic strata are found on Kotel'ny Island, where they comprise thick Ordovician platform carbonates that pass upward into Silurian and Devonian interbedded carbonates and cherts (Ershova et al., 2015b). In the De Long Islands, early Paleozoic rocks are recognized on Bennett, Henrietta and Jeannette Island (Kos' ko and Korago, 2009). On Bennett Island, early Cambrian to Early Ordovician fossil-bearing strata comprise a succession of interbedded marine sandstones, siltstones, shales and shelf carbonates with a general stratigraphic-upward deepening of the basin, and they are unconformably capped by Cretaceous basalts (Danukalova et al., 2014). By contrast, on Jeannette Island, early Paleozoic rocks constitute a volcano-sedimentary succession comprised by volcaniclastic rocks and minor tuffaceous breccias interlayered with subordinate dacitic to andesitic tuffs and volcanic flows, and intruded by mafic dikes and sills (Ershova et al., 2016). On Henrietta Island, the early Paleozoic sequence starts with a highly-similar volcano-sedimentary complex, but is overlain conformably by a clastic succession of polymict conglomerates, coarse sandstones and siltstones. Detrital zircon analysis of the volcaniclastic rocks from both Jeannette and Henrietta Island reveal a range of Precambrian ages, and loosely provide a Cambro-Ordovician maximum depositional age for the volcaniclastic sediments (Ershova et al., 2016). Direct dating of the volcanics and intrusives themselves, although complicated by the occurrence of zircon xenocrysts and later tectonothermal events, has reinforced that at least part of that magmatism was of latest Neoproterozoic to early Paleozoic age (Kos' ko and Korago, 2009; Ershova et al., 2016; Matushkin et al., 2016). Given that the inherited zircons in the magmatic rocks on both Henrietta and Jeannette Island are dominated by Neoproterozoic ages, and that Neoproterozoic crustal xenoliths are found in Cenozoic basalts on Zhokhova Island, it has been suggested that the De Long Islands are floored by Neoproterozoic basement, although it is nowhere exposed (Akinin et al., 2015).

The early to mid-Paleozoic affinity of the New Siberian Islands remains an outstanding question. On the basis of early Paleozoic faunas, Danukalova et al. (2014) concluded the islands were of Siberian affinity then. However, given the dominance of late Neoproterozoic and early Paleozoic ages among detrital zircons in Paleozoic rocks from the Anzhu and De Long Islands, others have suggested that their sediment source(s) was involved in Timanian and Caledonian orogenesis, implying an affinity to northern Baltica or (after the mid-Silurian) northern Laurussia (Ershova et al., 2015b; Ershova et al., 2016). Yet, early Paleozoic paleomagnetic data from the De Long Islands reveals that they occupied a very narrow band of mid-latitudes, between ~35° and 40° (ambiguous hemisphere), during the earliest Cambrian, Early Ordovician, Middle Ordovician and early Silurian (Metelkin et al., 2016; Zhdanova et al., 2016), which precludes them from having been tectonically coherent with any one of those continents then. Due to these significant paleogeographic uncertainties, the New Siberian Islands are not explicitly included in the plate model herein; they thus present an important target for further study.

4.5. The Kazakh terranes and Kazakhstania

Kazakhstania is a tectonic mosaic of microcontinenal fragments, island arcs, accretionary complexes, backarc basins and ophiolites, which was multiply deformed during numerous Paleozoic accretionary and collisional events, and strongly reshaped by late Paleozoic oroclinal bending. Because of this complex geologic history, the fundamental tectonic framework of Kazakhstania is still not well-understood, and the nature, age, divisions and indeed even the names of the principal tectonic units remain the subject of debate. To avoid further complicating the literature, I default in the following to popular terminology, but note that in some cases these terms may be inadequate or misleading, especially where they are applied across sparsely exposed and/or poorly studied regions. The major constituents of Kazakhstania probably did not assemble into one unified landmass until the mid-Paleozoic (Popov and Cocks, 2017), so for early Paleozoic time the terranes are instead collectively referred to as 'the Kazakh terranes'.

4.5.1. Kyrgyz Tianshan (Kyrgyzstan and southern Kazakhstan)

The Kyrgyz Tianshan, which continues beyond the borders of Kyrgyzstan into Tajikistan, eastern Uzbekistan, and southern Kazakhstan, is divided into the North, Middle and South Tianshan (Fig. 5). To the east, where the Tianshan Range crosses into northwest China, the range is referred to as the Chinese Tianshan to stress the distinct terrane terminology adopted there (as discussed in section 4.5.2 below). The Kyrgyz North Tianshan (hereafter KNT) is comprised by Mesoproterozoic continental fragments, variably metamorphosed Neoproterozoic to early Paleozoic metasediments, and large volumes of early Paleozoic granitoids (Kröner et al., 2013). To the north, the KNT is bounded by the Dzhalair-Naiman ophiolitic belt, which stretches NW–SE for more than 500 km and separates the KNT from the Chu-Yili microcontinent to the northeast (Windley et al., 2007). Ophiolitic rocks of the belt include harzburgite, lherzolite, gabbro, plagiogranite, dolerite, pillow basalt and chert, and siliciclastic turbidites which unconformably overlie them (Alexeiev et al., 2011). The crystallization age of the magmatic ophiolitic rocks is considered to be middle Cambrian on the basis of zircon ages from the plagiogranites (~521–513 Ma) (Kröner et al., 2007; Ryazantsev et al., 2009) and from early late Cambrian conodonts in the associated cherts (Alexeiev et al., 2011). The minimum age of the ophiolite is further constrained by the overlying siliciclastic turbidites, which are determined to be late Cambrian–Early Ordovician age on the basis of fossils and detrital zircons (Kröner et al., 2007; Alexeiev et al., 2011). The ophiolitic rocks are imbricated with a general top-to-the-southwest sense of motion and are structurally overthrust upon rocks of the KNT, which was otherwise characterized by passive margin sedimentation there until the late Early Ordovician (Alexeiev et al., 2011; Kröner et al., 2012). Such a relationship suggests that closure of the Dzhalair-Naiman basin proceeded by subduction to the north (Fig. 6), which is consistent with reports that Chu-Yili hosted early to late Cambrian (~534–508 Ma) arc-related magmatism, and bears relicts of late Cambrian–Early Ordovician HP metamorphism (Kröner et al., 2007; Alexeiev et al., 2011). Coincident with the timing of the obduction of the Dzhalair-Naiman ophiolitic belt, the northern flank of the KNT was subjected to ultra-high pressure (UHP) metamorphism in the Early Ordovician, according to a ~474 Ma Lu-Hf age from eclogite in the Aktyuz area (Rojas-Agramonte et al., 2013). Other observations, including a ~503 Ma detrital zircon age in the metamorphic protolith, a ~472 Ma post-kinematic granitoid and a ~470 Ma Ar–Ar mica cooling age on gneisses, indirectly reinforce that timing (Kröner et al., 2012).

Importantly, that scenario of Cambro-Ordovician Dzhalair-Naiman basin closure by subduction to the north beneath Chu-Yili is not undisputed. Popov et al. (2009) described latest Cambrian to mid-Ordovician siliciclastic slope and rise deposits that extend the length of the southwestern margin of Chu-Yili, and interpret that margin as having been passive across that interval. According to those authors, the middle Cambrian ophiolites of the Dzhalair-Naiman basin mark its initiation as a back-arc basin, and basin closure did not commence until the Middle Ordovician, when, they

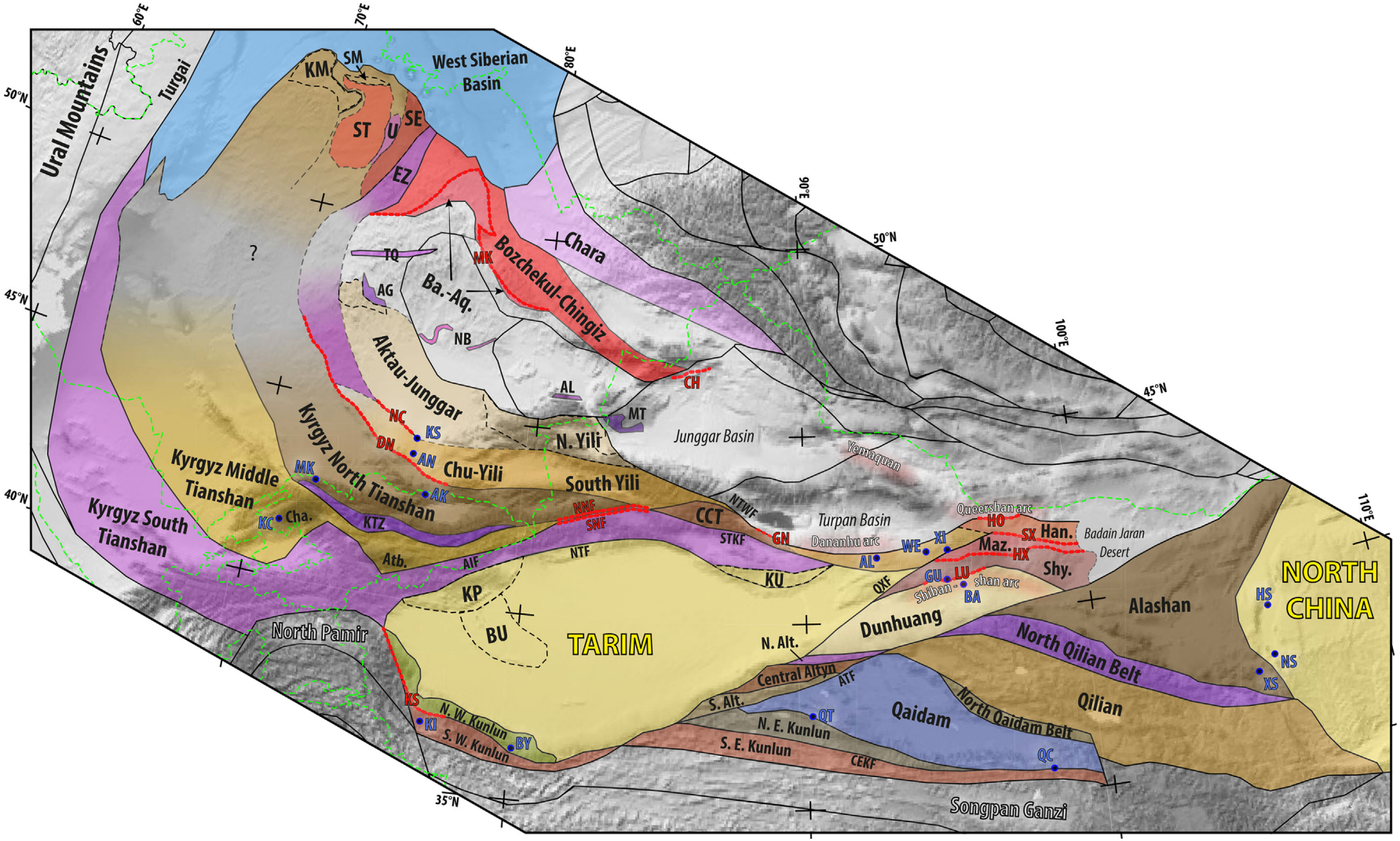

Figure 5. Overview map of Kazakhstania (section 4.5), Tarim (4.6), Beishan and Dunhuang (4.7), and Alashan, Qilian and Qaidam (4.8). Polygon colors depict generalized tectonic environment classifications: yellow, Tarim and North China cratons; brown shades, continental terranes/fragments; green shades, marginal fold-thrust belts; blue shades, sedimentary basins; red shades, continental/oceanic magmatic arcs; purple shades, oceanic/accretionary complexes. Terrane abbreviations: AG, Agadyr complex; AL, Alataw complex; Ba.-Aq, Baidaulet-Aqbastau belt; CCT, Chinese Central Tianshan; EZ, Erementau zone; Han., Hanshan; KM, Kokchetav massif; KTZ, Kyrgyz-Terskey zone ('Nikolaev Line'); Maz., Mazongshan; MT, Mayila-Tangbale complex; N. Alt., North Altyn belt; NB, North Balkhash complexes; S. Alt., South Altyn belt; SE, Selety zone; Shy., Shuangyingshan; SM, Shat massif; ST, Stepnyak zone; TQ, Teqturmas complex; U, Urumbai zone. Dashed red lines denote important boundaries discussed in the text: CH, Chagantaolegai and Hongguleleng mélanges; DN, Dzhalair-Naiman ophiolitic belt; GN, Gangou ophiolitic mélange; HO, Hongshishan ophiolite; HX, Hongliuhe-Xichangjing ophiolitic belt; KS, Kudi suture; LU, Liuyuan complex; MK, Maikan-Kyziltas belt; NC, Northeast boundary of Chu-Yili; NNF, North Natali fault; SNF, South Natali fault; SX, Shibanjing-Xiaohuangshan belt. Dashed black lines denote Precambrian continental blocks and basement uplifts: BU, Bachu uplift; KP, Kalpin uplift; KU, Kuruktag uplift. Blue circles denote areas discussed in the text: AK, Aktyuz area; AL, Alatage area; AN, Anrakhai area; BA, Baidunzi area; BY, Buya area; GU, Gubaoquan area; HS, Helanshan area; KC, Kassan metamorphic complex; KI, Kudi area; KS, Kanshengel; MK, Makbal complex; NS, Niushoushan area; QC, Qingshuiquan complex; QT, Qimantagh area; WE, Weiya area; XI, Xingxingxia area; XS, Xiangshan area. Other abbreviations: AIF, Atbashy-Inylchek fault; Atb, Atbashi Range; ATF, Altyn Tagh fault; CEKF, Central East Kunlun fault; Cha, Chatkal Range; NTF, North Tarim fault; NTWF, North Tianshan-Weiya fault; QXF, Qiemo-Xingxingxia fault; SKTF, South Tianshan-Kumishi fault. Dashed green lines delineate modern political boundaries for reference.

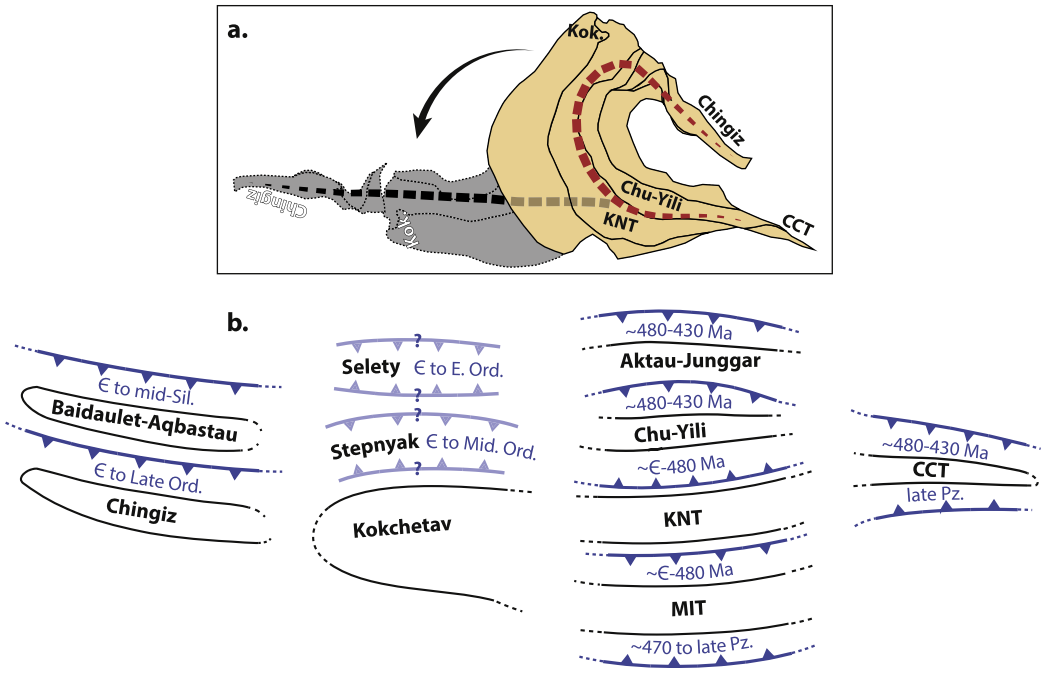

Figure 6. (a) The pre-late Paleozoic constituents of Kazakhstania (orange blocks) presently form an orocline (red dashed axis) that formed in the late Paleozoic. To consider pre-Devonian tectonics, the orocline must first be removed (gray blocks following black dashed axis). (b) Schematic illustration of the principal interpretations from section 4.5, concerning the early Paleozoic tectonic boundaries of Kazakhstania. Abbreviations: CCT = Chinese Central Tianshan; KNT = Kyrgyz North Tianshan; Kok. = Kokchetav; MIT = Kyrgyz Middle Tianshan. Blue dates relate to the timing of convergent margins (Table 1).

argue, subduction initiated beneath the north margin of the KNT. Although it is not clear why the northern flank of the KNT would have been subjected to Early Ordovician UHP metamorphism in this alternative model, the stratigraphic arguments raised by Popov et al. (2009) remain unaddressed and deserve further attention.

To the south, the KNT is separated from the Kyrgyz Middle Tianshan by the Kyrgyz-Terskey zone ('Nikolaev Line'), which is decorated by isolated exposures of early Cambrian to earliest Ordovician mafic-ultramafic rocks and cherts interpreted as dismembered ophiolitic complexes (Qian et al., 2009; Degtyarev et al., 2013). The Kyrgyz-Terskey zone also hosts more evolved Cambrian volcanic successions, some of which begin with pillow basalt before passing upward into differentiated basalt, andesite and dacite, and these have been interpreted as one or more island arcs within the collapsed Kyrgyz-Terskey ocean basin (De Grave et al., 2011a; Degtyarev et al., 2013). The late Cambrian to Early Ordovician closure of that basin—which could have been composite—was accompanied by HP-UHP metamorphism of the Makbal complex along the southern margin of the KNT, which occurred between ~510 Ma and 470 Ma (Rojas-Agramonte et al., 2013; Meyer et al., 2014). Folding and thrusting due to basin closure continued until the end of the Middle Ordovician (Degtyarev et al., 2013). Following the Early Ordovician closure of the Dzhalair-Naiman and Kyrgyz-Terskey basins (Table 1), the KNT was covered by Middle and Late Ordovician continental arc volcanics and mid-to-late Paleozoic volcano-sedimentary strata, and was widely intruded by granitoids of Middle Ordovician to Silurian age (Konopelko et al., 2008; Glorie et al., 2010; Kröner et al., 2013; Rojas-Agramonte et al., 2014). The origins of that voluminous Ordovician-Silurian magmatism were probably due in part to Early-Middle Ordovician orogenesis associated with basin closure on either side of the KNT, but likely also to continued subduction below the KNT either from the north, the south, or both.

South of the Kyrgyz-Terskey zone, the Kyrgyz Middle Tianshan (hereafter MIT) is typically described as the southeast extension of the so-called Ishim-Middle Tianshan (or Ishim-Naryn) microcontinent, which may span ~2000 km from eastern Kyrgyzstan to northern Kazakhstan (Windley et al., 2007; Kröner et al., 2017). The MIT comprises Precambrian crystalline complexes, Neoproterozoic volcanics and late Neoproterozoic to Middle or Late Ordovician marine sedimentary assemblages, namely shales, cherts and carbonates (Kröner et al., 2013). Notably, the MIT lacks Cambrian magmatic rocks, and Ordovician metavolcanic rocks are known only from the Chatkal and northern Atbashi ranges in the south of the MIT (Rojas-Agramonte et al., 2014; Alexeiev et al., 2016). The Ordovician metavolcanics there are dominated by rhyolites and dacites with subordinate intermediate to mafic volcanics, exhibit a calc-alkaline to sub-alkaline geochemistry, and are interpreted as products of a continental arc. U-Pb dating reveals that volcanism approximately spanned the Middle and Late Ordovician (~467–445 Ma) (Alexeiev et al., 2016). North of those arc volcanic rocks, a dismembered Ordovician ophiolitic assemblage has been identified along the northern slope of the Chatkal Range. The ophiolitic rocks include pyroxenite, gabbro, pillow basalt, turbidite, black shale and chert; the latter bearing Early to Middle Ordovician conodonts (Alexeiev et al., 2016). Those ophiolitic rocks are metamorphosed and structurally juxtaposed or unconformably overlain by unmetamorphosed Silurian strata. Those observations constrain the metamorphism of the ophiolitic assemblages to the Late Ordovician, which is coincident with the ~450 Ma high-grade metamorphism of the nearby Kassan metamorphic complex of the Chatkal Range (Alexeiev et al., 2016). This event may thus have marked closure of the basin between the arc and the MIT, which may only have been a short-lived backarc basin. Following that arc-continent collision, continental arc volcanism and plutonism appeared across the Middle Tianshan in the early Silurian and continued episodically into the late Paleozoic (Glorie et al., 2011b; Alexeiev et al., 2016) (Fig. 6; Table 1).

Further south, the Kyrgyz Middle Tianshan is separated from Tarim and the northern Pamirs by the South Tianshan, which,

although containing some pre-Devonian rocks, is recognized primarily as a late Paleozoic accretionary system (Jiang et al., 2014b; Klemd et al., 2015); further details of the South Tianshan are presented in section 4.6.1.

Concerning the paleobiogeography of the region, Cambrian and Early Ordovician faunas of the MIT bear a clear resemblance to those of South China (Popov et al., 2009), and Middle to Late Ordovician faunas of the MIT, KNT and Chu-Yili exhibit a strong affinity to the China blocks (particularly South China) and northern peri-Gondwana (Popov and Cocks, 2017). By contrast, the Ordovician faunal assemblages of the MIT, KNT and Chu-Yili are distinct from those of Baltica and Siberia.

4.5.2. Aktau-Junggar and Chinese Tianshan (eastern Kazakhstan and northwest China)

The northeastern margin of the Chu-Yili microcontinent is marked by a tectonic mélange exposed along the southern end of Lake Balkhash (Fig. 5). The mélange is comprised by structurally mixed units of radiolarian chert, turbidite, basalt and olistoliths of carbonate and quartzite, and it is interpreted as an accretionary complex (Popov et al., 2009). The radiolarian cherts largely lack clastic material, and bear conodonts that range in age from late Cambrian to Middle Ordovician, placing a maximum age on the operation of that accretionary complex. The occurrence of Ordovician intermediate and felsic volcanic rocks in Chu-Yili to the south of the mélange, as well as the attendant construction of an Ordovician basin there (inferred to be a forearc basin; Popov et al., 2009) suggests that subduction associated with that complex was south-dipping, beneath Chu-Yili. From the age and distribution of those volcanic and basinal successions, the north-facing active margin of Chu-Yili appears to have continued through the Early and Middle Ordovician before being interrupted in the Late Ordovician. Subsequently, arc magmatism re-initiated in the Silurian to the north of the Ordovician arc and continued through that period (Popov et al., 2009). Beyond the southern end of Lake Balkhash, the continuation of the tectonic boundary marked by that tectonic mélange is not firmly established, but to the southeast it appears to extend beyond Kanshengel and to the northwest it may continue into the Erementau zone that stretches to northern Kazakhstan (section 4.5.3) (Windley et al., 2007; Popov et al., 2009).

On the northeast side of that boundary, Precambrian rocks identified in central Kazakhstan (near Agadyr), eastern Kazakhstan, and in the Chinese North Tianshan of northwest China are thought to comprise a single, 800 km long, NW–SE elongate continental sliver, the Aktau-Junggar microcontinent (Windley et al., 2007) (Fig. 5). In the Chinese North Tianshan, the extension of this microcontinent is also called 'North Yili', to distinguish it from Precambrian units to the south ('South Yili'), which are likely correlative with the KNT or Chu-Yili (Wang et al., 2014a). The basement of Aktau-Junggar comprises Proterozoic metamorphic rocks, metasediments and metavolcanic rocks and is intruded by Neoproterozoic granitoids and unconformably overlain by latest Neoproterozoic to early Paleozoic strata, typified by fine-grained marine clastic rocks and carbonates (Degtyarev et al., 2006; Wang et al., 2011a; Liu et al., 2014a; Tretyakov et al., 2015). Paleozoic magmatism first appeared in Aktau-Junggar in the Ordovician, when Early and Late Ordovician (~480–440 Ma) granitoids intruded the basement in central Kazakhstan (Degtyarev et al., 2006) and Middle to Late Ordovician (~466–447 Ma) gabbros, diorites and granites invaded the Precambrian rocks of North Yili (Wang et al., 2012a; Huang et al., 2013b). A bimodal volcanic counterpart to that plutonism is also recognized in North Yili, where Early to Late Ordovician basalts and rhyolites occur (An et al., 2017). With the cessation of that magmatic episode, the Precambrian–early Paleozoic units of North Yili were deformed and metamorphosed during the Silurian to earliest Devonian (~443–413 Ma), in what has been interpreted as an accretionary event (Wang et al., 2011a), possibly marking its collision with Chu-Yili.

To the north of Aktau-Junggar, ophiolitic melanges and turbidites are recognized in a series of accretionary complexes of inferred to demonstrated Ordovician to Silurian age, which, together with a variety of late Paleozoic arc and accretionary complexes, form a NW–SE trending corridor separating Aktau-Junggar from the early Paleozoic sequences of the Chingiz belt of northeast Kazakhstan (section 4.5.4). Those early Paleozoic accretionary complexes have been classified in a variety of ways, but according to Degtyarev (2011) and Choulet et al. (2012b) they include the Teqturmas, Agadyr, North Balkhash and Alataw complexes (the Zhaman-Sarysu and North Balkhash complexes of Windley et al. (2007)), and the Mayila-Tangbale complex (Karamai complex of Windley et al. (2007)). In general, the age constraints on those accretionary complexes are poor. In the relatively well-constrained Mayila-Tangbale complex, an Ordovician to Silurian timing for subduction-accretion is interpreted from the constituents of melange there, which include late Neoproterozoic to Silurian ophiolitic and sedimentary rocks, Ordovician and Silurian volcaniclastic rocks dominated by a juvenile (Ordovician–Silurian) zircon population (Choulet et al., 2012a,b; Yang et al., 2012), and blocks of blueschist yielding Middle–Late Ordovician Ar–Ar ages (Zhang, 1997). The occurrence of late Silurian detrital zircons from blocks in that melange establishes its maximum depositional age, and it is sealed by late Silurian-Devonian terrigenous deposits (Choulet et al., 2012b). It is generally agreed that those accretionary complexes once comprised a contiguous, linear system along an early Paleozoic active margin, and have been since dismembered and dispersed by later tectonics, but due to their position in the interior of a late Paleozoic orocline, it is as-yet unclear if they belonged to a north-facing active margin along the north of Aktau-Junggar, a south-facing active margin along the south of the Chingiz belt, or both (Choulet et al., 2012b; Wang et al., 2012a). However, with reference to the Ordovician magmatism and Silurian deformation noted in Aktau-Junggar, it is reasonable to conclude that at least some of those complexes were associated with an Ordovician–Silurian subduction system along the northern margin of that block (Fig. 6; Table 1).

Across most of the 'South Yili', early Paleozoic rocks are lacking and the Precambrian basement is unconformably overlain by late Paleozoic volcanics and sediments (Wang et al., 2008; An et al., 2017). To the south, along and between the North and South Nalati faults that separate the Yili block from South Tianshan and Tarim, Ordovician to Silurian rocks occur as arc-type intermediate to felsic volcanics, volcaniclastics, clastic sediments, carbonates and I-type granitoids, and are collectively interpreted as relics of an early Paleozoic active margin (Gao et al., 2009; Qian et al., 2009; Wang et al., 2011b). However, the nature of the North and South Natali faults remain uncertain, so it is not yet clear if those rocks belong to the southern margin of the Yili block, the northern margin of Tarim, an independent continental strip ('the Chinese Central Tianshan'), or some combination therein. Some workers consider the boundary of the Yili block and northern Tarim to be comprised by only one true suture between ~82°E and ~85°E longitude, implying that an independent Chinese Central Tianshan does not exist there (Xiao et al., 2013). However, other workers have correlated the North and South Nalati faults with the Nikolaev Line and the Atbashy-Inylchek fault (which forms the boundary between the MIT and South Tianshan), respectively, meaning that the thin corridor between them is a tectonically distinct terrane (the Chinese Central Tianshan); or possibly an extension of the Krygzy Middle Tianshan (Gao et al., 2009; Qian et al., 2009). Still others

contend that a distinct Chinese Central Tianshan block exists, but that it extends much further south, to a discontinuous belt of Silurian–Devonian ophiolitic melanges in the South Tianshan, ~60 km south of the Atbashy-Inylchek-South Nalati fault (Charvet et al., 2011; Wang et al., 2011b); but see also Jiang et al. (2014b).

To the east of ~85°E, the existence of the 'Chinese Central Tianshan' (hereafter CCT) as a block rooted by continental basement becomes more certain, although whether the terrane represents the southeast extension of the Yili block (Xiao et al., 2013) or an independent continental ribbon (Huang et al., 2015b), is a matter of continuing debate. Here, the CCT is located between the North Tianshan-Weiya fault to the north and the South Tianshan-Kumishi fault to the south, and to the east it may continue beyond ~90°E, into the Xingxingxia microcontinent between the Turpan basin and north Beishan (see section 4.7). The CCT comprises a basement of Meso- to Neoproterozoic schist, gneiss, migmatite and metasedimentary rocks, unconformably overlain by metamorphosed Ordovician to Early Devonian volcano-sedimentary strata and Siluro-Devonian flysch, and intruded by early to late Paleozoic plutons (Ma et al., 2013; Huang et al., 2015b; Zhang et al., 2015). The early Paleozoic volcanic and intrusive rocks, which may have appeared as early as the late Cambrian (Wang et al., 2015), but certainly spanned ~475–420 Ma, include mafic, intermediate and felsic compositions, and reportedly exhibit the geochemical signature of subduction-related magmatism (Zhong et al., 2015), possibly compounded by Late Ordovician backarc extension (Zhang et al., 2016c) and Silurian crustal thickening (Dong et al., 2011b). Subsequently, in the Early Devonian, the CCT was invaded by A-type felsic intrusions that have been suggested to reflect a post-orogenic or extensional setting, followed by younger Devonian to Carboniferous plutons reflecting renewed subduction-related magmatism (Wang et al., 2015; Zhong et al., 2015). That broad early to middle Paleozoic magmatism is furthermore recorded in the detrital zircon populations of younger (late Paleozoic) sedimentary strata, which suggest that peak early Paleozoic magmatism occurred in the Late Ordovician (Ma et al., 2012; Zhang et al., 2015).

It is debated whether the subduction that gave rise to that Ordovician-Silurian magmatic arc was north- or south-dipping because the nature and history of the northern and southern terrane boundaries are themselves still ill-defined, but the data presently weigh in favor of south-directed subduction during the Ordovician to early Silurian followed by north-directed subduction in the Devonian and Carboniferous. Along the North Tianshan-Weiya fault, discontinuous exposures of ophiolitic melange are broadly considered to be of Cambrian–Ordovician age, and some locally include HP schists (Dong et al., 2011b; Wang et al., 2015). Among those melanges, the Gangou ophiolitic melange was deformed in the mid-Silurian (~430 Ma), intruded by an A-type granite at ~426 Ma and unconformably covered by Silurian flysch (Ma et al., 2013; Wang et al., 2015), suggesting that suturing there occurred prior to the end Silurian. By contrast, the South Tianshan-Kumishi fault contains ophiolitic rocks of Silurian to mid-Carboniferous age and is intruded by Late Carboniferous to Permian syn- to post-collisional granitoids (Qian et al., 2009; Jiang et al., 2014b; Wang et al., 2015). Together, those observations suggest that the CCT may have been the upper plate above a south-dipping subduction zone in the Ordovician and Silurian, until a mid-Silurian collision terminated subduction to the north and instigated north-dipping subduction beneath the south of the CCT (Fig. 6; Table 1). What exactly the CCT collided with in the north in the mid-Silurian remains unknown because exposed rocks of the Chinese North Tianshan to the north of the CCT are Devonian or younger, although it is commonly assumed that a fragment of Precambrian to early Paleozoic basement must be buried there (Wang et al., 2015).

4.5.3. Northern Kazakhstan

In northern Kazakhstan, the tectonic framework is cored by a Precambrian continental fragment—the Kokchetav microcontinent—comprising Mesoproterozoic crystalline basement covered by late Proterozoic and early Paleozoic clastic rocks and carbonates (Glorie et al., 2015) (Fig. 5). Similarities in the age of that basement with those of southern Kazakhstan have led to proposed correlations of the Kokchetav microcontinent with both the MIT and KNT, but direct physical ties are lacking. In its northeast, the Kokchetav microcontinent includes a belt of diamond and coesite-bearing HP-UHP metamorphic rocks that experienced peak metamorphic conditions during the early Cambrian (~540–520 Ma), before being exhumed in the middle to late Cambrian. It is widely accepted that part of that UHP metamorphic assemblage was formed from continental protoliths of Kokchetav derivation which were partly subducted in the latest Neoproterozoic to early Cambrian, but whether they were introduced to the subduction zone by subduction-erosion (wherein the Kokchetav microcontinent occupied an upper-plate position) (Glorie et al., 2015), or by partial subduction of the entire northeast passive margin of the Kokchetav microcontinent (wherein it would represent the lower plate) (Wilhem et al., 2012), is debated. Part of the problem that has frustrated resolution of this debate is the apparent absence of a coeval (Neoproterozoic–early Cambrian) magmatic arc. Probably Cambrian volcano-sedimentary successions have been identified in the east of the Kokchetav massif, but the volcanics are predominantly mafic in composition and (sparse) existing age constraints suggest the successions are likely of late middle to late Cambrian age (Degtyarev et al., 2016). In the Shat massif to the northeast of the Kokchetav HP-UHP belt, a succession of basic metavolcanics including rare rhyolites and felsic tuffs is inferred to be of pre-middle Cambrian age according to stratigraphic relationships, and thus could constitute the missing Neoproterozoic to early Cambrian arc, but this remains to be confirmed (Degtyarev et al., 2016).

In the middle to late Cambrian, exhumation of the HP-UHP Kokchetav belt occurred contemporaneously with deposition of coarse clastic strata and the eruption of mafic volcanics in the east of the Kokchetav massif, suggesting that post-collisional extension was operating there then, whereas in the central Kokchetav massif, middle to late Cambrian deposits were rather characterized by fine-grained clastic rocks and carbonates, reflecting stable platform-type conditions (Degtyarev et al., 2016). Conditions evidently changed in the Early to Middle Ordovician, when coarser clastic rocks were deposited across the central and eastern Kokchetav massif, together with ancillary volcanic rocks, mostly of mafic and intermediate composition. Subsequently, in the Middle to Late Ordovician, the region was characterized by the deposition of flysch, and in the Late Ordovician and Silurian the Kokchetav massif was intruded by large granitoid bodies, notably including the Zerenda, Krykkuduk and Borovoe complexes (Letnikov et al., 2009; Glorie et al., 2015).

To the northeast, the Kokchetav massif is flanked by the Stepnyak zone, comprising mostly Ordovician volcano-sedimentary rocks, the nature of which remains to be settled. According to one prevailing scheme, the zone constitutes a late Cambrian–Early Ordovician island arc complex that collided with the Kokchetav microcontinent in the Early to Middle Ordovician (Dobretsov et al., 2006; Korobkin and Smirnov, 2006). By that interpretation, the boundary of the Stepnyak zone and Kokchetav microcontinent must constitute an Early to Middle Ordovician subduction-accretion/collision zone, which Zhimulev et al. (2011) termed the North Kokchetav tectonic zone. Zhimulev et al. (2011) interpreted that zone as a collage of nappes, mostly comprising Kokchetav basement, that developed at ~490–470 Ma, based on $^{40}Ar/^{39}Ar$ ages on micas in schists and mylonitized gneisses along inferred

thrust boundaries (Glorie et al., 2015). The occurrence of olistostromes in deformed Early to Middle Ordovician strata in the east of the Kokchetav massif further supports tectonism there then (Korobkin and Smirnov, 2006). However, while not disputing the occurrence of an Early Ordovician tectonic event in the eastern Kokchetav massif, Degtyarev et al. (2016) have challenged the interpretation of the Stepnyak zone as an island arc complex. They argue that the composition and geochemistry of the late Cambrian and Ordovician volcanics of the Stepnyak zone and the occurrence of possibly Precambrian xenoliths in Late Ordovician granitoids there, together with the observation that the zone is framed to the north and east by small continental blocks, suggest that it is floored by continental crust—perhaps the same as that which forms the Kokchetav massif. Accordingly, those authors interpret the late Cambrian–Ordovician volcanism and tectonism in the Stepnyak zone as an expression of intraplate extension or subduction beneath the far-side of a joint Kokchetav-Stepnyak microcontinent (i.e. beneath the northeast of the Stepnyak zone), rather than subduction-collision between them (Degtyarev et al., 2016).

To the east of the Stepnyak zone lies a poorly characterized region that has been inconsistently subdivided, but often includes the so-called Selety zone (Şengör and Natal'In, 1996; Windley et al., 2007). That region is predominantly comprised by early to middle Cambrian volcanic and volcaniclastic rocks and late Cambrian to Early Ordovician cherty-terrigenous and carbonate strata (Degtyarev and Ryazantsev, 2007; Wilhem et al., 2012). Some authors have interpreted those Cambro-Ordovician sequences as a paired early Paleozoic accretionary complex (Urumbai zone) and Cambrian island arc (Selety arc) (Windley et al., 2007; Wilhem et al., 2012), or as a duplication of such paired complexes (the Ishkeolmes and Selety units of Şengör and Natal'In (1996)), but the present lack of detailed investigations of those rocks precludes a critical assessment of their nature and a satisfactory understanding of their history. Still further east, marking the divide between northern Kazakhstan and the Bozchekul-Chingiz domain (northeast Kazakhstan), is the possibly distinct Erementau zone, which is similarly poorly understood. Degtyarev (2011) described late Cambrian to Middle Ordovician cherty-terrigenous rocks, carbonates, and alkali basalt from that zone and interpreted it as a rift sequence, whereas others have recognized the zone as an accretionary complex and suture zone (Windley et al., 2007; Wilhem et al., 2012).

4.5.4. Chingiz

The core of northeast Kazakhstan is comprised by the Bozchekul-Chingiz-Tarbagatay (hereafter 'Chingiz') island arc-accretionary complex, which was active through most of the early Paleozoic (Şengör and Natal'In, 1996; Windley et al., 2007) (Fig. 5). The oldest rocks in the arc are early Cambrian ophiolitic rocks and bimodal volcanic rocks from northwest and central Chingiz, and they are interpreted to mark the initiation of the juvenile arc (Degtyarev, 2011). The establishment of the arc is further marked by the early–middle Cambrian appearance of differentiated volcanics displaying suprasubduction zone geochemical characteristics. In northwest and central Chingiz, island arc magmatism continued from the middle Cambrian to the middle Silurian, although the locus of magmatism jumped in the late Cambrian, and later began migrating southwest during the Middle Ordovician to Silurian (Levashova et al., 2009; Degtyarev, 2011). In the southeast of the Chingiz arc, magmatism may not have initiated until the Middle Ordovician (Choulet et al., 2012b). That the arc remained an intra-oceanic feature throughout its early Paleozoic development is evident by the consistently juvenile geochemical makeup of its arc magmatic rocks and the lack of continent-derived material in its early Paleozoic sedimentary rocks. Late Ordovician faunas from Chingiz, although presenting clear links to the Australasian region of Gondwana, also include genera distinct from those of the other Kazakh terranes (as well as Siberia and Baltica), reinforcing that Chingiz was somewhat isolated then (Popov and Cocks, 2017).

In northwest and central Chingiz, the southwest margin of the arc is bounded by the Maikan-Kyziltas (Esqembay-Balqybek) belt, which includes tectonically juxtaposed ophiolitic fragments, serpentinite melange and basalt-chert sequences of early Cambrian to Middle Ordovician age, together with flysch (Windley et al., 2007; Degtyarev, 2011). Possible continuations of that belt may occur in the southeast Chingiz where there are ophiolitic melanges bearing blocks of Cambrian to Late Ordovician mafic-ultramafic rocks, for example in the Chagantaolegai and Hongguleleng serpentinite melanges (Choulet et al., 2012b; Zhao and He, 2014). Alternatively, some of those melanges could frame the northern margin of the Chingiz belt (Chen et al., 2010). To the southwest of the Maikan-Kyziltas belt lies Ordovician volcanic and volcano-sedimentary complexes of the Baidaulet-Aqbastau belt that may have constituted an independent island arc (Windley et al., 2007; Degtyarev, 2011), or the second arc of a double arc system (together with the Chingiz arc) (Şengör and Natal'In, 1996). Cambrian–Ordovician calc-alkaline intrusive rocks are also recognized to the southeast, in the Mayila complex, and could represent a continuation of the Baidaulet-Aqbastau arc (Xu et al., 2012; Ren et al., 2014) (but see also section 4.5.2). Collision of the Baidaulet-Aqbastau and Chingiz arcs probably occurred in the Late Ordovician (Fig. 6; Table 1), when widespread conglomerates and olistostrome sequences were deposited in the Maikan-Kyziltas belt and in the southeast of the Chingiz arc (Degtyarev, 2011; Choulet et al., 2012b). Following collision of the Baidaulet-Aqbastau arc, arc magmatism continued in the Chingiz arc until the late Silurian, when volcanism waned and the region was characterized by the deposition of olistostromes and molasse and the intrusion of A-type granitoids (Levashova et al., 2009; Chen et al., 2010; Choulet et al., 2012b). Locally, late Silurian strata rest on older rocks above a prominent angular unconformity (Levashova et al., 2009). Arc magmatism resumed again in the Early Devonian to the south of the Chingiz arc, in the so-called 'Devonian arc' (Windley et al., 2007).

4.6. Tarim

4.6.1. North Tarim

Northern Tarim is separated from the Kyrgyz Middle Tianshan (MIT; section 4.5.1) and Chinese Central Tianshan (CCT; section 4.5.2) by the large South Tianshan complex, which is mainly comprised by Silurian, Devonian and Carboniferous metasediments (mostly marine and terrigenous clastic rocks, cherts and carbonates) (Safonova et al., 2016) (Fig. 5). Silurian–Devonian ophiolitic fragments and melange are found enclosed within that metasedimentary strata in both the north and the south of the South Tianshan, and in the north, along the Atbashy-Inylchek-South Nalati fault, the metasediments also host Devonian–Carboniferous HP/UHP metamorphic rocks (Jiang et al., 2014b; Klemd et al., 2015). It is broadly agreed that the South Tianshan is a mid-to-late Paleozoic accretionary complex that developed by consumption of the Tianshan Ocean that formerly separated the MIT/CCT and Tarim, but whether it was generated via north-dipping subduction beneath the MIT/CCT (Xiao et al., 2013), south-dipping subduction beneath Tarim (Charvet et al., 2011; Wang et al., 2011b), or both (Ge et al., 2014; Jiang et al., 2014b), is contentious. Accordingly controversial is the location and nature of the boundary between Tarim and the South Tianshan, which would only represent a true suture if subduction was north-dipping. Nevertheless, the North Tarim fault is recognized as an important first-order structure that broadly separates allocthonous rocks of the South Tianshan from para-autochthonous to autochthonous rocks of northern Tarim (Xiao

et al., 2013), and is commonly used, if non-genetically, to mark the boundary between them.

To the south of the North Tarim fault, the Paleozoic stratigraphy of the Tarim basin is well-characterized from well logs, seismic profiles and outcrops within basement uplifts. In the Kalpin and Bachu uplifts of northwest Tarim, thick and unmetamorphosed Neoproterozoic to late Paleozoic sedimentary sequences comprised predominantly by platform carbonates and fluvial to marine siliciclastic rocks rest unconformably upon Precambrian metamorphic basement (Carroll et al., 2001). Those sequences have conventionally been interpreted to reflect a long-lasting passive margin along the north margin of Tarim then (Bradley, 2008), but major unconformities occur in the Late Ordovician and Late Devonian (Carroll et al., 2001), and they are correlative with regional unconformities that can be traced across Tarim (Lin et al., 2012). The Late Ordovician unconformity in particular marks a prominent sedimentologic change from Cambrian–Middle Ordovician platform carbonates to exclusively siliciclastic deposits in the Silurian–Devonian. Paleocurrent indicators and clastic provenance analysis of Silurian–Devonian sandstones indicates that their sediment sources were recycled orogenic and volcanic provinces to the south and east (Carroll et al., 2001), where there were topographic highs at that time (Lin et al., 2012).

The case for mid-to-late Paleozoic south-dipping subduction beneath northern Tarim was first formulated from structural indications of northward vergence in high-grade metamorphic rocks and ophiolitic melange zones of the South Tianshan (Charvet et al., 2011; Wang et al., 2011b), but the significance of those observations and their relationship to the regional subduction polarity is debated (Xiao et al., 2013). However, there is a growing recognition of a belt of Silurian to mid-Devonian granitoids (~440–390 Ma) that stretch E–W across the southeast South Tianshan, and it now seems possible that belt comprises a magmatic arc that was situated above the north margin of Tarim (Huang et al., 2013a; Lin et al., 2013a; Ge et al., 2014; Jiang et al., 2014b). Presently, those granitoids are recognized to extend for ~500 km, from ~81°E to the western Kuruktag uplift. Notably, the Kuruktag uplift is regarded as a Precambrian basement block of Tarim (Shu et al., 2011; Zhang et al., 2013a), and thus the intrusion of Silurian to mid-Devonian arc-related granitoids there directly links that arc to the north margin of Tarim (Ge et al., 2014). The occurrence of a discontinuous belt of Silurian–Devonian ophiolitic melange in the south of the South Tianshan provides further support for the argument of south-dipping subduction (Jiang et al., 2014b). Although those melanges reside in allochthonous sheets, they are associated with a northward structural vergence and so cannot be derived from the ophiolitic belt along the north of the South Tianshan (Charvet et al., 2011; Wang et al., 2011b).

4.6.2. Southwest Tarim

The southwest margin of Tarim is flanked by the West Kunlun, which is divided by the Kudi suture into a northern belt (North West Kunlun; NWK) and a southern belt (South West Kunlun; SWK) (Fig. 5). The NWK is characterized by a Paleo-to-Neoproterozoic crystalline basement and Neoproterozoic metasedimentary rocks, unconformably overlain by Late Devonian-Carboniferous molasse, and it is considered to have comprised a coherent part of Tarim since the Neoproterozoic (Mattern and Schneider, 2000; Zhang et al., 2007a). In the Buya area in the southeast of the NWK, granites were intruded into the Proterozoic basement in the mid-Silurian (~430 Ma) (Ye et al., 2008). In contrast to the NWK, metamorphic basement rocks in the SWK that were previously assumed to be Paleo–Mesoproterozoic in age may rather be late Neoproterozoic to early Paleozoic (Zhang et al., 2007a). However, the occurrence of Mesoproterozoic detrital zircons in a paragneiss from the Kudi area suggests that older basement may be present (Xiao et al., 2005). In the early to mid-Paleozoic, the basement of the SWK was locally intruded by Cambrian granodiorites (~505 Ma), a large and terrane-parallel belt of Ordovician and early Silurian (~473–448 Ma and 435 Ma) high-K, calc-alkaline granitoids, and late Silurian–Early Devonian (~421–408 Ma) alkaline granites (Zhang et al., 2007a; Liao et al., 2010; Jia et al., 2013; Liu et al., 2014c). Late Ordovician-Silurian Ar–Ar ages from paragneisses of the metamorphic basement in the Kudi area are interpreted to date an episode of deformation that gave rise to ductile structures there (Xiao et al., 2002; Liao et al., 2010). Finally, those metamorphic basement rocks and early to mid-Paleozoic intrusive rocks were blanketed unconformably by molasse in the Late Devonian (Mattern and Schneider, 2000; Xiao et al., 2005).

The Kudi mafic-ultramafic complex, which presently forms a south-vergent klippe overthrust on the SWK, is recognized as a remnant of the former ocean basin that separated the NWK and SWK, together with volcanics and marbles to the north near the suture (Xiao et al., 2002). The volcanic sequence includes massive and pillowed basalts interbedded with cherts, intermediate volcanics, and volcaniclastic rocks, whereas the mafic-ultramafic complex to the south is comprised by layered harzburgite, dunite and gabbro situated above sheared serpentinite (Xiao et al., 2002; Liu et al., 2014c). The ultramafic-gabbroic rocks have yielded Cambrian ages (~526–510 Ma), and an imprecise Neoproterozoic Sm–Nd age (651 ± 53 Ma) (Liao et al., 2010; Liu et al., 2014c). From the volcanics near the suture to the north, a dacite yielded a late Cambrian age (~492 Ma) (Xiao et al., 2005; Liao et al., 2010; Liu et al., 2014c), and the associated marbles bear Cambrian–Ordovician crinoids (Xiao et al., 2002). Further age constraints are provided by Cambrian–Ordovician granitoids (~513–471 Ma) that invade the volcanic sequence and by Late Ordovician-Silurian radiolarian-bearing turbidites and cherts that overlie the volcanics (Xiao et al., 2002, 2005; Liu et al., 2014c).

Interpretations differ on the timing of the collision between the NWK and SWK, and the event has been variously assigned to the Early–Middle Ordovician (Xiao et al., 2005), Late Ordovician (Ye et al., 2008) and Silurian (Liu et al., 2014c), but the occurrence of the pre-Silurian early Paleozoic granitoids in the SWK establishes that subduction prior to the collision was southwest-dipping, beneath the SWK (Fig. 7; Table 1). The NWK (i.e. southwest Tarim) could thus have been passive prior to the arrival of the SWK, in which

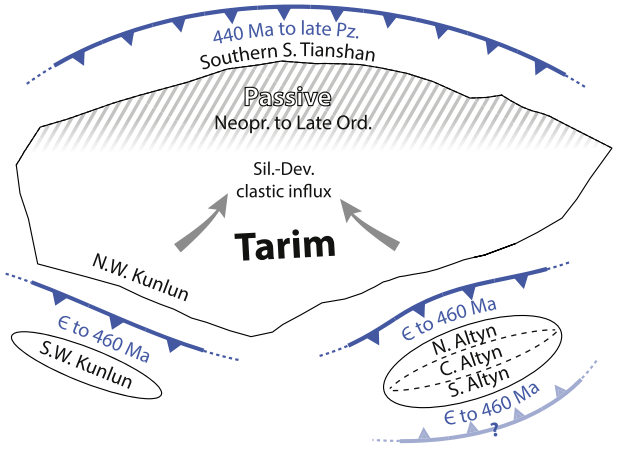

Figure 7. Schematic illustration of the principal interpretations from section 4.6, concerning the early Paleozoic tectonic boundaries of Tarim. Blue dates relate to the timing of convergent margins (Table 1).

case the Late Ordovician deformation of the NWK may register their collision. Indeed, following a stable Cambro–Ordovician interval characterized by the deposition of platform carbonates and basinal sediments, the entire southern half of Tarim was subjected to tectonism during the Middle–Late Ordovician, as evident by the development of thrusts, block uplifts, seismites and a regional unconformity (He et al., 2014, 2016; Liu et al., 2016b). Further support for a pre-Silurian collision comes from the geochemistry of Late Ordovician granitoids in the SWK, which Zhang et al. (2016b) classifies as early post-collisional products.

4.6.3. Southeast Tarim – Altyn orogen

Situated along the southeast margin of Tarim, bordered by the Dunhuang block (section 4.7) to the northeast and the Altyn Tagh fault to the southeast, the Altyn orogen is comprised by a central massif of Precambrian rocks—the Central Altyn block—flanked by two mobile belts: the North and South Altyn belts (Fig. 5).

The North Altyn belt borders the southern Dunhuang block and is mostly comprised by a mélange of Cambro–Ordovician volcano-sedimentary rocks, including basalts, tuffs, pelagic sediments, conodont-bearing chert, and carbonates, but also rare mafic and ultramafic intrusive rocks of presumed ophiolitic nature, an elongate lens of HP/LT metamorphic rocks, and voluminous granitoids (Zhang et al., 2017; Meng et al., 2017). Dating of HP eclogites and blueschists among the HP/LT rocks has yielded Cambro-Ordovician ages (Zhang et al., 2017), comparable to those of the ophiolitic rocks among the mélange (Gao et al., 2011), and the belt has thus been interpreted as a Cambro–Ordovician subduction-accretion complex. Correspondingly, subduction-related I-type granitoids of the belt have yielded late early Cambrian to Middle Ordovician ages, followed by the appearance of S-type granitoids in the Late Ordovician to Early Devonian (Liu et al., 2016a; Meng et al., 2017), which may reflect a change from active margin to a collisional or post-collisional environment.

To the south, across the Daban fault, the Central Altyn block is comprised by weakly metamorphosed Mesoproterozoic–Neoproterozoic metasedimentary and metavolcanic rocks that are intruded by Cambrian to early Silurian granitoids (Wu et al., 2009b; Liu et al., 2016a). To the south of those weakly metamorphosed Precambrian successions lie high-grade metamorphic rocks of the so-called 'Altyn complex' of the South Altyn belt (sometimes classified as part of the Central Altyn block) that also includes mafic-ultramafic rocks, granites and volcano-sedimentary rocks. The Altyn complex contains tonalitic-granodioritic gneisses, amphibolites and metasedimentary rocks, with lenses of eclogite, garnet peridotite, and mafic granulite. Dating of the granitic gneisses and metasedimentary rocks reveals that they formed from mostly Neoproterozoic protoliths that were strongly deformed in the mid-to-late Cambrian and Ordovician (Wang et al., 2013a). Accordingly, metamorphic ages derived from the HP-UHP rocks of the South Altyn reveal a mid-to-late Cambrian UHP eclogite-facies metamorphic event, followed by Ordovician retrograde granulite-facies metamorphism (Zhang et al., 2014a, 2015a). Among the Phanerozoic granitoids, crystallization ages span the Paleozoic—from late early Cambrian to the Permian—although distinct geochemical trends developed across that time, and magmatism peaked in the Middle Ordovician to Early Devonian (Liu et al., 2015a, 2016a). The earliest (late early Cambrian–Early Ordovician) granitoids are sparse, strongly deformed and present adakitic geochemical characteristics, whereas less-deformed Middle–Late Ordovician granitoids are more widespread and geochemically range from I- to S-type, and relatively undeformed Silurian to Devonian granitoids yield an A-type geochemistry (Kang et al., 2015; Liu et al., 2015a). Bimodal volcanic rocks also erupted in the Early Devonian, concurrent with the emplacement of A-type granites (Kang et al., 2015). Previously, the early Paleozoic mafic-ultramafic rocks of South Altyn, which include serpentinized dunite, harzburgite, gabbro and mafic volcanics, were all assumed to be ophiolitic fragments. However, the geochemistry of the Middle Ordovician to Silurian mafic-ultramafic rocks, together with the concurrent emplacement of S- and then A-type granitoids, rather suggests that the mafic-ultramafic successions are layered intrusions developed in a post-collisional extensional setting (Wang et al., 2014b); although pre-late Cambrian mafic-ultramafic rocks may still represent dismembered ophiolitic material (Liu et al., 2015a).

Owing to the very large displacements along the Altyn Tagh fault system, the lateral correlatives of the Altyn orogen are debated, but the rather different character and ages of the sequences in the North and South Altyn belts suggests that they may represent two distinct systems, as observed in the Qilian-Qaidam region to the east of the Altyn Tagh fault (section 4.8). However, the North Altyn belt—characterized by Cambro–Ordovician ophiolitic fragments, possibly subduction-related Cambrian to Middle Ordovician granitoids, and Late Ordovician to Devonian post-collisional intrusives—also resembles the sequence observed in the western Kunlun, and indeed the Middle–Late Ordovician tectonism observed across southern Tarim (section 4.6.2) is widely thought to be due to collision along the southeast of Tarim, in conjunction with the collision along its southwest (Lin et al., 2012; He et al., 2014, 2016) (Fig. 7; Table 1). The accompanying change in the style of magmatism in the South Altyn belt in the Middle Ordovician is consistent with a major collision at that time.

4.7. Beishan and Dunhuang

Beishan encompasses a wedge-shaped region situated between the southern terranes of Mongolia to the north (section 4.2), and the Dunhuang block, commonly presumed to be of Tarim affinity, to the south (Fig. 5). To the east, Beishan disappears beneath the Badain Jaran Desert of China and to the west it either merges with the Chinese Central Tianshan (section 4.5.2) or is tectonically juxtaposed against it along the Xingxingxia fault. The area is a complicated tectonic mosaic, comprised of E–W trending volcanic arcs, accretionary complexes, ophiolitic belts, and, controversially, blocks of Precambrian basement. Due to the intricacy of the region as well as the surge of recent investigations of it, the terrane concepts and subdivisions of Beishan are presently quite uncertain and prone to significant future modification. However, to facilitate the present discussion I here adopt the popular tectonic subdivisions of Xiao et al. (2010b) as a default working model. According to Xiao et al. (2010b), the constituents of Beishan can be recognized as a collage of Paleozoic arc-accretionary complexes that grew through a series of arc-arc and arc-continent collisions that continued through the Paleozoic. They recognized five principal units ('arcs'), from north to south: Queershan, Hanshan, Mazongshan, Shuangyingshan, and Shibanshan; each separated by a structural corridor decorated by ophiolitic mélange and interpreted as a suture.

The Queershan unit, according to Xiao et al. (2010b), comprises a series of Paleozoic volcanic arcs, characterized by differentiated volcanics and volcaniclastic rocks interbedded with turbidites and carbonates, stretching from the Ordovician to the Permian. Widespread and voluminous arc-related granitoids, which comprise large areas of the unit, were intruded in the Late Carboniferous to Permian. However, beyond being identified as an assemblage of Paleozoic arcs, the nature—whether continental or intra-oceanic—and affinity of the Queershan unit is unclear. To the west, possible correlatives include the Yemaquan and Dananhu arcs of the East Junggar region, both of which are reported to contain Ordovician to Carboniferous volcanic arc successions (Xiao et al., 2004; Long et al., 2012a). To the south, the Queershan unit is

bordered by ophiolitic rocks of the Hongshishan mélange, which comprises serpentinized ultramafic rocks, gabbros, diabase dikes, pillow basalts, cherts and limestones, juxtaposed against Carboniferous arc volcanic rocks (Xiao et al., 2010b). Sparse isotopic ages and fossils suggest that the Hongshishan ophiolite is Carboniferous-Permian in age, but precise constraints are lacking (Xiao et al., 2010b; Song et al., 2013a).

To the south of the Hongshishan ophiolite, the Hanshan unit has conventionally been considered a microcontinental fragment due to the widespread occurrence of high-grade gneisses and foliated granites of presumed Proterozoic age. However, modern dating efforts have largely revealed those crystalline rocks to be early–middle Paleozoic in age (Song et al., 2016). Clear examples of Proterozoic basement are recognized in the Alatage, Weiya and Xingxingxia areas of China, which probably constitute an extension of the Chinese Central Tianshan (He et al., 2015), but according to the Beishan terrane map of Xiao et al. (2010b), they are also correlative with the Hanshan unit. Others, however, have depicted an arbitrary boundary between the Xingxingxia area and the Hanshan unit (Liu et al., 2015b) or describe the Xingxingxia fault as the western boundary of Beishan; so the relationship between the Chinese Central Tianshan and Hanshan is not yet clear. At present, the oldest crystalline rocks identified in Hanshan to the east of the Xingxingxia region are Late Ordovician–Silurian granites and gneisses, preserved along its southern margin (Song et al., 2013b). To the south, the Hanshan unit is separated from the Mazongshan unit by the ophiolitic mélange-bearing Shibanjing-Xiaohuangshan belt. The ophiolites along this belt were previously thought to mark an ocean basin that closed in the early to middle Paleozoic according to the occurrence of Ordovician and Silurian fossils, but Zheng et al. (2013) have reported early Carboniferous crystallization ages (~345–336 Ma) from mafic rocks among the ophiolitic mélange.

In the Mazongshan unit, the age and nature of the oldest rocks is ill-defined. Metasedimentary sequences with Mesoproterozoic maximum depositional ages have been identified, but no Proterozoic crystalline rocks have been documented, and so the source of those Mesoproterozoic sediments—whether exotic (Song et al., 2016) or derived from yet unidentified local basement (Yu et al., 2016)—is unknown. The oldest crystalline rocks in Mazongshan are Cambrian and Early Ordovician gneisses and granites, but the intrusion of granites continued there from the Ordovician into the Devonian (Liu et al., 2015b; Song et al., 2015). Mazongshan also includes Ordovician–Silurian differentiated arc volcanics, volcaniclastic rocks, clastic sediments and carbonates (Ao et al., 2012; Song et al., 2015), and it is typically interpreted as an early Paleozoic intraoceanic arc (Xiao et al., 2010b). To the south, the mélange-decorated structural corridor separating Mazongshan from the Shuangyingshan unit contains the oldest ophiolitic material in Beishan, namely early Cambrian plagiogranites and gabbros, reported from the eastern Xichangjing and western Hongliuhe ophiolites (Ao et al., 2012; Tian et al., 2014; Cleven et al., 2015). However, Silurian to earliest Devonian crystallization ages have also been reported from gabbros and plagiogranites in the ophiolitic bodies along that mélange belt, reflecting a protracted Paleozoic history. In addition to the ophiolitic rocks, the corridor comprises deformed and metamorphosed Cambrian, Ordovician and Silurian clastic and pyroclastic rocks, Carboniferous to Permian clastic rocks and minor carbonates, and Permian basalts (Xiao et al., 2014). Estimates of the timing of emplacement of the ophiolites range from the Ordovician–Silurian (Ao et al., 2012) to Early Devonian (Cleven et al., 2015), or even the end-Permian (Tian et al., 2014). Despite that debated emplacement timing, it is broadly agreed that the bulk of the mélange belt developed in close association with an island arc, and the ophiolitic bodies probably initiated in a suprasubduction zone environment. Given that the northern margin of the Shuangyingshan unit to the south locally comprises a Cambrian to Silurian passive margin sequence (see below), the subduction system associated with that belt is commonly inferred to have been north-dipping, beneath the Mazongshan unit (Ao et al., 2012; Cleven et al., 2015). However, Tian et al. (2014) alternatively proposed that the belt represents a mid-to-late Paleozoic backarc basin. Given the otherwise contradictory age data, a composite history may in fact be most likely, wherein mid-to-late Paleozoic backarc development reactivated a former (early Paleozoic) subduction-collision system.

Definite Precambrian basement is known to occur in southern Beishan, as Neoproterozoic granitic gneisses have been documented in both the Gubaoquan area of the Shuangyingshan unit, and in the Baidunzi area of the Shibandun unit (Liu et al., 2015b; Yuan et al., 2015). Metasedimentary sequences with Mesoproterozoic maximum depositional ages have also been identified in the Shuangyingshan unit, but again a local (Beishan) source for those Mesoproterozoic sediments is so far unknown. The oldest Paleozoic rocks of the Shuangyingshan unit comprise Cambrian–Ordovician platform clastic rocks and carbonates, and are best exposed in the north (Ao et al., 2012). In the south, Paleozoic rocks are characterized by Ordovician to Carboniferous arc volcanic successions of calc-alkaline basalts, andesites, rhyolites, tuffs and volcaniclastic rocks interlayered with clastic sediments and carbonates (Mao et al., 2012a). Locally in southern Shuangyingshan, to the north of the Gubaoquan area, Ordovician eclogites occur (Liu et al., 2011a; Qu et al., 2011). Granitoids intruding the Shuangyingshan unit range in age from Silurian to Triassic (Liu et al., 2015b). In the structural corridor between the Shuangyingshan and Shibanshan units, intrusive rocks of the mafic-ultramafic Liuyuan complex have yielded Permian crystallization ages and are thrust imbricated with fossiliferous Permian sediments (Zhang et al., 2011; Mao et al., 2012b). Some have interpreted that complex as a Carboniferous–Permian backarc or post-collisional (intercontinental) basin, but the occurrence of Ordovician eclogites just to the north in the southern Shuangyingshan unit suggests the corridor had a longer tectonic history, and Mao et al. (2012b) proposed the Liuyuan complex may alternatively represent a relict forearc sliver.

In addition to locally exposed Neoproterozoic basement, the Shibanshan unit comprises high-grade metamorphic rocks of uncertain age, low greenschist-facies Devonian to Permian calc-alkaline volcanic rocks, volcaniclastic rocks, clastic sediments and carbonates, and abundant Carboniferous–Triassic granitic intrusions (Mao et al., 2012a,b). Xiao et al. (2010b) interpreted the Shibanshan unit as a continental margin arc constructed on the northern edge of the Dunhuang block, which has conventionally been presumed to comprise a Precambrian continental fragment dislocated from Tarim.

The Dunhuang block extends southeast to the Altyn Tagh fault and to the northwest it is bounded by the Qiemo-Xingxingxia fault. Proven Precambrian basement occurs as Archean-Paleoproterozoic tonalite-trondhjemite-granodiorite (TTG) gneisses and Paleoproterozoic amphibolites and mafic granulites in the south and east of the block, paralleling the bounding Altyn Tagh fault (Long et al., 2014; Zhao et al., 2015). In the Silurian to Early Devonian (~440–400 Ma), the Dunhuang block was subjected to an extensive tectono-thermal event associated with high-grade metamorphism and widespread granitoid plutonism, and that was followed by a second pulse of widespread granitoid plutonism in the Late Devonian–Carboniferous (Zong et al., 2012; Zhao et al., 2016). The mid-to-late Paleozoic products of those tectonothermal events are so pervasive in the Dunhuang block that Zhao et al. (2016) has questioned the concept of it as a cratonic block, suggesting that it may instead comprise a Paleozoic orogenic belt—perhaps representing a southward continuation of Beishan.

Due to the evident tectonic complexity of Beishan, these observations yield more questions than answers about the region's early Paleozoic paleogeographic evolution. Nevertheless, a few simple conclusions can be drawn (Table 1). Subduction was undoubtedly occurring along several of the domains of Beishan during the early Paleozoic, notably from the Ordovician onward. Although its affinity is not established, Xiao et al. (2010b) suggested that the Queershan unit could represent a segment of the south-facing early Paleozoic active margin of greater Siberia (central Mongolian terranes), which is consistent with the protracted arc-accretionary processes observed there. The location of the Queershan unit along that margin would also support a latest Paleozoic formation age for the Hongshishan mélange, due to final closure of the Paleoasian Ocean then (Domeier and Torsvik, 2014). The Dunhuang block and Shibanshan unit, in contrast to the other units of Beishan, are not associated with Ordovician subduction-related successions. However, volcanism appeared in the Shibanshan unit in the Devonian, and the Dunhuang block was marked by extensive metamorphism and magmatism in the Silurian–Early Devonian. Such an evolution is comparable to that of northern Tarim (section 4.6.1), where an early Paleozoic passive margin was perhaps supplanted by a north-facing active margin in the Silurian–Devonian. The affinity of the remaining units—Hanshan, Mazongshan and Shuangyingshan—remains an outstanding question. Although it is likely that they represented intraoceanic arc systems during the early to mid-Paleozoic, implied associations between the Hanshan unit and Chinese Central Tianshan and the occurrence of Mesoproterozoic sediments in the Mazongshan and Shuangyingshan unit (as well as Neoproterozoic gneisses in the latter) would suggest those units had earlier continental ties. In such case, they could collectively comprise a series of fringing arcs (or strike duplications of one) subjected to alternating and diachronous episodes of arc-backarc advance and retreat. However, given the present uncertainties in the nature, affinity, number, timing and polarity of subduction zones in Beishan, I did not attempt to incorporate the Hanshan, Mazongshan and Shuangyingshan units into the plate model; this presents an important area for future improvement.

4.8. Alashan, Qilian and Qaidam

Between the Altyn Tagh fault and Beishan to the northwest and the North China block to the east lie three Precambrian blocks—Alashan, Qilian and Qaidam—separated by two NW–SE trending mobile belts—the North Qilian belt and the North Qaidam belt (Fig. 5). To the west, the North Qilian and North Qaidam belts may continue into the Altyn orogen as the North and South Altyn (section 4.6.3), but are offset by ~400 km by the left-lateral Altyn Tagh fault; though this correlation is contested (Liu et al., 2012).

The Alashan block (also called the Alxa block) lies furthest to the northeast and is juxtaposed against the North China block, but the nature and timing of their amalgamation is unknown as neither a suture nor unambiguous evidence of subduction-related magmatism/metamorphism or collisional-deformation have been identified along their inferred boundary. Regarding the coherence of those blocks in the early to mid-Paleozoic, contradictory interpretations have been drawn from detrital zircon population comparisons (Hu et al., 2014a; Tang et al., 2014; Yuan and Yang, 2015a), paleomagnetic data (Huang et al., 1999a; Yuan and Yang, 2015b) and structural observations (Zhang et al., 2013b), of which none are definitive. Many of those studies were moreover conducted on rocks in the Helanshan, Niushoushan and Xiangshan regions, which are often assigned to westernmost North China or the North Qilian belt rather than Alashan (Liu et al., 2016d). Outside of those controversial regions, the Alashan block is comprised by early Precambrian crystalline basement, Neoproterozoic intrusive rocks and Late Carboniferous to Permian and younger cover. The Alashan block is therefore largely devoid of early Paleozoic rocks, excepting Late Ordovician–early Silurian diorites and granitoids and late Silurian–Devonian granites locally identified in the south of the block, and isolated exposures of Silurian diorite that have been reported from its east and northeast margins (Liu et al., 2016d; Zhou et al., 2016). Liu et al. (2016d) classified those Late Ordovician–Devonian magmatic rocks as arc-related and interpreted them as products of a south-dipping subduction system extending from the active north margin of North China (section 4.9.2) (Fig. 8; Table 1).

The North Qilian belt, which separates the Alashan block to the northeast from the Qilian block to the southwest, contains Neoproterozoic to early Paleozoic ophiolitic rocks, island-arc volcanic and plutonic rocks, HP metamorphic rocks, Silurian flysch and Devonian molasse, as well as younger sedimentary cover (Song et al., 2013c). The ophiolitic rocks, which variably include serpentinized peridotite, ultramafic-mafic cumulate rocks, massive gabbros and dolerites, sheeted dikes, massive and pillow basalts and sedimentary rocks including radiolarian chert, occur as nappes in two parallel, NW–SE trending belts. Zircons from gabbros in the northern belt have yielded latest Cambrian to Late Ordovician ages (~490–448 Ma), whereas gabbros from the southern belt have yielded distinctly older latest Neoproterozoic to late Cambrian ages (~550–496 Ma) (Song et al., 2013c). The northern ophiolite belt also differs from the southern one in that it contains a relative

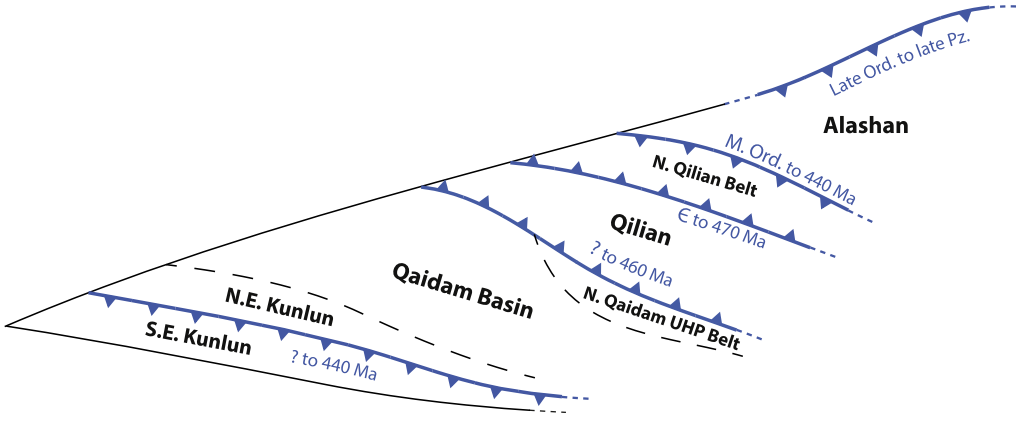

Figure 8. Schematic illustration of the principal interpretations from section 4.8, concerning the early Paleozoic tectonic boundaries of Alashan, Qilian and Qaidam. Blue dates relate to the timing of convergent margins (Table 1).

abundance of arc- and continent-derived rocks (Xia et al., 2012). Those ophiolitic belts are separated by a complex of arc volcanic rocks that includes Cambrian to earliest Ordovician (~517–487 Ma) tholeiitic to boninitic mafic rocks and late Cambrian to latest Ordovician (~494–445 Ma) dominantly felsic calc-alkaline volcanic rocks (Wang et al., 2005; Xia et al., 2012; Song et al., 2013c). Associated Cambrian–Late Ordovician felsic to mafic plutons (~520–450 Ma), inferred to be arc-related, occur in the arc volcanic complex but also intrude the ophiolitic rocks and the south margin of the North Qilian belt (Song et al., 2013c). Younger plutons of late Silurian–Devonian age occur to the north of the arc volcanic complex and are inferred to represent a phase of syn- to post-collisional magmatism, distinct from and post-dating the arc-related magmatism. Some of these late Silurian–Devonian intrusions appear to intrude into the southernmost margin of the Alashan block (Duan et al., 2015), which would imply that the North Qilian belt and Alashan block were united by that time.

Between the arc volcanic complex and the southern ophiolite belt of North Qilian, HP/LT metamorphic rocks occur in a dismembered, generally south-vergent belt that may represent the deep part of an accretionary wedge (Xiao et al., 2009; Zhang et al., 2012a). That metamorphic belt is comprised by blueschist- to eclogite-facies metamorphic blocks, ophiolitic slices and olistoliths enclosed by a blueschist- to eclogite-facies metasedimentary mélange (Zhang et al., 2012a; Song et al., 2013c). An Early Ordovician (~475 Ma) maximum depositional age for the mélange is provided by detrital zircons from the metasedimentary rocks (Zhang et al., 2012a). The Neoproterozoic–Cambrian protoliths of the HP rocks were subjected to eclogite-facies metamorphism in the Early–Middle Ordovician (~472–468 Ma), followed possibly by a younger metamorphic event in the late Silurian–Early Devonian (~421 Ma) (Song et al., 2006; Zhang et al., 2007b). Ar-Ar ages from the blueschists yield a comparable range of Ordovician–Early Devonian ages that are interpreted to date eclogite-facies retrogression following peak HP metamorphism in the Ordovician, and continued exhumation and cooling in the Silurian–Devonian (Song et al., 2013c). To the north of the arc volcanic complex lies a NW–SE trending belt of Silurian sedimentary rocks characterized by deposits of fine-grained siltstone and shale, but with coarser grained conglomerates and sandstones along the basin margins. Zircons from volcanic and granitoid clasts in those Silurian sedimentary rocks yield ages of ~515–429 Ma, indicating that the basin was substantially fed by the volcanic arc to its south. Together with the underlying ophiolitic rocks, the Silurian flysch was deformed and unconformably overlain by Early Devonian molasse and Late Devonian to Triassic platform-type strata (Xu et al., 2010).

To the southwest of the North Qilian belt, the Qilian block is comprised by Proterozoic high-grade metamorphic basement intruded by Neoproterozoic granites and early to mid-Paleozoic rocks, and unconformably covered by unmetamorphosed to low-grade Paleozoic–Mesozoic strata (Song et al., 2014; Huang et al., 2015a). Most of the studied early to mid-Paleozoic intrusive rocks are granitoids emplaced during the Late Ordovician to early Silurian (~460–440 Ma) (Huang et al., 2015a), although later Silurian-Devonian intrusives and intrusives of intermediate to mafic composition are also known (Yang et al., 2015; Tung et al., 2016). In the south of the Qilian block, the early Paleozoic sequence is reported to include marine sediments, arc volcanic and volcaniclastic rocks, and ophiolitic melange (Xiao et al., 2009; Song et al., 2014), and that region is sometimes treated as an independent block.

The North Qaidam UHP metamorphic belt separates the Qilian block to the northeast from the Qaidam block to the southwest and trends NW–SE, sub-parallel to the North Qilian belt. It is characterized by granitic gneisses that host blocks and lenses of metapelite, eclogite and garnet peridotite from which inclusions of coesite and diamond have been reported (Song et al., 2014). Early Paleozoic magmatic rocks have also been documented there and are broadly classified as Cambrian–Ordovician volcanic-plutonic complexes of island-arc affinity (Shi et al., 2006; Wu et al., 2009a) and syn- to post-collisional adakites and S-type granitoids of latest Ordovician to Devonian age (Yu et al., 2012; Huang et al., 2015a). Magmatic zircons from the metamorphic rocks reveal that the granitic gneisses were generated from Meso-Neoproterozoic protoliths, whereas the protoliths of the eclogites were basalts and ophiolitic rocks of Neoproterozoic (~870–750 Ma) and Cambrian (~540–500 Ma) age (Zhang et al., 2008, 2010; Song et al., 2014). Detrital zircons from the metapelites yield mostly Neoproterozoic ages, but also minor Paleoproterozoic and Mesoproterozoic age populations. Metamorphic zircon ages from those UHP rocks form a wide range between the late Cambrian and the Early Devonian, but mostly fall between ~460 Ma and 420 Ma (Mattinson et al., 2006; Zhang et al., 2008, 2010; Song et al., 2014). Zhang et al. (2010) interpreted that range of ages as a single UHP metamorphic event and suggested that the age range could be explained by slow subduction and/or by margin-parallel diachronism of continental subduction. Alternatively, observing that the HP-UHP metamorphic ages from the pelitic rocks form a more restricted range between ~440 Ma and 420 Ma compared with the eclogite ages that span the Ordovician and Silurian, Song et al. (2014) suggested that the earlier (Ordovician) eclogite ages reflect UHP metamorphism associated with oceanic subduction prior to the start of continental subduction in the Silurian.

Southwest of the North Qaidam UHP metamorphic belt lies the Mesozoic–Cenozoic Qaidam basin which is assumed to blanket Proterozoic crystalline basement of the Qaidam block that is everywhere concealed except along the North East Kunlun to the south (Song et al., 2014; Zhang et al., 2017). There, in the North East Kunlun, the basement is characterized by Proterozoic metamorphic rocks which are intruded by Neoproterozoic granitoids and covered by low-grade Ordovician-Silurian volcano-sedimentary strata and Late Devonian molasse (Xiong et al., 2014; Meng et al., 2015). In the west of the North East Kunlun, in the Qimantagh area, minor Cambrian to Ordovician magmatic rocks occur mostly as high-K calc-alkaline granitoids and possibly arc-related volcanics (Li et al., 2013; Wang et al., 2014b; Meng et al., 2015). More widespread granitoid magmatism occurred there in the Silurian and Devonian, but the affinity of those intrusives is ambiguous and they have been ascribed to a range of different settings (Chen et al., 2012; Meng et al., 2015).

To the south, the North East Kunlun is bordered by the South East Kunlun, which is comprised by Proterozoic basement covered by Ordovician–Silurian volcano-sedimentary strata and Late Devonian molasse, and intruded by Silurian–Devonian granitoids (Chen et al., 2012; Xiong et al., 2014). The North and South East Kunlun are divided by the Central East Kunlun fault, along which blocks of mafic-ultramafic rocks occur, and locally, in rocks associated with the North East Kunlun, granulites and eclogites (Zhang et al., 2017). The mafic-ultramafic rocks include peridotites, gabbros and mafic volcanic rocks and are inferred to represent ophiolitic fragments. Cambrian (~522–518 Ma) U–Pb zircon ages have been reported from gabbros of the Qingshuiquan complex (Meng et al., 2013). The timing of eclogite facies metamorphism of the HP metamorphic rocks is estimated to have occurred in the mid-Silurian (~428 Ma) and was followed by regional exhumation and cooling through the remainder of the Silurian and into the Devonian (Liu et al., 2005; Meng et al., 2013). However, peak metamorphism of the granulites has been determined as early–middle Cambrian, suggesting that the high-grade metamorphism of those rocks may reflect several metamorphic episodes (Meng et al., 2013).

The number of early Paleozoic subduction zones in the Alashan-Qilian-Qaidam region, as well as their affinity, duration and

polarity, are a matter of spirited debate that will certainly continue as new discoveries unfold. Given the distribution of HP and UHP metamorphic rocks, arc magmatic rocks, and ophiolitic belts as presently recognized, however, a general framework is emergent. HP and UHP metamorphic rocks in assemblages associated with the Qaidam block along both its north and south margins suggests that block entered both a north-dipping subduction zone to the north (below the Qilian block) and a south-dipping subduction zone to the south (below the South East Kunlun) as the lower plate (Fig. 8). While the timing of HP-UHP metamorphism along both of those margins remains unsettled (and possibly complicated by compound events), the prominence of Late Ordovician–early Silurian metamorphic ages, together with the widespread cessation of arc magmatism and the appearance of syn- to post-collisional plutonism at that time could suggest that subduction along both of those margins expired then (Table 1). The North Qilian belt, bearing HP metamorphic rocks and magmatic arc products was clearly the site of another subduction system, but based on the occurrence of two spatially and temporally distinct ophiolitic belts, I prefer the interpretation that it was the site of two successive subduction zones: an older, north-dipping subduction zone (beneath the south margin of the belt) was followed by instigation of a south-dipping subduction zone (below the north margin) (Fig. 8; Table 1). Cessation of the first subduction zone by collision with the Qilian block in the Early Ordovician could explain the occurrence of Early–Middle Ordovician HP metamorphism there, whereas the younger Silurian to Devonian metamorphic event could be attributed to the later closure of the northern basin and a collision with Alashan. The Ordovician–Silurian magmatic rocks in Alashan, in turn, could be related to another south-dipping subduction zone along the north of that block, as proposed by Liu et al. (2016d).

4.9. North China

4.9.1. Southern North China

The North and South China blocks are separated by the composite Qinling-Tongbai-Dabie-Sulu orogenic belt (Fig. 9), which chronicles a long-history of Paleozoic convergence that finally ended with the collision of North and South China in the Triassic. Relics of Paleozoic subduction and orogenesis are scarce to absent in the Dabie-Sulu, but are well-exposed in the Qinling-Tongbai. There, the North and South China blocks are separated by the North and South Qinling belts, which are in turn separated by the ophiolite-decorated Shangdan fault. The North Qinling is further subdivided into several WNW–ESE trending complexes—from north to south: the Kuanping complex, Erlangping complex, North Qinling complex and Shangdan ophiolite complex—and is bounded by the southern North China block to the north along the Luonan-Luanchuan fault, and by the Shangdan fault to the south. To the north of the Luonan-Luanchuan fault, the southern North China block is characterized by Archean to Proterozoic metamorphic basement unconformably overlain by Proterozoic to early Paleozoic strata, including Neoproterozoic to Ordovician platform carbonate

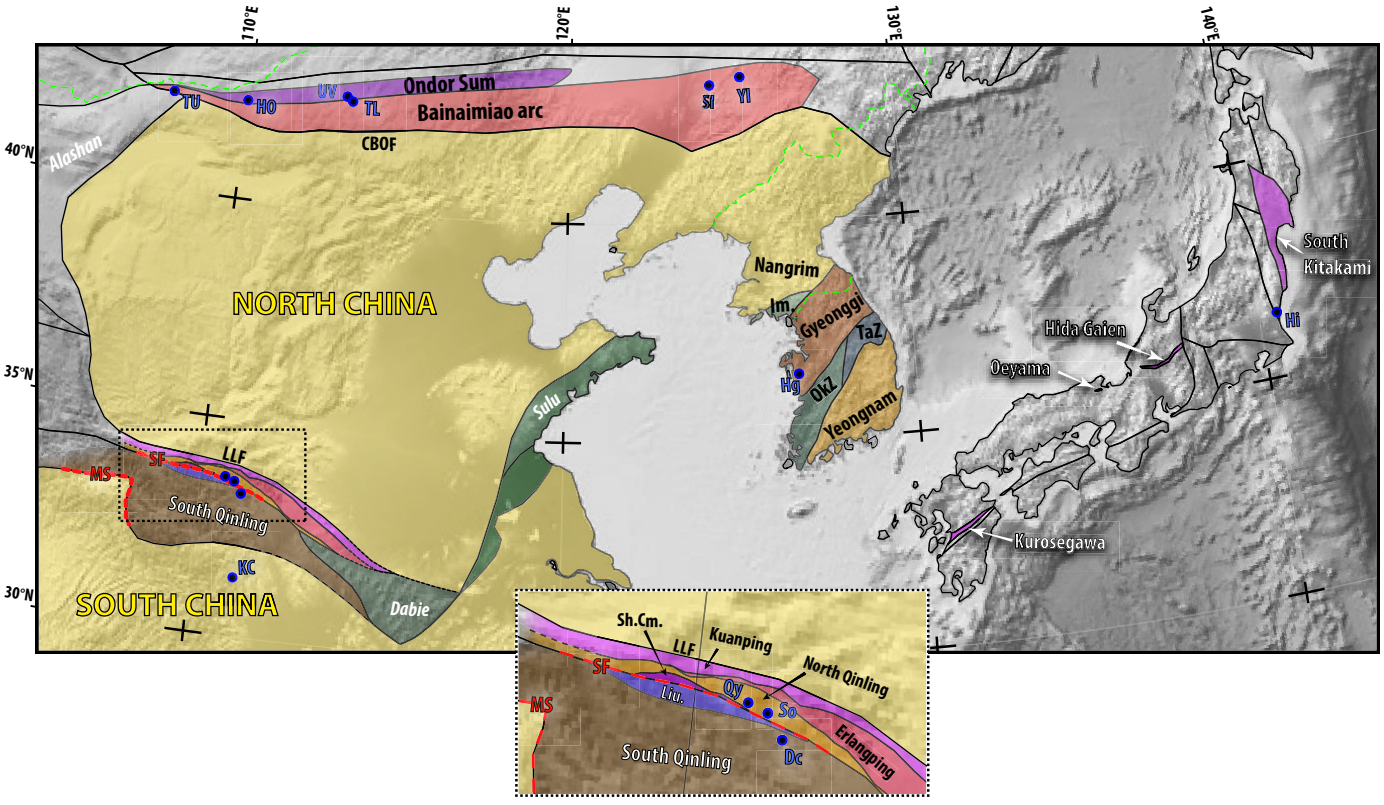

Figure 9. Overview map of North China (section 4.9), the Korean Peninsula (section 4.10), northern South China (section 4.11), and Japan (section 4.12); inset shows an enlargement of the southern margin of North China (dashed area). Polygon colors depict generalized tectonic environment classifications: yellow, North and South China cratons; brown shades, continental terranes/fragments; green shades, marginal mobile belts and HP-UHP terranes; blue shades, sedimentary basins; red shades, continental/oceanic magmatic arcs; purple shades, oceanic/accretionary complexes. Terrane abbreviations: Im., Imjingang belt; Liu., Liuling Group and Wuguan complex; OkZ, Okcheon zone; Sh. Cm., Shangdan ophiolite complex; TaZ, Taebaeskan zone. Dashed red lines denote important boundaries discussed in the text: MS, Mianlue suture zone; SH, Shangdan fault. Dashed green lines delineate modern political boundaries for reference. Blue circles denote areas discussed in the text: Dc, Duoling complex; Hg, Hongseong area; Hi, Hitachi area; HO, Hongqi area; KC, Kongling complex; Qy, Qingyouhe area; SI, Siping area; So, Songshugou area; TL, Tulinkai area; TU, Tugurige area, UV, Ulan Valley; YI, Yitong area. Other abbreviations: CBOF, Chifeng-Bayan Obo fault; LLF, Luonan-Luanchuan fault.

and clastic rocks (Wu and Zheng, 2013). Silurian and Devonian strata are absent from the southern North China block, and the early Paleozoic platform sequence is unconformably overlain by Carboniferous and Permian strata (Wu and Zheng, 2013).

South of the Luonan-Luanchuan fault, the Kuanping complex is comprised by greenschist to amphibolite-facies metabasaltic and metasedimentary rocks that are demonstrated to have Precambrian to early Paleozoic protoliths (Dong et al., 2011a; Wu and Zheng, 2013). Early–Middle Ordovician fossils and detrital zircons have been reported from the metasedimentary rocks, placing a maximum depositional age on the youngest strata (Cao et al., 2016). Sedimentologic and biostratigraphic observations from the least deformed metasedimentary units have indicated that the protoliths of those rocks were likely Neoproterozoic to early Paleozoic continental shelf and slope sediments (Wu and Zheng, 2013), although they have also been interpreted as remnants of an accretionary wedge (Bader et al., 2013; Cao et al., 2016) or a composite unit including a Meso-Neoproterozoic ophiolite (Dong and Santosh, 2016). Regional metamorphism of those rocks occurred in the early Silurian (~440–435 Ma), in conjunction with Silurian plutonism (Liu et al., 2011b). The metamorphic and plutonic rocks of the Kuanping complex are unconformably overlain by mid-Carboniferous to Permian strata in common with the southern North China block (Wu and Zheng, 2013).

The Erlangping complex to the south of the Kuanping complex is also characterized by greenschist to amphibolite-facies metaigneous and metasedimentary rocks, but perhaps exclusively of early Paleozoic age. Those rocks (or their protoliths) include ultramafic rocks, gabbro, diorite, massive and pillowed basalts, sheeted dikes, intermediate to felsic volcanics, fine-grained clastic rocks, radiolarian chert and carbonate rocks, that together may represent a dismembered ophiolitic sequence (Dong et al., 2011a; Bader et al., 2013). The cherts contain early Paleozoic fossils including radiolarians as young as Middle Ordovician (Dong and Santosh, 2016), or possibly Silurian (Wu and Zheng, 2013). Magmatism in the Erlangping complex spanned the late Cambrian to Early Devonian but became more voluminous after a brief hiatus in the mid-Ordovician (Wu and Zheng, 2013; Wang et al., 2013e). The tectonic affinity and compositional trends of that magmatism remain poorly characterized and controversial, but mafic magmatism appears to have been more prominent in the Ordovician, whereas in the Silurian it was more bimodal to dominantly felsic (Bader et al., 2013; Wang et al., 2013d), and notably included the intrusion of S-type granitoids (Dong and Santosh, 2016). Regional metamorphism of the Erlangping complex occurred in the early to mid-Silurian (~440–430 Ma), coeval with the metamorphism of the Kuanping complex (Liu et al., 2011b).

South of the Erlangping complex, the North Qinling complex is comprised by gneisses, mafic and felsic granulites, amphibolites, marbles, metapelites and granitoids. Important contributions to the metamorphic basement of the North Qinling occurred in the Meso-Neoproterozoic, but the occurrence of Paleoproterozoic and Archean detrital zircons in gneisses from that basement hints at the possible presence of older components there (Wu and Zheng, 2013). Medium-pressure granulite-facies metamorphism of the North Qinling complex occurred at ~440–420 Ma, and was associated with essentially coeval migmatization and intensified granitoid plutonism (~450–420 Ma) (Wu and Zheng, 2013; Wang et al., 2013e; Liu et al., 2014b). Although granitoid plutonism peaked in the Late Ordovician to mid-Silurian, magmatism in the North Qinling spanned from the Cambrian to the Early Devonian (Dong et al., 2011a; Wu and Zheng, 2013). The early expressions of that magmatism were mostly subduction-related gabbroic and granitic intrusions, which continued to be dominant from the late Cambrian to the Silurian, when S-type granitoids appeared (Dong and Santosh, 2016), although some late Cambrian granitoids have also been interpreted as products of crustal anatexis driven by orogenesis (Liu et al., 2016c). In the north of the North Qinling, eclogites occur as lenses or blocks in orthogneiss, paragneiss and schist, and coesite and diamond inclusions in zircon are reported both from the eclogites and their host rocks (Wang et al., 2013c). The eclogites were formed from mid-Neoproterozoic protoliths, possibly continental basalts, and were subjected to (U)HP metamorphism at ~490–485 Ma (Wu and Zheng, 2013; Wang et al., 2013c). (U)HP metamorphic rocks have also been documented in the south of the North Qinling. In the Qingyouhe area, Wang et al. (2014c) found a diamond inclusion in zircon from an amphibolite and inferred the associated ~490 U–Pb zircon age to date UHP metamorphism there. In the Songshugou area, HP granulites are estimated to have experienced peak HP metamorphism in the late Cambrian to Early Ordovician and are spatially associated with Neoproterozoic–Cambrian mafic-ultramafic rocks that probably comprise either a dismembered ophiolite or the off-scraped oceanic rocks of an accretionary complex (Bader et al., 2013; Li et al., 2014).

The south margin of the North Qinling complex is juxtaposed with the Shangdan ophiolitic complex (or Danfeng complex) which is recognized as an ophiolitic melange comprised by greenschist to amphibolite-facies ultramafic rocks, gabbros, basalts, diabase dikes, intermediate to acidic intrusions, pillow lavas and radiolarian cherts (Dong et al., 2011a). Cambrian–Ordovician (or Silurian?) radiolarian fossils in the cherts together with ~534–457 Ma zircon U-Pb ages from the gabbros establish a Cambrian-Ordovician age for those ophiolitic rocks (Dong et al., 2011a), although the intermediate intrusions are younger (~455–402 Ma) (Bader et al., 2013). The Shangdan ophiolitic complex is commonly interpreted as the suture zone between the North and South Qinling, with the Shangdan fault to the south of the ophiolite being taken as the discrete terrane boundary. However, immediately south of the Shangdan fault is a zone of intensively deformed thrust slices of low-grade metamorphosed sandstone, conglomerate, volcaniclastic rock and limestone that Dong et al. (2013) have collectively interpreted as a forearc accretionary prism developed along the southern active margin of the North Qinling. The composition of those clastic rocks indicates they were derived from a continental arc, and the detrital zircon population—which is dominated by Cambrian to Middle–Late Ordovician ages—implies that source was the North Qinling as Cambro-Ordovician magmatic rocks are unknown from the South Qinling (Dong et al., 2013). Thus, the terrane boundary between the North and South Qinling may lie slightly further south than the Shangdan fault, to the south of those forearc rocks, which furthermore suggest that the 'Shangdan Ocean' was still open when they were deposited. The age of deposition of those rocks, however, is a matter of continuing debate. According to Dong et al. (2013) their deposition occurred in the Late Ordovician to early Silurian based on the occurrence of ~455 Ma detrital zircons among clastic rocks in the west of the unit, and a ~435 Ma diabase dike that intrudes those strata. On the other hand, Yan et al. (2016) reported Late Devonian-earliest Carboniferous detrital zircons from metasedimentary rocks in the east of what was presumed to be the same unit (Wuguan complex) as well as intercalated earliest Carboniferous volcanics, and estimated its deposition age as Late Devonian to mid-Carboniferous.

Directly south of the Wuguan complex, and perhaps locally disconformably overlying part of it, is a thick succession of turbidites (Liuling Group) that is similarly critical to determining the age of Shangdan Ocean closure, but equally controversial. The age of the turbidites has been estimated as Middle to Late Devonian based on fossils, detrital zircons and from cross-cutting intrusions (Dong et al., 2013; Shi, 2016; Liao et al., 2017), but this presents a

stratigraphic problem if the Wuguan complex that they apparently locally overlie is indeed Late Devonian to mid-Carboniferous in age. Concerning their nature and provenance, the Liuling Group turbidites have been alternatively interpreted as an accretionary complex sourced only by sediments from the North Qinling—thereby implying the Shangdan Ocean remained open during their deposition as with the Wuguan complex (Yan et al., 2016)—or as a foreland basin sourced by sediments from both the North and South Qinling—indicating that the Shangdan Ocean was narrow or closed by the time of their deposition (Dong and Santosh, 2016). Thus, closure of the Shangdan Ocean can only presently be loosely constrained between the Silurian and the mid-Carboniferous. Nevertheless, it is clear that closure of that basin occurred by northward-dipping subduction given that early to mid-Paleozoic arc-related intrusions appear exclusively to the north of the South Qinling complex (section 4.11.2) (Wu and Zheng, 2013).

Distilling all the observations from this section: in contrast to the apparent passivity of southern North China (and of northwest South China; section 4.11.2) during the early Paleozoic, the North Qinling was undoubtedly associated with subduction-related magmatism from at least the late Cambrian to the Silurian, and it is interpreted to have comprised an independent terrane for much of that time. The occurrence of latest Cambrian–Early Ordovician eclogites on both the north and south margins of the North Qinling complex could suggest that subduction beneath it had commenced by that time, but the character of both the eclogites and their hosts rather suggest it was continental crust of the North Qinling itself which was partially subducted (Liu et al., 2016c). Due to the contemporaneous age of the (U)HP metamorphism along both margins, it has been proposed that the entire North Qinling complex was partially subducted, but this appears unlikely given that some pre-Early Ordovician intrusives from the complex exhibit typical igneous structures and otherwise lack evidence of having experienced such metamorphic conditions (Dong and Santosh, 2016; Liu et al., 2016c). Alternatively, the apparently contemporaneous timing of (U)HP metamorphism along both margins could be coincidental, and the North Qinling could have been caught between two opposed subduction zones in the middle to late Cambrian (Fig. 10). In any case, by the Early Ordovician the North Qinling was clearly situated above at least one subduction zone based on the arc magmatism that had appeared there then, but given that Cambrian–Ordovician (possibly Silurian) ophiolites flank the North Qinling on both sides, it was most likely lined by active margins both in the north and south. In the north, closure of the Erlangping basin probably occurred in the latest Ordovician to earliest Silurian, when regional metamorphism and S-type granitoid magmatism affected the Erlangping and Kuanping complexes, and the passive margin sequence of southern North China was interrupted (Fig. 10; Table 1). In the south, closure of the Shangdan basin could have also occurred in the Silurian or Devonian, but from the presently available evidence I favor the interpretation that it remained open until the mid-Carboniferous (Yan et al., 2016).

4.9.2. Northern North China

The northern boundary of the Precambrian North China craton is often taken as the Chifeng-Bayan Obo fault (Xiao et al., 2003; Zhang et al., 2014b) (Fig. 9). To the south of that fault, the craton is characterized by an Archean–Paleoproterozoic metamorphic basement unconformably overlain by a thick sequence of undeformed Proterozoic to early Paleozoic strata (Zhang et al., 2014b). The youngest rocks of the early Paleozoic sequence comprise Cambrian to Middle Ordovician marine clastic rocks and platform carbonates. In turn, those early Paleozoic rocks are unconformably overlain by Late Carboniferous and younger strata, marking a Late

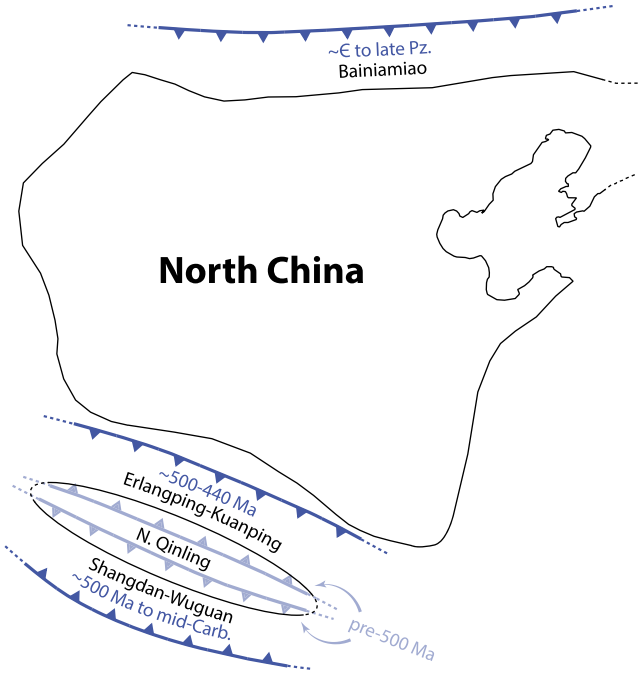

Figure 10. Schematic illustration of the principal interpretations from section 4.9, concerning the early Paleozoic tectonic boundaries of North China. Blue dates relate to the timing of convergent margins (Table 1).

Ordovician to Early Carboniferous depositional hiatus that was craton-wide (Cocks and Torsvik, 2013).

To the north of the Chifeng-Bayan Obo fault, the so-called Bainaimiao arc stretches from the Tugurige area in the west (~108°E) to the Siping-Yitong area in the east (~125°E), and consists mainly of greenschist to low amphibolite facies metasedimentary rocks, mafic to intermediate volcanic rocks, minor felsic lavas, volcaniclastic rocks, minor gabbros, diorites and granitoids (Xu et al., 2013; Zhang et al., 2014b). Those arc rocks are unconformably overlain by conglomerates, shallow marine clastic rocks and carbonates of late Silurian–Devonian age (Xu et al., 2013). The occurrence of ~460 Ma detrital zircons in the metasedimentary rocks of the arc indicates that they were derived from protoliths with depositional ages no older than Middle-Late Ordovician (Zhang et al., 2014b). Subsequent regional metamorphism of those rocks must have occurred prior to the deposition of the unmetamorphosed late Silurian cover and emplacement of an undeformed ~411 Ma pegmatite, but after emplacement of a meta-tuff and meta-diorite with emplacement ages of ~440 Ma and ~438 Ma, respectively (Zhang et al., 2013c, 2014b). The magmatic rocks are mostly calc-alkaline in composition, yield Ordovician to Silurian ages (~485–420 Ma), and are inferred to be subduction-related (Xu et al., 2013; Zhang et al., 2014b), but the precise duration and nature of magmatism there is not yet well-defined. Although no outcrops of Precambrian rock are recognized in the Bainiamiao arc, it has been surmised that a Precambrian basement may underlie the arc according to the isotopic composition of some of the magmatic rocks and the occurrence of Meso–Neoproterozoic detrital zircons in the metasedimentary rocks there (Xiao et al., 2003; Zhang et al., 2014b).

To the north, the Bainaimiao arc is juxtaposed against the Ondor Sum complex, which comprises ophiolitic rocks, arc volcanic rocks and mélange bearing blueschists and is commonly interpreted as a subduction-accretion complex (Xiao et al., 2003). In the Ulan Valley, where part of the complex is well-exposed, ophiolitic and calc-

alkaline volcanic rocks comprise the structural base of a north-dipping thrust stack. The ophiolitic rocks include pillow basalts, meta-gabbro, limestone and chert hosting late Precambrian to Cambrian fossils (De Jong et al., 2006). Those volcanic-sedimentary rocks are structurally overlain by pervasively deformed schists and mylonites with meta-basaltic lenses metamorphosed to greenschist or blueschist facies (De Jong et al., 2006; Shi et al., 2013). De Jong et al. (2006) estimated the timing of high-pressure metamorphism of those rocks to have occurred at ~450 Ma from Ar-Ar ages on phengite from the blueschist-facies quartzite mylonites, but glaucophane Ar-Ar ages of ~446 Ma and ~426 Ma have also been reported from the blueschists (Xiao et al., 2003). Stratigraphically, a minimum age for the high-pressure metamorphism and exhumation of the subduction-accretion complex is provided in the central Ondor Sum area, where the ophiolitic and high-pressure rocks are unconformably overlain by late Silurian–Early Devonian clastic rocks and carbonates (Xiao et al., 2003; Xu et al., 2013). Structurally, the Ondor Sum region is characterized by an NE–SW trending antiform, and thus the north dip of the thrust stack in the Ulan Valley is only a local attitude (Shi et al., 2013). Furthermore, formation of that antiform evidently post-dates the deposition of Carboniferous limestones in the Ondor Sum area, as they are likewise tilted. The antiform likely developed in the Permian–Triassic, when south-vergent thrusting grossly overprinted the structural grain of the region on a crustal scale (Zhang et al., 2014c). Consequently, the deduction of north-dipping subduction according to the apparent south-vergence of the Ondor Sum complex is probably not valid (Xiao et al., 2003). From a microstructural analysis, Shi et al. (2013) determined that syn-metamorphic deformation of the Ondor Sum complex was rather associated with a northwest structural vergence. To the west of the Ondor Sum area, possibly correlative greenschist-facies mélange belts with blocks of mafic-ultramafic rock and micaschist appear in the Hongqi and Tugurige areas, adjacent to Bainaimiao arc rocks (Shi et al., 2013; Xu et al., 2013). The Hongqi mélange includes ~485 Ma acidic volcanics, tuffaceous rock with Early to Middle Ordovician graptolites and microstructures indicating that syn-metamorphic deformation was associated with a northwest structural vergence (Shi et al., 2013).

Another notable exposure associated with the Ondor Sum complex occurs at Tulinkai, to the southeast of the Ulan Valley. There, a large, E–W elongate mafic body comprised predominantly of foliated amphibolite, diorite and gabbro overlies a base of serpentinized harzburgite-dunite of disputed nature (Jian et al., 2008; Shi et al., 2013). Felsic bodies with boninitic to adakitic geochemical affinities are abundant within the Tulinkai unit and alternatively cross-cut or conform to the host foliation. Crystallization ages from gabbros and tonalite genetically associated with the mafic rocks span the late Cambrian to Middle Ordovician (~490–457 Ma), whereas the felsic rocks range from the Early Ordovician to the mid-Silurian (~472–425 Ma) (Jian et al., 2008; Shi et al., 2013). Metamorphic zircons and metamorphic overgrowths on zircons from both the mafic rocks and the older (Ordovician) population of felsic rocks yield Late Ordovician-early Silurian metamorphic ages (~450–438 Ma) (Jian et al., 2008). Structurally, the Tulunkai unit overlies the Ondor Sum mélange, separated from it by a north-vergent thrust (Shi et al., 2013). In part according to whether the reported serpentinized harzburgite-dunite occurrence at the base of the Tulinkai unit is upheld, the unit could represent a supra-subduction zone ophiolite marking the initial stages of subduction initiation (Jian et al., 2008), or rather the basement of the Bainiamiao arc (Shi et al., 2013). In either case, the ~490 Ma tonalite from that unit indicates that subduction along the north margin of North China possibly initiated prior to the Early Ordovician.

Given the spatial relationship of the early Paleozoic arc and accretionary complex, together with structural indications from the latter, the polarity of that early Paleozoic subduction is interpreted to have been south-dipping, or directed beneath the north margin of the North China block (Fig. 10; Table 1). According to the age of the arc and ophiolitic rocks, subduction initiated at least by the late Cambrian and continued through the Ordovician and perhaps into the Silurian. However, the early to mid-Silurian deformation and metamorphism of the arc and concurrent exhumation of the fore-arc accretionary complex marked a significant change to the relative kinematics along that active margin. There is no evidence of an outboard collision at that time, but if the Bainaimiao arc was originally detached from the North China block by a marginal backarc that event could reflect collapse of the backarc and collision between the marginal arc and craton. Support for that is provided by seismic data which show northward-dipping structures in the middle and lower crust beneath the Bainaimiao arc that are interpreted to reflect southward thrusting of the arc onto the North China block (or conversely, northward underthrusting of North China beneath the arc) (Jian et al., 2016). Speculatively, that scenario could have been driven by advance of the trench due to subduction of progressively younger, hotter lithosphere, ultimately ending with ridge-subduction, slab detachment, cessation of subduction and regional uplift (Jian et al., 2016). Yet, if subduction terminated in the Silurian, its cessation was short-lived because subduction-related magmatism reappeared in northern North China by the Early Carboniferous, with indirect evidence suggesting that it perhaps re-initiated already in the Devonian (Domeier and Torsvik, 2014). It is therefore possible that convergence never actually ceased along the northern margin of North China in the mid-Paleozoic, but rather that convergence was briefly accommodated mostly by marginal shortening rather than subduction during the Silurian.

4.10. Korean peninsula

The treatment of Korea here is somewhat unique, because although it is widely agreed that the Precambrian blocks and Paleozoic mobile belts that today comprise the Korean peninsula were already components of the North and South China blocks prior to their Triassic collision, the details of their individual affinities (i.e. which parts of Korea correspond to which block of China) remain controversial. Korea comprises three Precambrian massifs—from north to south, the Nangrim, Gyeonggi and Yeongnam massifs—separated by Paleozoic–Mesozoic mobile belts and partly overlain by younger basins (Fig. 9). In the north, the Nangrim and Gyeonggi massifs are separated by the Imjingang belt, a fold-thrust belt comprised by late Paleozoic meta-sedimentary rocks that were deformed and metamorphosed in the Permo-Triassic, locally up to granulite facies (Kwon et al., 2009). In the south, the Gyeonggi and Yeongnam massifs are separated by the NE–SW trending Okcheon belt, which is commonly subdivided into the southwestern Okcheon zone and the northeastern Taebaeskan zone. The Okcheon zone is comprised of Neoproterozoic to Paleozoic metavolcanic and metasedimentary rocks that were variably metamorphosed up to amphibolite-facies, whereas the Taebaeskan zone contains weakly to non-metamorphosed Cambrian–Ordovician carbonates and siliciclastic rocks unconformably overlain by late Paleozoic sediments (Cho et al., 2013). Along the western margin of the Gyeonggi massif between those mobile belts, in the Hongseong area, Ordovician to Devonian metamorphic and metavolcanic rocks have been identified and interpreted to mark the occurrence of both subduction-related arc magmatism in the Ordovician and Silurian, and a Silurian–Devonian episode of high-grade metamorphism (Oh et al., 2014; Kim et al., 2015). However, the tectonic affinity and

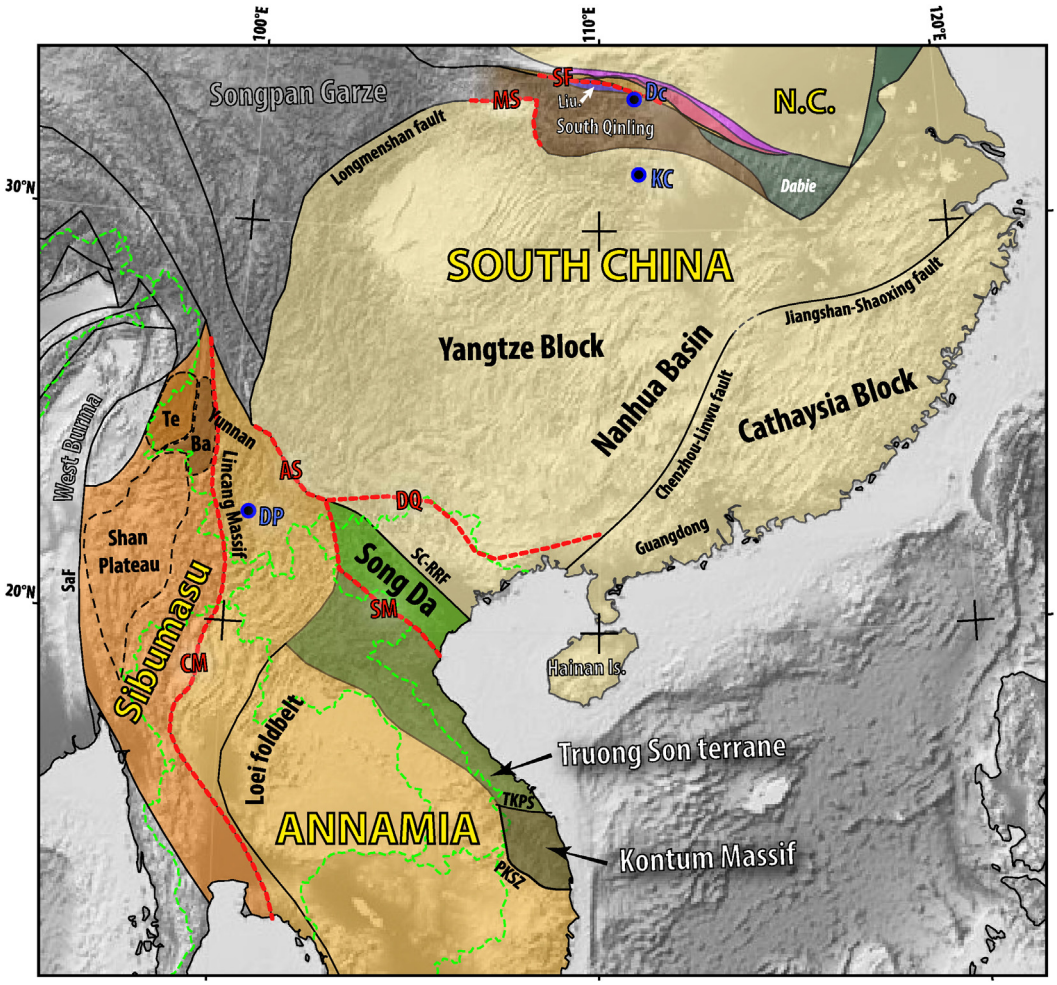

Figure 11. Overview map of South China (section 4.11), Annamia (section 4.13) and Sibumasu (section 4.14). Polygon colors depict generalized tectonic environment classifications: yellow, North and South China cratons; orange shades, Annamia and Sibumasu terranes; brown shades, microcontinental terranes/fragments; green shades, marginal metamorphic and mobile belts; blue shades, sedimentary basins; red shades, continental/oceanic magmatic arcs; purple shades, oceanic/accretionary complexes. Terrane abbreviations: Ba, Baoshan block; Liu., Liuling Group and Wuguan complex; Te, Tengchong block. Dashed red lines denote important boundaries discussed in the text: AS, Ailaoshan suture; CM, Changning-Menglian-Chiang Mai belt; DQ, Dian-Qiong suture; MS, Mianlue suture zone; SH, Shangdan fault; SM, Song Ma suture. Dashed green lines delineate modern political boundaries for reference. Blue circles denote areas discussed in the text: Dc, Duoling complex; DP, Dapingzhang; KC, Kongling complex. Other abbreviations: PKSZ, Po Ko shear zone; SaF, Sagaing fault; SC-RRF, Song Chay and Red River fault systems; TKPS, Tam Ky-Phuoc Son shear zone.

orientation of the Ordovician–Silurian active margin that generated those rocks is unclear. The discovery of Permo-Triassic eclogites in the Hongseong area has led to a proposal that the Triassic collisional orogen between North and South China (the Dabie-Sulu belt) continues into the Korean Peninsula through the Hongseong area, which could suggest that the Yeongnam and Gyeonggi massifs (southeast of the Hongseong area) are of South China affinity (Oh, 2006; Kwon et al., 2009). However, the continuation of the Dabie-Sulu belt into the Korean Peninsula remains controversial, and alternative proposals have placed it both further southeast, within the Okcheon belt, and further northwest, along the Imjingang belt, or outside of the Korean Peninsula altogether (Oh, 2006; Chang and Zhao, 2012). Obviously, the locations of the first-order terrane boundaries and the tectonic affinities of the various blocks of Korea need to be resolved before the rocks of the Hongseong area can be placed in their proper tectonic context.

4.11. South China

4.11.1. Central and southeastern South China

The South China block occupies most of present-day southeast China, and is bounded by the Qinling-Dabie-Sulu orogen to the north (where it borders North China; section 4.9.1), the Longmenshan fault to the northwest (where it meets Songpan-Garze), and the Ailaoshan-Song Ma fault to the southwest (where it borders Annamia; section 4.13) (Figs. 9 and 11). The terrane is comprised by two Precambrian cratons—the northwestern Yangtze block and the southeastern Cathaysia block—that first assembled together in the early Neoproterozoic, forming the Jiangnan orogen, but continued moving relative to one another, episodically, until the late Paleozoic. In the mid-Neoproterozoic, a phase of rifting between the cratons resulted in the formation of the regional Nanhua rift basin, but ultimately rifting ceased before true continental break-up. Subsequently, in the middle Paleozoic, Cathaysia and southeastern Yangtze were subjected to tectonism and magmatism during the so-called Kwangsian (or Wuyi-Yunkai) orogeny, which is attributed to continued relative motion between those cratons—perhaps collapse of the Nanhua basin—but is otherwise poorly understood. In the northeast of South China, the Jiangshan-Shaoxing fault is usually assumed to delineate the suture between those cratons, but the southwestern continuation of that suture through and beyond the Hunan Province is disputed, with multiple SW-trending faults to the southeast of the Jiangnan orogen having been proposed (Zhao and Cawood, 2012; Wang et al., 2013f). Given

the prolonged and uncertain history of relative motion between Yangtze and Cathaysia, in addition to the obfuscating effects of younger tectonics, it is not surprising that the suture is complex or cryptic in places. Nevertheless, for the sake of reference, the Chenzhou-Linwu fault is here adopted as the southwest continuation of the suture.

The Yangtze block is floored by Archean–Paleoproterozoic crystalline basement—comprising the oldest rocks known to the South China block—surrounded by tectonized late Mesoproterozoic to early Neoproterozoic rocks and Neoproterozoic magmatic rocks. In contrast, the oldest known rocks known from the Cathaysia block are Paleoproterozoic, although the presence of an Archean basement is suspected (Zhao and Cawood, 2012). The crystalline basement of those blocks is overlain by Neoproterozoic–early Paleozoic strata which are capped by a regional middle Paleozoic unconformity associated with Kwangsian orogenesis. In the Cathaysia block, that regional unconformable contact between the early and late Paleozoic is angular and the unconformity spans the Silurian, although in the southern areas it reaches further backward, into the Late Ordovician (Wang et al., 2013f). More locally, on Hainan Island and in the southern Guangdong Province of the Cathaysia block, an earlier Cambro-Ordovician unconformity is also recognized. In the southeastern Yangtze block, the regional middle Paleozoic unconformity mostly spans the Silurian, but towards the northwest the duration of the unconformity contracts as progressively younger Silurian strata appear below it, and the contact itself becomes less angular, ultimately becoming a paraconformity (Wang et al., 2013f; Jiang et al., 2014a). Beneath the unconformity, the nature of South China's early Paleozoic strata also exhibit a regional change from northwest to southeast, becoming generally more terrigenous, coarser and thicker toward the latter (Wang et al., 2010; Wu et al., 2010). In the Cathaysia block, the Cambro–Ordovician succession is dominated by siliciclastic rocks with minor limestone interbeds, whereas in the southeast Yangtze block, the Cambro–Ordovician is comprised by interstratified siliciclastic and carbonate rocks and in the central and northwest Yangtze block it is comprised by a carbonate platform overlain by Silurian shallow marine clastic rocks (Wang et al., 2013f; Jiang et al., 2014a; Yao et al., 2014; Chen et al., 2016). In accordance with that regional lithofacies gradation, paleocurrent data from Cambro–Ordovician strata in western Cathaysia and eastern Yangtze and early Silurian strata from central Yangtze reveal that sediment transport was generally NW-directed throughout the Cambrian to early Silurian (Wang et al., 2010). Importantly, that apparent transmission of sediment between the Cathaysia and Yangtze blocks, which is further corroborated by the similar detrital zircon age populations among their early Paleozoic strata (Wang et al., 2010), suggests that they remained contiguous following their Neoproterozoic amalgamation and subsequent (aborted) rifting, and were not separated by an early Paleozoic ocean basin (Wang et al., 2013f). Analyses of the detrital zircons from the early Paleozoic strata of Cathaysia and Yangtze have also revealed the existence of a late Neoproterozoic–Cambrian detrital zircon age population for which a source within South China is not known, implying that at least some of the early Paleozoic sediments are exotic (Wang et al., 2010; Yao et al., 2014; Chen et al., 2016). In this context, the detrital zircon age spectra from those early Paleozoic strata closely resemble those known from the east margin of northern Gondwana, suggesting that they could have shared a common sediment source, and thus that South China was possibly adjacent to northern India or western Australia then (Cawood et al., 2013). An argument for such a late Neoproterozoic–early Paleozoic positioning for South China has also been made on stratigraphic and biogeographic grounds (Jiang et al., 2003; Hughes et al., 2005).

Kwangsian orogenesis, which began in the Middle Ordovician and continued into the Devonian, was associated with intense deformation, metamorphism and magmatism in the Cathaysia block and, to a lesser degree, in the southeastern Yangtze block. In the southeast Yangtze block, Kwangsian deformation was characterized by thin-skinned, dominantly N-vergent folding, whereas in the Cathaysia block to the southeast, it was associated with thin and thick-skinned tectonism that included multiply-vergent folding and thrusting, and the development of large mylonitic shear zones (Faure et al., 2009; Shu et al., 2015). Transcurrent motion was probably also significant, notably along the many prominent NE–SW trending fault systems (Charvet et al., 2010). Regional metamorphism during the orogeny reached upper amphibolite to granulite-facies conditions in the Cathaysia block between ~460 Ma and 420 Ma, but diminished in intensity toward the eastern Yangtze block, where rocks only experienced greenschist-facies conditions (Li et al., 2010; Wang et al., 2013b). Magmatism during the Kwangsian was characterized by the voluminous emplacement of granites between ~460 Ma and 400 Ma, with peak activity in the Silurian. The granites, which were mostly emplaced into the Cathaysia block (but also appear in the southeast Yangtze block), are dominantly S-type, peraluminous granites, interpreted to have been produced by partial melting of South China's lower crust, with little input of juvenile mantle material (Wang et al., 2013f).

The explanation of the Kwangsian orogeny has proven challenging and controversial. One proposal is that there existed an ocean (the Huanan Ocean) between the Yangtze and Cathaysia blocks which closed at that time. However, the Cambrian–Ordovician rocks along the Jiangshan-Shaoxing fault show abundant shallow water sedimentary structures and there is evidence of continuous sedimentary transport from the Cathaysia block to the Yangtze block from detrital zircon age spectra and biostratigraphy. Similarly problematic is the utter lack of early Paleozoic ophiolitic suites, deep-sea silicates and subduction-related magmatic rocks, and the fact that the Kwangsian granites appear to have been sourced from the Precambrian basement with little input from magmas derived from juvenile crust. Alternatively, the Kwangsian may have been an intracontinental orogeny produced by relative movements between the Cathaysia and Yangtze blocks, without an intervening ocean between them (Xu et al., 2016). Although the details remain vague, such relative movements could have been far-field effects produced by dynamics occurring along South China's margins, notably southern South China, which the sedimentary record suggests was then in contact with northeast Gondwana (Table 1).

4.11.2. Northern South China

The north of South China is bordered by the Qinling-Tongbai-Dabie-Sulu orogenic belt (Figs. 9 and 11), which chronicles a long-history of Paleozoic convergence that ultimately ended in a Triassic collision between North and South China. Relics of the early Paleozoic history along that composite orogenic belt are largely absent in the Dabie-Sulu, but are well-exposed in the Qinling-Tongbai. The Qinling-Tongbai orogen can be subdivided into two WNW–ESE trending belts, the North and South Qinling, which are separated by the Shangdan fault that is associated with a mid-to-late Paleozoic suture. As discussed in section 4.9.1, the North Qinling was probably an independent terrane in the early Paleozoic, which ultimately collided with the southern margin of the North China block in the Late Ordovician–early Silurian. By contrast, the Precambrian to early Paleozoic assemblages of the South Qinling bear a strong resemblance to the passive northern margin of South China, and so seem to have had a very different early Paleozoic history.

The South Qinling lies to the south of the Shangdan fault and the controversial mid-Paleozoic metasedimentary successions of the Wuguan complex and Liuling Group (section 4.9.1), and to its south

the South Qinling is separated from northern South China by the Mianlue suture zone. The South Qinling is comprised by a greenschist to amphibolite-facies Precambrian basement overlain by Ediacaran to Triassic sedimentary strata. The oldest materials known from its basement are felsic gneisses from the Douling complex which have yielded protolith emplacement ages of ~2.5 Ga (Hu et al., 2013a). The age and composition of the Douling complex, which also includes schists, marbles and amphibolites, have drawn comparisons to the Archean–Proterozoic Kongling complex in the north of the Yangtze block (Guo et al., 2015), and an inference that those terranes were then unified (Dong and Santosh, 2016). Notably, both the Duoling and Kongling complexes were later intruded by granites in the mid-Neoproterozoic, strengthening that inference that the South Qinling and Yangtze blocks were united in the Proterozoic (Dong and Santosh, 2016).

Unconformably overlying the crystalline basement, the ~12 km thick sedimentary cover of the South Qinling begins with Ediacaran to Ordovician platform-type carbonate and clastic rocks and passes upwards into a very thick (~10 km) succession of Silurian to Devonian metagraywacke and shale, followed by minor and restricted late Paleozoic to Triassic deposits of shallow marine clastic rocks and limestones (Wu and Zheng, 2013). The Ordovician-Silurian transition in sedimentation style together with the thickness and composition of the Silurian succession is interpreted to reflect extensive subsidence of the South Qinling at the beginning of the Silurian, and was broadly concurrent with the emplacement of mafic dike swarms, A-type granites and carbonatite-syenite complexes in the South Qinling, suggesting the region may have been under large-scale extension then (Xu et al., 2008; Wu and Zheng, 2013; Nie et al., 2016a). To the south of the Mianlue suture zone, the Precambrian basement of the northern Yangtze block is likewise unconformably overlain by Ediacaran to Ordovician platform-type clastic rocks and carbonates followed by Silurian siltstones and shales, but Devonian–Carboniferous rocks are absent (Meng and Zhang, 2000; Dong and Santosh, 2016). The common pre-Devonian lithostratigraphy of the South Qinling and the northern Yangtze block thus indicates that they remained coherent through the Neoproterozoic and earliest Paleozoic, and their shared mid-Paleozoic subsidence punctuated by Late Ordovician–Silurian magmatism is taken to mark their breakup (Fig. 12; Table 1).

The Mianlue suture zone that separates the South Qinling and northern South China block comprises a tectonic mélange of dismembered ophiolitic fragments, a variety of volcanic rocks including ocean-island and island-arc volcanics as well as bimodal rocks, and blocks of continental and oceanic metasediments (Ji et al., 2016). A Silurian opening of the Mianlue Ocean is supported by Silurian bimodal volcanic rocks in the east of the Mianlue suture, and from Late Devonian to Carboniferous radiolarian faunas identified in cherts of the mélange (Dong and Santosh, 2016). Ultimately the Mianlue Ocean closed again in the Triassic when South China collided with the South Qinling (which by that time was already amalgamated with North China and the North Qinling following closure of the Shangdan Ocean; section 4.9.1.).

4.12. Japan

The Japanese islands are largely comprised by a stack of accretionary complexes that reflect a long history of convergence and growth along an active margin that has operated for nearly the entire Phanerozoic. Although early Paleozoic rocks are rare in Japan—mostly restricted to the Kurosegawa and Oeyama belts of southwest Japan, the Hida Gaien belt of central Honshu and the Hitachi area and South Kitakami belt of northeast Japan (Fig. 9)—they include arc-related granitoids, HP/LT metamorphic rocks, ophiolites and volcaniclastic sediments that clearly signify that subduction began there at least by the mid-Cambrian (Isozaki et al., 2010; Wakita, 2013). The earliest manifestation of that active margin are early to late Cambrian (~520–490 Ma) arc-related granitoids that have been recognized from small, isolated bodies in both northeast and southwest Japan, as well as from xenoliths in younger volcanics and from xenocrysts in accompanying metamorphic rocks (Sakashima et al., 2003; Tagiri et al., 2011; Isozaki et al., 2015). The spatial distribution of those presently meager igneous bodies suggests that they may once have constituted a Japan-wide magmatic arc—since destroyed by tectonic erosion—as does the occurrence of ~500 Ma detrital/inherited zircons among

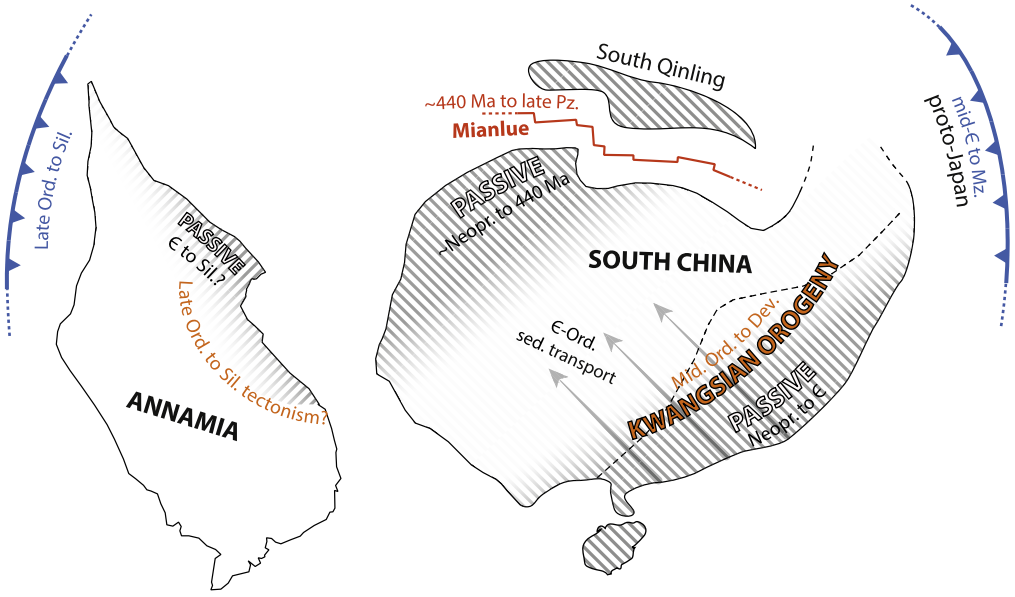

Figure 12. Schematic illustration of the principal interpretations from sections 4.11, 4.12 and 4.13, concerning the early Paleozoic tectonic boundaries of South China, Japan and Annamia. Blue/red dates relate to the timing of convergent/divergent margins (Table 1).

younger sedimentary rocks and granitoids across Japan. Subsequent to its Cambrian onset, subduction along that active margin continued through the Ordovician and Silurian, as evident by Ordovician-Silurian arc magmatism and high-grade metamorphism in both northeast and southwest Japan (Aoki et al., 2015; Isozaki et al., 2015), locally including HP/LT subduction-related metamorphism (Tsujimori et al., 2005), and the collection of Ordovician–Silurian volcaniclastic rocks and other sediments in arc-generated basins. The Ordovician–Silurian sedimentary successions have proven further useful in assessing Japan's early Paleozoic continental affinity, as both their early-middle Paleozoic biota and detrital zircon populations signal communication between Japan and its (at least formerly) neighboring terranes. The ages of detrital zircons from those Ordovician–Silurian sediments, as well as from inherited zircons among Japan's mid-Paleozoic granitoids, include significant Precambrian populations (notably late Mesoproterozoic–Neoproterozoic) that are unknown to Japan, but similar to the basement ages known from South China, suggesting that the latter may have acted as an important, if intermittent, sediment source for Japan (Aoki et al., 2015; Isozaki et al., 2015). The Ordovician–Silurian biota are less diagnostic, probably due in part to Japan's location in tropical latitudes at that time, but nonetheless reflect gross similarities with Australia, South China, North China and other central Asian terranes (Cocks and Torsvik, 2013; Williams et al., 2014), which imply a broad paleogeographic or paleo-latitudinal link with those regions then.

4.13. Annamia

Annamia comprises most of present day Vietnam, Laos, and Cambodia, as well as northeast Thailand and a strip of the Yunnan Province of China, and is generally delineated by the Changning-Menglian-Chiang Mai belt in the west (where it abuts Sibumasu) and the Ailaoshan-Song Ma suture in the northeast (where it borders South China), although its exact boundaries are still debated (Fig. 11). For example, Cai and Zhang (2009) suggested that the Dian-Qiong suture near the China-Vietnam political border is a Cenozoic structural duplication of the Ailaoshan-Song Ma suture, which would make northernmost Vietnam also a part of Annamia, rather than South China. Similarly, the Changning-Menglian-Chiang Mai belt includes several major north-south trending features that have been proposed to mark the discrete western boundary of Annamia (Metcalfe, 2013; Ridd, 2015).

Precambrian and early Paleozoic rocks of Annamia are widespread in Vietnam and eastern Laos, and are documented in the Yunnan Province of China, but are poorly studied in Cambodia and unknown from the Thai sector of the terrane, except for a restricted sequences of Silurian mudstones and rhyolites in the eastern Loei foldbelt (Ridd et al., 2011; Qian et al., 2015). In northern and central Vietnam and northeastern Laos, those Precambrian and early Paleozoic sequences are commonly divided into several distinct domains: the Kontum massif, the Truong Son terrane, and 'north Vietnam' (the Song Da belt and northeast Vietnam). The Kontum massif, which is bounded by the Po Ko shear zone to the west and the Tam Ky-Phuoc Son shear zone to the north, is characterized by generally high-grade metamorphic rocks (amphibolite to granulite facies) that contrast with the low-grade to unmetamorphosed early Paleozoic sedimentary rocks in the Truong Son terrane to the north. The Kontum massif was formerly thought to comprise Archean or Paleoproterozoic basement, but geochronological investigations have revealed a predominance of Ordovician–Silurian and Permo-Triassic metamorphic and magmatic ages, and the cores of detrital zircons from those rocks have yielded ages ranging back into the Meso- and Neoproterozoic (Usuki et al., 2009; Tran et al., 2014).

The NW–SE elongate Truong Son terrane extends from the Tam Ky-Phuoc Son shear zone in the southeast to the Song Ma suture in the north, and the early Paleozoic rocks there are characterized by low-grade to unmetamorphosed clastic rocks and carbonates of Ordovician and Silurian age, but possibly also of Cambrian age (Tong-Dzuy and Vu, 2011). Detrital zircons from those early Paleozoic rocks have yielded Archean and Paleoproterozoic ages for which there is no known source within Annamia, and so they are inferred to be derived from a previously adjacent continental terrane. From an age population analysis of those detrital zircons, Usuki et al. (2013) and Burrett et al. (2014) concluded that previously adjacent continent was most likely Qiangtang or the Tethyan Himalaya, both of which were probably outboard the Indian margin of Gondwana in the early Paleozoic (section 4.14). Higher grade metamorphic rocks in the Truong Son terrane, which occur along the Song Ma suture, are dominantly Permo-Triassic, but a few pelitic and garnet-phengite schists there have yielded monzanite inclusions and zoned monzanites of Silurian age, suggesting an earlier metamorphic event could have occurred there, as in the Kontum massif (Nakano et al., 2010). Magmatism in the Truong Son terrane was also mostly confined to the Permo-Triassic, but in the southeast of the terrane a granite yielded a U–Pb age of 438 Ma (Shi et al., 2015).

To the northeast of the Truong Son terrane, 'north Vietnam' (or the Song Da belt and northeast Vietnam, separated from one another by the Song Chay and Red River fault systems) includes Archean-Proterozoic basement and variably metamorphosed to unmetamorphosed clastic rocks and carbonates that span the early Paleozoic (Tong-Dzuy and Vu, 2011; Faure et al., 2014). As in the Truong Son terrane, north Vietnam was markedly affected by magmatism and metamorphism during the Permo-Triassic, but there are also indications that it experienced an earlier tectono-magmatic event in the Ordovician–Silurian (Roger et al., 2000; Żelaźniewicz et al., 2013; Nguyen et al., 2014).

In the southwest of the Yunnan Province of China, along the Changning-Menglian belt, early Paleozoic volcaniclastic rocks are reported from the eastern and western flanks of the Triassic Lincang granitic massif that formed during final closure of the Paleo-tethys Ocean. On the western flank of the Lincang granite, overlying schists of indefinite age, a metavolcanic sequence of basalt and andesite with minor dacite and rhyolite and interlayers of slate and phyllite has been dated as Late Ordovician (~456–459 Ma) and interpreted as a relic of a subduction-related magmatic arc (Nie et al., 2015). On the eastern side of the Lincang granite, exposures of the basement of the Simao basin around Dapingzhang comprise a Silurian dacite-andesite sequence including minor metabasalt, rhyolite, siltstone and chert, and an associated massive sulfide deposit, which together have been interpreted to reflect an arc-backarc environment (Lehmann et al., 2013; Nie et al., 2016b).

4.14. Northeast Gondwana

Following the final stages of Gondwana assembly in the early Cambrian, the northeast margin of Gondwana stretched for ~10,000 km, from the northwest Arabian-Nubian Shield, across the north Indian craton to the northeast corner of western Australia (Meert, 2003). However, the actual northeast rim of Gondwana then laid to the north of those Proterozoic cratons, and was comprised by continental terranes and microcontinents that are now scattered across southern Europe and central and south Asia. In the late Neoproterozoic to early Cambrian, concurrent with the final phases of Gondwana assembly, those marginal terranes were marked by intense deformation and magmatism associated with the Cadomian orogeny. In the west, to the north of the West African craton, that orogenic phase has been recognized to reflect the

operation of a continental magmatic arc that evolved, perhaps diachronously, into a transform system and finally a rift zone (Linnemann et al., 2008)—ultimately giving rise to the Rheic Ocean in the Cambro–Ordovician (Domeier, 2016). In the east, there is not a clear, margin-wide record of Cambro-Ordovician rifting, but evidence of the preceeding late Neoproterozoic–early Cambrian magmatic arc is widespread, and those magmatic rocks present an excellent Cadomian margin terrane identifier (Ustaömer et al., 2009; Moghadam et al., 2015). The principal terranes confirmed or commonly assumed to have occupied the northeast margin of Gondwana at the start of the Paleozoic include the Taurides and Pontides of Turkey, the Sanandaj-Sirjan, Alborz and Central Iran terranes of Iran, the Central Afghan terranes and part of the Pamirs, Qiangtang, Lhasa and the Tibetan Himalaya of the Tibetan Plateau, and Sibumasu in southeast Asia. In the following, these regions are each reviewed in turn.

4.14.1. Turkish terranes (Taurides and Pontides)

Turkey is divided into two principal tectonic domains: the northern Pontides and the southern Taurides, in addition to a corner of the Arabian platform that extends into the southeast of the country (Fig. 13). The Taurides exhibit strong Neoproterozoic-Paleozoic affinities to the northern margin of Gondwana, including Cadomian basement (Abbo et al., 2015), a common early Paleozoic stratigraphy including Late Ordovician glacial deposits (Monod et al., 2003; Ghienne et al., 2010), and typical Gondwanan faunas (Torsvik and Cocks, 2009). Following the Neoproterozoic–early Cambrian Cadomian orogenic cycle, the early Paleozoic sequence of the Taurides was mostly characterized by shallow marine platform sedimentation upon a broad passive margin, but was interrupted by mild tectonism and magmatism in the mid-to-Late Ordovician (Fig. 14; Table 1), as well as by the Hirnantian glaciation (Ghienne et al., 2010). Middle–Late Ordovician tectonism, which is recognized from a regional Middle Ordovician unconformity, the subsequent appearance of mass-flow deposits and the generation of a major NW–SE oriented sag basin that apparently spanned northeast Arabia, is commonly attributed to regional extension driven by continental rifting (Ghienne et al., 2010). Although post-Cadomian early Paleozoic magmatism is sparse in the Taurides, Middle and Late Ordovician metagranitoids interpreted to relate to that Mid-to-Late Ordovician rifting have been reported from the northwest of the Taurides, in the Tavşanlı zone (Okay et al., 2008b; Özbey et al., 2013).

The Pontides can be further subdivided into three tectonically distinct zones, from west to east: the Strandja (Istranca), Istanbul and Sakarya zones. The Strandja zone contains fragments of Cadomian basement which reveal that it formed part of the north Gondwanan margin in the late Neoproterozoic-earliest Paleozoic (Şahin et al., 2014), but its early Paleozoic history is largely unknown because Triassic metasedimentary rocks are the oldest strata covering the metamorphic basement (Okay, 2008). From detrital zircon analyses, Natal'in et al. (2012) deduced that some of the metasedimentary rocks of the metamorphic basement, including schists and paragneisses sometimes with amphibolite lenses, were likely derived from early Paleozoic sedimentary protoliths. They further considered the relative abundance of early Paleozoic zircons among those rocks to be a reflection of ongoing magmatism across that time, and suggested that the Strandja zone must comprise or have been near an early Paleozoic magmatic arc. At present, no early Paleozoic magmatic rocks have been identified in the Strandja zone, but Late Ordovician (~455 Ma) metamafic rocks interpreted to be derived from back-arc basalts have been identified in the adjacent Rhodope massif (Bonev et al., 2013), which may have shared a common tectonic history with the Strandja zone.

Like the Strandja zone, the early Paleozoic history of the Sakarya zone is very poorly known as the oldest sedimentary rocks overlying its metamorphic basement are Jurassic (Okay, 2008). Here too, however, the metamorphic basement has been derived in part from early Paleozoic sedimentary rocks, as revealed by the occurrence of early Paleozoic detrital zircons in metasedimentary rocks cross-cut by Early Devonian granitoids (Aysal et al., 2012). A prominent late Neoproterozoic age population among detrital zircons of some of those basement rocks has been used to correlate the basement of the Sakarya zone with the Cadomian margin of north Gondwana (Ustaömer et al., 2012), but its specific paleogeographic positioning then and its subsequent Paleozoic history remain unclear.

Unlike the Strandja and Sakarya zones, the strata of the Istanbul zone overlying the Precambrian crystalline basement spans most of the Paleozoic, beginning in the Early Ordovician and continuing into the Carboniferous. Notable differences in the sequence of that Paleozoic stratigraphy between the east and west of the Istanbul zone have led some to interpret the terrane to be composite—with a western Istanbul terrane (*sensu stricto*) and an eastern Zonguldak terrane—although others have interpreted the differences as facies changes across a singular block (Okay et al., 2008a; Ustaömer et al., 2011). In either case, both 'terranes' are floored by Precambrian basement that includes late Neoproterozoic magmatic rocks identified as products of the Cadomian orogenic cycle, and thus of presumed north Gondwanan affinity (Ustaömer et al., 2011). In the west of the Istanbul zone (the Istanbul 'terrane'), the Paleozoic sequence begins with Early Ordovician clastic rocks including conglomerates that are unconformably overlain by a continuous Middle–Late Ordovician to Early Carboniferous succession of shelf and slope-type clastic rocks and carbonates (Özgül, 2012). By contrast, in the east of the Istanbul zone (the Zonguldak 'terrane'), the Ordovician–Silurian sequence (which is reportedly continuous but notably includes Middle Ordovician conglomerates) is separated from overlying Devonian–Carboniferous rocks by an unconformity not observed in the west (Ustaömer et al., 2011; Bozkaya et al., 2012). Both the Early–Middle Ordovician unconformity in the west and the Silurian-Devonian unconformity in the east have been attributed to possible tectonism (Fig. 14; Table 1), but in neither case is the nature of such tectonism understood. This is in part due to the fact that the early Paleozoic paleogeography of the Istanbul zone is so poorly known. Although it is widely accepted that the Istanbul zone was located along the north margin of Gondwana in the Late Neoproterozoic–early Cambrian and had reached the southern margin of Laurussia by the Carboniferous (where it was affected by the Variscan orogeny), its intervening history is uncertain. Prevailing views consider that the Istanbul zone rifted from Gondwana either during the Ordovician—in which case it was associated with the Avalonian terranes—or during the Silurian–Devonian—wherein it would have been associated with the Variscan terranes. The conclusions drawn from paleontological, paleomagnetic and provenance studies of pre-Carboniferous rocks of the Istanbul zone have been mixed. Dean et al. (2000) considered Early and Middle Ordovician faunas from the east of the Istanbul zone to be cold-water types and similar to those of East Avalonia, whereas Sayar and Cocks (2013) found that, by the Late Ordovician, warmer-water faunas had appeared in the west of the Istanbul zone. However, Olempska et al. (2015) described Early Devonian ostracods from the west of the Istanbul zone and concluded that they shared strong similarities with the faunas of the peri-Gondwanan Variscan terranes and the northern margin of Gondwana itself. Paleomagnetic and detrital zircon studies of Early Ordovician rocks from the Istanbul zone have been used to argue for an Early Ordovician positioning of the Istanbul zone along the northwest of the Amazonian craton, but do not constrain its

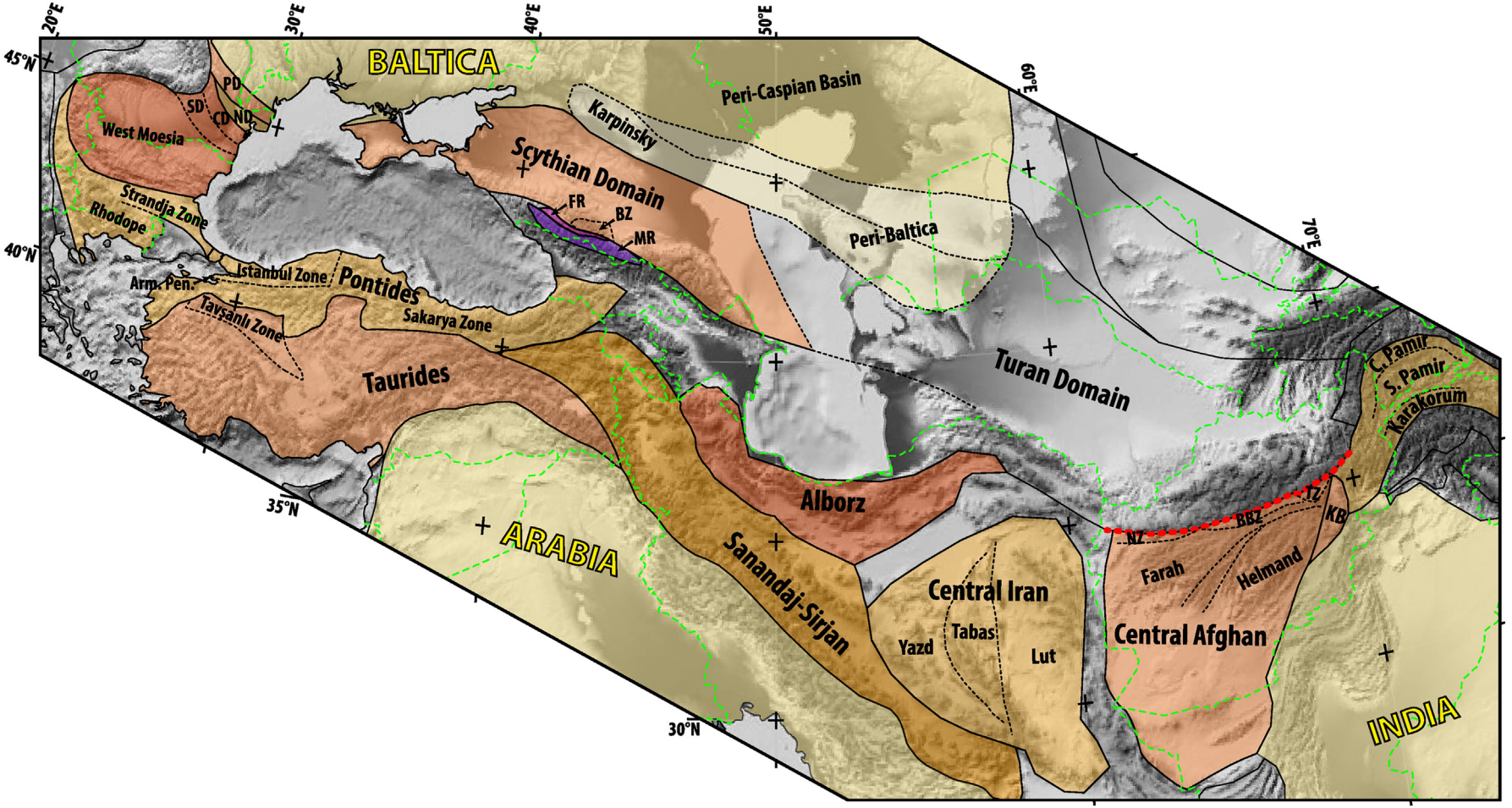

Figure 13. Overview map of Turkish, Iranian and Afghan terranes (section 4.14) and southeast Baltica (4.15). Abbreviations: Arm. Pen., Armutlu Peninsula; BBZ, Bande-Bayan zone; BZ, Bechasyn zone; CD, Central Dobrogea; FR, Fore Range zone; KB, Kabul block; MR, Main Range zone; ND, North Dobrogea; NZ, Nalbandan zone; PD, Pred-Dobrogea depression; SD, South Dobrogea; TZ, Turkman zone.

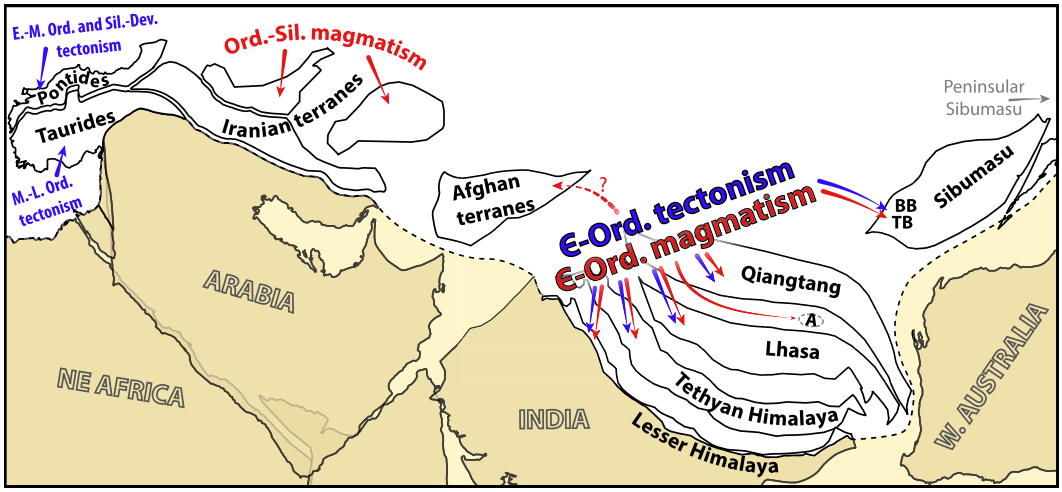

Figure 14. Schematic illustration of the principal observations from section 4.14, concerning the early Paleozoic tectonic boundaries of Northeast Gondwana. Blue/red dates relate to the timing of major tectonism/magmatism inferred to relate to important boundary dynamics (Table 1). Abbreviations: A = Amdo; BB = Baoshan block; TB = Tengchong block.

subsequent departure from Gondwana (Ustaömer et al., 2011; Oksum et al., 2015). A further complexity has been added by the recognition of ~460 Ma granitoids in the Armutlu Peninsula that lies between splayed strands of the North Anatolian fault at the boundary between the Istanbul and Sakarya zones. Interpreting the basement of that peninsula as a southern extension of the Istanbul zone, Okay et al. (2008a) speculated that the Middle–Late Ordovician plutonism there—which is otherwise unknown to the Istanbul zone—could reflect its rifting from Gondwana. However, that timing is significantly younger than the late Cambrian–Early Ordovician rifting of Avalonia and older than the late Silurian–Early Devonian rifting of the Variscan terranes, and moreover, a Middle–Late Ordovician syn-rift sequence is not manifest in the stratigraphy of the Istanbul zone.

4.14.2. Iranian terranes (Alborz, Central Iran, Sanandaj-Sirjan)

Iran comprises several tectonic blocks delineated by steep faults decorated by Paleozoic and Mesozoic ophiolites, and includes three large terranes that bear Neoproterozoic–Paleozoic sequences with strong north Gondwanan affinities, namely the Alborz, Central Iran and Sanandaj-Sirjan terranes (Fig. 13). Following Neoproterozoic–early Cambrian tectonism and magmatism associated with the Cadomian orogenic cycle along the northern margin of Gondwana, those terranes were characterized in early Paleozoic time by the deposition of shallow marine platform-type successions—as widely observed elsewhere along the Arabian margin of Gondwana—but with notable magmatic interruptions, mostly during the Late Ordovician–Silurian (Fig. 14; Table 1). The most voluminous example of such magmatism is the Soltan Maidan volcanics from the east of the Alborz terrane, a sequence of mafic volcanics interspersed with minor sedimentary horizons with a stratigraphic thickness that locally exceeds 1 km (Derakhshi and Ghasemi, 2015). Although the mafic volcanics have not been directly dated, they occur stratigraphically between Late Ordovician shales and Devonian conglomerates, and intraformational sedimentary units have yielded Late Ordovician to mid-Silurian microfossils, as well as granitic cobbles bearing zircons that gave a U–Pb age of ~434 Ma (Ghavidel-Syooki et al., 2011). The occurrence of conglomerates with relatively large (up to ~50 cm) Silurian granitic cobbles intercalated within those volcanics further suggests that contemporaneous felsic magmatism was also occurring in the region, although no sources have yet been identified. Late Ordovician mafic volcanics (Katian-Hirnantian age) also appear in the sedimentary units beneath the Soltan Maidan volcanics, as well as among low-grade metamorphic rocks of the Gorgan Schists to the northwest (Ghavidel-Syooki, 2008). In the Central Iran terrane, early Paleozoic mafic volcanics are recognized in the Niur Formation of the Tabas block, where they are stratigraphically bound between Late Ordovician and early Silurian shallow marine carbonates and clastic rocks (Hairapetian et al., 2011; Nowrouzi et al., 2014), and possibly Early Ordovician bimodal volcanics are reported from the northwest of the Yazd block (Hairapetian et al., 2015). Together, those Ordovician–Silurian bimodal to mafic-dominated magmatic pulses have conventionally been interpreted to reflect sluggish or recurring regional extension, ultimately giving rise to successful marginal rifting and the formation of the Paleotethys Ocean in the mid-Paleozoic (Stampfli et al., 1991; Alavi, 1996).

4.14.3. Central Afghan terranes and the Pamirs

Blocks of Precambrian basement and early Paleozoic strata are recognized from central Afghanistan and from the Hindu Kush ranges in the northeast. In central Afghanistan, a typical scheme distinguishes at least three Precambrian blocks, from west to east: the Farah block, the Helmand block and the Kabul block (Collett et al., 2015; Siehl, 2015) (Fig. 13). All three blocks contain deformed and metamorphosed Proterozoic basement, but early Paleozoic rocks are known only from the Farah and Helmand blocks (Abdullah and Chmyriov, 2008). The basement of the Farah block is exposed along, and directly south of, the so-called Middle Afghanistan fault-block zone, a narrow, E–W elongate and tectonically complex corridor that is thought to broadly demarcate the boundary between terranes of Eurasian and Gondwanan-affinity (i.e. the Paleotethys suture) (Siehl, 2015). The Precambrian basement exposures occur in a number of fault blocks along this corridor, including in the Nalbandan, Bande-Bayan and Turkman zones, but it has been speculated that the basement continues to the southwest, underlying the thick Mesozoic sedimentary pile of the Farah basin (Abdullah and Chmyriov, 2008; Siehl, 2015). Others, however, have considered it unlikely that Precambrian basement floors the Farah basin, and so the term Bande-Bayan block (as opposed to Farah block) is also present in the literature. The Precambrian basement of the Farah block is unconformably overlain by a Cambrian succession of clastic rocks, carbonates, and minor volcanic rocks including tuffs, but the occurrence of Ordovician and Silurian rocks is uncertain (Abdullah and Chmyriov, 2008). In the Helmand block, which lies to the southeast of the Farah block and

southwest of the Kabul block, the Proterozoic basement is unconformably overlain by a conformable sequence of Cambrian to late Paleozoic terrigenous clastic rocks and carbonates. In the north of the Helmand block, deformed S-type granitoids intruding the basement have been assigned a Cambro-Ordovician age based on a Rb-Sr whole rock age of 502 ± 24 Ma (Debon et al., 1987).

To the northeast of the Kabul block, the Karakorum and South and Central Pamir are commonly assumed to have occupied a similar position along the early Paleozoic north margin of Gondwana as those of the Afghan blocks to the west, but owing to the great inaccessibility of those regions, their geology remains very poorly studied. Nevertheless, Precambrian and early Paleozoic rocks have been documented in several areas. In the western Karakorum, a pre-Ordovician basement has been recognized and comprises a low-grade metasedimentary sequence of siltstones and quartzites intruded by pre-Ordovician granitoids (Le Fort et al., 1994). Unconformably overlying that basement are Early Ordovician shallow marine clastic rocks bearing peri-Gondwanan faunas—the oldest known to the Karakorum—which pass conformably upward into later Ordovician, Silurian and Devonian shallow marine clastic rocks and carbonates reflecting a stable continental shelf environment (Gaetani, 1997; Zanchi and Gaetani, 2011). A similar succession of early Paleozoic platform-type strata has also been recognized in southeast Karakorum, where the early Paleozoic rocks are reported to unconformably overlie Precambrian metadiorite (Rolland et al., 2002). Although their ages are not well-defined, those basement intrusives are likely late Neoproterozoic to Cambrian in age and so may be related to the same Cadomian magmatic cycle established elsewhere along the northern margin of Gondwana. In the South and Central Pamir, corresponding late Precambrian to possibly early Paleozoic granitoids have likewise been identified (Debon et al., 1987), and detrital zircon analyses of younger rocks there have revealed a significant population of Neoproterozoic to early Paleozoic grains (Schwab et al., 2004; Robinson et al., 2012). Early Paleozoic platform-type sedimentary successions, similar to those of Karakorum, are also reported from the Central Pamir, whereas early Paleozoic strata appear absent in the South Pamir (Gaetani, 1997; Siehl, 2015).

4.14.4. Qiangtang

Qiangtang lies in the middle of the Tibetan Plateau, between the Kunlun and Songpan Ganzi to the north and Lhasa to the south (Fig. 15). Its northern boundary is delimited by the Jinsha suture zone, and its southern boundary by the Bangong-Nujian suture. It is subdivided into North (or 'East') and South (or 'West') Qiangtang by the Longmu Tso-Shuanghu suture zone, which includes Cambrian to Silurian (504–437 Ma) gabbros and plagiogranites (Hu et al., 2014b; Zhai et al., 2016). It is presently unknown if North Qiangtang is floored by a crystalline basement, and the age of the oldest known rocks of the terrane—the meta-sedimentary Ningduo Group—is constrained only by the age of the youngest detrital zircons they bear, which are Late Neoproterozoic to early Cambrian (He et al., 2011). The next-oldest strata, and the oldest fossiliferous rocks of the terrane, are Ordovician and Silurian clastic rocks and carbonates, but they are rarely exposed, and mostly restricted to outcrops along the western Longmu Tso border (Xia et al., 2009). The Ordovician–Silurian rocks are unconformably overlain by similarly rarely-exposed Devonian strata, which exhibit an initial sequence of coarse clastic rocks and mafic to intermediate volcanics, followed by finer clastic rocks with fewer volcanic interbeds, and finally a succession of fossiliferous carbonates (Zhang et al., 2016a). The deposition of shallow marine clastic rocks and carbonates subsequently continued through the rest of the late Paleozoic (Zhu et al., 2013).

The nature of the basement of South Qiangtang is similarly poorly characterized, but middle Cambrian to Middle Ordovician (~510–470 Ma) granitoids intruding or associated with metasedimentary rocks which could represent the basement have been reported from the Duguer, Gemuri, and Rongma areas (Zhao et al., 2014b; Hu et al., 2015; Liu et al., 2016e). In the Rongma area, it has been established that those pre-Middle Ordovician metasedimentary rocks must have been deposited after ~590 Ma, as they bear detrital zircons of that age (Zhao et al., 2014b). Confirmed late Neoproterozoic strata are also recognized in the Dabure area where metasedimentary rocks are interbedded with Ediacaran basalts (Wang et al., 2016). In the Duguer area, some of the metasedimentary rocks cross-cut by Middle Ordovician intrusives are

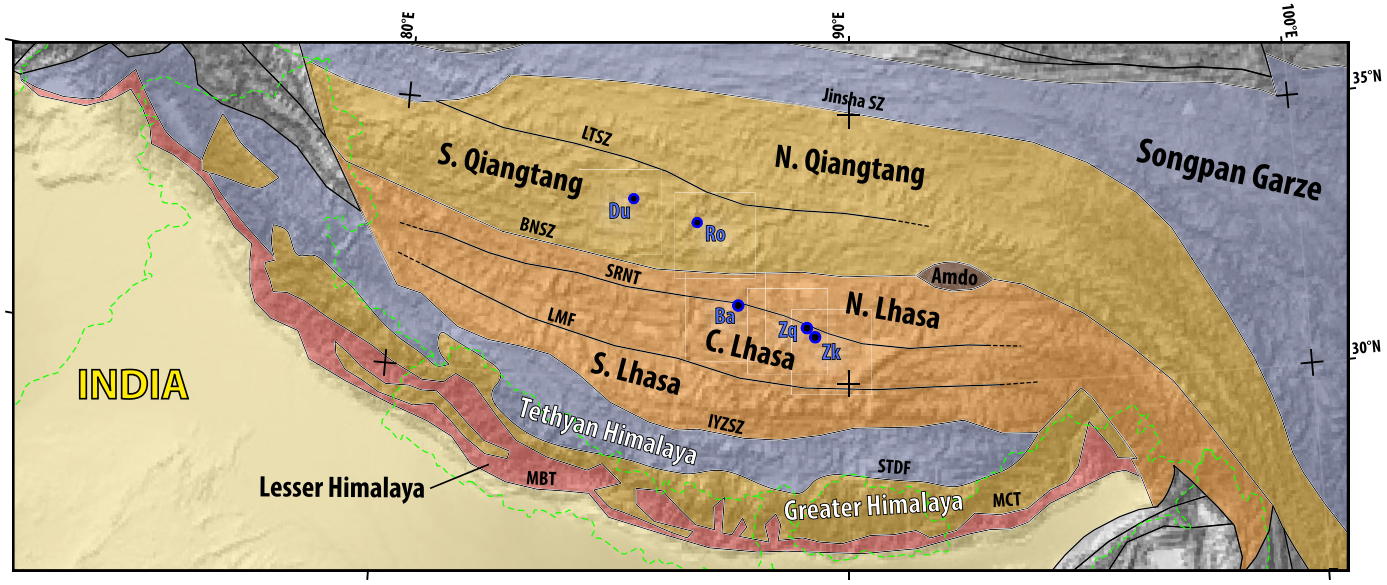

Figure 15. Overview map of Tibetan terranes (section 4.14). Blue circles denote areas discussed in the text: Ba, Banglei area; Du, Duguer area; Ro, Rongma area; Zk, Zhakang area; Zq, Zhaqian area. Other abbreviations: BNSZ, Bangong-Nujian suture zone; IYZSZ, Indus-Yarlung Zangbo suture zone; LMF, Luobadui-Milashan fault; LTSZ, Longmu Tso-Shuanghu suture zone; MBT, Main Boundary thrust; MCT, Main Central thrust; SRNT, Shiquan River-Nam Tso mélange zone; STDF, South Tibetan detachment fault.

evidently Cambro–Ordovician in age, as they bear Cambrian detrital zircons (Liu et al., 2017). Those Neoproterozoic to Cambrian metasediments were then deformed prior to the Middle Ordovician (Fig. 14; Table 1), at least in the Rongma area, where they are covered by Middle Ordovician conglomerates with angular unconformity and furthermore exhibit a tectonic foliation that is not observed in the overlying strata (Zhao et al., 2014b). Succeeding the Middle Ordovician basal conglomerates, Middle to Late Ordovician strata in South Qiangtang are mostly characterized by calcareous clastic rocks, locally interbedded with volcaniclastic rocks, followed by Silurian to Devonian shallow marine platform-type deposits (Zhu et al., 2013; Zhao, 2015). Although Middle–Late Ordovician bimodal volcanics (Liu et al., 2016e) and late Silurian HP granulites (Zhang et al., 2014d) outcropping to the north of Duguer are also attributed to South Qiangtang, those rocks occur along the Longmu Tso-Shuanghu suture zone, and so their early Paleozoic affinity is not certain.

4.14.5. Lhasa

Lhasa is positioned between Qiangtang and the Himalaya, bounded by the Bangong-Nujian suture to the north and the Indus-Yarlung Zangbo suture to the south (Fig. 15). Although traditionally treated as a singular terrane, accumulating evidence suggests that Lhasa is rather composite, and it is now commonly subdivided into a northern, central and southern block, demarcated by the Shiquan River-Nam Tso mélange zone in the north and the Luobadui-Milashan fault in the south (Zhu et al., 2013). Northern Lhasa is dominated by Mesozoic sediments and volcanics that are inferred to cover a basement of juvenile crust, although no rocks older than Middle Triassic have thus far been reported from the block (Zhu et al., 2013). Central Lhasa has a demonstrated Precambrian basement that, at least along the Shiquan River-Nam Tso mélange zone, bears relics of Neoproterozoic HP metamorphism and late amphibolite-facies retrogression during the early Paleozoic (~485 Ma) (Zhang et al., 2014f). The Precambrian basement is covered by Paleozoic metasedimentary and volcanic rocks including minor early Paleozoic strata that are divided by a Cambro–Ordovician angular unconformity which separates Cambrian sediments and volcanics from an Ordovician basal conglomerate and Ordovician to Devonian carbonates and shales (Zhu et al., 2013) (Fig. 14; Table 1). The Cambrian volcanics comprise early to middle Cambrian metarhyolites, ignimbrites and pyroclastic rocks interbedded within clastic sediments in the Zhaqian and Zhakang areas (Hu et al., 2013b; Ding et al., 2015) and a late Cambrian (~492 Ma) bimodal volcanic suite in the Banglei area (Zhu et al., 2012). Southern Lhasa, like Central Lhasa, is generally assumed to be floored by a Precambrian crystalline basement, but detrital zircons extracted from presumed Precambrian basement in the east of the terrane have yielded ages as young as latest Neoproterozoic (~550 Ma) (Dong et al., 2010). Together with a late Cambrian orthogneiss (~496 Ma) that cross-cuts those rocks, this suggests that at least some of the protoliths of the presumed Precambrian basement of South Lhasa could have been deposited in the earliest Paleozoic. Apart from some Late Devonian granites, post-Cambrian Paleozoic rocks are unknown from Southern Lhasa, and the next oldest strata is Triassic–Jurassic (Zhu et al., 2013).

4.14.6. Amdo

In the east of the Bangong-Nujian suture zone between Qiangtang and Lhasa lies an augen-shaped microcontinental block, the Amdo microcontinent, flanked both to its north and south by ophiolites (Fig. 15). The block is comprised by a crystalline basement of foliated orthogneisses with minor mafic granulites, amphibolites and migmatites, and metasedimentary cover rocks, which were together metamorphosed during the Jurassic (Zhang et al., 2012b). The magmatic protoliths of the crystalline basement were formed during two distinct phases of magmatism: an Early to mid-Neoproterozoic episode of granitoid magmatism (~920–800 Ma), followed by a Cambrian to Middle Ordovician phase of bimodal magmatism (~540–460 Ma) (Guynn et al., 2012; Zhang et al., 2012b). The metasedimentary cover strata, including marble, schist, phyllite and quartzite, are presently assumed to mostly represent late Paleozoic passive continental margin deposits, but neither their age nor tectonic environment are yet well established (Zhu et al., 2013).

4.14.7. Himalaya

Situated between Lhasa and India, the Himalayan orogen is bounded by the Indus-Yarlung Zangbo suture to the north and the Main Boundary thrust to the south (Fig. 15). The orogen is comprised of three principal units, from north to south: the Tethyan Himalaya, the Greater Himalaya and the Lesser Himalaya, which are separated from each other by the South Tibetan detachment fault and the Main Central thrust, respectively. The Lesser Himalaya comprises a thick sequence of Proterozoic to Cambrian strata, unconformably overlain by local Permian rift deposits and widespread Late Cretaceous to Eocene sediments (Brookfield, 1993; Valdiya, 1995). The Cambrian sediments there, which are characterized by shallow marine clastic rocks and carbonates, certainly span the early Cambrian, but possibly extend into the middle Cambrian (Hughes et al., 2005). In the Tethyan Himalaya to the north, Precambrian basement is likewise covered by Cambrian platform-type clastic rocks and carbonates, but there the Cambrian rocks are unconformably covered by low-grade sediments that were deposited near-continuously from the Ordovician to the Eocene (Liu and Einsele, 1994; Myrow et al., 2010). The Ordovician strata are characterized by arkosic clastic rocks, often floored by a basal conglomerate, whereas the subsequent Silurian and Devonian strata are typified by finer-grained, platform-type shales and carbonates (Gehrels et al., 2003; Myrow et al., 2010). Lying between the Lesser and Tethyan Himalaya and as isolated nappes overlying the Lesser Himalaya, the Greater Himalaya comprises a belt of medium to high-grade metamorphic rocks, including gneiss, migmatite, schist, and marble, with protolith ages that are poorly known but loosely bracketed as Neoproterozoic to Cambrian by detrital zircons and cross-cutting intrusions (Hodges et al., 1996; DeCelles et al., 2000; Myrow et al., 2003). Although it has been proposed that the Greater Himalaya could constitute an exotic terrane that collided with the Lesser Himalayan passive margin of India in the Cambro–Ordovician (DeCelles et al., 2000), the collective sedimentologic and stratigraphic (Myrow et al., 2010), paleobiologic (Hughes, 2016) and paleomagnetic (Torsvik et al., 2009) evidence weigh in favor of the alternative model in which the three units formed a continuous north-facing passive margin already by the beginning of the Cambrian (Myrow et al., 2003).

That an episode of early Paleozoic tectonism affected the Himalaya is perhaps most evident from the Cambro–Ordovician unconformity in the Tethyan Himalaya that is sealed by Ordovician molasse (Garzanti et al., 1986; Valdiya, 1995), but the Himalaya were also affected by strong early Paleozoic deformation (Bhargava et al., 2011), regional metamorphism (Gehrels et al., 2003) and extensive Cambrian to Ordovician magmatism (Cawood et al., 2007; Wang et al., 2012b) (Fig. 14; Table 1). The most significant early Paleozoic magmatic event in the Himalaya was the widespread intrusion of large volume granites into the Greater Himalaya sequence. Those granites are presently exposed as three orogen-parallel belts: as sheets in the Greater Himalaya sequence of the High Himalaya (Greater Himalaya granite belt), as tabular bodies and batholiths in the Greater Himalaya sequences of the Lesser Himalaya crystalline nappes to the south (Lesser Himalaya granite

belt), and as a string of gneissic domes in the Tethyan Himalaya to the north (Northern Himalaya gneiss domes), where they represent structural windows into the underlying Greater Himalaya sequence (Cawood et al., 2007). Geochemically, they are classified as peraluminous S-type granites and are inferred to be derived from crustal anatexis (Wang et al., 2012b). An array of age determinations have revealed that the bulk of those granites were emplaced between ~510 Ma and 470 Ma, while a few (questionable) older ages could suggest that plutonism initiated earlier, in the early Cambrian or latest Neoproterozoic (Cawood et al., 2007; Wang et al., 2012b). In addition to those intrusives, scattered examples of Cambrian volcanics, comprised by mafic to felsic tuffs and lavas, are recognized in the Tethyan Himalaya (Valdiya, 1995).

The records of early Paleozoic deformation in the Himalaya have been greatly obfuscated by intense Cenozoic deformation there, not least because the shortening directions associated with those deformation episodes may have been, at least locally, co-axial (Wiesmayr and Grasemann, 2002; Paulsen et al., 2007). However, in rare instances, unambiguous early Paleozoic structures have been identified where they are cross-cut by younger early Paleozoic features. In Cambrian rocks of the Tethyan Himalaya in the Spiti area of India, Wiesmayr and Grasemann (2002) observed mesoscopic folds truncated by the regional Cambro–Ordovician unconformity, which, following subtraction of subsequent deformation, restored to open, upright folds trending NW–SE. Correspondingly, from an analysis of calcite twins in Cambrian limestones of the same area of the Tethyan Himalaya, Paulsen et al. (2007) concluded that the region was subjected to NE–SW oriented shortening during the early Paleozoic. In the Dadeldhura and Kathmandu external thrust sheets of the Nepalese Himalaya, ductile deformation of Neoproterozoic–Cambrian metasedimentary rocks (the Bhimphedi Group; correlated with the Greater Himalaya sequence) has been constrained to the Cambrian–Early Ordovician by the occurrence of both deformed and undeformed cross-cutting intrusions (Gehrels et al., 2006a,b). Indirect evidence further suggests that deformation of those Neoproterozoic–Cambrian rocks in the Cambro-Ordovician was associated with north-south shortening and south-vergent thrusting (Gehrels et al., 2006a,b). More broadly, significant Cambro–Ordovician uplift of the Himalaya is inferred from the regional Cambro–Ordovician unconformity and by the abundance of first-cycle detritus, notably late Cambrian–Early Ordovician detrital zircons, in the overlying Ordovician molasse (Gehrels et al., 2006a; Bhargava et al., 2011). Given that those Cambro–Ordovician detrital zircons were almost certainly sourced from the Cambro–Ordovician granites intruded into the Greater Himalaya, their presence in the Ordovician molasse implies very rapid exhumation of those granitoids following their emplacement at depth. Contemporaneous with that early Paleozoic deformation, regional metamorphism of the Greater Himalaya sequence (including the Bhimphedi Group) is evident from Cambrian–Ordovician ages of monzanite inclusions in garnet (Gehrels et al., 2003, 2006a), and by the observation that some Cambro–Ordovician plutons contain Neoproterozoic to Cambrian metamorphic xenoliths with fabrics that predate the host intrusive (Cawood et al., 2007). Other Cambro–Ordovician intrusives are observed to cross-cut the metamorphic fabrics of their Neoproterozoic–Cambrian hosts directly.

4.14.8. Sibumasu

Sibumasu is a N–S elongate terrane that comprises much of eastern Myanmar, western Thailand and the Malay Peninsula, and it stretches south to northern Sumatra and north to the western Yunnan Province of China (Fig. 11). To the east, Sibumasu is juxtaposed against Annamia along the Changning-Menglian suture, and to the west it is bounded by the West Burma block along the Sagaing fault. In western Thailand and the Malay Peninsula, the early Paleozoic sequence of the terrane is broadly characterized by middle to late Cambrian shallow water siliciclastic rocks with tuffaceous interbeds that pass upwards into thick Ordovician to Silurian deep-water carbonates and shales (Lee, 2006; Ridd et al., 2011). Comparably, in the Shan Plateau of eastern Myanmar, Cambrian clastic rocks and local late Cambrian volcanics are overlain by Ordovician and Silurian carbonates and late Silurian–Early Devonian black shales (Mitchell et al., 2012). In contrast, in the western Yunnan Province of China, where the terrane is further subdivided into the Tengchong and Baoshan blocks, the Ordovician and Silurian sequence is dominated by coarser clastic rocks and is separated from underlying late Precambrian–Cambrian rocks, locally including middle to late Cambrian mafic volcanics, by a latest Cambrian–Early Ordovician unconformity (Zhang et al., 2014e; Li et al., 2016) (Fig. 14; Table 1). Those blocks also experienced voluminous early Paleozoic granitoid plutonism beginning in the middle Cambrian and continuing into the Middle–Late Ordovician (Liu et al., 2009; Li et al., 2016), whereas to the south in Sibumasu, early Paleozoic plutonism is known only from a few scattered granites and gneisses in northwestern and peninsular Thailand (Ridd et al., 2011; Lin et al., 2013b; Kawakami et al., 2014) and from the western edge of the Shan Plateau (Mitchell et al., 2012). Although the tectonic setting of those early Paleozoic plutons is still debated, together with local middle to late Cambrian volcanics scattered across Sibumasu and the latest Cambrian–Early Ordovician unconformity in Tengchong-Baoshan, they are most commonly attributed to active margin processes (Wang et al., 2013g; Li et al., 2016). Concerning its paleogeography, analyses of the faunas and detrital zircon populations of the early Paleozoic rocks of Sibumasu have revealed strong ties to northwestern Australia, but also notable faunal links to South China in the Late Ordovician (Fortey and Cocks, 1998; Cocks et al., 2005; Cai et al., 2017).

4.15. Baltica

4.15.1. East-Northeast Baltica (Timanide margin)

The early Paleozoic history of the eastern margin of Baltica is set between two major orogenic events that strongly affected the margin: the late Neoproterozoic Timanide orogeny and the late Paleozoic Uralian orogeny. The latter was a protracted event, beginning with the accretion of oceanic island-arcs in the Late Devonian and continuing until the collision with Kazakhstania in the Late Carboniferous, and it undoubtedly reshaped the pre-Devonian margin. Structurally and lithostratigraphically, the Urals are divided into several meridional zones that broadly characterize the various continental, oceanic, and island arc domains that were telescoped together during late Paleozoic orogenesis. The Main Uralian fault, which bisects the length of the range, represents the fundamental divide between western zones that collectively comprise the former (pre-Uralian) continental margin and its cover, and eastern zones that comprise former oceanic and island arc domains, now accreted along the continental margin (Ivanov et al., 2013). Because those western and eastern zones represent fundamentally different early Paleozoic domains, it is practical to consider them independently, and I begin with a discussion of the early Paleozoic continental margin, as it is known from the rocks preserved in the western zones.

Following major Timanide orogenesis in the late Neoproterozoic, the eastern margin of Baltica remained elevated during the early to middle Cambrian, and was characterized by a period of non-deposition then (Maslov et al., 1997; Sliaupa et al., 2006). Rare exposures of early Cambrian reef-bearing limestone and basalt occur in the southern Urals only as olistoliths within younger

Paleozoic sediments (Ryazantsev et al., 2008; Puchkov, 2013). Significant deposition along the margin first resumed with the appearance of late Cambrian to Early Ordovician rift facies, which unconformably overlie the Precambrian basement along the full length of the margin (although preserved only in restricted areas), from the northern polar Urals to the southern Urals (Maslov et al., 1997; Puchkov, 2002). Further south, contemporaneous Cambro-Ordovician subsidence is likewise inferred from seismic data and borehole records from the Peri-Caspian basin (Volozh et al., 2003; Sliaupa et al., 2006). The syn-rift deposits along the pre-Uralian margin include coarse, poorly-sorted, polymict conglomerates and sandstones interlayered with subalkaline basalts and rhyolitic tuffs, and exhibit large lateral thickness and facies variations (Puchkov, 2002). Following late Cambrian to Early Ordovician rifting, a passive margin was established and the deposition of continental shelf and slope-type sediments reigned through the rest of the Ordovician, Silurian and into the Devonian (Table 1). Clearly reflecting an east-facing passive margin, those deposits are characterized by a western facies of shallow water, reef-rich carbonates and terrigenous clastic rocks (continental shelf-type deposits) that pass eastward into deep water flysch, condensed units of shale and chert with pelagic faunas, and minor carbonates (continental slope and rise-type deposits) (Puchkov, 2002; Ivanov et al., 2013). Prior to the encroachment of island arcs in the Devonian, lithologic variations in those passive margin strata are mostly interpreted as changes in global eustasy, although a sharp regression in the mid-Silurian and a contemporaneous kink in regional tectonic subsidence curves may hint that the margin was affected by weak tectonism then (Sliaupa et al., 2006; Antoshkina, 2008). Another notable departure from typical passive margin conditions occurred in the Late Ordovician to early Silurian, when a variety of intrusives invaded several areas of the continental margin; but while the origins of those intrusives remain largely enigmatic, they have so-far been ascribed to mantle plume activity and not regional tectonism (Puchkov, 2013).

In contrast to those early to middle Paleozoic continental margin rocks to the west of the Main Uralian fault, early to middle Paleozoic rocks to the east of the fault (and in allochthons thrust westward over it) comprise a complicated mosaic of oceanic and island arc assemblages and, putatively, microcontinent blocks (Ivanov et al., 2013; Puchkov, 2013). Among the oceanic assemblages, mafic-ultramafic massifs interpreted as ophiolitic complexes are widespread, being distributed meridionally along the full length of the orogen as discrete bodies of various forms. In the southern Urals, a complete ophiolitic sequence is recognized in the Kempersay ophiolite in the Sakmara allochthon, where the mafic-ultramafic massif includes mantle peridotites, gabbroic rocks, sheeted dolerite dikes and basaltic pillow lavas associated with pelagic sediments (Savelieva et al., 1997). At the base of that ophiolitic massif is an amphibolite, dated at ~400 Ma, which is interpreted as a metamorphic sole formed during an episode of intraoceanic inversion (obduction) in the Uralian ocean basin (Savelieva et al., 2002). A similar ~415 Ma metamorphic age is also reported from the sole of the neighboring Khabarny ophiolitic massif (Belova et al., 2010). Other indications of late Silurian–Early Devonian tectonism in the southern Urals are reflected in ~420–400 Ma metamorphic ages reported from ophiolitic material along the Main Uralian fault, and in the occurrence of late Silurian–Early Devonian mafic dikes that crosscut many of the ophiolitic massifs there (Savelieva et al., 1997; Belova et al., 2010; Ryazantsev et al., 2015). The ophiolitic massifs themselves are estimated to be mostly Early to Middle Ordovician in age, according to the occurrence of Early–Middle Ordovician conodonts among their pelagic sediments, and from sparse isotopic ages (Savelieva et al., 2002; Puchkov, 2009). However, components of younger ophiolites are also present in the southern Urals, notably Early Devonian supra-subduction ophiolites associated with the initiation (or resumption) of subduction there then (Belova et al., 2010; Savelieva, 2011). Devonian ophiolites may also be present in the middle and northern Urals, where they comprise small, strongly dismembered bodies associated with Devonian sediments and volcanics, but they are poorly characterized. In the polar Urals, ophiolitic complexes are mostly represented by ultramafic bodies that include subordinate gabbros and sometimes dolerite dikes, but are always separated from their volcano-sedimentary components. Some of the ophiolitic complexes here too appear to be Cambro–Ordovician in age, according to sparse isotopic ages, but isotopic dating of the ultramafic rocks has also yielded Neoproterozoic ages, indicating that some components of those ultramafic massifs may be significantly older or recycled (Puchkov, 2009; Savelieva, 2011).

The oldest Paleozoic island arc vestiges recognized in the Urals are Middle to Late Ordovician volcanic successions in the southern Urals, which occur both in the Sakmara allochthon and to the north, along the Main Uralian fault. Those successions, which together are designated the Guberlya arc, comprise an initial sequence of Middle Ordovician pyroclastics, tuffs, basalts and minor rhyolites passing upward into a Late Ordovician volcanic series of basalts, andesites and rhyodacites (Dubinina and Ryazantsev, 2008; Ryazantsev et al., 2008). Arc magmatism of the Guberlya arc subsequently waned during the latest Ordovician, and ceased by the early Silurian, when the arc was capped by carbonaceous shales and cherts. Island arc magmatism resumed in the southern Urals in the Early Devonian, but in the Magnitogorsk zone to the east of the Guberlya arc (Brown et al., 2011). Arc magmatism there continued through the Late Devonian, when the Magnitogorsk arc collided with the margin of Baltica. In the middle, northern and polar Urals, island arc volcanism first appeared in the Late Ordovician as bimodal volcanic rocks of the nascent Tagil arc. In the Silurian, the Tagil arc evolved into a more differentiated system characterized by basaltic, andesitic and dacitic calc-alkaline lavas, abundant tuffs, volcaniclastic sediments and laterally equivalent carbonate and chert successions (Puchkov, 2013). In the mid-Silurian (~430–420 Ma), the Tagil arc was also invaded by large, zoned mafic-ultramafic bodies which, although poorly understood, are thought to be co-magmatic with the calc-alkaline volcanics on the basis of their spatial relationship and similar geochemistry (Herrington et al., 2005; Ivanov et al., 2013). In the Early Devonian, the locus of magmatism shifted eastward, and the former (western) axis of the arc was capped by carbonates, whereas in the east, magmatism continued into the Late Devonian (Herrington et al., 2005; Puchkov, 2013).

Purported Precambrian microcontinent fragments among rocks of the oceanic domain (east of the Main Uralian fault) occur in the East Uralian zone, to the east of the Ordovician–Devonian island arcs of the Magnitogorsk-Tagil zone. The East Uralian zone is comprised by tectonic lenses of variably metamorphosed Ordovician to Silurian basinal rocks and Devonian to Carboniferous volcaniclastic rocks and sediments, together with large granite-gneiss complexes (Görz et al., 2006). The expansive granites, which are Late Devonian to Permian in age, were conventionally thought to have been derived from the gneisses, which are preserved along the margins of the granites. On the basis of their high metamorphic grade and the premise that they pre-date the granites, the gneisses have long been assumed to represent Precambrian microcontinent blocks, possibly detached from the eastern margin of Baltica. However, isotopic dating of the gneisses has failed to detect any Precambrian components (Friberg et al., 2000; Görz et al., 2004), and has rather revealed the gneisses to be the deformed margins of the late Paleozoic granitoids (Görz et al., 2006). Consequently, there

exists, at present, no unequivocal evidence of microcontinents in the East Uralian zone.

To the east of the East Uralian zone lies the poorly exposed (and accordingly poorly understood) Trans-Uralian zone and Turgai belt, which are mostly comprised by mid-to-late Paleozoic accretionary complexes and Devonian–Carboniferous calc-alkaline volcano-plutonic complexes (Herrington et al., 2005; Hawkins et al., 2017). These have conventionally been interpreted to represent arc-accretionary systems of the active northwest margin of Kazakhstania, generated by east-dipping subduction of the Uralian Ocean beneath Kazakhstania prior to its Late Carboniferous collision with Baltica (Bea et al., 2002). Although Hawkins et al. (2017) argues that the Turgai belt may have already been assembled against the Uralian margin of Baltica by the late Early Carboniferous on the basis of similar mid-Carboniferous ore deposits in the Valerianovsky arc (of the Turgai belt) and Magnitogorsk arc.

4.15.2. Southeast Baltica (Scythian platform)

The early Paleozoic margin of southeast Baltica is challenging to investigate because it is extensively buried beneath a thick package of younger sedimentary cover, and so interpretations about its nature are mostly pieced together from geophysical survey data and scattered borehole observations. Nevertheless, from these data it is apparent that by the beginning of the Paleozoic, the craton of Baltica was flanked to the southeast by the Scythian platform, which broadly comprises a Precambrian basement overlain by early Paleozoic sediments and a great thickness of younger cover. From east to west, the Scythian platform spans the northern Caucasus region of southern Russia (between the Karpinsky Swell and the Greater Caucasus) and continues across Crimea and, controversially, may extend westward into the Pre-Dobrogea depression of southern Ukraine, Moldova and eastern Romania (Saintot et al., 2006; Starostenko et al., 2015) (Fig. 13). From boreholes in the Pre-Dobrogea depression, Seghedi (2012) constructed a synthetic stratigraphy for the Scythian platform there, characterized by a Neoproterozoic crystalline basement unconformably overlain by latest Neoproterozoic to early Cambrian conglomerates, sandstones and siltstones that grade upward into generally finer-grained Ordovician and early to middle Silurian clastic rocks and minor limestones. Those early Paleozoic rocks are capped by a late Silurian sedimentary hiatus and the Early Devonian strata that follow are characterized by an upward coarsening sedimentary sequence with interbedded andesitic to dacitic tuffs, overlain by Middle to Late Devonian carbonates. Because that early Paleozoic sequence closely mirrors others of the early Paleozoic passive margin of south Baltica—first interrupted in the Silurian by the arrival of Avalonia—Saintot et al. (2006) argue that the Pre-Dobrogea depression is actually a continuation of the craton rather than a component of the Scythian platform, but in any case the passive nature of the early Paleozoic margin there is well evident (Table 1).

The southern boundary of the Pre-Dobrogea depression is demarcated by the Sfântu Gheorghe fault, across which lies the North Dobrogea orogen and the Moesian platform, which together comprise a mosaic of Precambrian–Paleozoic blocks of uncertain early Paleozoic affinity, but possibly including Baltic, Avalonian and Gondwanan elements. The composite North Dobrogea orogen, which is separated from Moesia by the Peceneaga-Camena fault, includes variably metamorphosed and structurally-juxtaposed Neoproterozoic-Cambrian metamorphic basement complexes and Ordovician to Devonian sequences of deep marine sediments (in the north) and shelf sediments (in the south) (Seghedi, 2012). An Avalonian or Cadomian early Paleozoic affinity is broadly inferred for those units on the basis of detrital zircon populations from both the metamorphic complexes and the cover rocks, and the occurrence of late Neoproterozoic granites in the former (Balintoni and Balica, 2016). The north-south association of the Ordovician to Devonian deep and shallow water sedimentary successions there could also reflect a north-facing continental margin as would be expected along the early Paleozoic north margin of Gondwana (Oczlon et al., 2007).

The Moesian platform to the southwest of the North Dobrogea orogen is divided by the Intra-Moesian fault into West and East Moesia, and East Moesia is further subdivided by the NW–SE trending Capidava-Ovidiu fault into Central and South Dobrogea (Fig. 13). In Central Dobrogea, where the basement of the Moesian platform is exposed as Neoproterozoic amphibolite-facies metabasic rocks and metasediments, late Neoproterozoic turbidites in tectonic contact with the basement have yielded detrital zircon age spectra similar to those known from the early Paleozoic north margin of Gondwana (Seghedi, 2012; Balintoni and Balica, 2016). Those late Neoproterozoic turbidites furthermore bear volcanic clasts and indicators of north-directed paleoflow, consistent with a location along the north-facing active margin of Gondwana. In the South Dobrogea, early Paleozoic sedimentary strata include Ordovician tuffites and are capped by a mid-Silurian angular unconformity, followed by late Silurian argillites and an Early–Middle Devonian upward coarsening clastic sequence (Oczlon et al., 2007; Seghedi, 2012). Together, those observations may suggest that the Moesian platform (or part of it) traveled northward with Avalonia in the Ordovician and accreted to the southern margin of Baltica in the Silurian. However, along the Capidava-Ovidiu fault between the Central and South Dobrogea lies a sliver of putatively Paleoproterozoic basement (the 'Palazu terrane') that is speculated to be a detached fragment of Baltica. The positioning of that sliver could imply either that Paleozoic-Mesozoic strike-slip shuffling along the south margin of Baltica was complex (Oczlon et al., 2007), or that some of the assumed terrane affinities are erroneous. Owing to these uncertainties, North Dobrogea and the Moesian platform are excluded from the plate model.

In the Greater Caucasus, which demarcates the southern boundary of the Scythian platform between the Black and Caspian seas, early Paleozoic rocks are found in several orogen-parallel tectonostratigraphic zones, from north to south: the Bechasyn, Fore Range and Main Range zones (Fig. 13). In the Bechasyn zone, latest Neoproterozoic–Cambrian greenschist-facies metasedimentary and metavolcanic rocks are unconformably overlain by middle(?)–late Cambrian to Ordovician conglomerates and sandstones that pass conformably upward into Silurian–Early Devonian shales, limestones and cherts (Somin, 2011). The Silurian strata also include a horizon of conglomerate and limestone olistoliths bearing middle Cambrian faunas, which may reflect the occurrence of minor tectonism then. In the Fore Range zone to the south, which comprises a complicated mosaic of structurally juxtaposed Paleozoic assemblages, early Paleozoic rocks include an overturned Silurian ophiolite and a Silurian–Devonian volcano-sedimentary sequence of basalts, terrigenous sediments, chert, conglomerates with clasts of chert and volcanic rock, and olistostromes (Adamia et al., 2011; Somin, 2011). A variety of apparently middle to late Paleozoic metamorphic rocks there may also have early Paleozoic protoliths, but this remains to be substantiated. Similarly, in the Main Range zone, an array of late Paleozoic metamorphic rocks are thought to have been derived from early to middle Paleozoic sedimentary and volcanic protoliths with interpreted affinities ranging from continental rift sequences to supra-subduction ophiolites and island arc successions to accretionary complexes, but much about the ages and genesis of those successions remains to be clarified (Adamia et al., 2011; Somin, 2011).

4.16. North Kara terrane

As noted in section 4.1.1, the Taimyr Peninsula of northern Siberia is conventionally divided into three east-west trending domains: South, Central and North Taimyr (Fig. 2). South and Central Taimyr are understood to comprise the Neoproterozoic to mid-Carboniferous northwest-facing passive margin of Siberia, which was destroyed in the late Carboniferous by the arrival of allochthonous North Taimyr (Bradley, 2008; Pease and Scott, 2009). Owing to geological similarities between North Taimyr and the Severnaya Zemlya Archipelago, it is likely that those areas together comprise a larger microcontinent, and potential field data suggest that terrane may extend to the southwest to include the northeastern Kara Shelf (Lorenz et al., 2008). Here I follow Lorenz et al. (2008) in defining the 'North Kara terrane' (NKT) as extending from North Taimyr (in the southeast) to the edge of the South Kara basin (in the southwest) and northward to the continental edge of the Eurasia basin.

The oldest rocks of the NKT are deformed, low-grade metasedimentary sequences of Neoproterozoic to Cambrian age, and are exposed in North Taimyr and the Severnaya Zemlya Archipelago (on Bol'shevik and October Revolution Islands) (Lorenz et al., 2008; Pease and Scott, 2009), and probably on other small islands, such as those of the Izvesti Tsik Archipelago (Ershova et al., 2015a). Those metasedimentary sequences are dominated by sandstone, siltstone and mudstone cycles and are interpreted as turbidites; notably some coarse clastic horizons have been found to bear clasts of granite, felsic to intermediate volcanic rocks and schists (Lorenz et al., 2008). The top of the Cambrian sequence of the NKT is everywhere capped by an angular unconformity; the youngest deposits beneath the unconformity bear late Cambrian faunas (Lorenz et al., 2007). Above the basal conglomerates that seal the unconformity on October Revolution Island, finer-grained clastic strata pass upward into carbonates bearing Early Ordovician faunas and volcanic rocks that have yielded Cambro–Ordovician isotopic ages, revealing that the time-span represented by the unconformity was brief (Lorenz et al., 2007). The Early Ordovician volcanic rocks of October Revolution Island include andesites, trachytes, rhyolites and tuffs, and were emplaced concurrently with shallow intrusions of gabbro, syenite and granite into the Cambrian and Early Ordovician strata. The remainder of the Ordovician sequence there is characterized by medium- and fine-grained clastic rocks, carbonates, and locally thick Early to mid-Ordovician evaporites (Bogolepova et al., 2006).

Silurian–Devonian rocks of the NKT are widely exposed in the Severnaya Zemlya Archipelago excepting Bol'shevik Island. According to those sequences, in the early to mid-Silurian the NKT was dominated by the deposition of thick, platform carbonates, reflecting stable shelf conditions (Männik et al., 2009). In the late Silurian, red marls appeared, marking an early incursion of terrigenous material, followed by a thick sequence of coarse clastic rocks in the latest Silurian to Early Devonian (Lorenz et al., 2008). Those SiluroDevonian clastic deposits, which were transported from the west and northwest, are interpreted as molasse derived from the developing Caledonide orogen of northwest Baltica, correlative with the Old Red Sandstone facies of the British Isles.

Although it is well-accepted that the NKT was allocthonous to Siberia prior to their late Paleozoic unification, whether the NKT comprised an independent microcontinent during the early to mid-Paleozoic, or rather represented a prolongation of Baltica, is unsettled. Metelkin et al. (2005) presented early Paleozoic paleomagnetic data from Severnaya Zemlya and concluded that the NKT did not drift coherently with Baltica prior to the late Paleozoic. On the other hand, a number of independent observations seem to imply that the NKT was proximal to Baltica since the late Neoproterozoic. Detrital zircons from the Neoproterozoic–Cambrian turbidites of North Taimyr yield exclusively late Neoproterozoic ages that closely resemble the detrital zircon age spectra from similarly-aged turbidites in Novaya Zemlya, where there is furthermore a Cambro–Ordovician unconformity analogous to that observed on October Revolution Island (Pease and Scott, 2009). Regional potential field data also show a continuation of strong magnetic anomalies from the NKT into the northeast of Novaya Zemlya and the eastern Barents Sea, where no Paleozoic sutures are known (Lorenz et al., 2008; Daragan-Sushchova et al., 2014). Although not necessarily requiring tectonic coherence, Ordovician and Silurian faunas of the NKT bear a strong affinity to those of Baltica, suggesting that they were at least near one another then (Männik et al., 2009). Finally, the east- to southeast-transported Siluro–Devonian molasse of Severnaya Zemlya, if of Caledonian provenance as assumed, implies that the NKT and Baltica were juxtaposed at least by that time.

5. Paleomagnetic framework

In the following, the paleomagnetic data that constitute the quantitative paleogeographic framework used to construct the plate model are succinctly reviewed; new data compilations are also presented in Tables 2–4. Fig. 16 displays the data-based ('observed') apparent polar wander paths (APWPs), as computed for each of the major tectonic blocks, and a corresponding model-based APWP derived from the final plate model. Because paleomagnetic data from the Kazakh terranes have been subjected to vertical axis rotations (both locally and via regional oroclinal bending), they are treated separately; their inclination-only data is displayed in Fig. 17, where they are plotted against paleolatitudinal curves from the final plate model.

For Baltica and Gondwana, the early Paleozoic paleomagnetic compilation of Torsvik et al. (2012) was adopted, which includes 25 Cambrian to Silurian (500–419 Ma) poles from Baltica and 14 Cambrian to Early Devonian (500–409 Ma) poles from Gondwana. However, the temporal distribution of those poles is strongly heterogenous; using a 20-Ma moving window to construct an APWP, there are no poles defining the APWP of Gondwana at 430 and 420 Ma, and only one pole defining the path at 450, 440 and 410 Ma. Likewise, the APWP of Baltica nearly lacks definition at 440 Ma (one pole at 432 Ma). The splined paths of Torsvik et al. (2012) were therefore employed in the plate model (Fig. 16a,b). Notably, the sole pole defining the APWP of Gondwana at 410 Ma results in a sharp cusp in the path then, which is highly-smoothed by the alternative splined path. However, such a cusp could mark an important kinematic reorganization event, and thus presents a key feature to be evaluated through new paleomagnetic work.

The early Paleozoic paleomagnetic compilation for Siberia (Table 2) is taken from Torsvik et al. (2012) (updated from Cocks and Torsvik (2007)), with new poles added from Pavlov et al. (2012) and Powerman et al. (2013), yielding, in total, 30 poles from 510 Ma to 420 Ma. As discussed by Smethurst et al. (1998) and Pavlov et al. (2008), among others, early Paleozoic paleomagnetic poles derived from sites in the northwest of the Siberian craton (Anabar-Angara block) appear consistently westward offset from similarly-aged poles derived from sites in the southeast of the Siberian craton (Aldan block), suggesting that some post-early Paleozoic relative motion occurred between them. Such relative motion can be attributed to the Siluro–Devonian opening of the Vilyuy basin between those blocks, and from geological considerations Smethurst et al. (1998) (and references therein) and Pavlov et al. (2008) derived comparable estimates for the position of the pole of relative rotation between them: 60°N, 100°E and 62°N, 117°E, respectively. Although the uncertainty of the paleomagnetic data and the geometries of the APWPs do not lend themselves to a

Table 2
Paleomagnetic poles used in the construction of the plate model.

Block/Formation	Age	Glat (° N)	Glon (° E)	Plat	Plon	Ref
North Siberia						
Moyero River sediments	444	68	104	14	304	a
Angara River sediments*	455	58.5	99.8	29.5	320.2	b
Kulumbe section	461	68	88.8	24.1	332.4	c
Stolobovaya section	461	62.1	92.5	22	338	c
Moyero River sediments	463	68	104	23	338	a
Angara River sediments	468	58.5	99.8	35.2	333.2	b
Moyero River sediments	469	68	104	30	337	a
Guragir Formation*	470	68	88.8	30.9	332.7	a
Angara River sediments	475	58.5	99.8	36.4	338.2	b
Moyero River sediments	478	67.5	104	33.9	331.7	a
Uigur and Nizhneiltyk Formations	483	68	88.8	35.2	307.2	a
Moyero River sediments	483	68	104	40	318	a
Kulumbinskaya Formation	500	68	88.8	36.1	310.7	a
Moyero River sediments	500	68	104	37	318	a
Yunkyulyabit-Yuryakh Formation	507	70.9	122.6	36.4	319.6	a
Kulumbe River section	507	68	88.4	41.9	315.8	a
Khorbusuonka Amgan and Mayan seds.	507	71.5	124	43.7	320.5	a
South Siberia						
Nyuya and Lena River sediments*	432	60.6	116.3	17.6	282	d
Nyuya and Lena River sediments*	433	60.7	116.3	18.6	281.9	e
Lena River sediments*	449	60.5	116.4	21	289	a
Nyuya River sediments*	451	60.6	116.3	31.3	309.5	d
Kudrino section	461	57.7	107.99	21.1	323.4	c
Krivaya Luka Formation*	464	59.7	118.1	25.6	297.9	a
Krivaya Luka Formation*	464	59.7	118.1	28.2	307.1	a
Krivolutsky Suite	465	57.6	107.8	32.6	317	f
Lena River sediments*	468	59.8	118.1	32	319	a
Lena River redbeds*	470	60	114	25	317	a
Surinsk Formation*	480	58.3	109.61	42.2	308.1	a
Verkholensk Formation*	501	58.5	109.8	37.69	304	a
Maya River sediments	510	60	132	45.8	295	c
North China						
Zhaohuajing and Hanxia Groups	432	37.2	105.9	60.1	339	g
Middle Ordovician carbonates	464	37.3	109.3	31.5	327.7	h
Tianjinshan and Miboshan Formations	470	37.2	105.5	31.8	326.5	i
Late Cambrian-Ordovician carbonates	478	36	118	28.8	310.9	j
Early Ordovician carbonates	478	37.1	108.3	37.4	324.3	h
Zhaogezhuang area carbonates	480	39.7	118.5	32.9	294.6	k
Late Cambrian carbonates	491	37.2	109.2	31.7	329.6	h
Middle Cambrian sediments	503	37.2	109.2	37	326.7	h
South China						
Silurian sediments*	432	27.5	108	14.9	196.1	l
Silurian sediments*	432	28.5	109	4.9	194.7	m
Pagoda Formation, Sichuan Province	456	32.4	106.3	−45.8	191.3	n
Hongshiya Formation, Yunnan Province	*464*	*25.5*	*103*	*−38.9*	*235.7*	o
Xingshan-Zigui section, Hubei Province	*470*	*31.2*	*110.4*	*−38.4*	*154.9*	p
Douposi Formation, Wangcang section	503	31.9	105.9	−39.5	185.1	q
Douposi Formation, Guangyuan area	503	32.4	106.3	−51.3	166	r
Tarim						
"Devonian" redbeds	419	40.5	78.6	16.5	165	s
Silurian sediments	432	40.5	79.7	12.1	158.4	t
Aksu-Kalpin-Bachu area sediments	458	40.7	79.4	−40.7	183.3	u
Ordovician limestones	478	41.3	83.4	−20.4	180.6	t
North Kara						
Ust'spokoininskaya and Samoilovichskaya Fms.	423	79.6	96.3	10.5	183.5	v
Stroininskaya and Ozerninskaya Fms.	458	79.6	96.3	−10.1	212	v
Kruzhilikhinskaya and Kurchavinskaya Fms.	485	78.5	98.2	−26.9	255.5	v

Age: estimated numerical age of pole (in Ma); Glat/Glon: latitude/longitude of sampling site; Plat/Plon: latitude/longitude of paleomagnetic pole.
*Poles corrected for inclination shallowing (assuming $f = 0.6$) prior to construction of APWP (pole listings in Table 2 are *uncorrected*). Italicized poles are rejected. References: a, compiled in Cocks and Torsvik (2007); b, Pavlov et al. (2012); c, Pavlov et al. (2008); d, Powerman et al. (2013); e, Shatsillo et al. (2007); f, Rodionov et al. (2003); g, Huang et al. (2000a); h, Huang et al. (1999b), i, Huang et al. (1999a); j, Zhao et al. (1992); k, Yang et al. (2002); l, Huang et al. (2000b); m, Opdyke et al. (1987); n, Han et al. (2015); o, Fang et al. (1990); p, Hanning et al. (1998); q, Lixin et al. (1998); r, Yang et al. (2004); s, Li et al. (1990); t, Fang et al. (1996); u, Sun and Huang (2009); v, Metelkin et al. (2005).

Table 3
Apparent polar wander paths (APWPs) for the major continental blocks, built from data listed in Table 2 (after inclination correction).

Block/time (Ma)	N	Plat	Plon
North Siberia			
440	1	14.0	304.0
450	2	23.3	311.9
460	7	29.8	334.0
470	8	30.7	335.8
480	5	38.0	326.6
490	4	37.2	313.4
500	5	39.1	316.9
510	5	39.1	316.9
South Siberia			
430	2	11.6	283.0
440	3	13.0	285.0
450	2	24.7	298.8
460	7	27.9	313.0
470	7	30.2	313.1
480	2	36.3	314.1
490	1	49.4	310.0
500	2	44.1	300.2
510	2	44.1	300.2
Siberia combined			
400*	-	−4.7	118.4
410*	-	−7.4	114.1
420*	-	−10	112.3
430	2	−11.64	115.4
440	4	−13	119.4
450	4	−22.98	132.6
460	14	−27.18	150.4
470	15	−28.98	151.8
480	7	−36.51	147.2
490	5	−39.05	135.8
500	7	−39.92	136.9
510	7	−39.92	136.9
North China (spline path)			
430	-	59.8	339.3
440	-	48.7	337.5
450	-	39.4	334.9
460	-	33.6	330.3
470	-	32.3	322.0
480	-	33.3	312.7
490	-	33.5	320.9
500	-	35.5	327.2
South China (spline path)			
430	-	11.8	191.0
440	-	−13.3	191.5
450	-	−35.0	191.6
460	-	−48.2	190.4
470	-	−56.3	187.7
480	-	−56.5	187.7
490	-	−53.9	180.0
500	-	−47.8	177.2
Tarim (spline path)			
420	-	23.0	156.5
430	-	15.8	153.8
440	-	−2.3	158.7
450	-	−25.6	170.2
460	-	−37.6	181.8
470	-	−32.7	184.1
480	-	−19.1	180.8

N: number of input poles (for moving average calculations); Plat/Plon: latitude/longitude of paleomagnetic pole. The Siberian paths were built by moving average using a 20-Ma moving window. The combined Siberian path was constructed after a 13° rotation of the South Siberian poles about a pole at 60°N/110°E (see text).
*Interpolated poles taken from Torsvik et al. (2012). The North China, South China and Tarim APWPs are spline paths constructed without weighting and using a smoothing factor of 300.

rigorous identification of the exact position of the relative rotation, Pavlov et al. (2008) determined, from a least-squares approach, the best-fitting rotation pole to be at approximately 55°N, 112°E, substantiating the pole positions estimated from the geology and geometry of the Vilyuy basin. Application of a ~13°–14° rotation

Table 4
Inclination-only paleomagnetic data used in the construction of the plate model.

Block/formation	Age	Glat (° N)	Glon (° E)	Inc (°)	a95	Plat	Ref
North Tian Shan zone (south Kazakhstan/north Kyrgystan)							
Koiche Formation and late Silurian–Early Devonian rocks*	419	43.8	75.5	36.3	12.4	20.2	a
Botmoynak Formation, west Kyrgyz Range*	451	42.9	71.5	−18.1	8.8	−9.3	b
Almaly Formation, west Kyrgyz Range*	451	42.8	71.6	−28.0	4	−14.9	b
Late Caradocian sediments, Tabylgaty area*	451	41.7	74.2	−27.6	7	−14.6	b
Late Caradocian sediments, Toluk area*	451	41.9	73.5	−25.1	10.8	−13.2	b
Tertmasu Formation sandstones ('DUN' sites)*	456	41.7	74.3	−25.7	11.4	−13.5	c
Unkurtash Formation sandstones ('DOL-B' sites)*	460	41.9	75.7	−22.1	19.3	−11.5	c
Middle Ordovician redbeds*	464	42.6	73.8	−31.2	9	−16.9	d
Kurday Formation, Kendyktas Ridge*	464	43.0	74.9	−26.9	15	−14.2	a
Stepnyak zone (north-central Kazakhstan)							
Middle Ordovician volcanics, Saga Series	444	52.9	71.5	−19.3	7.2	−9.9	d
Late Ordovician volcanics, Ishim River valley	451	52.5	66.8	−24.3	8.8	−12.7	d
Late Ordovician volcanics and sediments, Bazarbay area	451	53.2	70.3	−21.8	9.5	−11.3	d
Boshekul-Chingiz zone (northeast Kazakhstan)							
Ludlovian volcanics, Chingiz Range	425	48.0	80.7	13.2	8.4	6.7	e
Early Silurian volcanics and redbeds, Chingiz Range	438	48.5	78.2	−2.8	13.3	−1.4	f
Early Ordovician sediments, central Chingiz Range*	478	48.8	79.0	−33	6.3	−18.0	g
Late Cambrian volcanics and sediments, central Chingiz Range	485	48.9	79.0	−35.2	9.8	−19.4	g

Age: estimated numerical age of magnetization (in Ma); Glat/Glon: latitude/longitude of sampling site; Inc: mean inclination; a95: 95% confidence ellipse (in degrees); Plat: paleolatitude.
*Inclinations corrected for inclination shallowing (assuming $f = 0.6$). References: a, Alexyutin et al. (2005); b, Bazhenov et al. (2003); c, Kirscher et al. (2017); d, Bazhenov et al. (2012); e, Levashova et al. (2009); f, Levashova et al. (2003); g, Collins et al. (2003).

about any of those poles yields comparably good fits between the Anabar-Angara and Aldan paleomagnetic data, but use of the 62°N, 117°E pole position implies that up to 200 km of shortening occurred to the SW of the pole, in the region immediately northwest of Lake Baikal. Some evidence of compressional structures in that region have been forwarded by Pavlov et al. (2008), but it is doubtful that they accommodated ~200 km of shortening. Furthermore, there are indications that Vilyuy rifting may have continued further southwest than commonly assumed (Cherepanova et al., 2013; Cherepanova and Artemieva, 2015), which would accordingly shift the location of the estimated rotation hinge. I therefore prefer to use a pole of 60°N, 110°E (approximate midpoint of the other listed poles), and a rotation of 13°, which reduces the magnitude of shortening to the southwest of the pole, but still respects the basin geometry and the paleomagnetic data (Fig. 16c; Table 3). Note, as an episode of deformation internal to Siberia, this rotation is only used to merge the Siberian paleomagnetic data and is not presently implemented in the plate model itself.

The paleomagnetic compilation for North and South China (Table 2) is modified and expanded from Cocks and Torsvik (2013), and includes eight early Paleozoic poles from North China and five from South China. The poles from North China span from 503 to 432 Ma, but only three are of similar (Early Ordovician) age, allowing calculation of a mean pole, and so a splined APWP was generated for North China (Fig. 16d; Table 3). Among the five poles from South China, two are from ~503 Ma and two are from ~432 Ma, allowing the calculation of two mean poles, but otherwise leaving only one individual Late Ordovician pole; a splined path was therefore also generated for South China (Fig. 16e; Table 3). Several additional early Paleozoic poles have been published for South China (two listed in Table 2), but their incorporation would yield a very improbable kinematic scenario wherein South China would be required to drift extremely rapidly from low to high-southerly latitudes and back again during the Ordovician (Fig. 16e).

For the Kazakh terranes, the data compilation is largely taken from Bazhenov et al. (2012), with minor additions from Kirscher et al. (2017) (Table 4). I also follow the simple terrane scheme of Bazhenov et al. (2012), in treating 'Kazakhstania' as three separate blocks during the early Paleozoic, which they label: 'North Tianshan' (NT), 'Stepnyak zone' (SK) and 'Boshekul-Chingiz zone' (BC). This terrane scheme is similar to the one introduced in section 4.5 (the present-day locations of NT, SK and BC are shown as dashed boundaries in Figs. 1 and 17), but is greatly simplified and includes only those blocks from which early Paleozoic paleomagnetic data are available. NT and SK are treated as coherent in the plate model, after back-rotating them (relative to one another) to their position prior to Devonian oroclinal bending (Fig. 6a), whereas BC is treated as independent. Because the Kazakh terranes have been widely affected by vertical axis rotations, declinations are discarded and only inclination data are used for reconstructions (Fig. 17). With the merging of similarly-aged data, the paleolatitude of the combined NT-SK is defined between ~465 Ma and 445 Ma, and at 420 Ma, and the paleolatitude of BC is defined at ~480 Ma, 438 Ma and 425 Ma.

The early Paleozoic paleomagnetic data from Tarim is very poor. The data compilation includes four early Paleozoic poles, but they are based on few samples and their ages are generally ill-constrained. Nevertheless, from these four poles the paleolatitude of Tarim can be crudely defined for the Ordovician (~468 Ma) and Silurian (~425 Ma); a poorly constrained spline path derived from these data is also presented in Table 3.

Concerning the central Mongolian terranes, possibly primary paleomagnetic data include an Ordovician pole from the Dzabkhan microcontinent (Kilian et al., 2016) and Silurian-Devonian results from the Lake-Khamsara zone (Bachtadse et al., 2000), in addition to suspected early Paleozoic remagnetizations from the Tuva-Mongolia (Kravchinsky et al., 2010) and Dzabkhan microcontinents (Evans et al., 1996). However, as these results are all younger than the inferred collision between the CMT and Siberia, and derived exclusively from blocks west of the Mongol-Okhotsk suture zone, they only serve to confirm that those blocks were coherent with Siberia in Ordovician–Silurian time. Because these data cannot be used to independently restore the CMT before its collision with Siberia, or Amuria after its rifting with the opening of the Mongol-Okhotsk Ocean, they are not considered further.

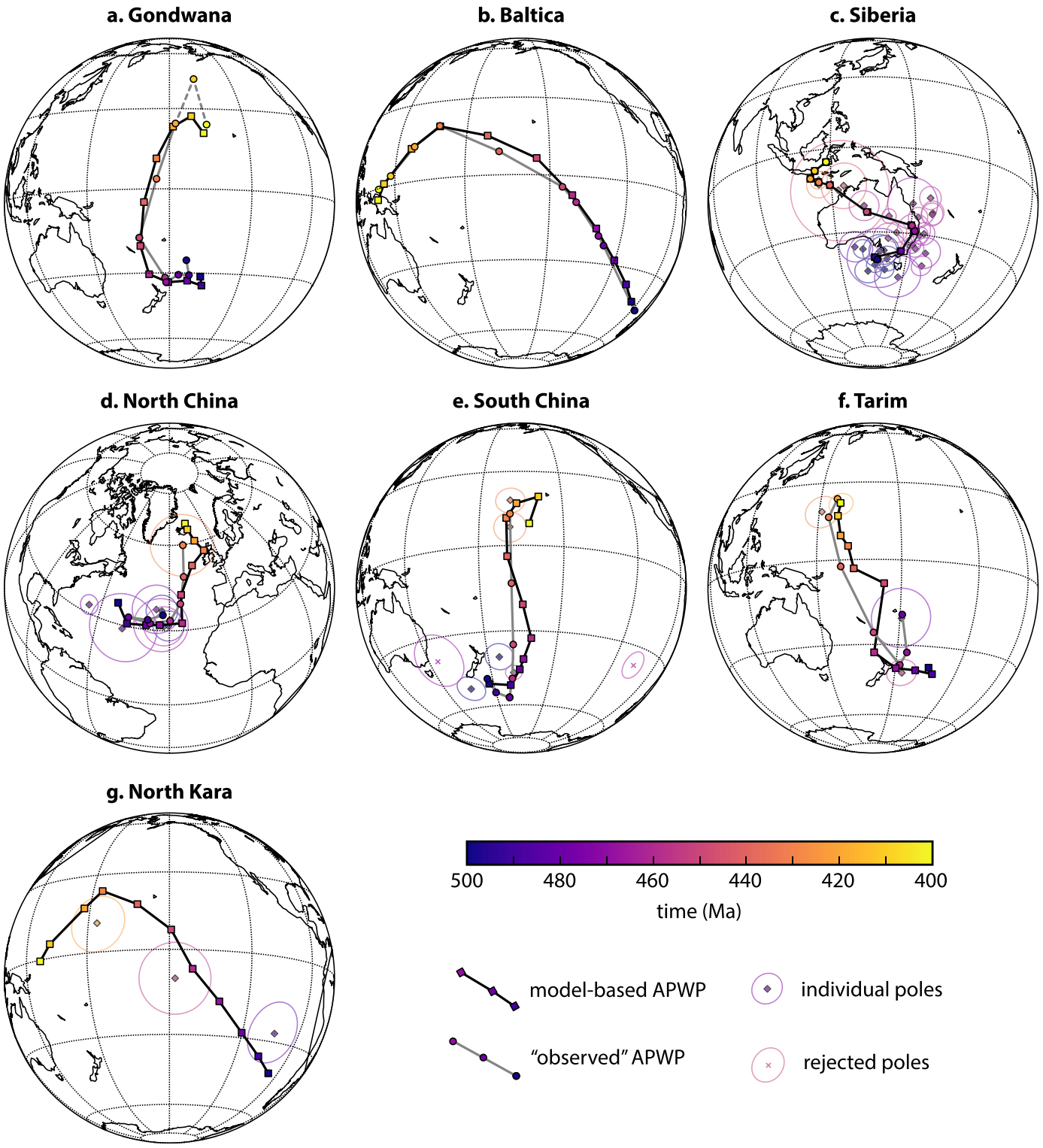

Figure 16. Paleomagnetic poles and apparent polar wander paths (APWPs) from Gondwana, Baltica, Siberia, North China, South China, Tarim and North Kara. Individual paleomagnetic poles are from Table 2 and data-based ('observed') APWPs are from Table 3 and Torsvik et al. (2012). Synthetic (model-based) APWPs are derived from the final plate model.

6. Plate model

This section presents the early Paleozoic (500–420 Ma) full-plate tectonic model of Asia that was constructed by the presented methodology (section 3), using the geologic and paleomagnetic data reviewed above (sections 4 and 5; Tables 1–4). The presentation of the model is broken into three time intervals: (1) Cambrian to Early Ordovician, (2) Middle to Late Ordovician and (3) Silurian. Each of these sub-sections begins with a discussion of the general paleogeographic context of the major blocks and terranes for that time interval, and then proceeds to discuss specific tectonic developments. Because it is helpful to describe orientations using both

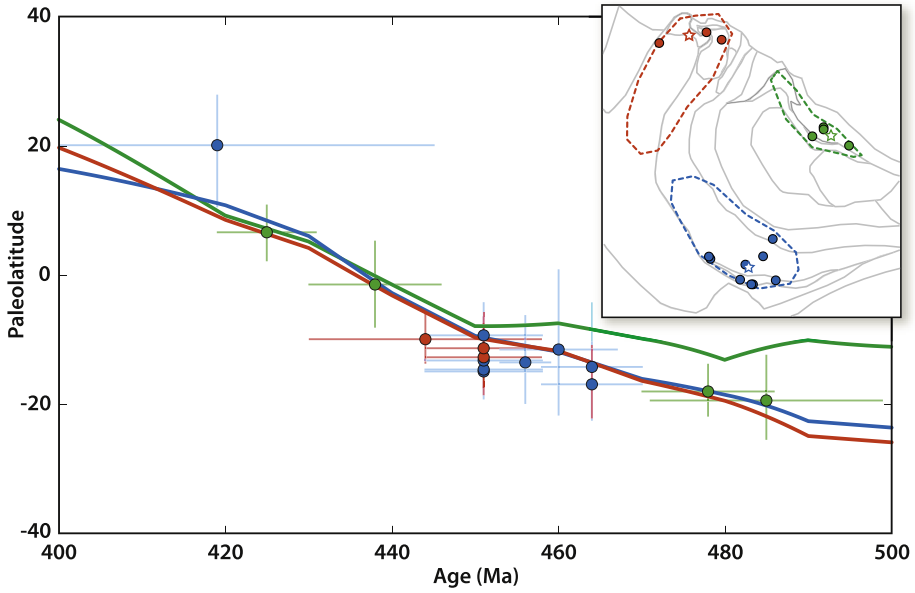

Figure 17. Paleolatitude estimates based on inclination-only data from the Kazakh terranes, listed in Table 4. The inset shows a schematic map of Kazakhstania (present-day), with the three simplified blocks from the plate model shown with dashed outlines: 'North Tianshan' zone (blue), 'Stepnyak' zone (red), and 'Boshekul-Chingiz' (green). The filled circles show the individual paleomagnetic sampling sites from these blocks, which correspond to a paleolatitude estimate of the same color. The three solid colored lines in the paleolatitude plot correspond to predicted paleolatitudes from the plate model for a given reference site (colored stars) within each of the blocks.

model-based (time-dependent) and present-day geographic reference systems, in the following I use *italics* when referring to model-based directions, to distinguish them from present-day directions (in normal font). Figs. 18–26 present instantaneous snapshots from the model in 10-Ma increments from 500 Ma to 420 Ma, in the paleomagnetic reference frame (i.e. relative to the spin-axis). The complete digital plate model, from which reconstructions can be generated for any arbitrary time between 500 Ma and 420 Ma, is available at: www.earthdynamics.org/data/Domeier2018_data.zip.

6.1. Cambrian to Early Ordovician (500–470 Ma)

6.1.1. Geography of the major continents

At the opening of the model at 500 Ma, the bulk of the building blocks of Asia were located in the southern hemisphere, bordered by the Iapetus Ocean to the *west* and the expansive landmass of Gondwana to the *east* and *south*. To the *north*, across the equator, the expansive Panthalassa Ocean occupied nearly the entire northern hemisphere and was largely devoid of continental material. With respect to the LLSVPs at depth, the blocks of Asia mostly occupied the longitudes between them, with the African LLSVP ('Tuzo') flanking them to the *east*, beneath East Gondwana, and the Pacific LLSVP ('Jason'), lying to the *west*, beneath the Iapetus (Fig. 18).

At this time, and continuing through the Early Ordovician, the paleomagnetic record for Gondwana is excellent (Torsvik et al., 2012). During the middle Cambrian, the position of Gondwana was such that northern Africa was at the South Pole, while the Iranian and Afghan terranes were at mid-southern latitudes and western Australia (northeastern Gondwana) straddled the equator. During the late Cambrian and Early Ordovician (Figs. 19–21), Gondwana mostly drifted about the South Pole, but by ~470 Ma it had moved slightly *northward*, so that most of Australia was north of the equator and the apparent position of the South Pole had drifted to the area of present-day northwest Algeria.

Middle Cambrian to Early Ordovician paleomagnetic data from Siberia are also ample, and establish that, at 500 Ma, Siberia was positioned between the equator and 30°S and was north-south inverted ('upside down') relative to its present-day orientation. Through the late Cambrian and Early Ordovician, Siberia slowly rotated clockwise and drifted *northward*, so that by 470 Ma the Aldan block was bestriding the equator.

The paleomagnetic data from Baltica are poor for the middle Cambrian to earliest Ordovician, as only two paleomagnetic poles are available between 530 Ma and 480 Ma, and, despite being considered the same age (~500 Ma), they lie ~35° apart (Torsvik et al., 2012). Nevertheless, those data reveal that during the middle Cambrian Baltica occupied mid-to-high southerly latitudes and was rotated at least 90°clockwise relative to its present-day orientation. Subsequently, between 500 Ma and 470 Ma, Baltica apparently rotated more than ~60° anticlockwise and, after 480 Ma, began drifting *northward*. At this later interval of the Early Ordovician (between 480 and 470 Ma) the motion of Baltica is well-established by seven independent poles.

The paleomagnetic data from North China for this interval, although sparse, are adequate to establish that it occupied the same low-latitudinal band between ~5° and 25°S from 500 Ma to 470 Ma. The paleolatitude for South China, on the other hand, is mostly interpolated during this interval, between middle Cambrian data that place South China at the equator and a Middle-Late Ordovician pole that places it at very low latitude (~10°). Annamia yields no paleomagnetic data for the entire early Paleozoic, and so it is unconstrained by direct observations, but as it bears a strong faunal affinity to South China and Gondwana across this time (Cocks and Torsvik, 2013), I assume it was adjacent to those terranes throughout the model.

Possibly primary paleomagnetic data from Ordovician rocks in northern Tarim have been reported by Fang et al. (1996) and Sun and Huang (2009). Age constraints from field tests are lacking from the former result, and the latter is only constrained to the pre-Late Devonian by a fold-test, but neither result resembles Late Paleozoic to Cenozoic data from Tarim. Together, those data suggest that Tarim was in low-to-moderate southern latitudes (~20°–30°S) and rotated ~110° counterclockwise relative to today. The polarity of those data are not firmly established, so it is alternatively possible that Tarim instead occupied low-to-moderate latitudes in the northern hemisphere then, but I deem this possibility far less likely for reasons discussed below.

Concerning the Kazakh terranes, paleomagnetic data from the Boshekul-Chingiz zone (BC) establish that it was at a latitude of ~20° in the latest Cambrian and Early Ordovician, whereas the paleolatitude of the North Tianshan (NT) and Stepnyak zones (SK) are effectively unconstrained during the Cambrian to Early Ordovician, according to very poor quality data. However, it is reasonable to assume that the NT and SK also occupied low-to-mid latitudes during this interval, as Middle Ordovician data place them at ~15°.

Following Torsvik et al. (2014), the absolute paleolongitude of the continents is estimated by the restoration of LIPs and kimberlites to the margins of the LLSVPs in the lowermost mantle, after correction for true polar wander (TPW). I have adopted the early Paleozoic TPW corrections presented by Torsvik et al. (2014). Although it should be noted that this is not strictly correct—because modifications made to the continental framework model of Torsvik et al. (2014) will in turn alter the TPW estimates derived from it—the changes made herein to the continental rotation model are of secondary order, and are therefore unlikely to be strongly disruptive to the original TPW estimates. In the future, full-plate models could be made in conjunction with new TPW estimations (wherein the full-plate model and TPW estimations are formulated iteratively and together), but this will be laborious and necessitates a global-scale approach, which is beyond the scope of the present work.

Estimation of the middle Cambrian paleolongitude of Gondwana is enabled by the eruption of the Kalkarindji LIP in northwest Australia at ~510 Ma, and by the emplacement of middle Cambrian kimberlites in southern Africa (Torsvik et al., 2014). Together with the middle Cambrian paleomagnetic constraints, these vestiges can be fit to the margins of Tuzo such that the Kalkarindji LIP is positioned above its northeastern margin, and the kimberlites of southern Africa are positioned over its southwest margin (Fig. 18; note that in Figs. 18–26 the reconstructions are presented in the paleomagnetic reference frame, but that the LLSVPs have been back-corrected for TPW to allow direct comparison between LIPs, kimberlites and the LLSVP margins).

Kimberlites were also emplaced into South China at ~510 Ma and into North China during the Early Ordovician (~483–475 Ma) (Fig. 20). Given the low latitudes of those blocks at that time, and the position determined for Gondwana, the simplest longitudinal positioning that would locate them above an LLSVP margin is a position directly *west* of northeast Gondwana (Australia), along the northwest margin of Tuzo. South China could alternatively be positioned over the southeast margin of Tuzo at 510 Ma, or on one of the margins of Jason. However, the former option would place South China on the far side of Gondwana (*north* of West Gondwana) with respect to its Early Devonian position (Domeier and Torsvik, 2014), requiring that South China drift to mid-northerly latitudes during the Ordovician or Silurian in order to skirt around Australia—in contradiction to the existing paleomagnetic data. The latter option would place South China far from Gondwana and directly adjacent to Laurentia, which was at equatorial latitudes and positioned over Jason then (Torsvik et al., 2014; Domeier, 2016). If Laurentia occupied the northern margin of Jason at 510 Ma, then South China would be restricted to the southern margin of that LLSVP, and would be trapped between Laurentia and the far-side of Gondwana for the duration of the early Paleozoic (i.e. analogous to the problem of it being positioned over the southeast margin of Tuzo). Alternatively, if Laurentia occupied the southern margin of Jason and South China the northern margin of that LLSVP, South China would avoid being boxed in by Laurentia, but would instead encounter problems migrating *eastward* past Baltica and Siberia to its Early Devonian position, as they occupied similar latitudes during the Ordovician and Silurian (Figs. 21–26).

The Early Ordovician positioning of North China is more restricted, as Laurentia occupied the northern margin of Jason, and Gondwana covered the southern margin of Tuzo. The sole alternative to the preferred position described above then would be to place North China on the southern margin of Jason, squeezed tightly between Laurentia and northwest Gondwana, but this would introduce considerable problems akin to those listed for South China. Accordingly, I prefer the simplest option, and place South China directly *west* of northeast Gondwana at this time, and North China to the *west* of South China.

No LIPs or kimberlites were emplaced into Baltica, Siberia, Tarim or the Kazakh terranes during the Cambrian or Early Ordovician, so their paleolongitudes are not directly constrained. However, because those continents and terranes shared the same southern hemisphere latitudes as Gondwana, the Cambro-Ordovician positioning of Gondwana greatly restricts the range of paleolongitudes that they could have occupied then. Baltica, being at high latitude during the middle and late Cambrian, is the continent most restricted in longitude by the positioning of Gondwana, and so its paleolongitude, while relative, can be robustly established.

As revealed by their paleomagnetic data, Siberia, the Kazakh terranes, and North and South China all shared broadly similar equatorial latitudes at this time, as did East Gondwana and Laurentia (Domeier, 2016), which significantly reduces the longitude options for Siberia and the Kazakh terranes. Given the position of Siberia at the beginning of the late Paleozoic, when it was located between Laurentia (to the *west*) and East Gondwana (to the *east*) (Domeier and Torsvik, 2014), and the fact that Laurentia, East Gondwana and Siberia all shared comparable latitudes throughout the early Paleozoic, Siberia must also have occupied a similar position between Laurentia and East Gondwana in the early Paleozoic, as it could not otherwise have skirted around those landmasses prior to the Devonian. Furthermore, beginning at ~480 Ma, Baltica began drifting *northward* from high latitude and entered into mid-latitudes in the Middle Ordovician before colliding with Laurentia at equatorial latitudes in the Silurian. Siberia must therefore have been *east* of Baltica by the time the latter entered into mid-latitudes in the Middle Ordovician, which further restricts its viable Early Ordovician longitude alternatives. Likewise, the Kazakh terranes, which were positioned between Siberia and North China at the start of the late Paleozoic (Domeier and Torsvik, 2014), broadly occupied the same paleolatitudes as Siberia and North China during the early Paleozoic, and so it is most likely that they were located in the same relative longitudinal position already at 500 Ma. Notably, this positioning raises some inconsistencies with respect to paleobiogeographical inferences (Popov et al., 2009; Popov and Cocks, 2017). An alternative solution could exploit the hemispheric ambiguity of the paleomagnetic data to place the Kazakh terranes in the northern hemisphere during the Cambrian and Ordovician, but this solution would not necessarily be more compatible with the paleobiologic data, and would moreover require greater kinematic complexity in the model (discussed below). I therefore prefer positioning the Kazakh terranes in the southern hemisphere at this time.

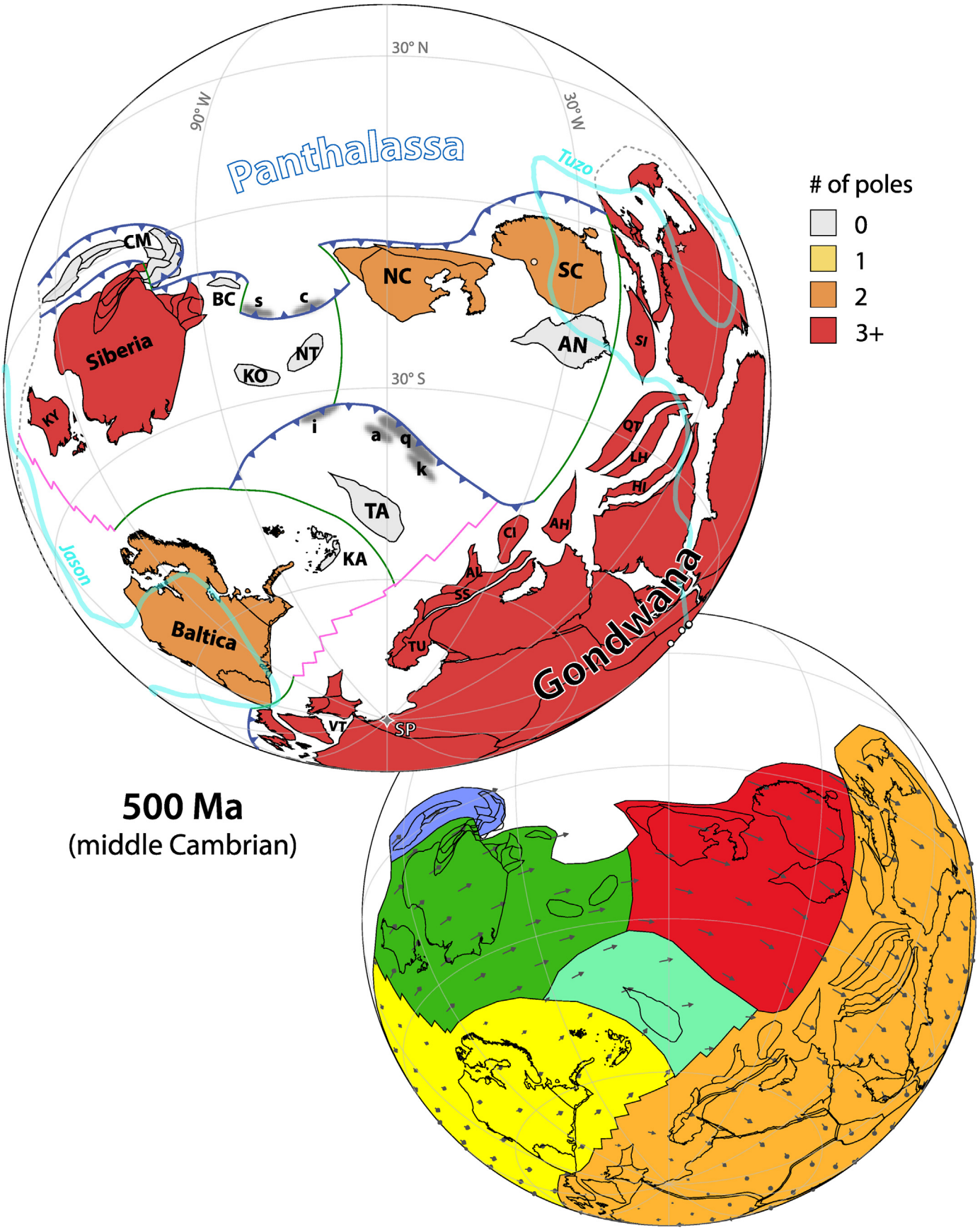

Figure 18. Plate model at 500 Ma. Upper panel: reconstruction showing simplified plate boundaries (blue: convergent, pink: divergent, green: transcurrent) and labels of some important features. The color of the continents is based on the number of paleomagnetic data contributing to their reconstruction at this time, based on a 20-Ma sliding window.

The Cambrian and Early Ordovician paleolongitude of Tarim is a challenge to establish because its paleolatitude is unconstrained prior to the late Early Ordovician. Nevertheless, given the paleogeography of the other blocks described above, if Tarim was at low-to-mid southern latitudes in the late Early Ordovician, as its paleomagnetic record suggests, and if it collided with North China at some point prior to the Devonian (section 6.2.3, below), then it must have occupied the space between Siberia and northern Gondwana, flanked by Baltica to the *southwest* and the Kazakh terranes and China blocks to the *north* and *northeast*.

As aforementioned, owing to the ambiguous polarity of Tarim's Ordovician paleomagnetic results, it is alternatively possible that Tarim occupied low-to-mid northern latitudes in the late Early Ordovician, in which case its paleolongitude would be almost totally unconstrained. However, this latter interpretation is unlikely for several reasons. First, adoption of that alternate polarity (placing Tarim in the northern hemisphere) would also invert Tarim's azimuthal orientation, requiring Tarim to rotate ~160° in ~30 Ma to reach its mid-Silurian orientation, as established by paleomagnetic data of known polarity. By contrast, the southern hemisphere option would only require Tarim to rotate ~20° over that interval. Second, Ordovician faunas from Tarim are similar to those found in other central Asian blocks, notably the Kazakh terranes and the North and South China blocks (Popov et al., 2009). If Tarim were situated at 20°–30° N in the Early to mid-Ordovician, it would have been largely isolated in the vast Panthalassa, and specifically separated from the North and South China blocks by ~30°–40° (considering latitude only); it would also be separated from the Kazakh terranes by a comparable distance if they too were in the southern hemisphere, as assumed here. In the southern hemisphere option, Tarim is proximal to those other China blocks. Finally, as will be discussed below, the *northern margins* of the Central Mongolian terranes, the Kazakh terranes, North China, and South China (Japan) were possibly all active from the Early Ordovician through the Devonian. If Tarim were in the northern hemisphere in the pre-Late Ordovician, but collided with North China at some point prior to the Devonian, then it must have passed across that extensive active margin interface. Although that is not an impossible scenario, it is considerably more complicated than the alternative wherein Tarim approaches North China from the other (*southern*) side, as will be illustrated below.

6.1.2. Merger of Siberia and the central Mongolian ribbon terrane

In the late Neoproterozoic and early Cambrian the south margin of Siberia, which was then *north-facing*, was clearly adjacent to an active margin. In the west, the Kuznetsk-Alatau and North Sayan arcs, as well as the Gorny Altai and West Sayan accretionary complexes associated with them, developed along an active margin that commenced at least by the late Neoproterozoic and which continued through the Cambrian (Figs. 3 and 4). Given that the arcs occur between the accretionary complexes (to the southwest) and the Siberian craton (to the northeast), subduction must have been directed beneath the arcs toward the craton, and the arcs were probably peri-cratonic, perhaps separated from Siberia by a minor backarc basin. Similarly, to the east, late Neoproterozoic and Cambrian island arc and subduction-accretion rocks of the Dzhida and Uda-Vitim zones are separated from the Siberian craton by late Neoproterozoic and Cambrian volcanic and terrigenous rocks of probable backarc affinity in the Hamar-Davaa, Olkhon and Barguzin-Ikat zones, an arrangement consistent with a then *north-facing* active margin there too (Figs. 18 and 19).

In the late Cambrian to Early Ordovician that active margin was strongly disrupted, as evident by widespread tectonism, intense metamorphism and the cessation of subduction-related magmatism in many of those former (late Neoproterozoic–Cambrian) marginal arcs. In the west, that event was associated with the convergence and collision of two arcs along the West Sayan zone (Fig. 4): the peri-Siberian North Sayan arc, and the late Neoproterozoic–Cambrian Lake Khamsara arc that likely represented the leading (active) edge of the Precambrian Tuva-Mongolia and Dzabkhan microcontinents, which constituted part of the larger central Mongolian ribbon terrane (CMT) then. The tectonism, metamorphism, and magmatic evolution in the eastern areas of south Siberia are more expansive and less well detailed, but are nonetheless understood to reflect a broad, oblique collision at that time, which is here ascribed to a collision between the CMT and peri-Siberia (Figs. 19 and 20). With that collision, the Neoproterozoic–Cambrian active margin of south Siberia was terminated, and central south Siberia would remain land-locked until the rifting of Amuria and the opening of the Mongol-Okhotsk Ocean in the Late Ordovician–Silurian (Fig. 23).

Whether subduction was occurring beneath the entire north margin of the CMT prior to its collision with peri-Siberia is unclear, but subduction was certainly active beneath the Lake Kharmsara arc along its northwestern edge, and evidently also beneath the northern Erguna block. Evidence of the collision itself is limited, but distributed throughout the north of the terrane: the cessation of arc magmatism in the Lake Kharmsara arc and Ordovician HP metamorphism in West Sayan, the observation of a pre-Silurian unconformity in the Ereendava zone, and the occurrence of high-grade metamorphism at ~500 Ma in the northern Erguna block. Along the southern margin of the CMT (facing *north* in the late Cambrian), north-dipping subduction probably began at least by the mid-Cambrian (if not already in the Neoproterozoic) and continued into the late Paleozoic (Figs. 4, 18–26). Evidence for such is best established in the east—where the Xing'an block may comprise a large early Paleozoic subduction-accretion complex, and early Paleozoic subduction-accretion complexes are also identified in the Songliao block—but also recognized by sparse relics of early Paleozoic accretionary complexes in south-central Mongolia, and perhaps also further west in the early Paleozoic arc assemblages of northern Beishan (Queershan arc and correlatives).

6.1.3. Assembly among the Kazakh terranes

To the *east* of southwest Siberia, terrane amalgamations were also occurring among the Kazakh terranes during the Cambro–Ordovician. In the comparatively well-understood Kyrgyz North Tianshan (KNT), terrane mergers occurred both along its north and south margins (Figs. 5 and 6). In the north, north-dipping subduction beneath the Chu-Yili microcontinent ended in a late

The dark gray polygons with lowercase letters depict minor terranes which are discussed in the text and kinematically modeled but not based on a present-day digitization. The thick, light blue lines show the outlines of the present-day large low shear velocity provinces (LLSVPs), based on the 1% slow SMEAN contour of Becker and Boschi (2002), after back-correction for true polar wander (TPW) using the TPW estimates of Torsvik et al. (2014). White dots denote kimberlite emplacements at ~500 Ma (gray dots/star denote kimberlite/large igneous province emplacements just prior to this reconstruction, at ~510 Ma). Gray dashed boundaries along the perimeter mark the arbitrary outer limit of the modeled domain and have no physical meaning. *Continent and major terrane abbreviations*: AH, Afghan terranes; AL, Alborz; AN, Annamia; BC, Boshekul-Chingiz zone; CI, Central Iran terranes; CM, Central Mongolian ribbon terrane; HI, Himalaya; KA, North Kara; KO, Kokchetav terrane; KY, Kolyma-Omolon; LH, Lhasa; NC, North China; NT, North Tianshan zone; QT, Qiangtang; SC, South China; SI, Sibumasu; SS, Sanandaj-Sirjan; TA, Tarim; TU, Turkish terranes; VT, Variscan terranes; *Minor terrane abbreviations*: a, Altyn belts; c, Chu-Yili; i, Kyrgyz Middle Tianshan; k, South West Kunlun; q, Qilian-Qaidam-North Qinling; s, Stepnyak-Selety. *Other abbreviations*: SP, South Pole. Lower panel: plate velocity field (plates are colored differently so that they are easily distinguished, but the colors are otherwise arbitrary).

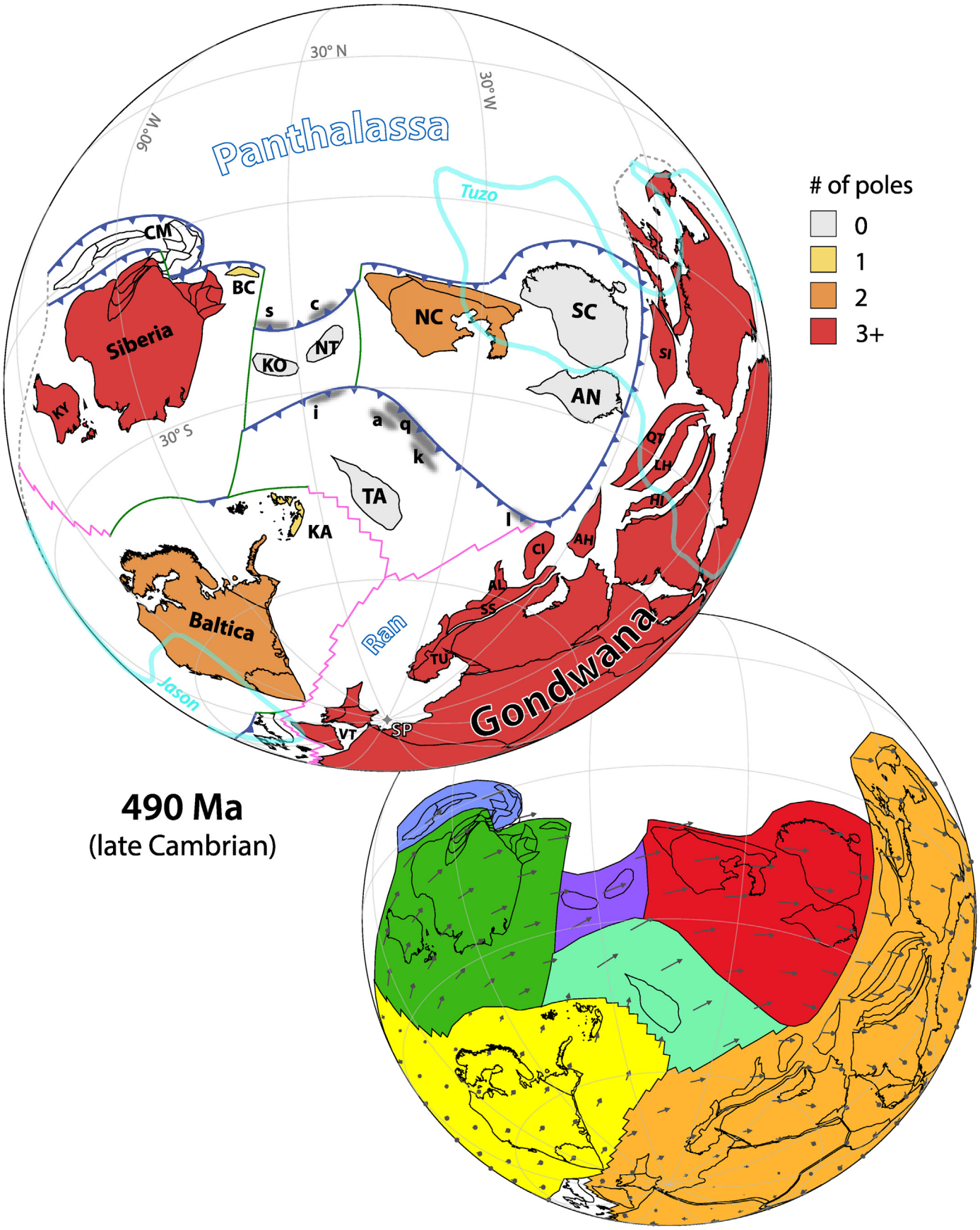

Figure 19. Plate model at 490 Ma. See Fig. 18 for a description of features. *New abbreviations:* l, 'Lincang arc'.

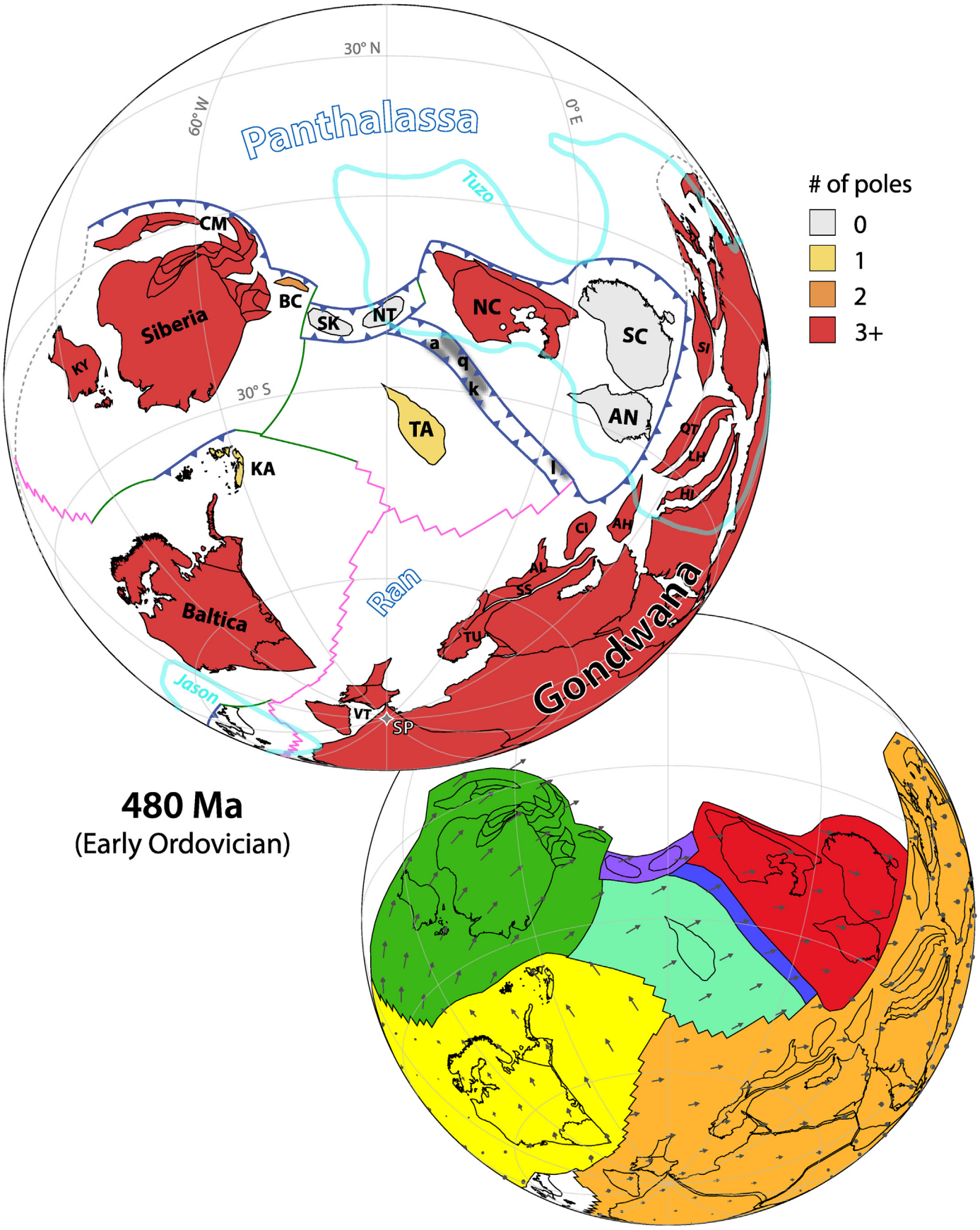

Figure 20. Plate model at 480 Ma. See Fig. 18 for a description of features. *New abbreviations:* SK, Stepnyak-Kokchetav zone.

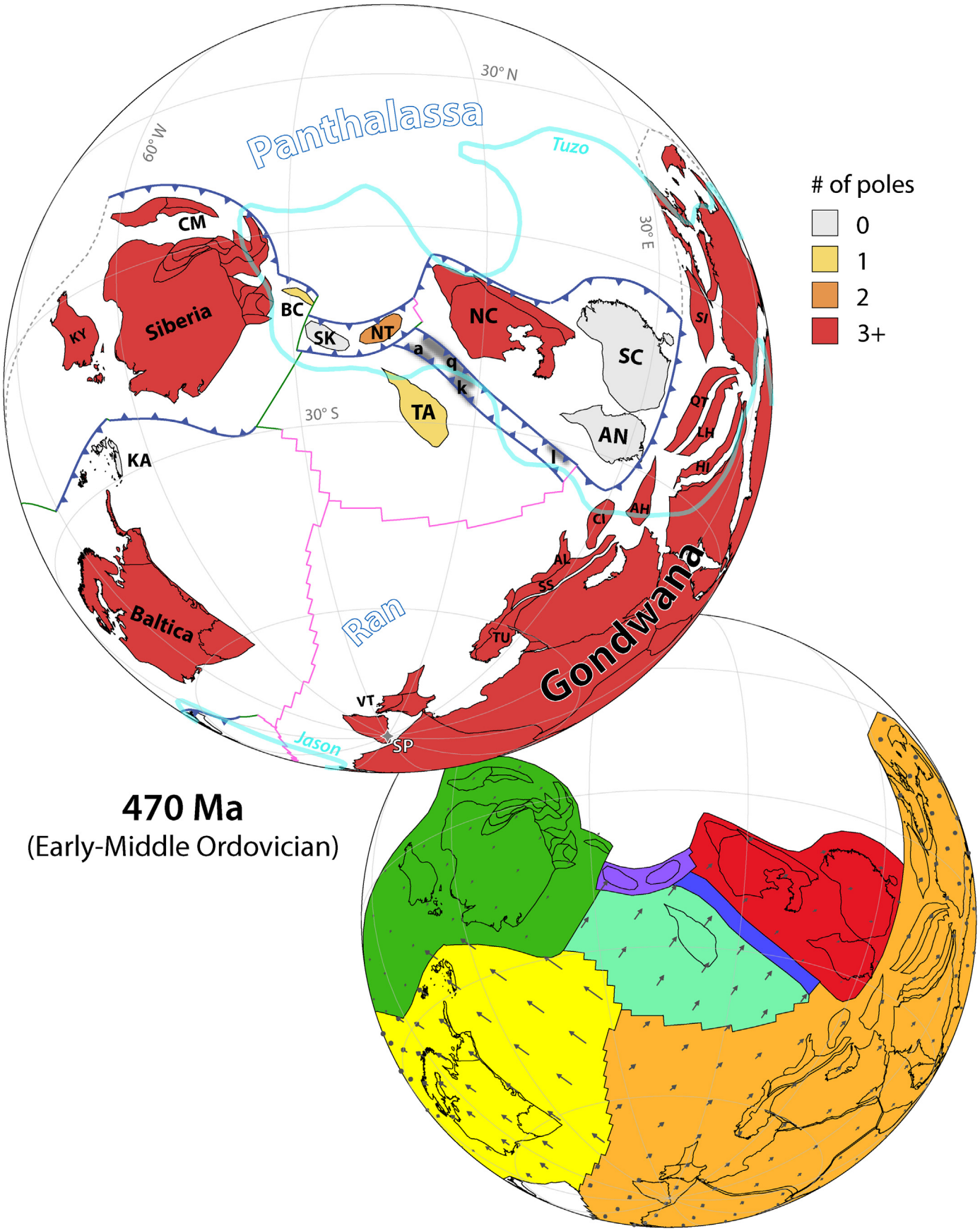

Figure 21. Plate model at 470 Ma. See Fig. 18 for a description of features.

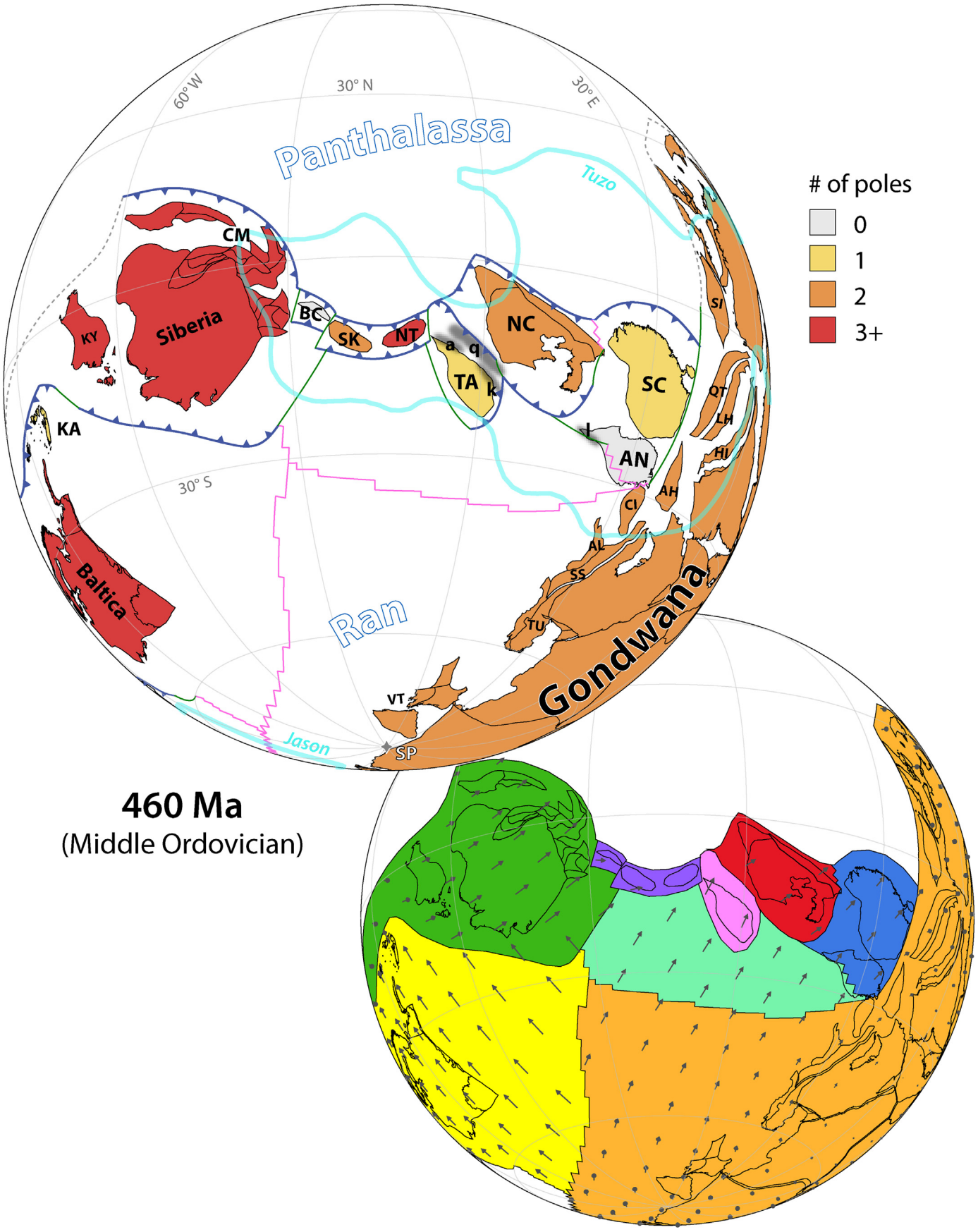

Figure 22. Plate model at 460 Ma. See Fig. 18 for a description of features.

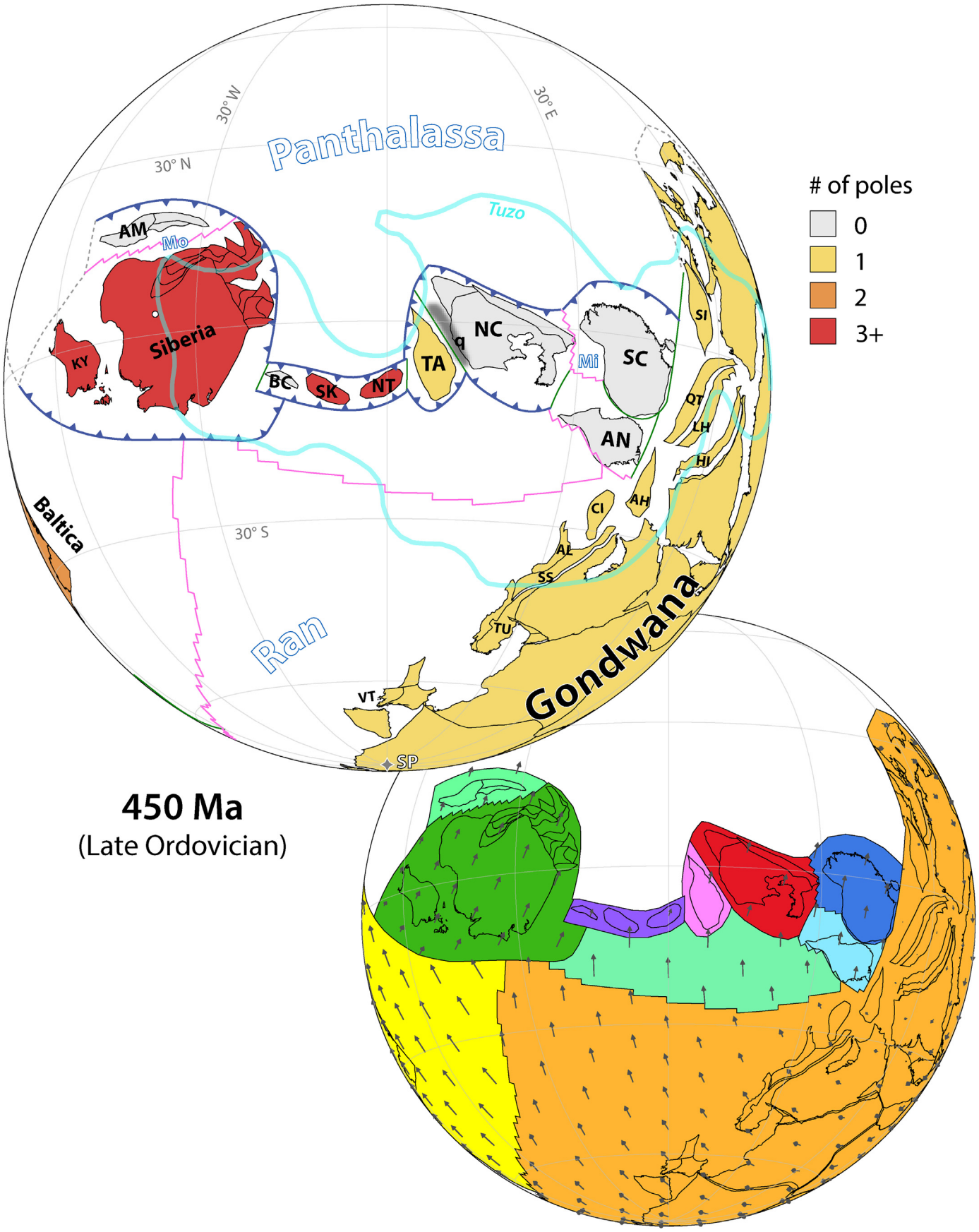

Figure 23. Plate model at 450 Ma. See Fig. 18 for a description of features. *New abbreviations:* AM, Amuria; Mi, Mianlue Ocean; Mo, Mongol-Okhotsk Ocean.

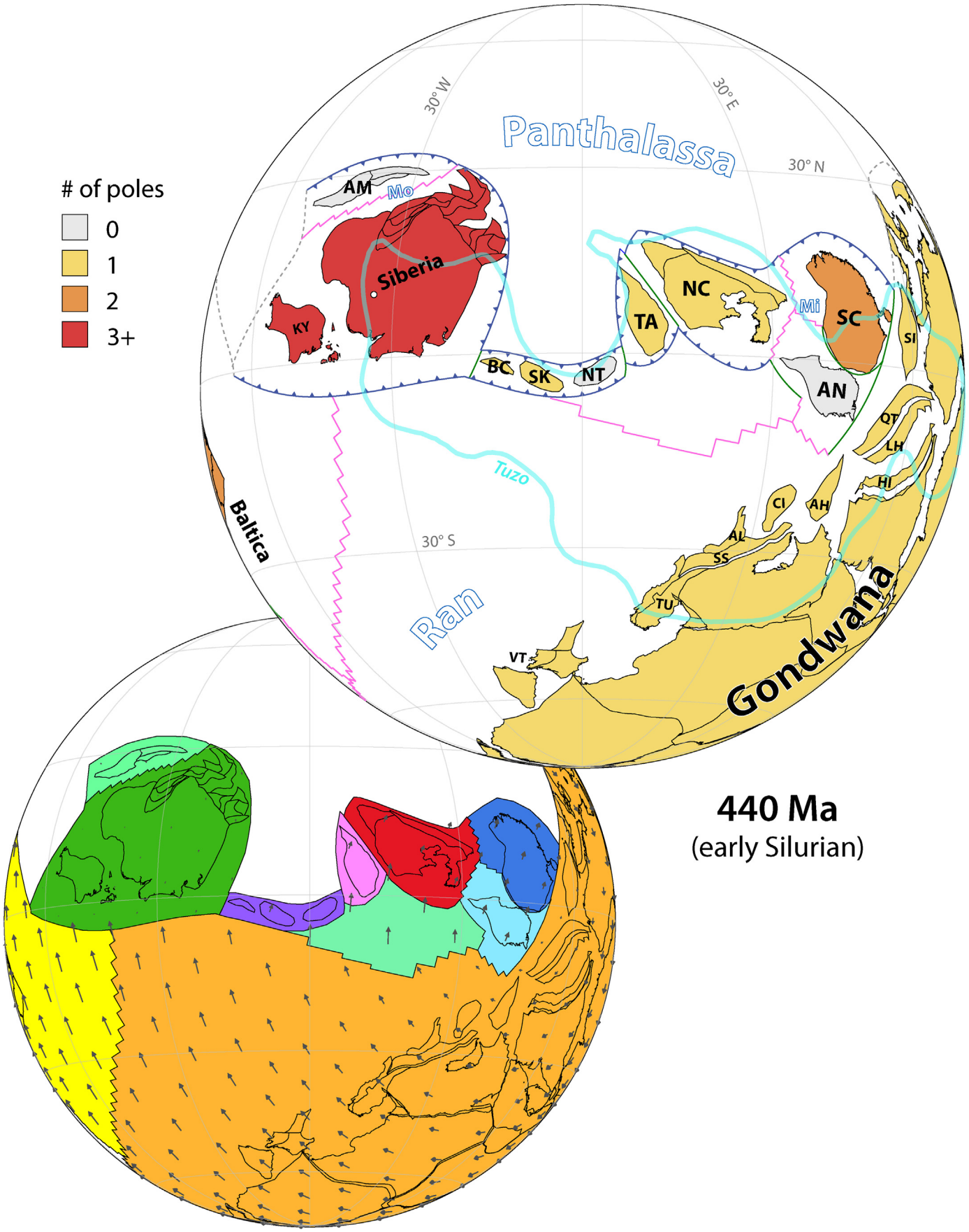

Figure 24. Plate model at 440 Ma. See Fig. 18 for a description of features.

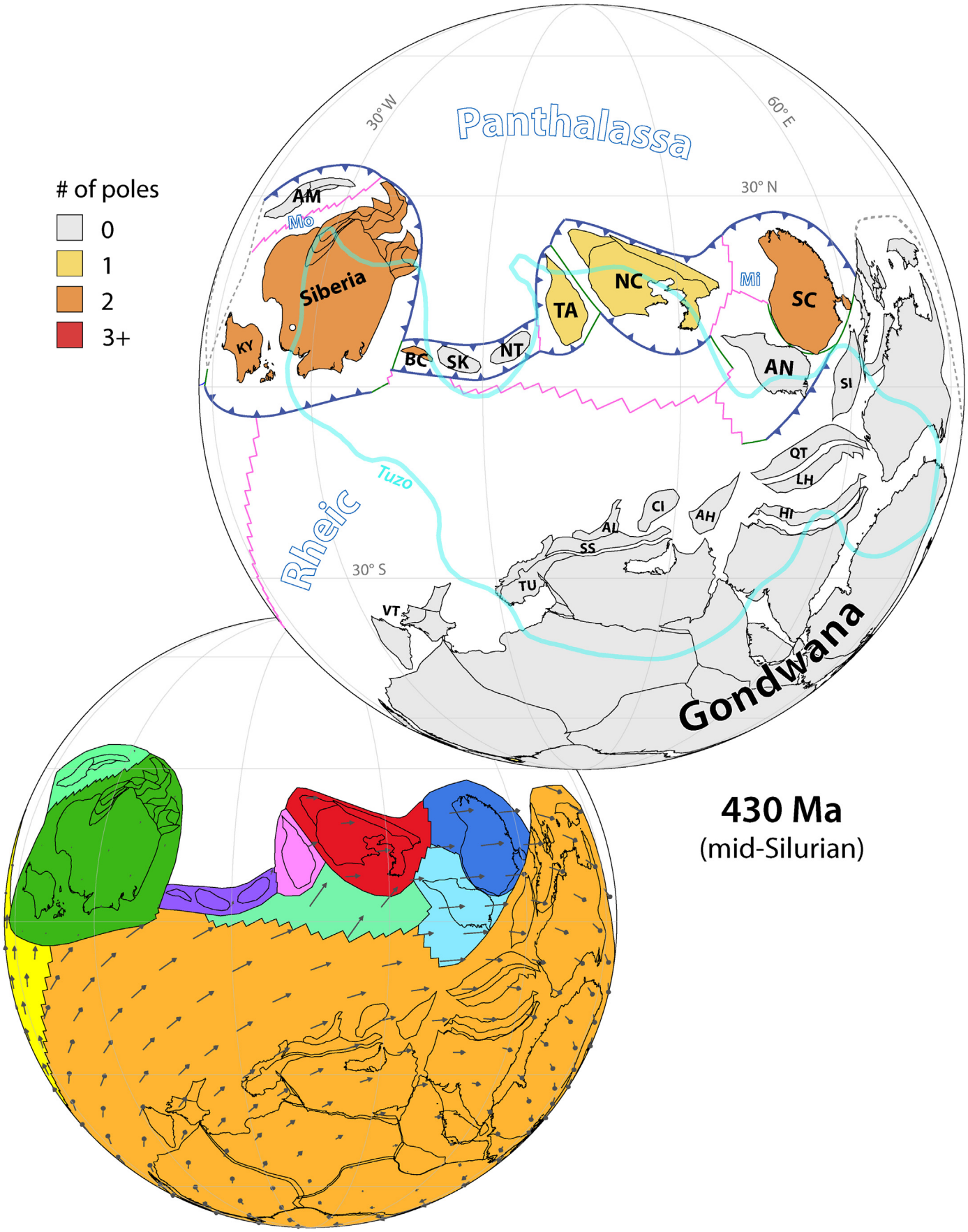

Figure 25. Plate model at 430 Ma. See Fig. 18 for a description of features.

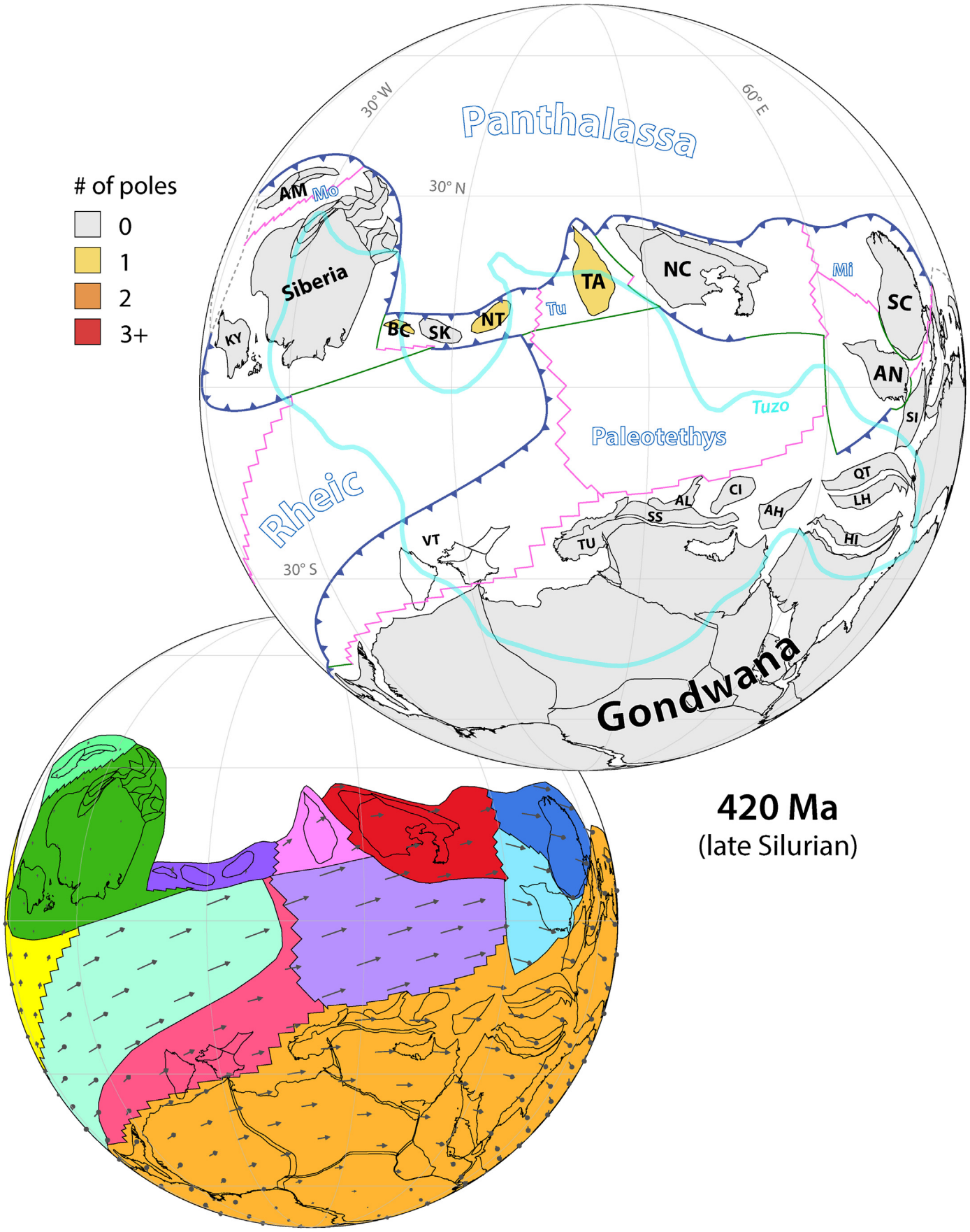

Figure 26. Plate model at 420 Ma. See Fig. 18 for a description of features. *New abbreviations:* Tu, Turkestan Ocean.

Cambrian–Early Ordovician collision between Chu-Yili and the KNT along the Dzhalair-Naiman belt. In the south, probably south-dipping subduction beneath the Kyrgyz Middle Tianshan (MIT) resulted in a similarly timed late Cambrian–Early Ordovician collision between the MIT and KNT along the Kyrgyz-Terskey zone. Although I have not explicitly included the Chu-Yili or MIT microcontinents in the model, Figs. 18 and 19 show those opposing middle to late Cambrian subduction systems, which converged toward the KNT (represented by the 'NT' block; section 5) until colliding with it by 480 Ma.

Following those opposing collisions and the termination of subduction in both the Dzhalair-Naiman and Kyrgyz-Terskey basins, subduction jumped outboard of the now-accreted terranes and resumed, with inverted polarity, both to the north and south of the enlarged KNT (Figs. 4 and 20). In the south, in the MIT, the appearance of subduction-related magmatism in the Chatkal and northern Atbashi ranges in the Ordovician is attributed to the relocation of subduction to the south margin of the MIT following closure of the Kyrgyz-Terskey basin. In the north, the initiation of south-dipping subduction beneath the north margin of Chu-Yili was marked by the construction of an accretionary complex and forearc basin there, and the eruption of Ordovician arc volcanics. South-dipping subduction continued there through the Ordovician and Silurian, with a brief interruption in the Late Ordovician (Popov et al., 2009). Subduction also initiated along the margin of Aktau-Junggar in the Early Ordovician, but as that terrane lacks early Paleozoic paleomagnetic data and its Ordovician faunas express its relative isolation from the other Kazakh terranes, I have not attempted to reconstruct it in the plate model. However, given the broad paleogeographic framework presented here, the mid-Paleozoic accretion of Aktau-Junggar to the northern margin of Chu-Yili would suggest that Aktau-Junggar came from the *north*, placing it in the Panthalassa (in equatorial to low northern latitudes) in the Cambro–Ordovician.

The spatial association of the northern and southern Kazakh terranes is not clear for the early Paleozoic, but the similar occurrence of subduction and accretion events during the Cambro–Ordovician permits the interpretation that they were lateral equivalents of the same tectonic system already at that time. The Kokchetav microcontinent, having experienced a Neoproterozoic-early Cambrian collisional event that resulted in local HP-UHP metamorphism, was subjected to post-orogenic extension in the middle Cambrian before becoming apparently passive in the late Cambrian. To the east in the Stepnyak zone, late Cambrian and Ordovician subduction-related arc rocks reveal the operation of an active margin at that time, although the location and orientation of the subduction zone has not yet been settled. If subduction occurred between the Kokchetav microcontinent and the Stepnyak zone, it must have been northeast-dipping beneath the latter, and ceased with an Early–Middle Ordovician collision between the Kokchetav microcontinent and Stepnyak zone along the North Kokchetav tectonic zone. In such case, the Cambro–Ordovician active margin of the Stepnyak zone could have been a *western* continuation of the *north-dipping* subduction zone between the KNT and Chu-Yili (Figs. 18 and 19). In the alternative interpretation of Degtyarev et al. (2016), where Cambro–Ordovician subduction was west-dipping beneath the combined Kokchetav microcontinent and Stepnyak zone, the polarity of subduction to the *north* of the southern and northern Kazakh terranes would have been different at that time, necessitating at least a transform boundary between those systems.

Further east of the Stepnyak zone, a broad area of Cambrian-Early Ordovician volcanic, cherty-terrigenous and carbonate rocks comprise the Urumbai, Selety and Erementau zones, which are poorly-understood but often recognized as a series of Cambrian–Early Ordovician island arc and subduction-accretion complexes that may represent a correlative of the Stepnyak system and/or the Chu-Yili system, or one or more independent arc terranes. In any case, as in the southern Kazakh terranes, the northern Kazakh terranes were defined by the merger of several subduction systems in the late Cambrian–Early Ordovician and by the end of that interval probably constituted a unified terrane. Given the many outstanding unknowns, the scenario presented in Figs. 18–20 represents only the simplest of many alternatives.

Prior to Devonian oroclinal bending, the Chingiz arc of northeast Kazakhstan was approximately azimuthally inverted ('upside down') in the early Paleozoic. Although the terrane was independent, paleomagnetic data reveal that Chingiz occupied the same low latitudes as those occupied by the other Kazakh terranes throughout the early Paleozoic, and it was probably positioned between southwest Siberia to the *west* and the other Kazakh terranes and North China to the *east*. As in southwest Siberia, the Chingiz arc clearly occupied the upper plate position above a *south-dipping* subduction zone that had initiated at least by the early Cambrian (Figs. 6, 18–20), in contrast to the apparent Cambrian passivity of the Kokchetav microcontinent and KNT. For this reason I prefer to tie the Chingiz arc to the southwest margin of Siberia at the beginning of the model, although paleomagnetic data suggest that it may have been at a slightly higher latitude than modeled during the Early Ordovician (Fig. 17). Unlike in southwest Siberia, *south-dipping* subduction continued beneath that arc through the Cambrian and Early Ordovician, and was not interrupted until the Middle or Late Ordovician arrival of the Baidaulet-Aqbastau arc.

It is important to note that this simple Cambro–Ordovician scenario for the Kazakh terranes conflicts with several paleobiogeographical inferences, most notably that the individual Kazakh terranes were still dispersed in the Ordovician and that they were all far from Siberia (Popov and Cocks, 2017). However, as can be seen from Figs. 18–20, the Kazakh terranes, the China blocks, Siberia and northeast Gondwana all occupy similar low latitudes, and these continents and terranes continue to occupy the same low latitudinal bands throughout the early Paleozoic (Figs. 21–26). This means that the Kazakh terranes do not have much opportunity to be strongly longitudinally shuffled with respect to the other continents and terranes, unless the paleomagnetic constraints are ignored. Still, the polarity of the Cambrian-Ordovician paleomagnetic data from the Kazah terranes is not known, so it is possible that the Kazakh terranes (or a subset of them) alternatively occupied low latitudes of the northern hemisphere, in which case they would have more longitudinal freedom of movement. However, this solution would leave the Kazakh terranes isolated in the Panthalassa, latitudinally separated from both South China and the northern margin of Gondwana, continents which they evidently have a strong faunal affinity to (Popov and Cocks, 2017). This solution would also greatly increase the complexity of the plate model by multiplying the number of independent subduction systems, because those associated with the Kazakh terranes could no longer exist as continuations of the Siberian and North/South China systems (as depicted in Figs. 18–20). This complexity becomes even more acute if the Kazakh terranes were dispersed and distributed on both sides of the equator, as proposed by Popov and Cocks (2017) (see their Fig. 13). The true paleogeographic framework most likely lies somewhere between the simplistic scenario adopted here and the complex archipelago model of Popov and Cocks (2017), but further work (particularly paleomagnetic) is needed to resolve this quandary.

6.1.4. Active margins of the China blocks

To the *east* of the Kazakh terranes, *south-dipping* Cambro-Ordovician subduction continued along the northern margin of

the North China block, and probably further *east* across the *north* margin of South China (comprised by the Japanese terranes) to the northeast margin of Gondwana. Thus, at ~500 Ma, active margins spanning a combined length of more than ~11,000 km ran from southern Siberia in the *west* to northeast Gondwana in the *east* (Fig. 18). With the inversion of *north-dipping* subduction along the *northern margins* of the Kazakh terranes at 480 Ma, that interface may have become an effectively continuous *south-dipping* subduction system (Fig. 20). In North China, relics of this active margin are recognized in the Bainaimiao arc and the Ondor Sum complex to its north, whereas relics of the same Cambro-Ordovician subduction zone along the *north* margin of South China are found in the scattered early Paleozoic rocks of the Japanese Islands.

6.1.5. The northeast margin of Gondwana

The early Paleozoic northeast margin of Gondwana is challenging to reconstruct because the blocks that comprised that margin have been dispersed and widely tectonized since then. On the other hand, the width of that former margin affords a wealth of opportunities to draw observations. The northeast margin of Gondwana stretched from the north Arabian peninsula and the Turkish terranes that may have lain to its north, to the Sibumasu terrane in the east, which flanked the north margin of western Australia. Conventionally, it was commonly assumed that, following Neoproterozoic–early Cambrian Cadomian orogenesis, that expansive margin remained largely passive during the late Cambrian and Early Ordovician, but as reviewed in section 4.14, there are actually signs of significant tectonism across wide swaths of it then (Fig. 14). In the west, sedimentation upon the Cadomian basement began with Early–Middle Ordovician conglomerates in the Istanbul and Zonguldak zones of Turkey, and in Iran and Afghanistan the Cambro-Ordovician witnessed the eruption of bimodal volcanics and the emplacement of S-type granitoids. Farther east, a regional Cambro–Ordovician unconformity, capped by Ordovician conglomerates, continues across Qiangtang, Lhasa, the Himalaya and the Tengchong and Baoshan blocks of northern Sibumasu; regions which were also widely affected by Cambro–Ordovician granitoid plutonism and bimodal volcanism. More locally, namely in the Himalaya, there are indications that late Cambrian–Early Ordovician interval was associated with intense deformation and regional metamorphism, which may have been elsewhere masked by later tectonics.

Although those observations suggest that some form of tectonism was occurring all along the margin of northeast Gondwana during the Cambro–Ordovician, the intensity of that tectonism appears to diminish from the east (Qiangtang, Lhasa, the Himalaya, northern Sibumasu) to the west (the Turkish, Iranian and Afghan terranes). Given the reconstructed position of South China and Annamia outboard of those eastern terranes, and the fact that South China drifted generally *southward* during the Cambro–Ordovician, I interpret the northeast margin of Gondwana there as a transpressional to highly-oblique convergent boundary (Figs. 18–21). Such an association could moreover explain the Cambro–Ordovician unconformity on Hainan Island (South China) as a counterpart of that tectonism (i.e. on the opposite side of the then-transpressive margin), and would also explain the NW-directed transport of sediments across South China during the early Paleozoic (Fig. 12), as well as the occurrence of late Neoproterozoic–Cambrian (Cadomian) detrital zircons in those sediments, for which a source within South China is not known.

In the west of the margin, along the Turkish and Iranian terranes, Cambro–Ordovician tectonism was more localized and punctuated, disturbing the seemingly otherwise widespread deposition of typical shallow marine passive margin sequences. This contrast between the western and eastern segments of the margin could reflect different tectonic environments associated with different boundary kinematics, which would imply that those margin segments were flanked by different plates. Further west along the northern margin of Gondwana, along the rim of Northwest Africa and Amazonia, the Cambro–Ordovician interval was associated with a major rift episode that culminated in the splitting of Avalonia from northwest Gondwana and the opening of the Rheic Ocean (Domeier, 2016). Conceivably, Cambro–Ordovician rifting along the north of Gondwana could have continued eastward from northwest Africa, perhaps exploiting transpressive lineaments left by the Cadomian orogeny. Indeed, the development of a divergent boundary somewhere between the Turkish/Iranian terranes of north Gondwana and the east margin of Baltica is necessary to accommodate the counterclockwise rotation and northward drift of the latter in Cambro–Ordovician time (Figs. 18–21), and I speculate that this divergent boundary evolved from an earlier (early Cambrian) transpressive boundary associated with the Cadomian cycle. In this context, the comparatively minor episodes of Ordovician and Silurian tectonism observed in the Turkish and Iranian terranes could be late stage post-rift relaxation effects, or the consequences of rift reactivation, but otherwise their occurrence is unexpected; further work is needed to clarify their nature. Notably, the switch from a transpressive boundary along the east of the northeast margin of Gondwana to a divergent boundary along its west necessitates a triple junction somewhere in between; the nature and identity of this boundary is considered in section 6.1.7.

6.1.6. The twist and drift of Baltica and Kara

In the late Neoproterozoic, northeastern Baltica was affected by the Timanide orogeny, which was perhaps related to the Cadomian orogeny that was taking place along the then-neighboring northern margin of Gondwana. Following that orogenic episode, the east margin of Baltica was subjected to Cambrian rifting, which as argued in the previous section, possibly reflected the conversion or reactivation of the former (Cadomian) transpressive boundary between east Baltica and north Gondwana, forming a new divergent boundary. While Cambrian rifting is documented from geologic vestiges along the east margin of Baltica, the development of such a divergent boundary between Baltica and Gondwana is moreover required by the available paleomagnetic constraints. The paleomagnetic data from Baltica reveal that it rotated counterclockwise through the Cambrian and began drifting northward at the beginning of the Ordovician (Figs. 18–21)—kinematics which can only be accomplished by the presence of a transform that evolves into a divergent boundary between Gondwana and Baltica. This conclusion is inescapable by the available paleomagnetic data alone; because both Baltica and north Gondwana shared the same southern polar latitudes, their relative paleolongitues are effectively fixed, and so uncertainties in their specific absolute paleolongitudes have no bearing on these kinematic inferences. Because the rifting of Avalonia and the opening of the Rheic Ocean were closely associated with this rifting between Baltica and north Gondwana in both a temporal and spatial sense, I speculate that they were dynamically related processes.

The tectonics that were taking place on the far (western) side of Baltica during the early Paleozoic—during which time it was mostly flanked by the Iapetus—are largely beyond the scope of this paper (see Domeier, 2016), but they are worth considering briefly at the opening of the model (at 500 Ma), when west Baltica was facing *north*, toward the north margin of Siberia (then *south-facing*) (Fig. 18). The Scandinavian margin of Baltica may have been passive throughout the early Paleozoic (Domeier, 2016), which is not a problem during the middle to late Cambrian when Baltica rotates

counterclockwise because Siberia, to its *north*, remained at the same latitude during that time and so their shared boundary can be simply modeled as a transform. However, in the latest Cambrian–Early Ordovician, Baltica began to drift *northward* while Siberia remained at effectively the same low latitude, such that Baltica began to encroach on Siberia, implying that there must have been an active margin somewhere between them then. Geologic records of a latest Cambrian–Early Ordovician active margin are unknown to the north margin of Siberia (South and Central Taimyr), and the northwest margin of Baltica is generally presumed to have been passive then (although see Jakob et al. (2017)), but evidence of Cambro–Ordovician tectonism and magmatism are documented in the North Kara terrane. As discussed in section 4.16, there are multiple geologic and geophysical arguments for early Paleozoic coherence between Baltica and the North Kara terrane (in their present assembly), and from a re-analysis of the paleomagnetic data of Metelkin et al. (2005), I conclude that no paleomagnetic-based argument can be made for a separation between North Kara and Baltica in the early Paleozoic. In conformity with the paleomagnetic data of Metelkin et al. (2005), I have modeled the North Kara terrane as a coherent unit of Baltica through the early Paleozoic. I therefore interpret the Cambro–Ordovician tectonism and magmatism observed in the North Kara terrane as a reflection of the active margin that must have otherwise been present between Baltica and Siberia at that time, and furthermore deduce that subduction there was *south-dipping* below North Kara (which was part of a greater Baltic plate) (Fig. 20).

6.1.7. Subduction and dynamics of the interior oceans

At 500 Ma, Gondwana, Baltica, Siberia, the Kazakh terranes and the China blocks together formed a triangular-shaped paleogeographic framework that enclosed a large internal ocean basin that occupied mostly mid-southern latitudes (~20°–70°S) (Fig. 18). At that time the basin was delimited to the *east* by northeast Gondwana, to the *southwest* it was flanked by northeast Baltica (and North Kara), to the *northwest* it was flanked by northwest Siberia, and to the *north* it was bordered by the Kazakh terranes and North and South China blocks. Very little of the history of that basin is established, as the paleogeography of the only major terrane which may have been located within it, Tarim, is also very poorly known. Nevertheless, I proceed with an attempt to decipher a possible first-order history of that basin from the observations gleaned from Tarim and from the scattered geologic observations from other continental fragments and oceanic and arc vestiges that may have once occupied it.

Northern Tarim, as known both from south of the North Tarim fault but also in the South Tianshan, and arguably east to the Dunhuang block and the Shibanshan unit of southern Beishan, was evidently passive in the late Cambrian and through the Early and Middle Ordovician (Figs. 5 and 7). According to the sparse paleomagnetic data, north Tarim was *southwest-facing* across that time, facing northeastern Baltica. Considering the established kinematics of Baltica during that interval, the boundary between north Tarim and northeast Baltica was likely initially a transform that may later have evolved into a spreading center (Figs. 18–21). The development of a spreading center to the *southwest* of north Tarim at some point prior to the mid-Ordovician is moreover necessary to accommodate the later *northward drift* of Tarim during the Late Ordovician to Silurian (section 6.2.6, below).

If Tarim was drifting *northward* already by the mid-Ordovician (and possibly earlier), while Siberia, the Kazakh terranes and the North and South China blocks to its *north* remained effectively at the same low southern latitudes, there must have been subduction occurring somewhere in the oceanic basin between them (i.e. between Tarim to the *south* and those other blocks to the *north*). With respect to the Kazakh terranes, such subduction—if active already in the Cambro-Ordovician—could have been associated with the northern active margin of the MIT, which evidently moved *northward* above a *south-dipping* subduction zone until colliding with the KNT in the Early Ordovician (Figs. 6, 18–20).

Unlike their *northern margins*, the *southern margins* of North and South China were passive during the Cambro–Ordovician, so any *eastward* continuation of the active northern margin of the MIT must have continued to the *south* of the China blocks. The southern margin of Tarim, which was *northeast-facing* during the Cambro–Ordovician (Figs. 18–20) according to Ordovician paleomagnetic data, was evidently also passive across that time. The eastward continuation of the MIT subduction zone, if one existed, must then have been intraoceanic, lying within the basin separating the southern margin of Tarim from the southern margins of North and South China (Fig. 18). Possible relics of such a Cambro-Ordovician intraoceanic subduction system include the subduction-related magmatic rocks and (U)HP metamorphic rocks in the North Qinling, to the south of the North China block (Fig. 9). As detailed in section 4.9.1, the North Qinling was independent from the North China block up until the Late Ordovician, when the Kuanping-Erlangping basin that separated them finally closed. In the late Cambrian-earliest Ordovician, the North Qinling unit was marked by (U)HP metamorphism along both its northern and southern margins, reflecting a significant tectonic event possibly associated with arc-continent collision(s). While I have not attempted to build a detailed scenario for this event (which coincides with or immediately preceeds the start of the model at 500 Ma), the (U)HP metamorphic vestiges from both the north and south margins of the North Qinling include components from the continental crust of the North Qinling itself, suggesting it was subjected to partial subduction along both sides (Fig. 10). This could occur if the North Qinling was trapped between two opposed subduction zones—with an analogous case presented above for the Kokchetav microcontinent and NKT—emphasizing the likely intraoceanic setting for the North Qinling, or at the very least underscoring its independence from the southern North China block then. In any case, following those (U)HP metamorphic events, the North Qinling occupied an upper plate position along (at least one) active margin through the Ordovician and into the Silurian, and I propose that it was partly this subduction system which accommodated Tarim's *northward drift* during the Ordovician.

Broadly similar while admittedly not altogether synchronous histories are observed amidst the complicated tectonic mosaic to the west of the Qinling; among the Qilian, Qaidam, Altyn and Kunlun belts (Fig. 5). In the Altyn orogen, as in the North Qinling, (U)HP metamorphism of Cambro–Ordovician age is documented along both its north and south margins, together with subduction-related magmatism that continued in the Altyn orogen through the mid-Ordovician. Likewise, in the Qilian-Qaidam and East Kunlun belts to the east of the Altyn orogen, and in the West Kunlun to the west of it, evidence of Cambrian and Ordovician subduction-related magmatism abounds, and more locally among those belts there is also evidence of Cambro–Ordovician high-grade metamorphism (sections 4.6.2 and 4.8).

A simple interpretation that emerges from those assembled observations is that the early Paleozoic ocean basin between Tarim, on the one side, and the Kazakh terranes and the North and South China blocks on the other, was host to at least one major intraoceanic subduction system during the Cambrian and Ordovician, and may have been the scene of a series of arc-continent collisions during the middle-late Cambrian, perhaps continuing into the Ordovician. This first-order picture is undoubtedly overly simplistic, and in reality it is likely that there was a series of intraoceanic arc and backarc systems, possibly resembling

something like that of southeast Asia today. While acknowledging that, I nevertheless overlook that complexity—in part because the present aim is to erect a first-order early Paleozoic framework, but also because many of the kinematic details necessary to properly reconstruct that intraoceanic system are still unknown—and proceed with a simplistic interpretation wherein all those elements, together with the MIT, comprised a single, elongate, *south-dipping* intraoceanic subduction system at 500 Ma (Fig. 18). Incidentally, a similar conceptualization was recently presented by Li et al. (in press), although they considered the arc system to be fringing Gondwana.

To the *east* of the North Qinling, the continuation of that intraoceanic system is uncertain. However, given that South China drifted *southward* along the northeast margin of Gondwana during the Cambro–Ordovician, and that the *south margin* of South China was passive at that time, the continuation of that intraoceanic subduction system must have continued all the way to the margin of Gondwana. As pointed out in section 6.1.5, the simultaneous occurrence of a transpressive boundary along the eastern segment of the northeast margin of Gondwana and a divergent to passive boundary along its western segment would necessitate a triple-junction somewhere between, and I accordingly suppose that the intersection of the intraoceanic subduction system with the northeast margin of Gondwana was that triple junction (Fig. 18).

6.2. Middle to Late Ordovician (470–445 Ma)

6.2.1. Geography of the major continents

The paleomagnetic records from Gondwana and Baltica are weak at the start of the Middle Ordovician and both records further deteoriate in the remainder of the period. Gondwana is defined by two poles between 470 Ma and 460 Ma, but only one pole between 460 Ma and 445 Ma (at 446 Ma) (Torsvik et al., 2012). Nevertheless, those data reveal that during the Middle and Late Ordovician Gondwana remained positioned such that northwest Africa was situated at southern polar latitudes and East Gondwana was straddling the equator (Figs. 21–23). The apparent position of the South Pole moved little over this time, specifically drifting from its position in the area of present-day northwest Algeria at 470 Ma to southern Morocco at 460 Ma and then to northeast Guinea by the end-Ordovician.

Baltica is likewise defined by three poles between 470 Ma and 460 Ma, but only two poles between 460 Ma and 445 Ma (Torsvik et al., 2012). Those data reveal that Baltica continued rotating counterclockwise during the Middle to Late Ordovician, and drifted *northward* from mid-southern latitudes at 470 Ma to low southern latitudes (~0°–30°S) by the close of the Ordovician.

The Middle to Late Ordovician paleomagnetic constraints from Siberia are excellent, and reveal that continent continued drifting *north* throughout the Ordovician, so that it was mostly in the northern hemisphere by the end of the period. Siberia also rotated slightly anticlockwise after 460 Ma, but remained north-south inverted ('upside down').

The Middle to Late Ordovician paleomagnetic records from the China blocks are poor. The record from North China includes only two Middle Ordovician poles, at 470 Ma and 464 Ma, which indicate that it was located between the equator and 20°S at that time. The Late Ordovician paleolatitude of North China is inferred via interpolation between those two Ordovician poles and its sole Silurian result, which reveals that after 460 Ma the block drifted more swiftly *northward*, crossing the equator to reach very low northern latitudes in the latest Ordovician. South China's record includes only one pole at ~456 Ma which indicates that it was also located at low southern latitudes then (~10°S). Interpolation between that result and South China's mid-Silurian data suggests that South China also drifted *northward* during the Late Ordovician, coming to straddle the equator by the end-Ordovician. The paleomagnetic record from Tarim likewise bears only one Middle–Late Ordovician pole. Its combined Ordovician paleomagnetic data place it at low-to-mid southern latitudes, whereas its Silurian results indicate that it had reached low-to-mid northern latitudes, thus revealing that Tarim too was drifting *northward* during the Middle–Late Ordovician.

Concerning the Kazakh terranes, the BC is not directly constrained by paleomagnetic data during the Middle to Late Ordovician, but the records from the NT and SK are excellent. Those data reveal that the NT and SK were at low southern latitudes (~10°–20°S) throughout the period. Furthermore, although pervasive vertical-axis rotations have hampered the use of paleomagnetic declinations among those data, the geographic distribution of the sampling sites is such that the inclinations alone can be used to roughly infer the orientation of the elongate NT-SK terranes (assuming they were united), the long-axis of which (presently oriented N–S to NW–SE) Bazhenov et al. (2012) showed to be then oriented approximately *east-west*.

Direct paleolongitudinal constraints are all but lacking during the Middle to Late Ordovician, as no LIPs erupted during that interval and kimberlites were only emplaced into northern Laurentia (at ~460 Ma and 450 Ma) and Siberia (at ~450 Ma) (Torsvik et al., 2014). Nevertheless, given the constraints from earlier and later times, those kimberlites are sufficient to infer that Siberia must have been located over the northwestern margin of Tuzo (Fig. 23), whereas northern Laurentia was positioned above the northern margin of Jason. Given that the equatorial band between Siberia (to the *west*) and Laurentia (to the *east*) accommodated the Kazakh terranes, the China blocks, and East Gondwana during the Late Ordovician, alternative longitudinal positions of Laurentia and Siberia are not possible due to space limitations. As before, with the absolute positioning of some key blocks (Laurentia and Siberia in this case), the relative longitudes of the remaining continents can be established through adoption of the simplest solution consistent with the paleomagnetic data. Accordingly, for Middle–Late Ordovician time, I have retained the general configuration of all the blocks between Siberia (to the *west*) and northeast Gondwana (to the *east*) as they were in the late Cambrian–Early Ordovician. Or, more pertinently, I have retained this configuration from their Early Devonian arrangement, which they must ultimately evolve to.

6.2.2. An extensive active margin interface with the Panthalassa

At the end of the Early Ordovician, an extensive, equatorial, *south-dipping* subduction interface ran from the *northern* margin of the CMT in the *west*, across the *northern* margins of the Kazakh terranes and North and South China blocks to the northeast margin of Gondwana (Fig. 18). Geologic vestiges from across those continental margins indicate that subduction continued along them through the Ordovician and Silurian and into the late Paleozoic (Figs. 19–26).

Interestingly, the apparent continuity and stability of that vast subduction interface may explain why the array of continental blocks and terranes collected between Siberia and northeast Gondwana were not strongly reshuffled during the early Paleozoic, as well as why their collective motions were similar and restrained. That wide, long-lived, near-equatorial subduction system may have played a first-order role in controlling the early Paleozoic kinematics of those continents and terranes, keeping them largely locked in place and kinematically semi-coupled. It also largely isolated those continents from the kinematics of the vast Panthalassa to the *north*, such that our knowledge of that domain (not modeled here) will always be extremely limited. Although I have

modeled the subduction system as a single, effectively continuous lineament (i.e. without large breaks or duplications), it is again most likely that the system was rather more complicated by backarcs and arc duplications, as in the case of the present-day southwest Pacific. One example of such an arc duplication is the Baidaulet-Aqbastau arc, which collided with the Boshekul-Chingiz zone in the Late Ordovician. Prior to its collision with the Boshekul-Chingiz zone, both arcs were simultaneously active, and probably associated with subduction systems of like-polarity (Şengör and Natal'In, 1996) (Figs. 6, 22 and 23).

6.2.3. A compound collision between Tarim and North China

From its Early–Middle Ordovician position at about 30°S, Tarim's Middle Ordovician *northward drift* brought it increasingly closer to the string of low-latitude continents and terranes lying between Siberia and northeast Gondwana then, and by the end of the Late Ordovician, Tarim must have collided with one of them (Figs. 21–23). Following the arguments presented in section 6.1.7, Tarim's *northward drift* in the Middle Ordovician, as in the Cambro–Ordovician, was accommodated by a *south-dipping* intraoceanic subduction zone lying between Tarim and North China. As also discussed in that section, the Cambrian history of that intraoceanic system—which is here assumed to have included elements now preserved in the Kunlun, Altyn, Qilian, Qaidam and North Qinling belts—probably involved bi-vergent arc-continent or arc-arc collisions, so that there were lithospheric scale weaknesses bounding both margins of that elongate system. Because many of the constituent blocks and belts of that elongate system preserve Cambrian to Silurian subduction-related relics along both margins, it isn't clear from the geology which of those margins was active at any given time during that interval, and moreover their present-day relative orientations are not necessarily reflective of their early Paleozoic configuration (Li et al., in press). Yet, if that intraoceanic system was correlative with the MIT in the *west*, as proposed in section 6.1.7, it is likely that the *northern margin* of that intraoceanic system was active in the late Cambrian and Early Ordovician, and thus associated with a *south-dipping* subduction zone (Figs. 18–20).

To accommodate the *northward drift* of Tarim behind that intraoceanic system, the *south-dipping* subduction zone must have been rolling back during the Early–Middle Ordovician. At ~480 Ma, however, the MIT collided with the KNT, at which point subduction jumped to the far (*south*) side of the MIT and switched polarity (to *north-dipping*). Conceivably, that local subduction polarity inversion could have had a wider effect, inducing *north-dipping* subduction beneath the *southern margin* of the intraoceanic arc system to the *east*, if such subduction was not already in operation (Fig. 20). Subduction could then have been briefly operating along both margins of that elongate arc system, facilitating the convergence of North China and Tarim on both sides.

At about 460 Ma, a collision occurred between the southern margin of Tarim (then facing *northeast*) and the *southwest* margin of the elongate arc system, resulting in the accretion of the South West Kunlun and Altyn belts to southern Tarim (Figs. 21 and 22). That collision could have driven further internal tectonism within the elongate arc system by the telescoping of minor intra-arc or back-arc basins, and could thus relate to the Middle-Late Ordovician collisions that evidently occurred among elements of the Qilian and Qaidam belts (section 4.8). However, along the *north* margin of the elongate arc system, subduction may have locally persisted through the latest Ordovician, ending by a collision between North Qinling-Qilian-Qaidam and North China-Alashan in the early Silurian. According to the progressive *northward drift* and clockwise rotation of Tarim through the Late Ordovician and into the Silurian as modeled, I further speculate that this compound series of Late Ordovician to early Silurian collisions could have occurred under a broadly transpressive regime after ~460 Ma (Figs. 23 and 24). During the Middle Ordovician, Tarim drifted *northward* past the KNT and its northern margin intersected the expansive equatorial subduction interface described above; its northern margin hence abruptly became active in the latest Ordovician or early Silurian (Figs. 7, 23 and 24). Tarim's southwest margin likewise became active following the collision and accretion of the South West Kunlun at 460 Ma.

The fate of the intraoceanic arc system further to the *southeast* is difficult to discern. Because South China, like North China, drifted *southward* until the Middle–Late Ordovician, when it reversed course and began drifting *northward*, I infer that *south-dipping* subduction beneath the intraoceanic arc to the *south* of South China and Annamia continued until ~460 Ma (Figs. 21 and 22). The cessation of subduction along that segment of the intraoceanic arc system could have been due to the collisions occurring to the *northwest*, between the intraoceanic arc and Tarim and North China, but it is perhaps more likely that subduction there ceased due the arrival of Annamia to the trench. Unfortunately, the early Paleozoic history of western Annamia is not well-known, but it is intriguing to note the occurrence of early Paleozoic volcaniclastic rocks and particularly Middle–Late Ordovician metavolcanic rocks in the northwest of Annamia (Yunnan Province of China) (section 4.13), which could be remnants of that intraoceanic arc system or an expression of Annamia's collision with it—and which otherwise would be unexpected given the prevailing passive margin conditions in northwest South China and Annamia during the Ordovician (Fig. 12). To accommodate the *northward drift* of South China following the cessation of subduction along the intraoceanic arc system, I assume the former convergent margin evolved to become a divergent boundary (Figs. 22 and 23). This divergent boundary would have specifically developed adjacent to the Iranian terranes along the northeast margin of Gondwana, and could potentially explain the appearance of bimodal to mafic-dominated magmatism there in the Late Ordovician–Silurian (section 4.14.2).

Although there are admittedly many assumptions and uncertainties bound up in this scenario, and in some instances a relaxed usage of ages, it is important to highlight the fact that the paleomagnetically-determined *northward drift* of Tarim during the Ordovician, coupled with the comparative latitudinal-stability of North China during that time, requires that a subduction zone was operating somewhere between the two. The two continental margins that were facing each other then, southern Tarim and southern North China, were both passive according to the geological evidence reviewed, implying that subduction between them was intraoceanic. Although the choices I have made about the positioning, polarity and uniformity of the intraoceanic system are highly provisional, I contend that this is presently the simplest scenario that meets the majority of the available observations.

6.2.4. The peculiar Kwangsian orogeny

Broadly coincident with the mid-Ordovician reversal of South China's drift (from *south* to *north-directed*) was the onset of the extensive Kwangsian orogeny in South China. Kwangsian orogenesis continued from the Middle Ordovician into the Devonian and was associated with intense deformation, metamorphism and magmatism, but conspicuously affected the interior of South China more so than its margins (section 4.11.1). Given the significant role that transcurrent motion evidently played in Kwangsian orogenesis, and that the orogen seems to have partly nucleated on the pre-existing suture zone between the Yangtze and Cathaysia cratons, it is compelling to consider the Kwangsian event to be an intracontinental orogeny driven by the far-field effect of transpression between southern South China and northeast Gondwana

(Figs. 21–23). On the inferred conjugate margin of northeast Gondwana (along Qiangtang, Lhasa, the Himalaya and Sibumasu), Cambro-Ordovician tectonism and magmatism had largely abated by the beginning of the Middle Ordovician. This diminution of tectonism and magmatism along northeast Gondwana concurrent with the initiation of the Kwangsian orogeny in South China may signify the end of active convergence between South China and northeast Gondwana, and a switch to transcurrent tectonism, then mostly accommodated by deformation in South China.

Although presently poorly detailed, indications of Ordovician-Silurian metamorphism and magmatism along eastern Annamia (in the Kontum massif, Truong Son terrane and 'north Vietnam'; section 4.13), which are otherwise puzzling, could also relate to the Kwangsian orogeny, and would accordingly further cement the ties between Annamia, South China and northeast Gondwana across that time.

6.2.5. The birth of the Mongol-Okhotsk and Mianlue oceans

In the latest Ordovician–early Silurian, two new oceans began to develop: the Mongol-Okhotsk Ocean between southern Siberia and northern Amuria, and the Mianlue Ocean between northern South China and the South Qinling (Fig. 23). The Mongol-Okhotsk Ocean likely commenced in response to continued subduction below the southern margin of the central Mongolian terranes, and seems to have partly nucleated on the former collisional boundary between the CMT and southern Siberia (Fig. 19). The exact age of the Mongol-Okhotsk's origination is not known; the oldest dated rocks from the basin are late Silurian radiolarian cherts, but they sit atop older dolerites of ocean island-affinity (section 4.1.4). Here I assume a latest Ordovician opening for the Mongol-Okhotsk Ocean (450 Ma). From its latest Ordovician opening, the Mongol-Okhotsk Ocean continued to widen through most of the remainder of the Paleozoic (Domeier and Torsvik, 2014), and did not ultimately close until the latest Jurassic-earliest Cretaceous (Van der Voo et al., 2015).

The opening of the Mianlue Ocean by the rifting of the South Qinling from the northern rim of South China was marked by a regional Ordovician–Silurian transition in sedimentation style and the emplacement of mafic dike swarms (section 4.11.2). The reason for the Mianlue Ocean's opening is not known, but from the reconstructed continenal framework it could be seen as somewhat self-emergent by the differential movements of North China and South China beginning in the Middle–Late Ordovician (Figs. 22 and 23). Whether that differential movement was instigated by the interaction of South China with northeast Gondwana, North China with Tarim, a combination of the two, or something else altogether is a rather dynamical question that cannot be addressed here. Owing to the signs of metamorphism and magmatism in eastern Annamia at this time, I also speculate that Mianlue Ocean opening may have been associated with differential motions between South China and Annamia, and model a transform between them through the latest Ordovician and Silurian (Figs. 23–26). Following its opening, the Mianlue Ocean remained open through to the collision between North and South China in the Triassic, although the South Qinling (not explicitly modeled here) collided with North China already in the late Paleozoic (section 4.9.1) (Domeier and Torsvik, 2014).

6.2.6. Spreading and subduction in the expanding internal oceans

With the continued *northward drift* of both Baltica and Tarim, and their relative *east-west drift* from one another, the oceans between Baltica, Tarim and northern Gondwana must have widened during the Middle and Late Ordovician (Figs. 21–23). Following from the Early Ordovician framework, I assume that basin widening was accommodated by a simple triad of divergent boundaries, meeting at a ridge-ridge-ridge triple junction. The position and orientation of the those divergent boundaries are thus derived from the kinematics of Baltica, Tarim and Gondwana, and the simple assumptions about how ridges behave as discussed in section 3.

To the *northwest*, those internal oceans were flanked by Siberia. According to the relative motions between Siberia, Baltica and Tarim (the latter two describing the motion of the oceanic lithosphere adject to Siberia), the boundary between Siberia and those oceans was partly convergent, and partly transcurrent during the Middle Ordovician (Figs. 21 and 22). Although the active margin between Siberia and Baltica during the Early Ordovician was inferred to be *south-dipping* (beneath North Kara), such a *south-dipping* subduction zone could not have continued further *east* beyond North Kara because it would have resulted in a collision between northern Siberia (as the lower plate) and that *south-dipping* subduction zone by ~470 Ma, for which there is no evidence in the South and Central Taimyr. Instead, I infer that subduction to the *east* of North Kara first initiated as a *north-dipping* subduction system at 470 Ma, by the foundering of a transform segment left behind North Kara as it passed by northern Siberia (Figs. 20 and 21). Because there is also no evidence of a Middle Ordovician continental arc in Taimyr, I assume that this arc was formed outboard the margin of northern Siberia, and specifically postulate that this was the subduction system where the Middle–Late Ordovician intra-oceanic Guberlya and Tagil arcs developed (section 4.15.1). These arcs, together with the later Magnitogorsk arc, fringed northern Siberia until the late Paleozoic, when they collided in a stepwise manner with the passive margin of east Baltica (Domeier and Torsvik, 2014).

6.3. Silurian (445–420 Ma)

6.3.1. Geography of the major continents

No paleomagnetic constraints are available from Gondwana for the duration of the Silurian (which, as an aside, is a remarkable deficiency in need of remedy), so its motion is entirely interpolated for this time (Torsvik et al., 2012). According to this interpolation, Gondwana mostly rotated clockwise over this interval, with the apparent position of the South Pole moving from the Northwest Africa craton (present-day northeast Guinea) at the opening of the Silurian to southernmost Amazonia (present-day north Argentina) by the close of the period. Due to the clockwise rotation of the landmass over this interval, the orientation of the northeast margin of Gondwana changed from a NNE–SSW orientation at 445 Ma to an ENE–WSW orientation by the end-Silurian (Figs. 24–26). Western Australia correspondingly moved from low northern latitudes to low southern latitudes during this time.

Paleomagnetic constraints from Baltica are poor for the early Silurian, but at 430 Ma Baltica collided with Laurentia to form Laurussia (Domeier, 2016), and the late Silurian paleomagnetic dataset from Laurussia is excellent (Torsvik et al., 2012). During the early Silurian Baltica continued to drift *northward* while rotating anticlockwise, such that by 430 Ma, when it collided with Laurentia, it was straddling the equator. Following the fusion of Baltica and Laurentia into the new landmass of Laurussia, that continent drifted slowly *southward* for the remainder of the Silurian, so that by the end of the Silurian the bulk of Laurussia was in the southern hemisphere.

Siberia's Silurian paleomagnetic record is weak, including only three poles, and with no paleomagnetic data between 432 Ma and 360 Ma. The early to middle Silurian paleomagnetic data indicate that the continent continued to drift *northward* across that time, so that by ~430 Ma the entirety of Siberia occupied low latitudes (0–30°) in the northern hemisphere. Interpolating between 430 Ma and 360 Ma, Siberia continued to drift *north* and rotate

clockwise; by 360 Ma Siberia had rotated ~45° clockwise from its orientation at 430 Ma.

The Silurian paleomagnetic data from the Kazakh terranes includes only two poles from the NT and SK and two from the BC. Collectively, those data reveal that the Kazakh terranes occupied equatorial latitudes during the Silurian, drifting *northward* from low southern latitudes in the early Silurian to reach low northern latitudes by the late Silurian. Although the specific distribution of those terranes is not well constrained, I consider it simplest to assume that they maintained an approximately *east-west* alignment, similar to that inferred for the combined NT-SK terranes in the Ordovician. Alternatively, they could have begun to rotate (either as a unified Kazakhstania or as a collection of semi-coherent blocks) slowly clockwise to reach the NW–SE orientation they evidently had by the Early-Middle Devonian (Bazhenov et al., 2012).

The Silurian paleomagnetic records from the China blocks are also weak. South China has only two Silurian poles, which are of the same age (~432 Ma). Nevertheless, interpolation between those poles and the Ordovician data reveals that South China moved *northward* during the early Silurian, whereas interpolation between that position and South China's Devonian setting suggests that it remained in low northern latitudes during the late Silurian.

No Silurian paleomagnetic data are available from the North China block itself due to the expansive Late Ordovician–Early Carboniferous stratigraphic hiatus there. However, Huang et al. (2000a) presented paleomagnetic data from Silurian sedimentary rocks in the southeast of the Alashan terrane, which could be used as a proxy for the North China block if the Alashan terrane was already united with it then. From the same area of the Alashan terrane, Huang et al. (1999a) presented an Early–Middle Ordovician paleomagnetic pole which coincides with similarly-aged poles from the North China block, thereby suggesting that Alashan (or at least its southeast domain) was coherent with the North China block by that time. Accordingly, I assume that Alashan was coherent with the North China block by the Ordovician and employ the Silurian pole to reconstruct North China, but caution that this assumption is challenged by post-Ordovician paleomagnetic data from other areas of the Alashan block which do not coincide with coeval data from the North China block (Huang et al., 2000a). The Silurian paleomagnetic pole employed places the North China block at low, northern latitudes (~15°) and with an orientation only slightly clockwise-rotated relative to today, effectively the same as it had in the Early–Middle Ordovician.

From Silurian–Devonian sedimentary rocks in northwest Tarim, Li et al. (1990) and Fang et al. (1996) reported possibly primary paleomagnetic data, which are at least constrained to be of pre-Early Permian age according to baked contact tests. Taken as primary, those data suggest that Tarim was rotated ~90° counterclockwise (relative to today) and had reached low-to-moderate northern latitudes (~20°–30°N) by the late Silurian. Having been in low southern latitudes in the Late Ordovician, Tarim must have drifted *northward* during the Silurian, crossing the equator in the latest Ordovician-early Silurian.

As in the Middle to Late Ordovician, direct paleolongitudinal constraints for the Silurian are sparse, and restricted to kimberlite emplacements in northwest Laurentia (at ~441 Ma and 435 Ma) and northeast Siberia (at ~442 Ma and 430 Ma) (Figs. 24 and 25) (Torsvik et al., 2014). The emplacement of kimberlites into those continents during both the Late Ordovician and Silurian suggests that they remained positioned over the same LLSVP margins across that time; or, in other words, Laurentia remained over the northern margin of Jason and Siberia lingered above the northwest margin of Tuzo. Although the early Silurian drift of Gondwana permits Laurentia to be alternatively positioned over the southern margin of Jason by the time kimberlites were emplaced into it at ~441 Ma, that positioning would require Laurentia (and Baltica) to drift *westward* at an astonishingly rapid rate (~60 cm/yr) between the Late Ordovician and early Silurian, which I deem unlikely. With the absolute paleolongitudes of Laurentia and Siberia again determined, the relative longitudes of the remaining continents can again be inferred from the paleomagnetic constraints and the geographic demands of earlier and later times.

6.3.2. The active margin interface with the Panthalassa

The extensive active margin interface with the Panthalassa—comprised, from *west* to *east*, by the southern margin of Amuria, the southwest margin of Siberia, and the *northern* margins of the Kazakh terranes, Tarim, North China and South China—continued from the Late Ordovician through the Silurian (Figs. 23–26). Between the Late Ordovician and early Silurian that broad subduction zone migrated slightly *northward*, and in the *east* that *northward* retreat of the trench continued through the Silurian, in tandem with the *northward drift* of the China blocks then. Owing to the clockwise rotation of Gondwana during the Silurian, that active margin may have been further elongated to span more than 15,000 km by the end of the Silurian (Fig. 26). As earlier, in the Ordovician, that active margin may have been effectively continuous, meaning that the kinematic communication between the Asian continental blocks and the vast Panthalassa Ocean to their *north* was minimal.

6.3.3. Dispersal and spreading amidst the equatorial continental train

At the beginning of the Silurian, the collection of continents and terranes between Siberia, to the *west*, and northeast Gondwana, to the *east*, was close-fitting (Fig. 24), as it had been throughout the Ordovician. However, from about the mid-Silurian, the clockwise rotation of Gondwana resulted in a *southeastward drift* of northeast Gondwana, or a movement directed away from Siberia, which continued to linger above the northwest margin of Tuzo then (Figs. 25 and 26). Because South China, Annamia and northeast Gondwana were locked up in a transpressive orogeny, that *southeastward displacement* of northeast Gondwana may also have carried South China and Annamia with it. The ensuing separation between North China and South China would then have been taken up by the pre-exising, and by-then rapidly expanding, Mianlue Ocean.

Further to the *west* along the equatorial continental train, the Silurian *northward drift* of Tarim was partly accommodated by continued transcurrent motion along its shared boundary with North China, meaning that tectonism continued along the Altyn, Qilian, Qaidaim, Kunlun and North Qinling belts. On the far (northern) side of Tarim, subduction seems to have continued from the Ordovician, but local spreading may also have begun between northern Tarim and the KNT in the late Silurian, ultimately opening the Turkestan Ocean that would later collapse again in the late Paleozoic (Domeier and Torsvik, 2014). Still further *west*, the Mongol-Okhotsk Ocean between south Siberia and Amuria continued to expand behind the active *northern* margin of the latter.

6.3.4. Spreading and subduction in the internal oceans

As in the Late Ordovician, throughout the Silurian a vast interior ocean occupied the void between the equatorial band of continents and terranes to the *north*, Gondwana to the *southeast* and Baltica to the *west* (Figs. 23–26). The ridge-ridge-ridge triple junction that had characterized that domain in the Early to Middle Ordovician was consumed by subduction (beneath peri-Siberia) in the Late Ordovician (Figs. 22 and 23), so that by early Silurian time the two remaining ridges were distant from one another (Fig. 24). The

continued *northward drift* of Baltica in the early Silurian engendered continued spreading along the *southwestern* of those two ridges, resulting in expansion of the Ran Ocean separating Baltica from northwest Gondwana (the Ran Ocean is a *northeast* extension of the Rheic Ocean separating Avalonia and northwest Gondwana; after the mid-Silurian merger of Avalonia and Baltica, the Rheic and Ran oceans became unified and are together referred to as the 'Rheic Ocean' from then). However, following the collision between Baltica and Laurentia at ~430 Ma, *north-dipping* subduction initiated beneath the *southern margin* of Laurussia, and the Rheic Ocean began to narrow from that time (Domeier and Torsvik, 2014; Domeier, 2016).

The *northeastern* ridge—which was formerly tied to the kinematics of Tarim but had become decoupled from it following Tarim's collision with the intraoceanic arc and North China in the Middle-Late Ordovician (Figs. 22 and 23)—was considerably reduced in length by the start of the Silurian, due to subduction beneath Siberia and the Kazakh terranes. To the *north* of that ridge was an independent oceanic plate which through Silurian time was subducting to the *north* beneath southwest Tarim and southern North China. By the latest Silurian that plate had vanished and so too the ridge that separated it from northeast Gondwana to the *south*. At end-Silurian time, with subduction encroaching directly onto the expansive oceanic margins of the greater Gondwana plate from two sides (beneath Laurussia to the *west* and Siberia, the Kazakh terranes and North China to the *north*), I infer that a major plate reorganization occurred, notably including the instigation of a new subduction zone outboard of northwest Gondwana and the inception of a new ridge-ridge-ridge triple junction behind it (Fig. 26). Although the *northward* continuation of that *east-dipping* subduction zone (and the *north-south oriented* ridge behind it) from the northwest margin of Gondwana is speculative, its development along the margin of Gondwana itself is dictated by the geologic history of the Variscan terranes (Domeier and Torsvik, 2014). I specifically elected to model this late Silurian reorganization in a manner similar to the starting framework of Domeier and Torsvik (2014), so that these models may be linked, but further work needs to be done on refining the details of Variscan terrane evolution in these models (Franke et al., 2017).

7. Discussion and outlook

Although I hope that this model will prove valuable as something of a contextual tectonic reference for Asia, and as a basic framework to be further tested and refined (or refuted), it is, at best, provisional. Much remains to be done. There are a great number of glaring deficiencies (some of which I have declared, but many others which I have not) that remain to be addressed—and many of the choices that I have made will expectedly beget critical and novel questions. Alternative scenarios need to be considered. And there also remains the matter of evaluating the present model itself, on the basis of its many quantitative aspects. However, this paper is long, and by now the reader is undoubtedly weary. My intention is therefore to keep this discussion brief, and to defer a richer treatment of these many important themes to future works.

Of the forseeable questions and concerns, perhaps the most salient is: to what extent is this model believable? It is not presently possible to answer this question with a percent-error estimate, or a confidence level (although it is thought-provoking to ponder how that could be achieved), but a brief qualitative consideration should prove illuminating. Considering first the paleolatitudes of the various continents and terranes, most all (save Annamia) have enough early Paleozoic paleomagnetic data to work out at least the first-order latitudinal framework. This is clear from Figs. 18–26, where most blocks are colored yellow, orange or red (denoting the presence of paleomagnetic constraints) for most of the modeled time interval. Crucially, many of those blocks—namely Siberia, the Kazakh terranes, North China, South China and northeastern Gondwana—are directly constrained to the same low latitudinal bands by that paleomagnetic data. This observation is critical because it reveals that those blocks never had the opportunity to be strongly re-shuffled (in a longitudinal sense) during the early Paleozoic, implying that they maintained effectively the same paleogeographic arrangement that they are known to have had in the late Paleozoic. For example, North China is reconstructed between Siberia (to the *west*) and South China (to the *east*) in the Devonian (Domeier and Torsvik, 2014); because paleomagnetic data from those three continents reveal that they occupied effectively the same latitudes from 500 Ma to 410 Ma, North China must have always been positioned between Siberia (to the *west*) and South China (to the *east*). The gaps noted in those early Paleozoic paleomagnetic records, at least for the major blocks, never seem protracted enough to otherwise conceal the north-south displacements that would be required to allow such longitudinal shuffling. As aforementioned, a possible exception to this is presented by the Kazakh terranes, whose paleomagnetic data could be used to restore them to low latitudes in the northern hemisphere in the Cambrian and Ordovician, but this solution raises additional kinematic complexities and doesn't otherwise better explain the existing geologic and paleobiologic data.

The corollary, then, is that the sufficiently good early Paleozoic paleomagnetic record from the continental blocks of Asia affords a reliable restoration of their absolute paleolatitudes, as well as an effective estimate of their relative paleolongitudes. The relative paleolongitudinal framework of the model is therefore robust even without the proposed absolute paleolongitudinal constraints. Nevertheless, the absolute paleolongitudes can provide a useful starting point for dynamical exercises, including those designed to evaluate the kinematics of the model itself, and those using the model as an input for numerical mantle simulations. One particularly striking aspect of the model that arises from application of the absolute paleolongitudinal constraints is the appearance of a regional vorticity in the Cambro-Ordovician (Figs. 18 and 19) and mid-to-late Silurian (Figs. 25 and 26). Future work, and in particular the completion of a global early Paleozoic full-plate model will be required to determine if these modeled kinematics are physically viable.

Concerning the veracity of the modeled plate boundaries, much can again be hung on the underlying continental framework. The extensive and enduring, near-equatorial, *south-dipping* subduction system running from Siberia to South China, for example, is derived from geological observations, but its kinematics are directly linked to the kinematics of the continents. Intriguingly, it may well have been that expansive subduction system that kept the low-latitudinal string of continents and terranes in line for so long, in turn allowing their relative paleolongitudes to be confidently deduced. As a closing admission, however, I would call attention to an important assumption in my reconstruction of the plate boundaries amidst the oceans between the major continental blocks. Tarim acts as a lynchpin of sorts, helping to establish the kinematics of intraoceanic subduction to the *north* of it, as well as spreading to its *south*. I have made a case for why I consider it most likely that Tarim was in the southern hemisphere in the Cambrian and Ordovician, but the ambiguity of its paleomagnetic data alternatively permits its restoration in the northern hemisphere then. If, in the end, it turns out that Tarim occupied the latter, the kinematics of the interior oceans as modeled here would be doubtful, and many details of the presented model would need to be reconsidered.

Acknowledgements

I thank Trond Torsvik and Robin Cocks for innumerous discussions about the paleogeography of the early Paleozoic, and for laying much of the groundwork that this paper stands upon. I also thank Trond for providing feedback on an early version of this manuscript and Robin for providing a thorough and constructive review. This work was supported by the Research Council of Norway (RCN) through its Centres of Excellence funding scheme, project 223272 (CEED), and through RCN project 250111.

References

Abbo, A., Avigad, D., Gerdes, A., Güngör, T., 2015. Cadomian basement and Paleozoic to Triassic siliciclastics of the Taurides (Karacahisar dome, south-central Turkey): paleogeographic constraints from U–Pb–Hf in zircons. Lithos 227, 122–139.

Abdullah, S., Chmyriov, V.M. (Eds.), 2008. Geology and Mineral Resources of Afghanistan. British Geological Survey Occasional Publication No. 15.

Adamia, S., Zakariadze, G., Chkhotua, T., Sadradze, N., Tsereteli, N., Chabukiani, A., Gventsadze, A., 2011. Geology of the Caucasus: a review. Turkish Journal of Earth Sciences 20 (5), 489–544.

Akinin, V.V., Gottlieb, E.S., Miller, E.L., Polzunenkov, G.O., Stolbov, N.M., Sobolev, N.N., 2015. Age and composition of basement beneath the De Long archipelago, Arctic Russia, based on zircon U–Pb geochronology and O–Hf isotopic systematics from crustal xenoliths in basalts of Zhokhov Island. Arktos 1 (1), 1–10.

Alavi, M., 1996. Tectonostratigraphic synthesis and structural style of the Alborz Mountain system in northern Iran. Journal of Geodynamics 21 (1), 1–33.

Alexeiev, D., Kröner, A., Hegner, E., Rojas-Agramonte, Y., Biske, Y.S., Wong, J., Geng, H., Ivleva, E., Mühlberg, M., Mikolaichuk, A., 2016. Middle to Late Ordovician arc system in the Kyrgyz Middle Tianshan: from arc-continent collision to subsequent evolution of a Palaeozoic continental margin. Gondwana Research 39, 261–291.

Alexeiev, D., Ryazantsev, A., Kröner, A., Tretyakov, A., Xia, X., Liu, D., 2011. Geochemical data and zircon ages for rocks in a high-pressure belt of Chu-Yili Mountains, southern Kazakhstan: implications for the earliest stages of accretion in Kazakhstan and the Tianshan. Journal of Asian Earth Sciences 42 (5), 805–820.

Alexyutin, M., Bachtadse, V., Alexeiev, D., Nikitina, O., 2005. Palaeomagnetism of Ordovician and Silurian rocks from the Chu-Yili and Kendyktas mountains, south Kazakhstan. Geophysical Journal International 162 (2), 321–331.

An, F., Zhu, Y., Wei, S., Lai, S., 2017. The zircon U–Pb and Hf isotope constraints on the basement nature and Paleozoic evolution in northern margin of Yili Block, NW China. Gondwana Research 43, 41–54.

Antoshkina, A.I., 2008. Late Ordovician–Early Silurian facies development and environmental changes in the Subpolar Urals. Lethaia 41 (2), 163–171.

Ao, S., Xiao, W., Han, C., Li, X., Qu, J., Zhang, J., Guo, Q., Tian, Z., Abrajevitch, A., Van der Voo, R., 2012. Cambrian to early Silurian ophiolite and accretionary processes in the Beishan collage, NW China: implications for the architecture of the Southern Altaids. Geological Magazine 149 (4), 606.

Aoki, K., Isozaki, Y., Yamamoto, A., Sakata, S., Hirata, T., 2015. Mid-Paleozoic arc granitoids in SW Japan with Neoproterozoic xenocrysts from South China: new zircon U–Pb ages by LA-ICP-MS. Journal of Asian Earth Sciences 97, 125–135.

Aysal, N., Öngen, S., Peytcheva, I., Keskin, M., 2012. Origin and evolution of the Havran Unit, Western Sakarya basement (NW Turkey): new LA-ICP-MS U-Pb dating of the metasedimentary-metagranitic rocks and possible affiliation to Avalonian microcontinent. Geodinamica Acta 25 (3–4), 226–247.

Bachtadse, V., Pavlov, V., Kazansky, A., Tait, J., 2000. Siluro-Devonian paleomagnetic results from the Tuva Terrane (southern Siberia, Russia): implications for the paleogeography of Siberia. Journal of Geophysical Research: Solid Earth 105 (B6), 13509–13518.

Badarch, G., Dickson Cunningham, W., Windley, B.F., 2002. A new terrane subdivision for Mongolia: implications for the Phanerozoic crustal growth of Central Asia. Journal of Asian Earth Sciences 21 (1), 87–110.

Bader, T., Franz, L., Ratschbacher, L., Capitani, C., Webb, A.A.G., Yang, Z., Pfänder, J.A., Hofmann, M., Linnemann, U., 2013. The Heart of China revisited: II Early Paleozoic (ultra) high-pressure and (ultra) high-temperature metamorphic Qinling orogenic collage. Tectonics 32 (4), 922–947.

Balintoni, I., Balica, C., 2016. Peri-Amazonian provenance of the Euxinic Craton components in Dobrogea and of the North Dobrogean Orogen components (Romania): a detrital zircon study. Precambrian Research 278, 34–51.

Bazhenov, M.L., Collins, A.Q., Degtyarev, K.E., Levashova, N.M., Mikolaichuk, A.V., Pavlov, V.E., Van der Voo, R., 2003. Paleozoic northward drift of the North Tien Shan (Central Asia) as revealed by Ordovician and Carboniferous paleomagnetism. Tectonophysics 366 (1), 113–141.

Bazhenov, M.L., Levashova, N.M., Degtyarev, K.E., Van der Voo, R., Abrajevitch, A.V., McCausland, P.J., 2012. Unraveling the early–middle Paleozoic paleogeography of Kazakhstan on the basis of Ordovician and Devonian paleomagnetic results. Gondwana Research 22 (3), 974–991.

Bea, F., Fershtater, G., Montero, P., 2002. Granitoids of the Uralides: implications for the evolution of the orogen. In: Mountain Building in the Uralides: Pangea to the Present, vol. 132. American Geophysical Union Monograph Series, pp. 211–232.

Becker, T.W., Boschi, L., 2002. A comparison of tomographic and geodynamic mantle models. Geochemistry, Geophysics, Geosystems 3 (1).

Belichenko, V., Geletii, N., Barash, I., 2006. Barguzin microcontinent (Baikal mountain area): the problem of outlining. Russian Geology and Geophysics (Geologiya i Geofizika) 47 (10), 1035–1045.

Belova, A., Ryazantsev, A., Razumovsky, A., Degtyarev, K., 2010. Early Devonian suprasubduction ophiolites of the southern Urals. Geotectonics 44 (4), 321–343.

Bhargava, O.N., Frank, W., Bertle, R., 2011. Late Cambrian deformation in the Lesser Himalaya. Journal of Asian Earth Sciences 40 (1), 201–212.

Bogolepova, O.K., Gubanov, A.P., Pease, V.L., 2006. The Ordovician of the Severnaya Zemlya Archipelago, Russia. Newsletters on Stratigraphy 42 (1), 21–41.

Bonev, N., Ovtcharova-Schaltegger, M., Moritz, R., Marchev, P., Ulianov, A., 2013. Peri-Gondwanan Ordovician crustal fragments in the high-grade basement of the Eastern Rhodope Massif, Bulgaria: evidence from U-Pb LA-ICP-MS zircon geochronology and geochemistry. Geodinamica Acta 26 (3–4), 207–229.

Boyden, J.A., Müller, R.D., Gurnis, M., Torsvik, T.H., Clark, J.A., Turner, M., Ivey-Law, H., Watson, R.J., Cannon, J.S., 2011. Next-generation plate-tectonic reconstructions using GPlates. In: Geoinformatics: Cyberinfrastructure for the Solid Earth Sciences. Cambridge University Press, pp. 95–113.

Bozkaya, Ö., Yalçın, H., Göncüoğlu, M.C., Murphy, B., 2012. Mineralogic evidences of a mid-Paleozoic tectono-thermal event in the Zonguldak terrane, northwest Turkey: implications for the dynamics of some Gondwana-derived terranes during the closure of the Rheic Ocean. Canadian Journal of Earth Sciences 49 (4), 559–575.

Bradley, D.C., 2008. Passive margins through earth history. Earth-Science Reviews 91 (1), 1–26.

Brookfield, M., 1993. The Himalayan passive margin from Precambrian to Cretaceous times. Sedimentary Geology 84 (1), 1–35.

Brown, D., Herrington, R., Alvarez-Marron, J., 2011. Processes of arc-continent collision in the uralides. In: Arc-continent Collision. Frontiers in Earth Sciences, Springer Verlag, pp. 311–340.

Burenjargal, U., Okamoto, A., Kuwatani, T., Sakata, S., Hirata, T., Tsuchiya, N., 2014. Thermal evolution of the Tseel terrane, SW Mongolia and its relation to granitoid intrusions in the Central Asian Orogenic Belt. Journal of Metamorphic Geology 32 (7), 765–790.

Burrett, C., Zaw, K., Meffre, S., Lai, C.K., Khositanont, S., Chaodumrong, P., Udchachon, M., Ekins, S., Halpin, J., 2014. The configuration of Greater Gondwana—evidence from LA ICPMS, U–Pb geochronology of detrital zircons from the Palaeozoic and Mesozoic of Southeast Asia and China. Gondwana Research 26 (1), 31–51.

Buslov, M., Geng, H., Travin, A., Otgonbaatar, D., Kulikova, A., Ming, C., Stijn, G., Semakov, N., Rubanova, E., Abildaeva, M., 2013. Tectonics and geodynamics of Gorny Altai and adjacent structures of the Altai–Sayan folded area. Russian Geology and Geophysics 54 (10), 1250–1271.

Buslov, M., Watanabe, T., Saphonova, I.Y., Iwata, K., Travin, A., Akiyama, M., 2002. A Vendian-Cambrian island arc system of the Siberian continent in Gorny Altai (Russia, Central Asia). Gondwana Research 5 (4), 781–800.

Bussien, D., Gombojav, N., Winkler, W., Von Quadt, A., 2011. The Mongol–Okhotsk Belt in Mongolia—an appraisal of the geodynamic development by the study of sandstone provenance and detrital zircons. Tectonophysics 510 (1), 132–150.

Cai, F., Ding, L., Yao, W., Laskowski, A.K., Xu, Q., Zhang, J.E., Sein, K., 2017. Provenance and tectonic evolution of Lower Paleozoic–Upper Mesozoic strata from Sibumasu terrane, Myanmar. Gondwana Research 41, 325–336.

Cai, J.X., Zhang, K.J., 2009. A new model for the Indochina and South China collision during the Late Permian to the Middle Triassic. Tectonophysics 467 (1), 35–43.

Cai, K., Sun, M., Yuan, C., Long, X., Xiao, W., 2011a. Geological framework and Paleozoic tectonic history of the Chinese Altai, NW China: a review. Russian Geology and Geophysics 52 (12), 1619–1633.

Cai, K., Sun, M., Yuan, C., Zhao, G., Xiao, W., Long, X., Wu, F., 2011b. Prolonged magmatism, juvenile nature and tectonic evolution of the Chinese Altai, NW China: evidence from zircon U–Pb and Hf isotopic study of Paleozoic granitoids. Journal of Asian Earth Sciences 42 (5), 949–968.

Cao, H., Li, S., Zhao, S., Yu, S., Li, X., Somerville, I., 2016. Detrital zircon geochronology of Neoproterozoic to early Paleozoic sedimentary rocks in the North Qinling Orogenic Belt: implications for the tectonic evolution of the Kuanping Ocean. Precambrian Research 279, 1–16.

Carroll, A.R., Graham, S.A., Chang, E.Z., McKnight, C., 2001. Sinian through Permian tectonostratigraphic evolution of the northwestern Tarim basin, China. In: Paleozoic and Mesozoic Tectonic Evolution of Central Asia: From Continental Assembly to Intracontinental Deformation, vol. 194. Geological Society of America, Memoir, pp. 47–70.

Cawood, P.A., Johnson, M.R., Nemchin, A.A., 2007. Early Palaeozoic orogenesis along the Indian margin of Gondwana: tectonic response to Gondwana assembly. Earth and Planetary Science Letters 255 (1), 70–84.

Cawood, P.A., Wang, Y., Xu, Y., Zhao, G., 2013. Locating South China in Rodinia and Gondwana: a fragment of greater India lithosphere? Geology 41 (8), 903–906.

Chang, K.H., Zhao, X., 2012. North and South China suturing in the east end: what happened in Korean Peninsula? Gondwana Research 22 (2), 493–506.

Charvet, J., Shu, L., Faure, M., Choulet, F., Wang, B., Lu, H., Le Breton, N., 2010. Structural development of the Lower Paleozoic belt of South China: genesis of an intracontinental orogen. Journal of Asian Earth Sciences 39 (4), 309–330.

Charvet, J., Shu, L., Laurent-Charvet, S., Wang, B., Faure, M., Cluzel, D., Chen, Y., De Jong, K., 2011. Palaeozoic tectonic evolution of the Tianshan belt, NW China. Science China Earth Sciences 54 (2), 166–184.
Chen, B., Jahn, B., Tian, W., 2009. Evolution of the Solonker suture zone: constraints from zircon U–Pb ages, Hf isotopic ratios and whole-rock Nd–Sr isotope compositions of subduction-and collision-related magmas and forearc sediments. Journal of Asian Earth Sciences 34 (3), 245–257.
Chen, J.F., Han, B.F., Ji, J.Q., Zhang, L., Xu, Z., He, G.Q., Wang, T., 2010. Zircon U–Pb ages and tectonic implications of Paleozoic plutons in northern West Junggar, North Xinjiang, China. Lithos 115 (1), 137–152.
Chen, Q., Sun, M., Long, X., Zhao, G., Yuan, C., 2016. U–Pb ages and Hf isotopic record of zircons from the late Neoproterozoic and Silurian–Devonian sedimentary rocks of the western Yangtze Block: implications for its tectonic evolution and continental affinity. Gondwana Research 31, 184–199.
Chen, X., Gehrels, G., Yin, A., Li, L., Jiang, R., 2012. Paleozoic and Mesozoic basement magmatisms of Eastern Qaidam Basin, Northern Qinghai-Tibet Plateau: LA-ICP-MS zircon U-Pb geochronology and its geological significance. Acta Geologica Sinica-English Edition 86 (2), 350–369.
Cherepanova, Y., Artemieva, I., 2015. Density heterogeneity of the cratonic lithosphere: a case study of the Siberian craton. Gondwana Research 28 (4), 1344–1360.
Cherepanova, Y., Artemieva, I.M., Thybo, H., Chemia, Z., 2013. Crustal structure of the Siberian craton and the West Siberian basin: an appraisal of existing seismic data. Tectonophysics 609, 154–183.
Cho, M., Cheong, W., Ernst, W.G., Yi, K., Kim, J., 2013. SHRIMP U-Pb ages of detrital zircons in metasedimentary rocks of the central Ogcheon fold-thrust belt, Korea: evidence for tectonic assembly of Paleozoic sedimentary protoliths. Journal of Asian Earth Sciences 63, 234–249.
Choulet, F., Cluzel, D., Faure, M., Lin, W., Wang, B., Chen, Y., Wu, F.Y., Ji, W., 2012a. New constraints on the pre-Permian continental crust growth of Central Asia (West Junggar, China) by U–Pb and Hf isotopic data from detrital zircon. Terra Nova 24 (3), 189–198.
Choulet, F., Faure, M., Cluzel, D., Chen, Y., Lin, W., Wang, B., Jahn, B.-m, 2012b. Architecture and evolution of accretionary orogens in the Altaids collage: the early Paleozoic West Junggar (NW China). American Journal of Science 312 (10), 1098–1145.
Cleven, N., Lin, S., Guilmette, C., Xiao, W., Davis, B., 2015. Petrogenesis and implications for tectonic setting of Cambrian suprasubduction-zone ophiolitic rocks in the central Beishan orogenic collage, Northwest China. Journal of Asian Earth Sciences 113, 369–390.
Cocks, L.R.M., Fortey, R., Lee, C., 2005. A review of Lower and Middle Palaeozoic biostratigraphy in west peninsular Malaysia and southern Thailand in its context within the Sibumasu Terrane. Journal of Asian Earth Sciences 24 (6), 703–717.
Cocks, L.R.M., Torsvik, T.H., 2007. Siberia, the wandering northern terrane, and its changing geography through the Palaeozoic. Earth-Science Reviews 82 (1), 29–74.
Cocks, L.R.M., Torsvik, T.H., 2013. The dynamic evolution of the Palaeozoic geography of eastern Asia. Earth-Science Reviews 117, 40–79.
Collett, S., Faryad, S.W., Mosazai, A.M., 2015. Polymetamorphic evolution of the granulite-facies Paleoproterozoic basement of the Kabul Block, Afghanistan. Mineralogy and Petrology 109 (4), 463–484.
Collins, A.Q., Degtyarev, K.E., Levashova, N.M., Bazhenov, M.L., Van der Voo, R., 2003. Early Paleozoic paleomagnetism of East Kazakhstan: implications for paleolatitudinal drift of tectonic elements within the Ural–Mongol belt. Tectonophysics 377 (3), 229–247.
Danukalova, M., Kuzmichev, A., Korovnikov, I., 2014. The Cambrian of Bennett Island (New Siberian Islands). Stratigraphy and Geological Correlation 22 (4), 347–369.
Daoudene, Y., Gapais, D., Ledru, P., Cocherie, A., Hocquet, S., Donskaya, T.V., 2009. The Ereendavaa Range (north-eastern Mongolia): an additional argument for Mesozoic extension throughout eastern Asia. International Journal of Earth Sciences 98 (6), 1381–1393.
Daragan-Sushchova, L., Petrov, O., Daragan-Sushchov, Y.I., Vasil'ev, M., 2014. Structure of the North Kara Shelf from results of seismostratigraphic analysis. Geotectonics 48 (2), 139–150.
De Grave, J., Glorie, S., Buslov, M.M., Izmer, A., Fournier-Carrie, A., Batalev, V.Y., Vanhaecke, F., Elburg, M., 2011a. The thermo-tectonic history of the Song-Kul plateau, Kyrgyz Tien Shan: Constraints by apatite and titanite thermochronometry and zircon U/Pb dating. Gondwana Research 20 (4), 745–763.
De Grave, J., Glorie, S., Zhimulev, F.I., Buslov, M.M., Elburg, M., Vanhaecke, F., 2011b. Emplacement and exhumation of the Kuznetsk-Alatau basement (Siberia): implications for the tectonic evolution of the Central Asian Orogenic Belt and sediment supply to the Kuznetsk, Minusa and West Siberian Basins. Terra Nova 23 (4), 248–256.
De Jong, K., Xiao, W., Windley, B.F., Masago, H., Lo, C.H., 2006. Ordovician $^{40}Ar/^{39}Ar$ phengite ages from the blueschist-facies Ondor Sum subduction-accretion complex (Inner Mongolia) and implications for the early Paleozoic history of continental blocks in China and adjacent areas. American Journal of Science 306 (10), 799–845.
Dean, W., Monod, O., Rickards, R., Demir, O., Bultynck, P., 2000. Lower Palaeozoic stratigraphy and palaeontology, Karadere–Zirze area, Pontus mountains, northern Turkey. Geological Magazine 137 (5), 555–582.
Debon, F., Afzali, H., Le Fort, P., Sonet, J., 1987. Major intrusive stages in Afghanistan: Typology, age and geodynamic setting. Geologische Rundschau 76 (1), 245–264.
DeCelles, P.G., Gehrels, G.E., Quade, J., LaReau, B., Spurlin, M., 2000. Tectonic implications of U-Pb zircon ages of the Himalayan orogenic belt in Nepal. Science 288 (5465), 497–499.
Degtyarev, K., 2011. Tectonic evolution of Early Paleozoic Island-arc systems and continental crust formation in the Caledonides of Kazakhstan and the North Tien Shan. Geotectonics 45 (1), 23–50.
Degtyarev, K., Ryazantsev, A., 2007. Cambrian arc-continent collision in the Paleozoides of Kazakhstan. Geotectonics 41 (1), 63–86.
Degtyarev, K., Ryazantsev, A., Tretyakov, A., Tolmacheva, T.Y., Yakubchuk, A., Kotov, A., Salnikova, E., Kovach, V., 2013. Neoproterozoic-Early Paleozoic tectonic evolution of the western part of the Kyrgyz Ridge (Northern Tian Shan) caledonides. Geotectonics 47 (6), 377–417.
Degtyarev, K., Shatagin, K., Kotov, A., Sal'nikova, E., Luchitskaya, M., Yakovleva, S., Plotkina, Y.V., Fedoseenko, A., 2006. Early paleozoic granitoids of the Aqtau-Dzungar microcontinent (Central Kazakhstan). Doklady Earth Sciences 411 (1), 1204–1208.
Degtyarev, K., Tolmacheva, T.Y., Tretyakov, A., Kotov, A., Shatagin, K., 2016. Cambrian to Lower Ordovician complexes of the Kokchetav Massif and its fringing (Northern Kazakhstan): structure, age, and tectonic settings. Geotectonics 50 (1), 71–142.
Demoux, A., Kröner, A., Badarch, G., Jian, P., Tomurhuu, D., Wingate, M.T., 2009a. Zircon ages from the Baydrag block and the Bayankhongor ophiolite zone: time constraints on late Neoproterozoic to Cambrian subduction-and accretion-related magmatism in central Mongolia. The Journal of Geology 117 (4), 377–397.
Demoux, A., Kröner, A., Liu, D., Badarch, G., 2009b. Precambrian crystalline basement in southern Mongolia as revealed by SHRIMP zircon dating. International Journal of Earth Sciences 98 (6), 1365–1380.
Derakhshi, M., Ghasemi, H., 2015. Soltan Maidan Complex (SMC) in the eastern Alborz structural zone, northern Iran: magmatic evidence for Paleotethys development. Arabian Journal of Geosciences 8 (2), 849–866.
Dijkstra, A.H., Brouwer, F.M., Cunningham, W.D., Buchan, C., Badarch, G., Mason, P.R., 2006. Late Neoproterozoic proto-arc ocean crust in the Dariv Range, Western Mongolia: a supra-subduction zone end-member ophiolite. Journal of the Geological Society 163 (2), 363–373.
Ding, H., Zhang, Z., Dong, X., Yan, R., Lin, Y., Jiang, H., 2015. Cambrian ultrapotassic rhyolites from the Lhasa terrane, south Tibet: evidence for Andean-type magmatism along the northern active margin of Gondwana. Gondwana Research 27 (4), 1616–1629.
Dobretsov, N., Buslov, M., Yu, U., 2004. Fragments of oceanic islands in accretion–collision areas of Gorny Altai and Salair, southern Siberia, Russia: early stages of continental crustal growth of the Siberian continent in Vendian–Early Cambrian time. Journal of Asian Earth Sciences 23 (5), 673–690.
Dobretsov, N., Buslov, M., Zhimulev, F., Travin, A., Zayachkovsky, A., 2006. Vendian-Early Ordovician geodynamic evolution and model for exhumation of ultrahigh and high-pressure rocks from the Kokchetav subduction-collision zone (Northern Kazakhstan). Russian Geology and Geophysics 47, 428–444.
Dobretsov, N.L., Buslov, M.M., 2004. Serpentinitic mélanges associated with HP and UHP rocks in Central Asia. International Geology Review 46 (11), 957–980.
Domeier, M., 2016. A plate tectonic scenario for the Iapetus and Rheic Oceans. Gondwana Research 36, 275–295.
Domeier, M., Torsvik, T.H., 2014. Plate tectonics in the late Paleozoic. Geoscience Frontiers 5 (3), 303–350.
Domeier, M., Torsvik, T.H., 2018. Full-plate modelling in pre-Jurassic time. Geological Magazine 1–20. https://doi.org/10.1017/S0016756817001005 (in press).
Dong, X., Zhang, Z., Santosh, M., 2010. Zircon U-Pb chronology of the Nyingtri group, southern Lhasa terrane, Tibetan Plateau: implications for Grenvillian and Pan-African provenance and Mesozoic-Cenozoic metamorphism. The Journal of Geology 118 (6), 677–690.
Dong, Y., Liu, X., Neubauer, F., Zhang, G., Tao, N., Zhang, Y., Zhang, X., Li, W., 2013. Timing of Paleozoic amalgamation between the North China and South China Blocks: evidence from detrital zircon U–Pb ages. Tectonophysics 586, 173–191.
Dong, Y., Santosh, M., 2016. Tectonic architecture and multiple orogeny of the Qinling Orogenic Belt, Central China. Gondwana Research 29 (1), 1–40.
Dong, Y., Zhang, G., Neubauer, F., Liu, X., Genser, J., Hauzenberger, C., 2011a. Tectonic evolution of the Qinling orogen, China: review and synthesis. Journal of Asian Earth Sciences 41 (3), 213–237.
Dong, Y., Zhang, G., Neubauer, F., Liu, X., Hauzenberger, C., Zhou, D., Li, W., 2011b. Syn-and post-collisional granitoids in the Central Tianshan orogen: geochemistry, geochronology and implications for tectonic evolution. Gondwana Research 20 (2), 568–581.
Donskaya, T., Gladkochub, D., Fedorovsky, V., Mazukabzov, A., Cho, M., Cheong, W., Kim, J., 2013. Synmetamorphic granitoids (~490 Ma) as accretion indicators in the evolution of the Ol'khon terrane (*western Cisbaikalia*). Russian Geology and Geophysics 54 (10), 1205–1218.
Duan, J., Li, C., Qian, Z., Jiao, J., 2015. Geochronological and geochemical constraints on the petrogenesis and tectonic significance of Paleozoic dolerite dykes in the southern margin of Alxa Block, North China Craton. Journal of Asian Earth Sciences 111, 244–253.

Dubinina, S., Ryazantsev, A., 2008. Conodont stratigraphy and correlation of the Ordovician volcanogenic and volcanogenic sedimentary sequences in the South Urals. Russian Journal of Earth Sciences 10, 1–31.
Ershova, V., Prokopiev, A., Khudoley, A., Shneider, G., Andersen, T., Kullerud, K., Makar'ev, A., Maslov, A., Kolchanov, D., 2015a. Results of UePb (LAeICPMS) Dating of Detrital Zircons from Metaterrigenous Rocks of the Basement of the North Kara Basin. Doklady Earth Sciences 464, 997–1000.
Ershova, V.B., Lorenz, H., Prokopiev, A.V., Sobolev, N.N., Khudoley, A.K., Petrov, E.O., Estrada, S., Sergeev, S., Larionov, A., Thomsen, T.B., 2016. The De Long Islands: a missing link in unraveling the Paleozoic paleogeography of the Arctic. Gondwana Research 35, 305–322.
Ershova, V.B., Prokopiev, A.V., Khudoley, A.K., Sobolev, N.N., Petrov, E.O., 2015b. Detrital zircon ages and provenance of the Upper Paleozoic successions of Kotel'ny Island (New Siberian Islands archipelago). Lithosphere 7 (1), 40–45.
Evans, D., Zhuravlev, A.Y., Budney, C., Kirschvink, J., 1996. Palaeomagnetism of the Bayan Gol Formation, western Mongolia. Geological Magazine 133 (4), 487–496.
Fang, D.J., Jin, G.H., Jiang, L.P., Wang, P.Y., Wang, Z.L., 1996. Paleozoic paleomagnetic results and the tectonic significance of Tarim Plate. Acta Geophysica Sinica 39, 532–542.
Fang, W., Van der Voo, R., Liang, Q., 1990. Ordovician paleomagnetism of eastern Yunnan, China. Geophysical Research Letters 17 (7), 953–956.
Faure, M., Lepvrier, C., Van Nguyen, V., Van Vu, T., Lin, W., Chen, Z., 2014. The South China Block-Indochina collision: where, when, and how? Journal of Asian Earth Sciences 79, 260–274.
Faure, M., Shu, L., Wang, B., Charvet, J., Choulet, F., Monié, P., 2009. Intracontinental subduction: a possible mechanism for the Early Palaeozoic Orogen of SE China. Terra Nova 21 (5), 360–368.
Fortey, R., Cocks, L., 1998. Biogeography and palaeogeography of the Sibumasu terrane in the Ordovician: a review. In: Biogeography and Geological Evolution of SE Asia. Backhuys Publishers, pp. 43–56.
Franke, W., Cocks, L.R.M., Torsvik, T.H., 2017. The Palaeozoic Variscan oceans revisited. Gondwana Research 48, 257–284.
Friberg, M., Larionov, A., Petrov, G., Gee, D., 2000. Paleozoic amphibolite–granulite facies magmatic complexes in the hinterland of the Uralide Orogen. International Journal of Earth Sciences 89 (1), 21–39.
Gaetani, M., 1997. The Karakorum block in central Asia, from Ordovician to Cretaceous. Sedimentary Geology 109 (3–4), 339–359.
Gao, J., Long, L., Klemd, R., Qian, Q., Liu, D., Xiong, X., Su, W., Liu, W., Wang, Y., Yang, F., 2009. Tectonic evolution of the South Tianshan orogen and adjacent regions, NW China: geochemical and age constraints of granitoid rocks. International Journal of Earth Sciences 98 (6), 1221–1238.
Gao, X., Xiao, P., Guo, L., Dong, Z., Xi, R., 2011. Opening of an early Paleozoic limited oceanic basin in the northern Altyn area: constraints from plagiogranites in the Hongliugou-Lapeiquan ophiolitic mélange. Science China Earth Sciences 54 (12), 1871–1879.
Garzanti, E., Casnedi, R., Jadoul, F., 1986. Sedimentary evidence of a Cambro-Ordovician orogenic event in the northwestern Himalaya. Sedimentary Geology 48 (3–4), 237–265.
Ge, R., Zhu, W., Wilde, S.A., He, J., Cui, X., Wang, X., Bihai, Z., 2014. Neoproterozoic to Paleozoic long-lived accretionary orogeny in the northern Tarim Craton. Tectonics 33 (3), 302–329.
Ge, W., Wu, F., Zhou, C., Rahman, A.A., 2005. Emplacement age of the Tahe granite and its constraints on the tectonic nature of the Ergun block in the northern part of the Da Hinggan Range. Chinese Science Bulletin 50 (18), 2097–2105.
Gehrels, G.E., DeCelles, P.G., Martin, A., Ojha, T., Pinhassi, G., Upreti, B., 2003. Initiation of the Himalayan orogen as an early Paleozoic thin-skinned thrust belt. GSA Today 13 (9), 4–9.
Gehrels, G.E., DeCelles, P.G., Ojha, T., Upreti, B., 2006a. Geologic and U-Th-Pb geochronologic evidence for early Paleozoic tectonism in the Kathmandu thrust sheet, central Nepal Himalaya. Geological Society of America Bulletin 118 (1–2), 185–198.
Gehrels, G.E., DeCelles, P.G., Ojha, T., Upreti, B., 2006b. Geologic and U–Pb geochronologic evidence for early Paleozoic tectonism in the Dadeldhura thrust sheet, far-west Nepal Himalaya. Journal of Asian Earth Sciences 28 (4), 385–408.
Ghavidel-Syooki, M., 2008. Palynostratigraphy and Palaeogeography of the Upper Ordovician Gorgan Schists (Southeastern Caspian sea), Eastern Alborz Mountain ranges, Northern Iran. Comunicações Geológicas 123–155.
Ghavidel-Syooki, M., Hassanzadeh, J., Vecoli, M., 2011. Palynology and isotope geochronology of the Upper Ordovician–Silurian successions (Ghelli and Soltan Maidan Formations) in the Khoshyeilagh area, eastern Alborz Range, northern Iran; stratigraphic and palaeogeographic implications. Review of Palaeobotany and Palynology 164 (3), 251–271.
Ghienne, J.F., Monod, O., Kozlu, H., Dean, W., 2010. Cambrian–Ordovician depositional sequences in the Middle East: a perspective from Turkey. Earth-Science Reviews 101 (3), 101–146.
Gladkochub, D., Donskaya, T., 2009. Overview of geology and tectonic evolution of the Baikal-Tuva area. In: Biosilica in Evolution, Morphogenesis, and Nanobiotechnology. Progress in Molecular and Subcellular Biology, vol. 47. Springer, pp. 3–26.
Gladkochub, D.P., Donskaya, T.V., Wingate, M.T., Poller, U., Kröner, A., Fedorovsky, V.S., Mazukabzov, A.M., Todt, W., Pisarevsky, S.A., 2008. Petrology, geochronology, and tectonic implications of c. 500 Ma metamorphic and igneous rocks along the northern margin of the Central Asian Orogen (Olkhon terrane, Lake Baikal, Siberia). Journal of the Geological Society 165 (1), 235–246.
Glorie, S., De Grave, J., Buslov, M., Elburg, M., Stockli, D., Gerdes, A., 2010. Multi-method chronometric constraints on the evolution of the Northern Kyrgyz Tien Shan granitoids (Central Asian Orogenic Belt): from emplacement to exhumation. Journal of Asian Earth Sciences 38 (3), 131–146.
Glorie, S., De Grave, J., Buslov, M., Zhimulev, F., Izmer, A., Vandoorne, W., Ryabinin, A., Vanhaecke, F., Elburg, M., 2011a. Formation and Palaeozoic evolution of the Gorny-Altai–Altai-Mongolia suture zone (South Siberia): zircon U/Pb constraints on the igneous record. Gondwana Research 20 (2), 465–484.
Glorie, S., De Grave, J., Buslov, M., Zhimulev, F., Stockli, D., Batalev, V., Izmer, A., Vanhaecke, F., Elburg, M., 2011b. Tectonic history of the Kyrgyz South Tien Shan (Atbashi-Inylchek) suture zone: the role of inherited structures during deformation-propagation. Tectonics 30 (6).
Glorie, S., Zhimulev, F., Buslov, M., Andersen, T., Plavsa, D., Izmer, A., Vanhaecke, F., De Grave, J., 2015. Formation of the Kokchetav subduction–collision zone (northern Kazakhstan): insights from zircon U–Pb and Lu–Hf isotope systematics. Gondwana Research 27 (1), 424–438.
Gordienko, I., Bulgatov, A., Ruzhentsev, S., Minina, O., Klimuk, V., Vetluzhskikh, L., Nekrasov, G., Lastochkin, N., Sitnikova, V., Metelkin, D., 2010. The Late Riphean–Paleozoic history of the Uda–Vitim island arc system in the Transbaikalian sector of the Paleoasian Ocean. Russian Geology and Geophysics 51 (5), 461–481.
Gordienko, I., Filimonov, A., Minina, O., Gornova, M., Medvedev, A.Y., Klimuk, V., Elbaev, A., Tomurtogoo, O., 2007. Dzhida island-arc system in the Paleoasian Ocean: structure and main stages of Vendian-Paleozoic geodynamic evolution. Russian Geology and Geophysics 48 (1), 91–106.
Gordienko, I., Kovach, V., Elbaev, A., Kotov, A., Sal'nikova, E., Reznitskii, L., Yakovleva, S., Anisimova, I., 2012. Collisional granitoids of the Dzhida zone of the Central Asian Fold belt, Southwestern Transbaikalia: age and conditions of the formation. Petrology 20 (1), 40–58.
Görz, I., Bombach, K., Kroner, U., Ivanov, K., 2004. Protolith and deformation age of the Gneiss-Plate of Kartali in the southern East Uralian Zone. International Journal of Earth Sciences 93 (4), 475–486.
Görz, I., Kroner, U., Ivanov, K., 2006. The formation of gneisses in the Southern East Uralian Zone—a result of Late Palaeozoic granite ascent and emplacement. Journal of Asian Earth Sciences 27 (4), 402–415.
Guo, J.L., Wu, Y.B., Gao, S., Jin, Z.M., Zong, K.Q., Hu, Z.C., Chen, K., Chen, H.H., Liu, Y.S., 2015. Episodic Paleoarchean-Paleoproterozoic (3.3–2.0 Ga) granitoid magmatism in Yangtze Craton, South China: implications for late Archean tectonics. Precambrian Research 270, 246–266.
Gurnis, M., Turner, M., Zahirovic, S., DiCaprio, L., Spasojevic, S., Müller, R.D., Boyden, J., Seton, M., Manea, V.C., Bower, D.J., 2012. Plate tectonic reconstructions with continuously closing plates. Computers & Geosciences 38 (1), 35–42.
Guynn, J., Kapp, P., Gehrels, G.E., Ding, L., 2012. U–Pb geochronology of basement rocks in central Tibet and paleogeographic implications. Journal of Asian Earth Sciences 43 (1), 23–50.
Hairapetian, V., Mohibullah, M., Tilley, L.J., Williams, M., Miller, C.G., Afzal, J., Pour, M.G., Hejazi, S.H., 2011. Early Silurian carbonate platform ostracods from Iran: a peri-Gondwanan fauna with strong Laurentian affinities. Gondwana Research 20 (2), 645–653.
Hairapetian, V., Pour, M.G., Popov, L.E., Hejazi, S.H., Holmer, L.E., Evans, D., Sharafi, A., 2015. Ordovician of the Anarak Region: implications in understanding Early Palaeozoic history of Central Iran. Stratigraphy 12 (2), 22–30.
Han, Z., Yang, Z., Tong, Y., Jing, X., 2015. New paleomagnetic results from Late Ordovician rocks of the Yangtze Block, South China, and their paleogeographic implications. Journal of Geophysical Research: Solid Earth 120 (7), 4759–4772.
Hanning, W., Rixiang, Z., Lixin, B., Bin, G., Jianjun, L., 1998. Revised apparent polar wander path of the Yangtze Block and its tectonic implications. Science in China Series D: Earth Sciences 41, 78–90.
Hawkins, T., Smith, M., Herrington, R., Maslennikov, V., Boyce, A., Jeffries, T., Creaser, R., 2017. The geology and genesis of the iron skarns of the Turgai belt, northwestern Kazakhstan. Ore Geology Reviews 85, 216–246.
He, B., Jiao, C., Xu, Z., Cai, Z., Zhang, J., Liu, S., Li, H., Chen, W., Yu, Z., 2016. The paleotectonic and paleogeography reconstructions of the Tarim Basin and its adjacent areas (NW China) during the late Early and Middle Paleozoic. Gondwana Research 30, 191–206.
He, B., Qiao, X., Jiao, C., Xu, Z., Cai, Z., Guo, X., Zhang, Y., 2014. Palaeo-earthquake events during the late Early Palaeozoic in the central Tarim Basin (NW China). Geologos 20 (2), 105–123.
He, S., Li, R., Wang, C., Zhang, H., Ji, W., Yu, P., Gu, P., Shi, C., 2011. Discovery of ~4.0 Ga detrital zircons in the Changdu Block, North Qiangtang, Tibetan Plateau. Chinese Science Bulletin 56 (7), 647–658.
He, Z.Y., Klemd, R., Zhang, Z.M., Zong, K.Q., Sun, L.X., Tian, Z.L., Huang, B.T., 2015. Mesoproterozoic continental arc magmatism and crustal growth in the eastern Central Tianshan Arc Terrane of the southern Central Asian Orogenic Belt: geochronological and geochemical evidence. Lithos 236, 74–89.
Helo, C., Hegner, E., Kröner, A., Badarch, G., Tomurtogoo, O., Windley, B.F., Dulski, P., 2006. Geochemical signature of Paleozoic accretionary complexes of the Central Asian Orogenic Belt in South Mongolia: constraints on arc environments and crustal growth. Chemical Geology 227 (3), 236–257.
Herrington, R.J., Zaykov, V.V., Maslennikov, V.V., Brown, D., Puchkov, V.N., 2005. Mineral deposits of the Urals and links to geodynamic evolution. Economic Geology 100, 1069–1095.

Hodges, K., Parrish, R., Searle, M., 1996. Tectonic evolution of the central Annapurna range, Nepalese Himalayas. Tectonics 15 (6), 1264–1291.
Hu, J., Gong, W., Wu, S., Liu, Y., Liu, S., 2014a. LA-ICP-MS zircon U-Pb dating of the Langshan Group in the Northeast margin of the Alxa block, with tectonic implications. Precambrian Research 255 (2), 756–770.
Hu, J., Liu, X., Chen, L., Qu, W., Li, H., Geng, J., 2013a. A ~2.5 Ga magmatic event at the northern margin of the Yangtze craton: evidence from U-Pb dating and Hf isotope analysis of zircons from the Douling Complex in the South Qinling orogen. Chinese Science Bulletin 58 (28–29), 3564–3579.
Hu, P.Y., Zhai, Q.G., Jahn, B.M., Wang, J., Li, C., Lee, H.Y., Tang, S.H., 2015. Early Ordovician granites from the South Qiangtang terrane, northern Tibet: implications for the early Paleozoic tectonic evolution along the Gondwanan proto-Tethyan margin. Lithos 220, 318–338.
Hu, P., Li, C., Wang, M., Xie, C., Wu, Y., 2013b. Cambrian volcanism in the Lhasa terrane, southern Tibet: record of an early Paleozoic Andean-type magmatic arc along the Gondwana proto-Tethyan margin. Journal of Asian Earth Sciences 77, 91–107.
Hu, P., Li, C., Wu, Y., Xie, C., Wang, M., Li, J., 2014b. Opening of the Longmu Co–Shuanghu–Lancangjiang ocean: constraints from plagiogranites. Chinese Science Bulletin 59 (25), 3188–3199.
Huang, B., Otofuji, Y.I., Yang, Z., Zhu, R., 2000a. New Silurian and Devonian palaeomagnetic results from the Hexi Corridor terrane, northwest China, and their tectonic implications. Geophysical Journal International 140 (1), 132–146.
Huang, B., Otofuji, Y., Yang, Z., 1999a. Paleomagnetic constraints on the tectonic relationship between the Alashan/Hexi Corridor terrane and the North China Block. Geophysical Research Letters 26 (6), 787–790.
Huang, B., Yang, Z., Otofuji, Y.I., Zhu, R., 1999b. Early Paleozoic paleomagnetic poles from the western part of the North China Block and their implications. Tectonophysics 308 (3), 377–402.
Huang, H., Niu, Y., Nowell, G., Zhao, Z., Yu, X., Mo, X., 2015a. The nature and history of the Qilian Block in the context of the development of the Greater Tibetan Plateau. Gondwana Research 28 (1), 209–224.
Huang, H., Zhang, Z., Santosh, M., Zhang, D., Zhao, Z., Liu, J., 2013a. Early Paleozoic tectonic evolution of the South Tianshan collisional belt: evidence from geochemistry and zircon U-Pb geochronology of the Tie'reke Monzonite Pluton, Northwest China. The Journal of Geology 121 (4), 401–424.
Huang, K., Opdyke, N.D., Zhu, R., 2000b. Further paleomagnetic results from the Silurian of the Yangtze Block and their implications. Earth and Planetary Science Letters 175 (3), 191–202.
Huang, Z., Long, X., Kröner, A., Yuan, C., Wang, Q., Sun, M., Zhao, G., Wang, Y., 2013b. Geochemistry, zircon U–Pb ages and Lu–Hf isotopes of early Paleozoic plutons in the northwestern Chinese Tianshan: petrogenesis and geological implications. Lithos 182, 48–66.
Huang, Z., Long, X., Kröner, A., Yuan, C., Wang, Y., Chen, B., Zhang, Y., 2015b. Neoproterozoic granitic gneisses in the Chinese Central Tianshan Block: implications for tectonic affinity and Precambrian crustal evolution. Precambrian Research 269, 73–89.
Hughes, N.C., 2016. The Cambrian palaeontological record of the Indian subcontinent. Earth-Science Reviews 159, 428–461.
Hughes, N.C., Peng, S., Bhargava, O., Ahluwalia, A., Walia, S., Myrow, P.M., Parcha, S., 2005. Cambrian biostratigraphy of the Tal Group, Lesser Himalaya, India, and early Tsanglangpuan (late early Cambrian) trilobites from the Nigali Dhar syncline. Geological Magazine 142 (1), 57–80.
Inger, S., Scott, R., Golionko, B., 1999. Tectonic evolution of the Taimyr Peninsula, northern Russia: implications for Arctic continental assembly. Journal of the Geological Society 156 (6), 1069–1072.
Isozaki, Y., Aoki, K., Nakama, T., Yanai, S., 2010. New insight into a subduction-related orogen: a reappraisal of the geotectonic framework and evolution of the Japanese Islands. Gondwana Research 18 (1), 82–105.
Isozaki, Y., Ehiro, M., Nakahata, H., Aoki, K., Sakata, S., Hirata, T., 2015. Cambrian plutonism in Northeast Japan and its significance for the earliest arc-trench system of proto-Japan: New U–Pb zircon ages of the oldest granitoids in the Kitakami and Ou Mountains. Journal of Asian Earth Sciences 108, 136–149.
Ivanov, A.V., Demonterova, E.I., Gladkochub, D.P., Donskaya, T.V., 2014. The Tuva–Mongolia Massif and the Siberian Craton–are they the same? A comment on 'Age and provenance of the Ergunahe Group and the Wubinaobao Formation, northeastern Inner Mongolia, NE China: implications for tectonic setting of the Erguna Massif' by Zhang et al. International Geology Review 56 (8).
Ivanov, K., Puchkov, V., Fyodorov, Y.N., Erokhin, Y.V., Pogromskaya, O., 2013. Tectonics of the Urals and adjacent part of the West-Siberian platform basement: main features of geology and development. Journal of Asian Earth Sciences 72, 12–24.
Jakob, J., Alsaif, M., Corfu, F., Andersen, T.B., 2017. Age and origin of thin discontinuous gneiss sheets in the distal domain of the magma-poor hyperextended pre-Caledonian margin of Baltica, southern Norway. Journal of the Geological Society 174 (3), 557–571.
Ji, X.Z., Yang, L.Q., Santosh, M., Li, N., Zhang, C., Zhang, Z.C., Han, R., Li, Z.C., Wu, C.J., 2016. Detrital zircon geochronology of Devonian quartzite from tectonic mélange in the Mianlue Suture Zone, Central China: provenance and tectonic implications. International Geology Review 58 (12), 1510–1527.
Jia, R.Y., Jiang, Y.H., Liu, Z., Zhao, P., Zhou, Q., 2013. Petrogenesis and tectonic implications of early Silurian high-K calc-alkaline granites and their potassic microgranular enclaves, western Kunlun orogen, NW Tibetan Plateau. International Geology Review 55 (8), 958–975.
Jian, P., Kröner, A., Jahn, B.M., Windley, B.F., Shi, Y., Zhang, W., Zhang, F., Miao, L., Tomurhuu, D., Liu, D., 2014. Zircon dating of Neoproterozoic and Cambrian ophiolites in West Mongolia and implications for the timing of orogenic processes in the central part of the Central Asian Orogenic Belt. Earth-Science Reviews 133, 62–93.
Jian, P., Kröner, A., Shi, Y., Zhang, W., Liu, Y., Windley, B.F., Jahn, B.-m., Zhang, L., Liu, D., 2016. Age and provenance constraints on seismically-determined crustal layers beneath the Paleozoic southern Central Asian Orogen, Inner Mongolia, China. Journal of Asian Earth Sciences 123, 119–141.
Jian, P., Liu, D., Kröner, A., Windley, B.F., Shi, Y., Zhang, F., Shi, G., Miao, L., Zhang, W., Zhang, Q., 2008. Time scale of an early to mid-Paleozoic orogenic cycle of the long-lived Central Asian Orogenic Belt, Inner Mongolia of China: implications for continental growth. Lithos 101 (3), 233–259.
Jian, P., Liu, D., Kröner, A., Windley, B.F., Shi, Y., Zhang, W., Zhang, F., Miao, L., Zhang, L., Tomurhuu, D., 2010. Evolution of a Permian intraoceanic arc–trench system in the Solonker suture zone, Central Asian Orogenic Belt, China and Mongolia. Lithos 118 (1), 169–190.
Jiang, B., Sinclair, H.D., Niu, Y., Yu, J., 2014a. Late Neoproterozoic–Early Paleozoic evolution of the South China Block as a retroarc thrust wedge/foreland basin system. International Journal of Earth Sciences 103 (1), 23–40.
Jiang, G., Sohl, L.E., Christie-Blick, N., 2003. Neoproterozoic stratigraphic comparison of the Lesser Himalaya (India) and Yangtze block (south China): paleogeographic implications. Geology 31 (10), 917–920.
Jiang, T., Gao, J., Klemd, R., Qian, Q., Zhang, X., Xiong, X., Wang, X., Tan, Z., Chen, B., 2014b. Paleozoic ophiolitic mélanges from the South Tianshan Orogen, NW China: geological, geochemical and geochronological implications for the geodynamic setting. Tectonophysics 612, 106–127.
Jiang, Y., Sun, M., Kröner, A., Tumurkhuu, D., Long, X., Zhao, G., Yuan, C., Xiao, W., 2012. The high-grade Tseel Terrane in SW Mongolia: an Early Paleozoic arc system or a Precambrian sliver? Lithos 142, 95–115.
Jiang, Y., Sun, M., Zhao, G., Yuan, C., Xiao, W., Xia, X., Long, X., Wu, F., 2011. Precambrian detrital zircons in the Early Paleozoic Chinese Altai: their provenance and implications for the crustal growth of central Asia. Precambrian Research 189 (1), 140–154.
Kang, L., Xiao, P.X., Gao, X.F., Xi, R.G., Yang, Z.C., 2015. Age, petrogenesis and tectonic implications of Early Devonian bimodal volcanic rocks in the South Altyn, NW China. Journal of Asian Earth Sciences 111, 733–750.
Kawakami, T., Nakano, N., Higashino, F., Hokada, T., Osanai, Y., Yuhara, M., Charusiri, P., Kamikubo, H., Yonemura, K., Hirata, T., 2014. U-Pb zircon and CHIME monazite dating of granitoids and high-grade metamorphic rocks from the Eastern and Peninsular Thailand—a new report of Early Paleozoic granite. Lithos 200, 64–79.
Kelty, T.K., Yin, A., Dash, B., Gehrels, G.E., Ribeiro, A.E., 2008. Detrital-zircon geochronology of Paleozoic sedimentary rocks in the Hangay–Hentey basin, north-central Mongolia: implications for the tectonic evolution of the Mongol–Okhotsk Ocean in central Asia. Tectonophysics 451 (1), 290–311.
Khudoley, A.K., Guriev, G.A., 2003. Influence of syn-sedimentary faults on orogenic structure: examples from the Neoproterozoic–Mesozoic east Siberian passive margin. Tectonophysics 365 (1), 23–43.
Khudoley, A.K., Prokopiev, A.V., Chamberlain, K.R., Ernst, R.E., Jowitt, S.M., Malyshev, S.V., Zaitsev, A.I., Kropachev, A.P., Koroleva, O.V., 2013. Early Paleozoic mafic magmatic events on the eastern margin of the Siberian Craton. Lithos 174, 44–56.
Kilian, T., Swanson-Hysell, N., Bold, U., Crowley, J., Macdonald, F., 2016. Paleomagnetism of the Teel basalts from the Zavkhan terrane: implications for Paleozoic paleogeography in Mongolia and the growth of continental crust. Lithosphere 8 (6), 699–715.
Kim, S.W., Kwon, S., Park, S.I., Yi, K., Santosh, M., Ryu, I.C., 2015. Early to Middle Paleozoic arc magmatism in the Korean Peninsula: constraints from zircon geochronology and geochemistry. Journal of Asian Earth Sciences 113, 866–882.
Kirscher, U., Bachtadse, V., Mikolaichuk, A., Kröner, A., Alexeiev, D., 2017. Palaeozoic evolution of the North Tianshan based on palaeomagnetic data–transition from Gondwana towards Pangaea. International Geology Review 59 (16), 1–18.
Klemd, R., Gao, J., Li, J.L., Meyer, M., 2015. Metamorphic evolution of (ultra)-high-pressure subduction-related transient crust in the South Tianshan Orogen (Central Asian Orogenic Belt): geodynamic implications. Gondwana Research 28 (1), 1–25.
Konopelko, D., Biske, G., Seltmann, R., Kiseleva, M., Matukov, D., Sergeev, S., 2008. Deciphering Caledonian events: timing and geochemistry of the Caledonian magmatic arc in the Kyrgyz Tien Shan. Journal of Asian Earth Sciences 32 (2), 131–141.
Korobkin, V., Smirnov, A., 2006. Paleozoic tectonics and geodynamics of volcanic arcs in northern Kazakhstan. Russian Geology and Geophysics 47 (4), 458–470.
Kos'ko, M., Korago, E., 2009. Review of geology of the new Siberian islands between the Laptev and the East Siberian Seas, North East Russia. Stephan Mueller Special Publication Series 4, 45–64.
Kovach, V., Salnikova, E., Wang, K.L., Jahn, B.M., Chiu, H.Y., Reznitskiy, L., Kotov, A., Iizuka, Y., Chung, S.L., 2013. Zircon ages and Hf isotopic constraints on sources of clastic metasediments of the Slyudyansky high-grade complex, southeastern Siberia: implication for continental growth and evolution of the Central Asian Orogenic Belt. Journal of Asian Earth Sciences 62, 18–36.
Kozakov, I., Sal'nikova, E., Wang, T., Didenko, A., Plotkina, Y.V., Podkovyrov, V., 2007. Early Precambrian crystalline complexes of the Central Asian microcontinent: age, sources, tectonic position. Stratigraphy and Geological Correlation 15 (2), 121–140.

Kravchinsky, V.A., Sklyarov, E.V., Gladkochub, D.P., Harbert, W.P., 2010. Paleomagnetism of the Precambrian Eastern Sayan rocks: implications for the Ediacaran–Early Cambrian paleogeography of the Tuva-Mongolian composite terrane. Tectonophysics 486 (1), 65–80.
Kröner, A., Alexeiev, D., Hegner, E., Rojas-Agramonte, Y., Corsini, M., Chao, Y., Wong, J., Windley, B.F., Liu, D., Tretyakov, A., 2012. Zircon and muscovite ages, geochemistry, and Nd–Hf isotopes for the Aktyuz metamorphic terrane: evidence for an Early Ordovician collisional belt in the northern Tianshan of Kyrgyzstan. Gondwana Research 21 (4), 901–927.
Kröner, A., Alexeiev, D., Kovach, V., Rojas-Agramonte, Y., Tretyakov, A., Mikolaichuk, A., Xie, H., Sobel, E., 2017. Zircon ages, geochemistry and Nd isotopic systematics for the Palaeoproterozoic 2.3 to 1.8 Ga Kuilyu Complex, East Kyrgyzstan–the oldest continental basement fragment in the Tianshan orogenic belt. Journal of Asian Earth Sciences 135, 122–135.
Kröner, A., Alexeiev, D., Rojas-Agramonte, Y., Hegner, E., Wong, J., Xia, X., Belousova, E., Mikolaichuk, A., Seltmann, R., Liu, D., 2013. Mesoproterozoic (Grenville-age) terranes in the Kyrgyz North Tianshan: zircon ages and Nd–Hf isotopic constraints on the origin and evolution of basement blocks in the southern Central Asian Orogen. Gondwana Research 23 (1), 272–295.
Kröner, A., Kovach, V., Belousova, E., Hegner, E., Armstrong, R., Dolgopolova, A., Seltmann, R., Alexeiev, D., Hoffmann, J., Wong, J., 2014. Reassessment of continental growth during the accretionary history of the Central Asian Orogenic Belt. Gondwana Research 25 (1), 103–125.
Kröner, A., Lehmann, J., Schulmann, K., Demoux, A., Lexa, O., Tomurhuu, D., Štípská, P., Liu, D., Wingate, M.T., 2010. Lithostratigraphic and geochronological constraints on the evolution of the Central Asian Orogenic Belt in SW Mongolia: early Paleozoic rifting followed by late Paleozoic accretion. American Journal of Science 310 (7), 523–574.
Kröner, A., Windley, B., Badarch, G., Tomurtogoo, O., Hegner, E., Jahn, B., Gruschka, S., Khain, E., Demoux, A., Wingate, M., 2007. Accretionary growth and crust formation in the Central Asian Orogenic Belt and comparison with the Arabian-Nubian shield. Geological Society of America Memoirs 200, 181–209.
Kurihara, T., Tsukada, K., Otoh, S., Kashiwagi, K., Chuluun, M., Byambadash, D., Boijir, B., Gonchigdorj, S., Nuramkhan, M., Niwa, M., 2009. Upper Silurian and Devonian pelagic deep-water radiolarian chert from the Khangai–Khentei belt of Central Mongolia: evidence for Middle Paleozoic subduction–accretion activity in the Central Asian Orogenic Belt. Journal of Asian Earth Sciences 34 (2), 209–225.
Kwon, S., Sajeev, K., Mitra, G., Park, Y., Kim, S.W., Ryu, I.C., 2009. Evidence for Permo-Triassic collision in far east Asia: the Korean collisional orogen. Earth and Planetary Science Letters 279 (3), 340–349.
Le Fort, P., Tongiorgi, M., Gaetani, M., 1994. Discovery of a crystalline basement and Early Ordovician marine transgression in the Karakorum mountain range, Pakistan. Geology 22 (10), 941–944.
Lee, C.P., 2006. The Cambrian of Malaysia. Palaeoworld 15 (3), 242–255.
Lehmann, B., Zhao, X., Zhou, M., Du, A., Mao, J., Zeng, P., Henjes-Kunst, F., Heppe, K., 2013. Mid-Silurian back-arc spreading at the northeastern margin of Gondwana: the Dapingzhang dacite-hosted massive sulfide deposit, Lancangjiang zone, southwestern Yunnan, China. Gondwana Research 24 (2), 648–663.
Letnikov, F., Kotov, A., Degtyarev, K., Sal'nikova, E., Levchenkov, O., Shershakova, M., Shershakov, A., Rizvanova, N., Makeev, A., Tolkachev, M., 2009. Silurian granites of northern Kazakhstan: U-Pb age and tectonic position. Stratigraphy and Geological Correlation 17 (3), 275–282.
Levashova, N.M., Degtyarev, K.E., Bazhenov, M.L., Collins, A.Q., Van der Voo, R., 2003. Middle Paleozoic paleomagnetism of east Kazakhstan: post-Middle Devonian rotations in a large-scale orocline in the central Ural–Mongol belt. Tectonophysics 377 (3), 249–268.
Levashova, N.M., Van der Voo, R., Abrajevitch, A.V., Bazhenov, M.L., 2009. Paleomagnetism of mid-Paleozoic subduction-related volcanics from the Chingiz Range in NE Kazakhstan: the evolving paleogeography of the amalgamating Eurasian composite continent. Geological Society of America Bulletin 121 (3–4), 555–573.
Li, G.J., Wang, Q.F., Huang, Y.H., Gao, L., Yu, L., 2016. Petrogenesis of middle Ordovician peraluminous granites in the Baoshan block: implications for the early Paleozoic tectonic evolution along East Gondwana. Lithos 245, 76–92.
Li, S., Zhao, S., Liu, X., Cao, H., Yu, S., Li, X., Somerville, I., Yu, S., Suo, Y., 2018. Closure of the Proto-Tethys Ocean and Early Paleozoic amalgamation of microcontinental blocks in East Asia. Earth-Science Reviews. https://doi.org/10.1016/j.earscirev.2017.01.011 (in press).
Li, W., Neubauer, F., Liu, Y., Genser, J., Ren, S., Han, G., Liang, C., 2013. Paleozoic evolution of the Qimantagh magmatic arcs, Eastern Kunlun Mountains: constraints from zircon dating of granitoids and modern river sands. Journal of Asian Earth Sciences 77, 183–202.
Li, Y., McWilliams, M., Sharps, R., Cox, A., Li, Y., Li, Q., Gao, Z., Zhang, Z., Zhai, Y., 1990. A Devonian paleomagnetic pole from red beds of the Tarim Block, China. Journal of Geophysical Research: Solid Earth 95 (B12), 19185–19198.
Li, Y., Zhou, H.W., Li, Q.L., Xiang, H., Zhong, Z.Q., Brouwer, F.M., 2014. Palaeozoic polymetamorphism in the North Qinling orogenic belt, Central China: insights from petrology and *in situ* titanite and zircon U–Pb geochronology. Journal of Asian Earth Sciences 92, 77–91.
Li, Y., Zhou, H., Brouwer, F.M., Wijbrans, J.R., Zhong, Z., Liu, H., 2011. Tectonic significance of the Xilin Gol Complex, Inner Mongolia, China: petrological, geochemical and U–Pb zircon age constraints. Journal of Asian Earth Sciences 42 (5), 1018–1029.
Li, Z.X., Li, X.H., Wartho, J.A., Clark, C., Li, W.X., Zhang, C.L., Bao, C., 2010. Magmatic and metamorphic events during the early Paleozoic Wuyi-Yunkai orogeny, southeastern South China: new age constraints and pressure-temperature conditions. Geological Society of America Bulletin 122 (5–6), 772–793.
Liao, S.Y., Jiang, Y.H., Jiang, S.Y., Yang, W.Z., Zhou, Q., Jin, G.D., Zhao, P., 2010. Subducting sediment-derived arc granitoids: evidence from the Datong pluton and its quenched enclaves in the western Kunlun orogen, northwest China. Mineralogy and Petrology 100 (1–2), 55–74.
Liao, X.Y., Wang, Y.W., Liu, L., Wang, C., Santosh, M., 2017. Detrital zircon U-Pb and Hf isotopic data from the Liuling Group in the South Qinling belt: provenance and tectonic implications. Journal of Asian Earth Sciences 134, 244–261.
Lin, C., Yang, H., Liu, J., Rui, Z., Cai, Z., Zhu, Y., 2012. Distribution and erosion of the Paleozoic tectonic unconformities in the Tarim Basin, Northwest China: significance for the evolution of paleo-uplifts and tectonic geography during deformation. Journal of Asian Earth Sciences 46, 1–19.
Lin, W., Chu, Y., Ji, W., Zhang, Z., Shi, Y., Wang, Z., Li, Z., Wang, Q., 2013a. Geochronological and geochemical constraints for a middle Paleozoic continental arc on the northern margin of the Tarim block: implications for the Paleozoic tectonic evolution of the South Chinese Tianshan. Lithosphere 5 (4), 355–381.
Lin, Y.L., Yeh, M.W., Lee, T.Y., Chung, S.L., Iizuka, Y., Charusiri, P., 2013b. First evidence of the Cambrian basement in Upper Peninsula of Thailand and its implication for crustal and tectonic evolution of the Sibumasu terrane. Gondwana Research 24 (3), 1031–1037.
Linnemann, U., Pereira, F., Jeffries, T.E., Drost, K., Gerdes, A., 2008. The Cadomian Orogeny and the opening of the Rheic Ocean: the diachrony of geotectonic processes constrained by LA-ICP-MS U–Pb zircon dating (Ossa-Morena and Saxo-Thuringian Zones, Iberian and Bohemian Massifs). Tectonophysics 461 (1), 21–43.
Liu, C., Wu, C., Gao, Y., Lei, M., Qin, H., 2016a. Age, composition, and tectonic significance of Palaeozoic granites in the Altyn orogenic belt, China. International Geology Review 58 (2), 131–154.
Liu, G., Einsele, G., 1994. Sedimentary history of the Tethyan basin in the Tibetan Himalayas. Geologische Rundschau 83 (1), 32–61.
Liu, H., Somerville, I.D., Lin, C., Zuo, S., 2016b. Distribution of Palaeozoic tectonic superimposed unconformities in the Tarim Basin, NW China: significance for the evolution of palaeogeomorphology and sedimentary response. Geological Journal 51 (4), 627–651.
Liu, H., Wan, B., Shu, L., Jahn, B.M., Lizuka, Y., 2014a. Detrital zircon ages of Proterozoic meta-sedimentary rocks and Paleozoic sedimentary cover of the northern Yili Block: implications for the tectonics of microcontinents in the Central Asian Orogenic Belt. Precambrian Research 252, 209–222.
Liu, L., Kang, L., Cao, Y., Yang, W., 2015a. Early Paleozoic granitic magmatism related to the processes from subduction to collision in South Altyn, NW China. Science China Earth Sciences 58 (9), 1513–1522.
Liu, L., Liao, X., Wang, Y., Wang, C., Santosh, M., Yang, M., Zhang, C., Chen, D., 2016c. Early Paleozoic tectonic evolution of the North Qinling Orogenic Belt in Central China: insights on continental deep subduction and multiphase exhumation. Earth-Science Reviews 159, 58–81.
Liu, L., Wang, C., Cao, Y.T., Chen, D.L., Kang, L., Yang, W.Q., Zhu, X.H., 2012. Geochronology of multi-stage metamorphic events: Constraints on episodic zircon growth from the UHP eclogite in the South Altyn, NW China. Lithos 136, 10–26.
Liu, Q., Wu, Y.B., Wang, H., Gao, S., Qin, Z.W., Liu, X.C., Yang, S.H., Gong, H.J., 2014b. Zircon U–Pb ages and Hf isotope compositions of migmatites from the North Qinling terrane and their geological implications. Journal of Metamorphic Geology 32 (2), 177–193.
Liu, Q., Zhao, G., Sun, M., Eizenhöfer, P.R., Han, Y., Hou, W., Zhang, X., Wang, B., Liu, D., Xu, B., 2015b. Ages and tectonic implications of Neoproterozoic ortho- and paragneisses in the Beishan Orogenic Belt, China. Precambrian Research 266, 551–578.
Liu, Q., Zhao, G., Sun, M., Han, Y., Eizenhöfer, P.R., Hou, W., Zhang, X., Zhu, Y., Wang, B., Liu, D., 2016d. Early Paleozoic subduction processes of the Paleo-Asian Ocean: insights from geochronology and geochemistry of Paleozoic plutons in the Alxa Terrane. Lithos 262, 546–560.
Liu, S., Hu, R., Gao, S., Feng, C., Huang, Z., Lai, S., Yuan, H., Liu, X., Coulson, I.M., Feng, G., 2009. U–Pb zircon, geochemical and Sr–Nd–Hf isotopic constraints on the age and origin of Early Palaeozoic I-type granite from the Tengchong–Baoshan Block, Western Yunnan Province, SW China. Journal of Asian Earth Sciences 36 (2), 168–182.
Liu, X., Chen, B., Jahn, B.M., Wu, G., Liu, Y., 2011a. Early Paleozoic (ca. 465 Ma) eclogites from Beishan (NW China) and their bearing on the tectonic evolution of the southern Central Asian Orogenic Belt. Journal of Asian Earth Sciences 42 (4), 715–731.
Liu, X., Jahn, B.M., Hu, J., Li, S., Liu, X., Song, B., 2011b. Metamorphic patterns and SHRIMP zircon ages of medium-to-high grade rocks from the Tongbai orogen, central China: implications for multiple accretion/collision processes prior to terminal continental collision. Journal of Metamorphic Geology 29 (9), 979–1002.
Liu, Y., Genser, J., Neubauer, F., Jin, W., Ge, X., Handler, R., Takasu, A., 2005. $^{40}Ar/^{39}Ar$ mineral ages from basement rocks in the eastern Kunlun Mountains, NW China, and their tectonic implications. Tectonophysics 398 (3), 199–224.
Liu, Y., Li, C., Xie, C., Fan, J., Wu, H., 2017. Detrital zircon U–Pb ages and Hf isotopic composition of the Ordovician Duguer quartz schist, central Tibetan Plateau: constraints on tectonic affinity and sedimentary source regions. Geological Magazine 154 (3), 558–570.

Liu, Y., Li, C., Xie, C., Fan, J., Wu, H., Jiang, Q., Li, X., 2016e. Cambrian granitic gneiss within the central Qiangtang terrane, Tibetan Plateau: implications for the early Palaeozoic tectonic evolution of the Gondwanan margin. International Geology Review 58 (9), 1043–1063.
Liu, Z., Jiang, Y.H., Jia, R.Y., Zhao, P., Zhou, Q., Wang, G.-C., Ni, C.-Y., 2014c. Origin of Middle Cambrian and Late Silurian potassic granitoids from the western Kunlun orogen, northwest China: a magmatic response to the Proto-Tethys evolution. Mineralogy and Petrology 108 (1), 91–110.
Lixin, B., Rixiang, Z., Harming, W., Bin, G., Jianjun, L., 1998. New Cambrian paleomagnetic pole for Yangtze block. Science in China Series D: Earth Sciences 41, 66–71.
Long, X., Yuan, C., Sun, M., Kröner, A., Zhao, G., 2014. New geochemical and combined zircon U–Pb and Lu–Hf isotopic data of orthogneisses in the northern Altyn Tagh, northern margin of the Tibetan plateau: implication for Archean evolution of the Dunhuang Block and crust formation in NW China. Lithos 200, 418–431.
Long, X., Yuan, C., Sun, M., Safonova, I., Xiao, W., Wang, Y., 2012a. Geochemistry and U–Pb detrital zircon dating of Paleozoic graywackes in East Junggar, NW China: insights into subduction–accretion processes in the southern Central Asian Orogenic Belt. Gondwana Research 21 (2), 637–653.
Long, X., Yuan, C., Sun, M., Xiao, W., Wang, Y., Cai, K., Jiang, Y., 2012b. Geochemistry and Nd isotopic composition of the Early Paleozoic flysch sequence in the Chinese Altai, Central Asia: evidence for a northward-derived mafic source and insight into Nd model ages in accretionary orogen. Gondwana Research 22 (2), 554–566.
Long, X., Yuan, C., Sun, M., Xiao, W., Zhao, G., Wang, Y., Cai, K., Xia, X., Xie, L., 2010. Detrital zircon ages and Hf isotopes of the early Paleozoic flysch sequence in the Chinese Altai, NW China: new constrains on depositional age, provenance and tectonic evolution. Tectonophysics 480 (1), 213–231.
Lorenz, H., Gee, D.G., Whitehouse, M.J., 2007. New geochronological data on Palaeozoic igneous activity and deformation in the Severnaya Zemlya Archipelago, Russia, and implications for the development of the Eurasian Arctic margin. Geological Magazine 144 (1), 105–125.
Lorenz, H., Männik, P., Gee, D., Proskurnin, V., 2008. Geology of the Severnaya Zemlya archipelago and the North Kara terrane in the Russian High Arctic. International Journal of Earth Sciences 97 (3), 519–547.
Ma, X., Shu, L., Jahn, B.M., Zhu, W., Faure, M., 2012. Precambrian tectonic evolution of Central Tianshan, NW China: constraints from U–Pb dating and in situ Hf isotopic analysis of detrital zircons. Precambrian Research 222, 450–473.
Ma, X., Shu, L., Santosh, M., Li, J., 2013. Petrogenesis and tectonic significance of an early Palaeozoic mafic-intermediate suite of rocks from the Central Tianshan, northwest China. International Geology Review 55 (5), 548–573.
Makrygina, V., Belichenko, V., Reznitsky, L., 2007. Types of paleoisland arcs and back-arc basins in the northeast of the Paleoasian Ocean (from geochemical data). Russian Geology and Geophysics 48 (1), 107–119.
Männik, P., Bogolepova, O., Poldvere, A., Gubanov, A., 2009. New data on Ordovician–Silurian conodonts and stratigraphy from the Severnaya Zemlya archipelago, Russian Arctic. Geological Magazine 146 (4), 497–516.
Mao, Q., Xiao, W., Fang, T., Wang, J., Han, C., Sun, M., Yuan, C., 2012a. Late Ordovician to early Devonian adakites and Nb-enriched basalts in the Liuyuan area, Beishan, NW China: implications for early Paleozoic slab-melting and crustal growth in the southern Altaids. Gondwana Research 22 (2), 534–553.
Mao, Q., Xiao, W., Windley, B.F., Han, C., Qu, J., Ao, S., Zhang, J.e., Guo, Q., 2012b. The Liuyuan complex in the Beishan, NW China: a Carboniferous–Permian ophiolitic fore-arc sliver in the southern Altaids. Geological Magazine 149 (3), 483–506.
Maslov, A., Erdtmann, B.D., Ivanov, K., Ivanov, S., Krupenin, M., 1997. The main tectonic events, depositional history, and the palaeogeography of the southern Urals during the Riphean-early Palaeozoic. Tectonophysics 276 (1), 313–335.
Mattern, F., Schneider, W., 2000. Suturing of the Proto-and Paleo-Tethys oceans in the western Kunlun (Xinjiang, China). Journal of Asian Earth Sciences 18 (6), 637–650.
Matthews, K.J., Maloney, K.T., Zahirovic, S., Williams, S.E., Seton, M., Müller, R.D., 2016. Global plate boundary evolution and kinematics since the late Paleozoic. Global and Planetary Change 146, 226–250.
Mattinson, C., Wooden, J., Liou, J., Bird, D., Wu, C., 2006. Age and duration of eclogite-facies metamorphism, North Qaidam HP/UHP terrane, western China. American Journal of Science 306 (9), 683–711.
Matushkin, N.Y., Metelkin, D., Vernikovsky, V., Travin, A., Zhdanova, A., 2016. Geology and Age ofMafic Magmatism on Jeannette Island (De Long Archipelago) d Implications for Paleotectonic Reconstructions for the Arctic. Doklady Earth Sciences 467 (1), 219–223.
Meert, J.G., 2003. A synopsis of events related to the assembly of eastern Gondwana. Tectonophysics 362 (1), 1–40.
Meng, F., Cui, M., Wu, X., Ren, Y., 2015. Heishan mafic–ultramafic rocks in the Qimantag area of Eastern Kunlun, NW China: remnants of an early Paleozoic incipient island arc. Gondwana Research 27 (2), 745–759.
Meng, F., Zhang, J., Cui, M., 2013. Discovery of Early Paleozoic eclogite from the East Kunlun, Western China and its tectonic significance. Gondwana Research 23 (2), 825–836.
Meng, L., Chen, B., Zhao, N., Wu, Y., Zhang, W., He, J., Wang, B., Han, M., 2017. The distribution, geochronology and geochemistry of early Paleozoic granitoid plutons in the North Altun orogenic belt, NW China: implications for the petrogenesis and tectonic evolution. Lithos 268–271, 399–417.
Meng, Q.R., Zhang, G.W., 2000. Geologic framework and tectonic evolution of the Qinling orogen, central China. Tectonophysics 323 (3), 183–196.
Metcalfe, I., 2013. Gondwana dispersion and Asian accretion: tectonic and palaeogeographic evolution of eastern Tethys. Journal of Asian Earth Sciences 66, 1–33.
Metelkin, D., 2013. Kinematic reconstruction of the Early Caledonian accretion in the southwest of the Siberian paleocontinent based on paleomagnetic results. Russian Geology and Geophysics 54 (4), 381–398.
Metelkin, D., Vernikovsky, V., Tolmacheva, T.Y., Matushkin, N.Y., Zhdanova, A., Pisarevsky, S., 2016. First paleomagnetic data for the New Siberian Islands: implications for Arctic paleogeography. Gondwana Research 37, 308–323.
Metelkin, D.V., Vernikovsky, V.A., Kazansky, A.Y., Bogolepova, O.K., Gubanov, A.P., 2005. Paleozoic history of the Kara microcontinent and its relation to Siberia and Baltica: paleomagnetism, paleogeography and tectonics. Tectonophysics 398 (3), 225–243.
Meyer, M., Klemd, R., Hegner, E., Konopelko, D., 2014. Subduction and exhumation mechanisms of ultra-high and high-pressure oceanic and continental crust at Makbal (Tianshan, Kazakhstan and Kyrgyzstan). Journal of Metamorphic Geology 32 (8), 861–884.
Miao, L., Fan, W., Liu, D., Zhang, F., Shi, Y., Guo, F., 2008. Geochronology and geochemistry of the Hegenshan ophiolitic complex: implications for late-stage tectonic evolution of the Inner Mongolia-Daxinganling Orogenic Belt, China. Journal of Asian Earth Sciences 32 (5), 348–370.
Mitchell, A., Chung, S.L., Oo, T., Lin, T.H., Hung, C.H., 2012. Zircon U–Pb ages in Myanmar: magmatic–metamorphic events and the closure of a neo-Tethys ocean? Journal of Asian Earth Sciences 56, 1–23.
Moghadam, H.S., Khademi, M., Hu, Z., Stern, R.J., Santos, J.F., Wu, Y., 2015. Cadomian (Ediacaran–Cambrian) arc magmatism in the ChahJam–Biarjmand metamorphic complex (Iran): magmatism along the northern active margin of Gondwana. Gondwana Research 27 (1), 439–452.
Monod, O., Kozlu, H., Ghienne, J.F., Dean, W., Günay, Y., Hérissé, A.L., Paris, F., Robardet, M., 2003. Late Ordovician glaciation in southern Turkey. Terra Nova 15 (4), 249–257.
Myrow, P.M., Hughes, N.C., Goodge, J.W., Fanning, C.M., Williams, I.S., Peng, S., Bhargava, O.N., Parcha, S.K., Pogue, K.R., 2010. Extraordinary transport and mixing of sediment across Himalayan central Gondwana during the Cambrian–Ordovician. Geological Society of America Bulletin 122 (9–10), 1660–1670.
Myrow, P.M., Hughes, N.C., Paulsen, T., Williams, I., Parcha, S.K., Thompson, K., Bowring, S.A., Peng, S.C., Ahluwalia, A., 2003. Integrated tectonostratigraphic analysis of the Himalaya and implications for its tectonic reconstruction. Earth and Planetary Science Letters 212 (3), 433–441.
Nakano, N., Osanai, Y., Sajeev, K., Hayasaka, Y., Miyamoto, T., Minh, N.T., Owada, M., Windley, B., 2010. Triassic eclogite from northern Vietnam: inferences and geological significance. Journal of Metamorphic Geology 28 (1), 59–76.
Natal'in, B.A., Sunal, G., Satir, M., Toraman, E., 2012. Tectonics of the Strandja Massif, NW Turkey: history of a long-lived arc at the northern margin of Palaeo-Tethys. Turkish Journal of Earth Sciences 21 (5), 755–798.
Nguyen, T.T.B., Hieu, P.T., Hai, T.T., ANH, B.T., Xuan, N.T., Cung, D.M., 2014. Petrogenesis and zircon U–Pb ages of the Thien Ke granitic pluton in the Tam Dao region: implications for early Paleozoic tectonic evolution in NE Vietnam. Journal of Mineralogical and Petrological Sciences 109 (5), 209–221.
Nie, H., Wan, X., Zhang, H., He, J.F., Hou, Z.H., Siebel, W., Chen, F., 2016a. Ordovician and Triassic mafic dykes in the Wudang terrane: evidence for opening and closure of the South Qinling ocean basin, central China. Lithos 266, 1–15.
Nie, X., Feng, Q., Metcalfe, I., Baxter, A.T., Liu, G., 2016b. Discovery of a Late Devonian magmatic arc in the southern Lancangjiang zone, western Yunnan: geochemical and zircon U–Pb geochronological constraints on the evolution of Tethyan ocean basins in SW China. Journal of Asian Earth Sciences 118, 32–50.
Nie, X., Feng, Q., Qian, X., Wang, Y., 2015. Magmatic record of Prototethyan evolution in SW Yunnan, China: geochemical, zircon U–Pb geochronological and Lu–Hf isotopic evidence from the Huimin metavolcanic rocks in the southern Lancangjiang zone. Gondwana Research 28 (2), 757–768.
Nokleberg, W.J., Parfenov, L.M., Monger, J.W., Norton, I.O., Chanďuk, A.I., Stone, D.B., Scotese, C.R., Scholl, D.W., Fujita, K., 2000. Phanerozoic Tectonic Evolution of the Circum-North Pacific. USGS Professional Paper 1626.
Nowrouzi, Z., Moussavi-Harami, R., Mahboubi, A., Gharaie, M.H.M., Ghaemi, F., 2014. Petrography and geochemistry of Silurian Niur sandstones, Derenjal Mountains, East Central Iran: implications for tectonic setting, provenance and weathering. Arabian Journal of Geosciences 7 (7), 2793–2813.
Oczlon, M.S., Seghedi, A., Carrigan, C.W., 2007. Avalonian and Baltican terranes in the Moesian Platform (southern Europe, Romania, and Bulgaria) in the context of Caledonian terranes along the southwestern margin of the East European craton. Geological Society of America Special Papers 423, 375–400.
Oh, C.W., Imayama, T., Yi, S.B., Kim, T., Ryu, I.C., Jeon, J., Yi, K., 2014. Middle Paleozoic metamorphism in the Hongseong area, South Korea, and tectonic significance for Paleozoic orogeny in northeast Asia. Journal of Asian Earth Sciences 95, 203–216.
Oh, C.W., 2006. A new concept on tectonic correlation between Korea, China and Japan: histories from the late Proterozoic to Cretaceous. Gondwana Research 9 (1), 47–61.
Okay, A.I., 2008. Geology of Turkey: a synopsis. Anschnitt 21, 19–42.
Okay, A.I., Bozkurt, E., Satır, M., Yiğitbaş, E., Crowley, Q.G., Shang, C.K., 2008a. Defining the southern margin of Avalonia in the Pontides: geochronological data from the Late Proterozoic and Ordovician granitoids from NW Turkey. Tectonophysics 461 (1), 252–264.

Okay, A.I., Satır, M., Shang, C.K., 2008b. Ordovician metagranitoid from the Anatolide-Tauride Block, northwest Turkey: geodynamic implications. Terra Nova 20 (4), 280–288.
Oksum, E., Hisarlı, Z.M., Çinku, M.C., Ustaömer, T., Orbay, N., 2015. New paleomagnetic results from Ordovician sedimentary rocks from NW Anatolia: tectonic implications for the paleolatitudinal position of the Istanbul Terrane. Tectonophysics 664, 14–30.
Olempska, E., Nazik, A., Çapkinoğlu, Ş., Saydam-Demiray, D.G., 2015. Lower Devonian ostracods from the Istanbul area, Western Pontides (NW Turkey): Gondwanan and peri-Gondwanan affinities. Geological Magazine 152 (2), 298–315.
Opdyke, N.D., Huang, K., Xu, G., Zhang, W., Kent, D.V., 1987. Paleomagnetic results from the Silurian of the Yangtze paraplatform. Tectonophysics 139 (1–2), 123–132.
Özbey, Z., Ustaömer, T., Robertson, A.H., Ustaömer, P.A., 2013. Tectonic significance of Late Ordovician granitic magmatism and clastic sedimentation on the northern margin of Gondwana (Tavşanlı Zone, NW Turkey). Journal of the Geological Society 170 (1), 159–173.
Özgül, N., 2012. Stratigraphy and some structural features of the İstanbul Paleozoic. Turkish Journal of Earth Sciences 21 (6), 817–866.
Pan, S., Zheng, J., Griffin, W., Chu, L., Xu, Y., Li, Y., Ma, Q., Wang, D., 2014. Precambrian tectonic attribution and evolution of the Songliao terrane revealed by zircon xenocrysts from Cenozoic alkali basalts, Xilinhot region, NE China. Precambrian Research 251, 33–48.
Pankhurst, R.J., Rapela, C.W., Fanning, C.M., Márquez, M., 2006. Gondwanide continental collision and the origin of Patagonia. Earth-Science Reviews 76 (3), 235–257.
Parfenov, L.M., Natapov, L.M., Sokolov, S.D., Tsukanov, N.V., 1993. Terrane analysis and accretion in North-East Asia. Island Arc 2 (1), 35–54.
Paulsen, T.S., Demosthenous, C.M., Myrow, P.M., Hughes, N.C., Parcha, S., 2007. Paleostrain stratigraphic analysis of calcite twins across the Cambrian–Ordovician unconformity in the Tethyan Himalaya, Spiti and Zanskar valley regions, India. Journal of Asian Earth Sciences 31 (1), 44–54.
Pavlov, V., Bachtadse, V., Mikhailov, V., 2008. New Middle Cambrian and Middle Ordovician palaeomagnetic data from Siberia: Llandelian magnetostratigraphy and relative rotation between the Aldan and Anabar–Angara blocks. Earth and Planetary Science Letters 276 (3), 229–242.
Pavlov, V., Veselovskiy, R., Shatsillo, A., Gallet, Y., 2012. Magnetostratigraphy of the Ordovician Angara/Rozhkova river section: further evidence for the Moyero reversed superchron. Izvestiya, Physics of the Solid Earth 48 (4), 297–305.
Pease, V., Scott, R., 2009. Crustal affinities in the Arctic Uralides, northern Russia: significance of detrital zircon ages from Neoproterozoic and Palaeozoic sediments in Novaya Zemlya and Taimyr. Journal of the Geological Society 166 (3), 517–527.
Pelechaty, S.M., 1996. Stratigraphic evidence for the Siberia-Laurentia connection and Early Cambrian rifting. Geology 24 (8), 719–722.
Pfänder, J., Kröner, A., 2004. Tectono-magmatic evolution, age and emplacement of the Agardagh Tes-Chem ophiolite in Tuva, Central Asia: crustal growth by island arc accretion. Developments in Precambrian Geology 13, 207–221.
Popov, L.E., Bassett, M.G., Zhemchuzhnikov, V.G., Holmer, L.E., Klishevich, I.A., 2009. Gondwanan faunal signatures from Early Palaeozoic terranes of Kazakhstan and Central Asia: evidence and tectonic implications. Geological Society, London, Special Publications 325 (1), 23–64.
Popov, L.E., Cocks, L.R.M., 2017. Late Ordovician palaeogeography and the positions of the Kazakh terranes through analysis of their brachiopod faunas. Acta Geologica Polonica 67 (3), 323–380.
Powerman, V., Shatsillo, A., Coe, R., Zhao, X., Gladkochub, D., Buchwaldt, R., Pavlov, V., 2013. Palaeogeography of the Siberian platform during middle Palaeozoic Times (~450–400 Ma): new palaeomagnetic evidence from the Lena and Nyuya rivers. Geophysical Journal International 194 (3), 1412–1440.
Puchkov, V., 2002. Paleozoic evolution of the East European continental margin involved in the Uralide orogeny. In: Mountain Building in the Uralides: Pangea to the Present, vol. 132. American Geophysical Union Monograph Series, pp. 9–31.
Puchkov, V., 2013. Structural stages and evolution of the Urals. Mineralogy and Petrology 107 (1), 3–37.
Puchkov, V.N., 2009. The evolution of the Uralian orogen. Geological Society, London, Special Publications 327 (1), 161–195.
Qian, Q., Gao, J., Klemd, R., He, G., Song, B., Liu, D., Xu, R., 2009. Early Paleozoic tectonic evolution of the Chinese South Tianshan Orogen: constraints from SHRIMP zircon U–Pb geochronology and geochemistry of basaltic and dioritic rocks from Xiate, NW China. International Journal of Earth Sciences 98 (3), 551–569.
Qian, X., Feng, Q., Yang, W., Wang, Y., Chonglakmani, C., Monjai, D., 2015. Arc-like volcanic rocks in NW Laos: geochronological and geochemical constraints and their tectonic implications. Journal of Asian Earth Sciences 98, 342–357.
Qu, J., Xiao, W., Windley, B., Han, C., Mao, Q., Ao, S., Zhang, J., 2011. Ordovician eclogites from the Chinese Beishan: implications for the tectonic evolution of the southern Altaids. Journal of Metamorphic Geology 29 (8), 803–820.
Ren, R., Han, B.F., Xu, Z., Zhou, Y.Z., Liu, B., Zhang, L., Chen, J.F., Su, L., Li, J., Li, X.H., 2014. When did the subduction first initiate in the southern Paleo-Asian Ocean: new constraints from a Cambrian intra-oceanic arc system in West Junggar, NW China. Earth and Planetary Science Letters 388, 222–236.
Ridd, M.F., 2015. East flank of the Sibumasu block in NW Thailand and Myanmar and its possible northward continuation into Yunnan: a review and suggested tectono-stratigraphic interpretation. Journal of Asian Earth Sciences 104, 160–174.
Ridd, M.F., Barber, A.J., Crow, M.J. (Eds.), 2011. The Geology of Thailand. Geological Society of London, 617 pp.
Robinson, A.C., Ducea, M., Lapen, T.J., 2012. Detrital zircon and isotopic constraints on the crustal architecture and tectonic evolution of the northeastern Pamir. Tectonics 31 (2).
Rodionov, V., Dekkers, M., Khramov, A., Gurevich, E., Krijgsman, W., Duermeijer, C., Heslop, D., 2003. Paleomagnetism and cyclostratigraphy of the Middle Ordovician Krivolutsky suite, Krivaya Luka section, southern Siberian platform: record of non-synchronous NRM-components or a non-axial geomagnetic field? Studia Geophysica et Geodaetica 47 (2), 255–274.
Roger, F., Leloup, P.H., Jolivet, M., Lacassin, R., Trinh, P.T., Brunel, M., Seward, D., 2000. Long and complex thermal history of the Song Chay metamorphic dome (Northern Vietnam) by multi-system geochronology. Tectonophysics 321 (4), 449–466.
Rojas-Agramonte, Y., Herwartz, D., García-Casco, A., Kröner, A., Alexeiev, D.V., Klemd, R., Buhre, S., Barth, M., 2013. Early Palaeozoic deep subduction of continental crust in the Kyrgyz North Tianshan: evidence from Lu–Hf garnet geochronology and petrology of mafic dikes. Contributions to Mineralogy and Petrology 166 (2), 525–543.
Rojas-Agramonte, Y., Kröner, A., Alexeiev, D., Jeffreys, T., Khudoley, A., Wong, J., Geng, H., Shu, L., Semiletkin, S., Mikolaichuk, A., 2014. Detrital and igneous zircon ages for supracrustal rocks of the Kyrgyz Tianshan and palaeogeographic implications. Gondwana Research 26 (3–4), 957–974.
Rolland, Y., Picard, C., Pêcher, A., Carrio, E., Sheppard, S.M., Oddone, M., Villa, I.M., 2002. Presence and geodynamic significance of Cambro-Ordovician series of SE Karakoram (N Pakistan). Geodinamica Acta 15 (1), 1–21.
Rudnev, S., Babin, G., Kovach, V., Kiseleva, V.Y., Serov, P., 2013. The early stages of island-arc plagiogranitoid magmatism in Gornaya Shoriya and West Sayan. Russian Geology and Geophysics 54 (1), 20–33.
Rudnev, S., Borisov, S., Babin, G., Levchenkov, O., Makeev, A., Serov, P., Matukov, D., Plotkina, Y.V., 2008. Early Paleozoic batholiths in the northern part of the Kuznetsk Alatau: composition, age, and sources. Petrology 16 (4), 395–419.
Rudnev, S., Izokh, A., Kovach, V., Shelepaev, R., Terent'eva, L., 2009. Age, composition, sources, and geodynamic environments of the origin of granitoids in the northern part of the Ozernaya zone, western Mongolia: growth mechanisms of the Paleozoic continental crust. Petrology 17 (5), 439–475.
Ruppen, D., Knaf, A., Bussien, D., Winkler, W., Chimedtseren, A., von Quadt, A., 2014. Restoring the Silurian to Carboniferous northern active continental margin of the Mongol–Okhotsk Ocean in Mongolia: Hangay–Hentey accretionary wedge and seamount collision. Gondwana Research 25 (4), 1517–1534.
Ruzhentsev, S., Nekrasov, G., 2009. Tectonics of the Aga zone, Mongolia-Okhotsk belt. Geotectonics 43 (1), 34–50.
Ryazantsev, A., Degtyarev, K., Kotov, A., Sal'nikova, E., Anisimova, I., Yakovleva, S., 2009. Ophiolite Sections of the Dzhalair-Nayman Zone, South Kazakhstan: Their Structure and Age Substantiation. Doklady Earth Sciences 427 (2), 902–906.
Ryazantsev, A., Dubinina, S., Kuznetsov, N., Belova, A., 2008. Ordovician lithotectonic complexes in allochthons of the southern Urals. Geotectonics 42 (5), 368–395.
Ryazantsev, A., Savelieva, G., Razumovsky, A., 2015. Dike complexes in ophiolites of the Urals. Geotectonics 49 (3), 193–209.
Rytsk, E.Y., Kovach, V., Yarmolyuk, V., Kovalenko, V., Bogomolov, E., Kotov, A., 2011. Isotopic structure and evolution of the continental crust in the East Transbaikalian segment of the Central Asian Foldbelt. Geotectonics 45 (5), 349–377.
Safonova, I., Biske, G., Romer, R., Seltmann, R., Simonov, V., Maruyama, S., 2016. Middle Paleozoic mafic magmatism and ocean plate stratigraphy of the South Tianshan, Kyrgyzstan. Gondwana Research 30, 236–256.
Safonova, I.Y., Buslov, M., Iwata, K., Kokh, D., 2004. Fragments of Vendian-Early Carboniferous oceanic crust of the Paleo-Asian Ocean in foldbelts of the Altai-Sayan region of Central Asia: geochemistry, biostratigraphy and structural setting. Gondwana Research 7 (3), 771–790.
Şahin, S.Y., Aysal, N., Güngör, Y., Peytcheva, I., Neubauer, F., 2014. Geochemistry and U–Pb zircon geochronology of metagranites in Istranca (Strandja) Zone, NW Pontides, Turkey: implications for the geodynamic evolution of Cadomian orogeny. Gondwana Research 26 (2), 755–771.
Saintot, A., Stephenson, R.A., Stovba, S., Brunet, M.F., Yegorova, T., Starostenko, V., 2006. The evolution of the southern margin of Eastern Europe (Eastern European and Scythian platforms) from the latest Precambrian-Early Palaeozoic to the Early Cretaceous. Geological Society, London, Memoirs 32 (1), 481–505.
Sakashima, T., Terada, K., Takeshita, T., Sano, Y., 2003. Large-scale displacement along the Median Tectonic Line, Japan: evidence from SHRIMP zircon U–Pb dating of granites and gneisses from the South Kitakami and paleo-Ryoke belts. Journal of Asian Earth Sciences 21 (9), 1019–1039.
Savelieva, G., 2011. Ophiolites in European Variscides and Uralides: geodynamic settings and metamorphism. Geotectonics 45 (6), 439–452.
Savelieva, G., Sharaskin, A.Y., Saveliev, A., Spadea, P., Gaggero, L., 1997. Ophiolites of the southern Uralides adjacent to the East European continental margin. Tectonophysics 276 (1), 117–137.
Savelieva, G., Sharaskin, A.Y., Saveliev, A., Spadea, P., Pertsev, A., Babarina, I., 2002. Ophiolites and zoned mafic–ultramafic massifs of the Urals: a comparative analysis and some tectonic implications. In: Mountain Building in the Uralides: Pangea to the Present, vol. 132. American Geophysical Union Monograph Series, pp. 135–153.

Sayar, C., Cocks, L.R.M., 2013. A new Late Ordovician Hirnantia brachiopod Fauna from NW Turkey, its biostratigraphical relationships and palaeogeographical setting. Geological Magazine 150 (3), 479–496.
Schwab, M., Ratschbacher, L., Siebel, W., McWilliams, M., Minaev, V., Lutkov, V., Chen, F., Stanek, K., Nelson, B., Frisch, W., 2004. Assembly of the Pamirs: age and origin of magmatic belts from the southern Tien Shan to the southern Pamirs and their relation to Tibet. Tectonics 23 (4).
Seghedi, A., 2012. Palaeozoic formations from Dobrogea and pre-Dobrogea–an overview. Turkish Journal of Earth Sciences 21 (5), 669–721.
Şengör, A., Natal'In, B., 1996. Paleotectonics of Asia: fragments of a synthesis. In: The Tectonic Evolution of Asia. Cambridge University Press, pp. 486–640.
Şengör, A., Natal'In, B., Burtman, V., 1993. Evolution of the Altaid tectonic collage and Palaeozoic crustal growth in Eurasia. Nature 364 (6435), 299–307.
Seton, M., Müller, R., Zahirovic, S., Gaina, C., Torsvik, T., Shephard, G., Talsma, A., Gurnis, M., Turner, M., Maus, S., 2012. Global continental and ocean basin reconstructions since 200 Ma. Earth-Science Reviews 113 (3), 212–270.
Shatsillo, A., Paverman, V., Pavlov, V., 2007. Middle Paleozoic segment of the apparent polar wander path from the Siberian platform: new paleomagnetic evidence for the Silurian of the Nyuya-Berezovskii facial province. Izvestiya Physics of the Solid Earth 43 (10), 880–889.
Shi, G., Faure, M., Xu, B., Zhao, P., Chen, Y., 2013. Structural and kinematic analysis of the Early Paleozoic Ondor Sum-Hongqi mélange belt, eastern part of the Altaids (CAOB) in Inner Mongolia, China. Journal of Asian Earth Sciences 66, 123–139.
Shi, J., 2016. An Investigation of Multi-generation Folds in Liuling Group South of the Shangdan Suture Zone in the Qinling Belt. The University of Western Ontario Electronic Thesis and Dissertation Repository, 4169, 198 pp.
Shi, M.F., Lin, F.C., Fan, W.Y., Deng, Q., Cong, F., Tran, M.D., Zhu, H.P., Wang, H., 2015. Zircon U–Pb ages and geochemistry of granitoids in the Truong Son terrane, Vietnam: tectonic and metallogenic implications. Journal of Asian Earth Sciences 101, 101–120.
Shi, R., Yang, J., Wu, C., Tsuyoshi, I., Takafumi, H., 2006. Island arc volcanic rocks in the north Qaidam UHP belt, northern Tibet plateau: evidence for ocean–continent subduction preceding continent–continent Subduction. Journal of Asian Earth Sciences 28 (2), 151–159.
Shu, L., Deng, X., Zhu, W., Ma, D., Xiao, W., 2011. Precambrian tectonic evolution of the Tarim Block, NW China: new geochronological insights from the Quruqtagh domain. Journal of Asian Earth Sciences 42 (5), 774–790.
Shu, L., Wang, B., Cawood, P.A., Santosh, M., Xu, Z., 2015. Early Paleozoic and Early Mesozoic intraplate tectonic and magmatic events in the Cathaysia Block, South China. Tectonics 34 (8), 1600–1621.
Siehl, A., 2015. Structural setting and evolution of the Afghan orogenic segment–a review. Geological Society, London, Special Publications 427, 57–88.
Sliaupa, S., Fokin, P., Lazauskiene, J., Stephenson, R.A., 2006. The Vendian-Early Palaeozoic sedimentary basins of the East European Craton. Geological Society, London, Memoirs 32 (1), 449–462.
Smethurst, M.A., Khramov, A.N., Torsvik, T.H., 1998. The Neoproterozoic and Palaeozoic palaeomagnetic data for the Siberian Platform: from Rodinia to Pangea. Earth-Science Reviews 43 (1), 1–24.
Somin, M.L., 2011. Pre-Jurassic basement of the Greater Caucasus: brief overview. Turkish Journal of Earth Sciences 20 (5), 545–610.
Song, D., Xiao, W., Han, C., Li, J., Qu, J., Guo, Q., Lin, L., Wang, Z., 2013a. Progressive accretionary tectonics of the Beishan orogenic collage, southern Altaids: insights from zircon U–Pb and Hf isotopic data of high-grade complexes. Precambrian Research 227, 368–388.
Song, D., Xiao, W., Han, C., Tian, Z., 2013b. Geochronological and geochemical study of gneiss–schist complexes and associated granitoids, Beishan Orogen, southern Altaids. International Geology Review 55 (14), 1705–1727.
Song, D., Xiao, W., Windley, B.F., Han, C., Tian, Z., 2015. A Paleozoic Japan-type subduction-accretion system in the Beishan orogenic collage, southern Central Asian Orogenic Belt. Lithos 224, 195–213.
Song, D., Xiao, W., Windley, B.F., Han, C., Yang, L., 2016. Metamorphic complexes in accretionary orogens: insights from the Beishan collage, southern Central Asian Orogenic Belt. Tectonophysics 688, 135–147.
Song, S., Niu, Y., Su, L., Xia, X., 2013c. Tectonics of the North Qilian orogen, NW China. Gondwana Research 23 (4), 1378–1401.
Song, S., Niu, Y., Su, L., Zhang, C., Zhang, L., 2014. Continental orogenesis from ocean subduction, continent collision/subduction, to orogen collapse, and orogen recycling: the example of the North Qaidam UHPM belt, NW China. Earth-Science Reviews 129, 59–84.
Song, S., Zhang, L., Niu, Y., Su, L., Song, B., Liu, D., 2006. Evolution from oceanic subduction to continental collision: a case study from the Northern Tibetan Plateau based on geochemical and geochronological data. Journal of Petrology 47 (3), 435–455.
Sorokin, A., Kotov, A., Sal'nikova, E., Kudryashov, N., Velikoslavinskii, S., Yakovleva, S., Fedoseenko, A., Plotkina, Y.V., 2011. Early paleozoic granitoids in the Lesser Khingan terrane, Central Asian Foldbelt: age, geochemistry, and geodynamic interpretations. Petrology 19 (6), 601–617.
Stampfli, G., Marcoux, J., Baud, A., 1991. Tethyan margins in space and time. Palaeogeography, Palaeoclimatology, Palaeoecology 87 (1), 373–409.
Stampfli, G.M., Borel, G., 2002. A plate tectonic model for the Paleozoic and Mesozoic constrained by dynamic plate boundaries and restored synthetic oceanic isochrons. Earth and Planetary Science Letters 196 (1), 17–33.
Starostenko, V., Janik, T., Yegorova, T., Farfuliak, L., Czuba, W., Środa, P., Thybo, H., Artemieva, I., Sosson, M., Volfman, Y., 2015. Seismic model of the crust and upper mantle in the Scythian Platform: the DOBRE-5 profile across the north western Black Sea and the Crimean Peninsula. Geophysical Journal International 201 (1), 406–428.
Steinberger, B., Torsvik, T.H., 2008. Absolute plate motions and true polar wander in the absence of hotspot tracks. Nature 452 (7187), 620–623.
Štípská, P., Schulmann, K., Lehmann, J., Corsini, M., Lexa, O., Tomurhuu, D., 2010. Early Cambrian eclogites in SW Mongolia: evidence that the Palaeo-Asian Ocean suture extends further east than expected. Journal of Metamorphic Geology 28 (9), 915–933.
Stone, D., Minyuk, P., Kolosev, E., 2003. New paleomagnetic paleolatitudes for the Omulevka terrane of northeast Russia: a comparison with the Omolon terrane and the eastern Siberian platform. Tectonophysics 377 (1), 55–82.
Sun, L.S., Huang, B.C., 2009. New paleomagnetic result for Ordovician rocks from the Tarim Block, Northwest China and its tectonic implications. Chinese Journal of Geophysics 52 (7), 1836–1848.
Sun, M., Yuan, C., Xiao, W., Long, X., Xia, X., Zhao, G., Lin, S., Wu, F., Kröner, A., 2008. Zircon U–Pb and Hf isotopic study of gneissic rocks from the Chinese Altai: progressive accretionary history in the early to middle Palaeozoic. Chemical Geology 247 (3), 352–383.
Sun, W., Chi, X.G., Zhao, Z., Pan, S.Y., Liu, J.F., Zhang, R., Quan, J.Y., 2014. Zircon geochronology constraints on the age and nature of 'Precambrian metamorphic rocks' in the Xing'an block of Northeast China. International Geology Review 56 (6), 672–694.
Tagiri, M., Dunkley, D.J., Adachi, T., Hiroi, Y., Fanning, C., 2011. SHRIMP dating of magmatism in the Hitachi metamorphic terrane, Abukuma Belt, Japan: evidence for a Cambrian volcanic arc. Island Arc 20 (2), 259–279.
Tang, J., Xu, W.L., Wang, F., Wang, W., Xu, M.J., Zhang, Y.H., 2013. Geochronology and geochemistry of Neoproterozoic magmatism in the Erguna Massif, NE China: petrogenesis and implications for the breakup of the Rodinia supercontinent. Precambrian Research 224, 597–611.
Tang, Q., Li, C., Zhang, M., Ripley, E.M., Wang, Q., 2014. Detrital zircon constraint on the timing of amalgamation between Alxa and Ordos, with exploration implications for Jinchuan-type Ni-Cu ore deposit in China. Precambrian Research 255 (2), 748–755.
Taylor, J.P., Webb, L.E., Johnson, C.L., Heumann, M.J., 2013. The lost South Gobi microcontinent: protolith studies of metamorphic tectonites and implications for the evolution of continental crust in Southeastern Mongolia. Geosciences 3 (3), 543–584.
Tong-Dzuy, T., Vu, K. (Eds.), 2011. Stratigraphic Units of Vietnam, second ed. Vietnam National University Publisher. 556 pp.
Tian, Z., Xiao, W., Windley, B.F., Lin, L.N., Han, C., Zhang, J.E., Wan, B., Ao, S., Song, D., Feng, J., 2014. Structure, age, and tectonic development of the Huoshishan–Niujuanzi ophiolitic mélange, Beishan, southernmost Altaids. Gondwana Research 25 (2), 820–841.
Torsvik, T.H., Burke, K., Steinberger, B., Webb, S.J., Ashwal, L.D., 2010. Diamonds sampled by plumes from the core-mantle boundary. Nature 466 (7304), 352–355.
Torsvik, T.H., Cocks, L.R.M., 2009. The Lower Palaeozoic palaeogeographical evolution of the northeastern and eastern peri-Gondwanan margin from Turkey to New Zealand. Geological Society, London, Special Publications 325 (1), 3–21.
Torsvik, T.H., Paulsen, T.S., Hughes, N.C., Myrow, P.M., Ganerød, M., 2009. The Tethyan Himalaya: palaeogeographical and tectonic constraints from Ordovician palaeomagnetic data. Journal of the Geological Society 166 (4), 679–687.
Torsvik, T.H., Steinberger, B., Cocks, L.R.M., Burke, K., 2008. Longitude: linking Earth's ancient surface to its deep interior. Earth and Planetary Science Letters 276 (3), 273–282.
Torsvik, T.H., van der Voo, R., Doubrovine, P.V., Burke, K., Steinberger, B., Ashwal, L.D., Trønnes, R.G., Webb, S.J., Bull, A.L., 2014. Deep mantle structure as a reference frame for movements in and on the Earth. Proceedings of the National Academy of Sciences 111 (24), 8735–8740.
Torsvik, T.H., Van der Voo, R., Preeden, U., Mac Niocaill, C., Steinberger, B., Doubrovine, P.V., van Hinsbergen, D.J., Domeier, M., Gaina, C., Tohver, E., 2012. Phanerozoic polar wander, palaeogeography and dynamics. Earth-Science Reviews 114 (3), 325–368.
Tran, H.T., Zaw, K., Halpin, J.A., Manaka, T., Meffre, S., Lai, C.K., Lee, Y., Van Le, H., Dinh, S., 2014. The Tam Ky-Phuoc Son shear zone in Central Vietnam: tectonic and metallogenic implications. Gondwana Research 26 (1), 144–164.
Tretyakov, A., Degtyarev, K., Shatagin, K., Kotov, A., Sal'nikova, E., Anisimova, I., 2015. Neoproterozic anorogenic rhyolite-granite volcanoplutonic association of the Aktau-Mointy sialic massif (Central Kazakhstan): age, source, and paleotectonic position. Petrology 23 (1), 22–44.
Tsujimori, T., Liou, J., Wooden, J., Miyamoto, T., 2005. U-Pb dating of large zircons in low-temperature jadeitite from the Osayama serpentinite melange, Southwest Japan: insights into the timing of serpentinization. International Geology Review 47 (10), 1048–1057.
Tung, K.A., Yang, H.Y., Yang, H.J., Smith, A., Liu, D., Zhang, J., Wu, C., Shau, Y.H., Wen, D.J., Tseng, C.Y., 2016. Magma sources and petrogenesis of the early–middle Paleozoic backarc granitoids from the central part of the Qilian block, NW China. Gondwana Research 38, 197–219.
Ustaömer, P.A., Ustaömer, T., Collins, A.S., Robertson, A.H., 2009. Cadomian (Ediacaran–Cambrian) arc magmatism in the Bitlis Massif, SE Turkey: magmatism along the developing northern margin of Gondwana. Tectonophysics 473 (1), 99–112.
Ustaömer, P.A., Ustaömer, T., Gerdes, A., Zulauf, G., 2011. Detrital zircon ages from a Lower Ordovician quartzite of the Istanbul exotic terrane (NW Turkey):

evidence for Amazonian affinity. International Journal of Earth Sciences 100 (1), 23–41.
Ustaömer, P.A., Ustaömer, T., Robertson, A., 2012. Ion Probe U-Pb dating of the Central Sakarya Basement: a peri-Gondwana terrane intruded by Late Lower Carboniferous subduction/collision-related granitic rocks. Turkish Journal of Earth Sciences 21 (6), 905–932.
Usuki, T., Lan, C.Y., Wang, K.L., Chiu, H.Y., 2013. Linking the Indochina block and Gondwana during the Early Paleozoic: evidence from U–Pb ages and Hf isotopes of detrital zircons. Tectonophysics 586, 145–159.
Usuki, T., Lan, C.Y., Yui, T.F., Iizuka, Y., Van Vu, T., Tran, T.A., Okamoto, K., Wooden, J.L., Liou, J.G., 2009. Early Paleozoic medium-pressure metamorphism in central Vietnam: evidence from SHRIMP U-Pb zircon ages. Geosciences Journal 13 (3), 245–256.
Valdiya, K., 1995. Proterozoic sedimentation and Pan-African geodynamic development in the Himalaya. Precambrian Research 74 (1), 35–55.
Van der Voo, R., van Hinsbergen, D.J., Domeier, M., Spakman, W., Torsvik, T.H., 2015. Latest Jurassic–earliest Cretaceous closure of the Mongol-Okhotsk Ocean: a paleomagnetic and seismological-tomographic analysis. Geological Society of America Special Papers 513, 589–606.
Volkova, N., Travin, A., Yudin, D., 2011. Ordovician blueschist metamorphism as a reflection of accretion-collision events in the Central Asian orogenic belt. Russian Geology and Geophysics 52 (1), 72–84.
Volozh, Y.A., Antipov, M., Brunet, M.F., Garagash, I., Lobkovskii, L., Cadet, J.P., 2003. Pre-Mesozoic geodynamics of the Precaspian basin (Kazakhstan). Sedimentary Geology 156 (1), 35–58.
Vyssotski, A., Vyssotski, V., Nezhdanov, A., 2006. Evolution of the West Siberian Basin. Marine and Petroleum Geology 23 (1), 93–126.
Wakita, K., 2013. Geology and tectonics of Japanese islands: a review–the key to understanding the geology of Asia. Journal of Asian Earth Sciences 72, 75–87.
Walker, J.D., Geissman, J.W., Bowring, S., Babcock, L., 2013. The Geological Society of America geologic time scale. Geological Society of America Bulletin 125 (3–4), 259–272.
Wang, B., Faure, M., Shu, L., Cluzel, D., Charvet, J., De Jong, K., Chen, Y., 2008. Paleozoic tectonic evolution of the Yili Block, western Chinese Tianshan. Bulletin de la Société Géologique de France 179 (5), 483–490.
Wang, B., Jahn, B.M., Lo, C.H., Shu, L.S., Wu, C.Y., Li, K.S., Wang, F., 2011a. Structural analysis and $^{40}Ar/^{39}Ar$ thermochronology of Proterozoic rocks in Sailimu area (NW China): implication to polyphase tectonics of the North Chinese Tianshan. Journal of Asian Earth Sciences 42 (5), 839–853.
Wang, B., Jahn, B.M., Shu, L., Li, K., Chung, S.L., Liu, D., 2012a. Middle-Late Ordovician arc-type plutonism in the NW Chinese Tianshan: implication for the accretion of the Kazakhstan continent in Central Asia. Journal of Asian Earth Sciences 49, 40–53.
Wang, B., Liu, H., Shu, L., Jahn, B.M., Chung, S.L., Zhai, Y., Liu, D., 2014a. Early Neoproterozoic crustal evolution in northern Yili Block: insights from migmatite, orthogneiss and leucogranite of the Wenquan metamorphic complex in the NW Chinese Tianshan. Precambrian Research 242, 58–81.
Wang, B., Shu, L., Faure, M., Jahn, B.M., Cluzel, D., Charvet, J., Chung, S.L., Meffre, S., 2011b. Paleozoic tectonics of the southern Chinese Tianshan: insights from structural, chronological and geochemical studies of the Heiyingshan ophiolitic mélange (NW China). Tectonophysics 497 (1), 85–104.
Wang, C., Liu, L., Xiao, P.X., Cao, Y.T., Yu, H.Y., Meert, J.G., Liang, W.T., 2014b. Geochemical and geochronologic constraints for Paleozoic magmatism related to the orogenic collapse in the Qimantagh–South Altyn region, northwestern China. Lithos 202–203, 1–20.
Wang, C., Liu, L., Yang, W.Q., Zhu, X.H., Cao, Y.T., Kang, L., Chen, S.F., Li, R.S., He, S.P., 2013a. Provenance and ages of the Altyn Complex in Altyn Tagh: implications for the early Neoproterozoic evolution of northwestern China. Precambrian Research 230, 193–208.
Wang, C.Y., Zhang, Q., Qian, Q., Zhou, M.F., 2005. Geochemistry of the Early Paleozoic Baiyin volcanic rocks (NW China): implications for the tectonic evolution of the North Qilian orogenic belt. The Journal of Geology 113 (1), 83–94.
Wang, D., Zheng, J., Ma, Q., Griffin, W.L., Zhao, H., Wong, J., 2013b. Early Paleozoic crustal anatexis in the intraplate Wuyi–Yunkai orogen, South China. Lithos 175, 124–145.
Wang, H., Wu, Y.B., Gao, S., Liu, X.C., Liu, Q., Qin, Z.W., Xie, S.W., Zhou, L., Yang, S.H., 2013c. Continental origin of eclogites in the North Qinling terrane and its tectonic implications. Precambrian Research 230, 13–30.
Wang, H., Wu, Y.B., Gao, S., Zheng, J.P., Liu, Q., Liu, X.C., Qin, Z.W., Yang, S.H., Gong, H.J., 2014c. Deep subduction of continental crust in accretionary orogen: evidence from U–Pb dating on diamond-bearing zircons from the Qinling orogen, central China. Lithos 190, 420–429.
Wang, H., Wu, Y.B., Qin, Z.W., Zhu, L.Q., Liu, Q., Liu, X.C., Gao, S., Wijbrans, J.R., Zhou, L., Gong, H.J., 2013d. Age and geochemistry of Silurian gabbroic rocks in the Tongbai orogen, central China: implications for the geodynamic evolution of the North Qinling arc–back-arc system. Lithos 179, 1–15.
Wang, M., Li, C., Ming-Xie, C., 2016. Dating of detrital zircons from the Dabure clastic rocks: the discovery of Neoproterozoic strata in southern Qiangtang, Tibet. International Geology Review 58 (2), 216–227.
Wang, M., Zhang, J., Zhang, B., Qi, G., 2015. An Early Paleozoic collisional event along the northern margin of the Central Tianshan Block: constraints from geochemistry and geochronology of granitic rocks. Journal of Asian Earth Sciences 113 (1), 325–338.
Wang, X., Wang, T., Zhang, C., 2013e. Neoproterozoic, Paleozoic, and Mesozoic granitoid magmatism in the Qinling Orogen, China: constraints on orogenic process. Journal of Asian Earth Sciences 72, 129–151.
Wang, X., Zhang, J., Santosh, M., Liu, J., Yan, S., Guo, L., 2012b. Andean-type orogeny in the Himalayas of South Tibet: implications for early Paleozoic tectonics along the Indian margin of Gondwana. Lithos 154, 248–262.
Wang, Y., Fan, W., Zhang, G., Zhang, Y., 2013f. Phanerozoic tectonics of the South China Block: key observations and controversies. Gondwana Research 23 (4), 1273–1305.
Wang, Y., Xing, X., Cawood, P.A., Lai, S., Xia, X., Fan, W., Liu, H., Zhang, F., 2013g. Petrogenesis of early Paleozoic peraluminous granite in the Sibumasu Block of SW Yunnan and diachronous accretionary orogenesis along the northern margin of Gondwana. Lithos 182, 67–85.
Wang, Y., Yuan, C., Long, X., Sun, M., Xiao, W., Zhao, G., Cai, K., Jiang, Y., 2011c. Geochemistry, zircon U–Pb ages and Hf isotopes of the Paleozoic volcanic rocks in the northwestern Chinese Altai: petrogenesis and tectonic implications. Journal of Asian Earth Sciences 42 (5), 969–985.
Wang, Y., Zhang, F., Fan, W., Zhang, G., Chen, S., Cawood, P.A., Zhang, A., 2010. Tectonic setting of the South China Block in the early Paleozoic: resolving intracontinental and ocean closure models from detrital zircon U-Pb geochronology. Tectonics 29 (6).
Wegener, A., 1912. Die entstehung der kontinente. Geologische Rundschau 3 (4), 276–292.
Wiesmayr, G., Grasemann, B., 2002. Eohimalayan fold and thrust belt: implications for the geodynamic evolution of the NW-Himalaya (India). Tectonics 21 (6).
Wilhem, C., Windley, B.F., Stampfli, G.M., 2012. The Altaids of Central Asia: a tectonic and evolutionary innovative review. Earth-Science Reviews 113 (3), 303–341.
Williams, M., Wallis, S., Oji, T., Lane, P.D., 2014. Ambiguous biogeographical patterns mask a more complete understanding of the Ordovician to Devonian evolution of Japan. Island Arc 23 (2), 76–101.
Windley, B.F., Alexeiev, D., Xiao, W., Kröner, A., Badarch, G., 2007. Tectonic models for accretion of the Central Asian Orogenic Belt. Journal of the Geological Society 164 (1), 31–47.
Wu, C., Wooden, J.L., Robinson, P.T., Gao, Y., Wu, S., Chen, Q., Mazdab, F.K., Mattinson, C., 2009a. Geochemistry and zircon SHRIMP U-Pb dating of granitoids from the west segment of the North Qaidam. Science in China Series D: Earth Sciences 52 (11), 1771–1790.
Wu, C., Yang, J., Robinson, P.T., Wooden, J.L., Mazdab, F.K., Gao, Y., Wu, S., Chen, Q., 2009b. Geochemistry, age and tectonic significance of granitic rocks in north Altun, northwest China. Lithos 113 (3), 423–436.
Wu, F.Y., Sun, D.Y., Ge, W.C., Zhang, Y.B., Grant, M.L., Wilde, S.A., Jahn, B.M., 2011. Geochronology of the Phanerozoic granitoids in northeastern China. Journal of Asian Earth Sciences 41 (1), 1–30.
Wu, G., Chen, Y., Chen, Y., Zeng, Q., 2012. Zircon U–Pb ages of the metamorphic supracrustal rocks of the Xinghuadukou Group and granitic complexes in the Argun massif of the northern Great Hinggan Range, NE China, and their tectonic implications. Journal of Asian Earth Sciences 49, 214–233.
Wu, G., Chen, Y., Sun, F., Liu, J., Wang, G., Xu, B., 2015. Geochronology, geochemistry, and Sr–Nd–Hf isotopes of the early Paleozoicigneous rocks in the Duobaoshan area, NE China, and their geological significance. Journal of Asian Earth Sciences 97, 229–250.
Wu, L., Jia, D., Li, H., Deng, F., Li, Y., 2010. Provenance of detrital zircons from the late Neoproterozoic to Ordovician sandstones of South China: implications for its continental affinity. Geological Magazine 147 (6), 974–980.
Wu, Y.B., Zheng, Y.F., 2013. Tectonic evolution of a composite collision orogen: an overview on the Qinling–Tongbai–Hong'an–Dabie–Sulu orogenic belt in central China. Gondwana Research 23 (4), 1402–1428.
Xia, J., Wang, L., Zhong, H., Tong, J., Lu, R., Wang, M., 2009. Discovery of large-scale Silurian ancient delta deposition system in Longmu Co area. Qinghai-Tibet plateau, China and its significance, Geology Bulletin of China 28, 1267–1275.
Xia, X., Song, S., Niu, Y., 2012. Tholeiite–Boninite terrane in the North Qilian suture zone: implications for subduction initiation and back-arc basin development. Chemical Geology 328, 259–277.
Xiao, W.J., Zhang, L.C., Qin, K.Z., Sun, S., Li, J.L., 2004. Paleozoic accretionary and collisional tectonics of the Eastern Tianshan (China): implications for the continental growth of central Asia. American Journal of Science 304 (4), 370–395.
Xiao, W., Han, C., Liu, W., Wan, B., Zhang, J.e., Ao, S., Zhang, Z., Song, D., Tian, Z., Luo, J., 2014. How many sutures in the southern Central Asian Orogenic Belt: insights from East Xinjiang–West Gansu (NW China)? Geoscience Frontiers 5 (4), 525–536.
Xiao, W., Huang, B., Han, C., Sun, S., Li, J., 2010a. A review of the western part of the Altaids: a key to understanding the architecture of accretionary orogens. Gondwana Research 18 (2), 253–273.
Xiao, W., Mao, Q., Windley, B., Han, C., Qu, J., Zhang, J., Ao, S., Guo, Q., Cleven, N., Lin, S., 2010b. Paleozoic multiple accretionary and collisional processes of the Beishan orogenic collage. American Journal of Science 310 (10), 1553–1594.
Xiao, W., Santosh, M., 2014. The western Central Asian Orogenic Belt: a window to accretionary orogenesis and continental growth. Gondwana Research 25 (4), 1429–1444.
Xiao, W., Windley, B., Hao, J., Li, J., 2002. Arc-ophiolite obduction in the Western Kunlun Range (China): implications for the Palaeozoic evolution of central Asia. Journal of the Geological Society 159 (5), 517–528.
Xiao, W., Windley, B., Liu, D.Y., Jian, P., Liu, C., Yuan, C., Sun, M., 2005. Accretionary tectonics of the Western Kunlun Orogen, China: a Paleozoic–early Mesozoic, long-lived active continental margin with implications for the growth of southern Eurasia. The Journal of Geology 113 (6), 687–705.

Xiao, W., Windley, B.F., Allen, M.B., Han, C., 2013. Paleozoic multiple accretionary and collisional tectonics of the Chinese Tianshan orogenic collage. Gondwana Research 23 (4), 1316–1341.
Xiao, W., Windley, B.F., Hao, J., Zhai, M., 2003. Accretion leading to collision and the Permian Solonker suture, Inner Mongolia, China: termination of the central Asian orogenic belt. Tectonics 22 (6).
Xiao, W., Windley, B.F., Yong, Y., Yan, Z., Yuan, C., Liu, C., Li, J., 2009. Early Paleozoic to Devonian multiple-accretionary model for the Qilian Shan, NW China. Journal of Asian Earth Sciences 35 (3), 323–333.
Xiong, F., Ma, C., Jiang, H.a., Liu, B., Huang, J., 2014. Geochronology and geochemistry of Middle Devonian mafic dykes in the East Kunlun orogenic belt, Northern Tibet Plateau: implications for the transition from Prototethys to Paleotethys orogeny. Chemie der Erde-Geochemistry 74 (2), 225–235.
Xu, B., Charvet, J., Chen, Y., Zhao, P., Shi, G., 2013. Middle Paleozoic convergent orogenic belts in western Inner Mongolia (China): framework, kinematics, geochronology and implications for tectonic evolution of the Central Asian Orogenic Belt. Gondwana Research 23 (4), 1342–1364.
Xu, B., Zhao, P., Wang, Y., Liao, W., Luo, Z., Bao, Q., Zhou, Y., 2015. The pre-Devonian tectonic framework of Xing'an-Mongolia orogenic belt (XMOB) in north China. Journal of Asian Earth Sciences 97, 183–196.
Xu, C., Campbell, I.H., Allen, C.M., Chen, Y., Huang, Z., Qi, L., Zhang, G., Yan, Z., 2008. U–Pb zircon age, geochemical and isotopic characteristics of carbonatite and syenite complexes from the Shaxiongdong, China. Lithos 105 (1), 118–128.
Xu, Y.J., Cawood, P.A., Du, Y.S., 2016. Intraplate orogenesis in response to Gondwana assembly: Kwangsian Orogeny, South China. American Journal of Science 316 (4), 329–362.
Xu, Y., Du, Y., Cawood, P.A., Yang, J., 2010. Provenance record of a foreland basin: detrital zircon U–Pb ages from Devonian strata in the North Qilian Orogenic Belt, China. Tectonophysics 495 (3), 337–347.
Xu, Z., Han, B.F., Ren, R., Zhou, Y.Z., Zhang, L., Chen, J.F., Su, L., Li, X.H., Liu, D.Y., 2012. Ultramafic–mafic mélange, island arc and post-collisional intrusions in the Mayile Mountain, West Junggar, China: implications for Paleozoic intra-oceanic subduction–accretion process. Lithos 132, 141–161.
Yan, Z., Fu, C., Wang, Z., Yan, Q., Chen, L., Chen, J., 2016. Late Paleozoic subduction–accretion along the southern margin of the North Qinling terrane, central China: evidence from zircon U-Pb dating and geochemistry of the Wuguan Complex. Gondwana Research 30, 97–111.
Yang, G., Li, Y., Santosh, M., Gu, P., Yang, B., Zhang, B., Wang, H., Zhong, X., Tong, L., 2012. A Neoproterozoic seamount in the Paleoasian Ocean: evidence from zircon U–Pb geochronology and geochemistry of the Mayile ophiolitic mélange in West Junggar, NW China. Lithos 140, 53–65.
Yang, H., Zhang, H., Luo, B., Zhang, J., Xiong, Z., Guo, L., Pan, F., 2015. Early Paleozoic intrusive rocks from the eastern Qilian orogen, NE Tibetan Plateau: petrogenesis and tectonic significance. Lithos 224, 13–31.
Yang, Z., Otofuji, Y.I., Sun, Z., Huang, B., 2002. Magnetostratigraphic constraints on the Gondwanan origin of North China: Cambrian/Ordovician boundary results. Geophysical Journal International 151 (1), 1–10.
Yang, Z., Sun, Z., Yang, T., Pei, J., 2004. A long connection (750–380 Ma) between South China and Australia: paleomagnetic constraints. Earth and Planetary Science Letters 220 (3), 423–434.
Yao, W.H., Li, Z.X., Li, W.X., Li, X.H., Yang, J.H., 2014. From Rodinia to Gondwanaland: a tale of detrital zircon provenance analyses from the southern Nanhua Basin, South China. American Journal of Science 314 (1), 278–313.
Yarmolyuk, V., Kovach, V., Kovalenko, V., Salnikova, E., Kozlovskii, A., Kotov, A., Yakovleva, S., Fedoseenko, A., 2011. Composition, sources, and mechanism of continental crust growth in the Lake Zone of the Central Asian Caledonides: I. Geological and geochronological data. Petrology 19 (1), 55–78.
Yarmolyuk, V., Kovalenko, V., Sal'nikova, E., Kozakov, I., Kotov, A., Kovach, V., Vladykin, N., Yakovleva, S., 2005. U-Pb age of syn- and post-metamorphic granitoids from South Mongolia: evidence for the presence of Grenvillides in the Central Asian Foldbelt. Doklady Earth Sciences 404, 986–990.
Ye, H.M., Li, X.H., Li, Z.X., Zhang, C.-L., 2008. Age and origin of high Ba–Sr appinite–granites at the northwestern margin of the Tibet Plateau: implications for early Paleozoic tectonic evolution of the Western Kunlun orogenic belt. Gondwana Research 13 (1), 126–138.
Yu, J., Guo, L., Li, J., Li, Y., Smithies, R.H., Wingate, M.T., Meng, Y., Chen, S., 2016. The petrogenesis of sodic granites in the Niujuanzi area and constraints on the Paleozoic tectonic evolution of the Beishan region, NW China. Lithos 256, 250–268.
Yu, S., Zhang, J., Del Real, P.G., 2012. Geochemistry and zircon U–Pb ages of adakitic rocks from the Dulan area of the North Qaidam UHP terrane, north Tibet: constraints on the timing and nature of regional tectonothermal events associated with collisional orogeny. Gondwana Research 21 (1), 167–179.
Yuan, W., Yang, Z., 2015a. The Alashan Terrane was not part of North China by the Late Devonian: evidence from detrital zircon U–Pb geochronology and Hf isotopes. Gondwana Research 27 (3), 1270–1282.
Yuan, W., Yang, Z., 2015b. The Alashan Terrane did not amalgamate with North China block by the Late Permian: evidence from Carboniferous and Permian paleomagnetic results. Journal of Asian Earth Sciences 104, 145–159.
Yuan, Y., Zong, K., He, Z., Klemd, R., Liu, Y., Hu, Z., Guo, J., Zhang, Z., 2015. Geochemical and geochronological evidence for a former early Neoproterozoic microcontinent in the South Beishan Orogenic Belt, southernmost Central Asian Orogenic Belt. Precambrian Research 266, 409–424.
Zanchi, A., Gaetani, M., 2011. The geology of the Karakoram range, Pakistan: the new 1: 100,000 geological map of Central-Western Karakoram. Italian Journal of Geosciences 130 (2), 161–262.
Żelaźniewicz, A., Hòa, T.T., Larionov, A.N., 2013. The significance of geological and zircon age data derived from the wall rocks of the Ailao Shan–Red River Shear Zone, NW Vietnam. Journal of Geodynamics 69, 122–139.
Zeng, Q.D., Liu, J.M., Chu, S.X., Wang, Y.B., Sun, Y., Duan, X.X., Zhou, L.L., Qu, W.J., 2014. Re–Os and U–Pb geochronology of the Duobaoshan porphyry Cu–Mo–(Au) deposit, northeast China, and its geological significance. Journal of Asian Earth Sciences 79, 895–909.
Zhai, Q.G., Jahn, B.M., Wang, J., Hu, P.Y., Chung, S.L., Lee, H.Y., Tang, S.H., Tang, Y., 2016. Oldest Paleo-Tethyan ophiolitic mélange in the Tibetan Plateau. Geological Society of America Bulletin 128 (3–4), 355–373.
Zhang, C.L., Zou, H.-B., Li, H.K., Wang, H.Y., 2013a. Tectonic framework and evolution of the Tarim Block in NW China. Gondwana Research 23 (4), 1306–1315.
Zhang, C., Lu, S., Yu, H., Ye, H., 2007a. Tectonic evolution of the Western Kunlun orogenic belt in northern Qinghai-Tibet Plateau: evidence from zircon SHRIMP and LA-ICP-MS U-Pb geochronology. Science in China Series D: Earth Sciences 50 (6), 825–835.
Zhang, G., Song, S., Zhang, L., Niu, Y., 2008. The subducted oceanic crust within continental-type UHP metamorphic belt in the North Qaidam, NW China: evidence from petrology, geochemistry and geochronology. Lithos 104 (1), 99–118.
Zhang, H., Yang, T., Hou, Z., Bian, Y., 2016a. Devonian Nb-enriched basalts and andesites of north-central Tibet: evidence for the early subduction of the Paleo-Tethyan oceanic crust beneath the North Qiangtang Block. Tectonophysics 682, 96–107.
Zhang, J.X., Mattinson, C.G., Yu, S., Li, Y., 2014a. Combined rutile–zircon thermometry and U–Pb geochronology: New constraints on Early Paleozoic HP/UHT granulite in the south Altyn Tagh, north Tibet, China. Lithos 200, 241–257.
Zhang, J., Li, J., Xiao, W., Wang, Y., Qi, W., 2013b. Kinematics and geochronology of multistage ductile deformation along the eastern Alxa block, NW China: new constraints on the relationship between the North China Plate and the Alxa block. Journal of Structural Geology 57, 38–57.
Zhang, J., Li, J., Yu, S., Meng, F., Mattinson, C., Yang, H., Ker, C., 2012a. Provenance of eclogitic metasediments in the north Qilian HP/LT metamorphic terrane, western China: geodynamic implications for early Paleozoic subduction-erosion. Tectonophysics 570, 78–101.
Zhang, J., Mattinson, C., Yu, S., Li, J., Meng, F., 2010. U–Pb zircon geochronology of coesite-bearing eclogites from the southern Dulan area of the North Qaidam UHP terrane, northwestern China: spatially and temporally extensive UHP metamorphism during continental subduction. Journal of Metamorphic Geology 28 (9), 955–978.
Zhang, J., Meng, F., Wan, Y., 2007b. A cold Early Palaeozoic subduction zone in the North Qilian Mountains, NW China: petrological and U-Pb geochronological constraints. Journal of Metamorphic Geology 25 (3), 285–304.
Zhang, J., Yu, S., Mattinson, C., 2017. Early Paleozoic polyphase metamorphism in northern Tibet, China. Gondwana Research 41, 267–289.
Zhang, L., 1997. The $^{40}Ar/^{39}Ar$ metamorphic ages of Tangbale blueschists and their geological significance in West Junggar of Xinjiang. Chinese Science Bulletin 42 (22), 1902–1904.
Zhang, Q., Liu, Y., Huang, H., Wu, Z., Zhou, Q., 2016b. Petrogenesis and tectonic implications of the high-K Alamas calc-alkaline granitoids at the northwestern margin of the Tibetan Plateau: geochemical and Sr–Nd–Hf–O isotope constraints. Journal of Asian Earth Sciences 127, 137–151.
Zhang, S.H., Zhao, Y., Ye, H., Liu, J.M., Hu, Z.C., 2014b. Origin and evolution of the Bainaimiao arc belt: implications for crustal growth in the southern Central Asian orogenic belt. Geological Society of America Bulletin 126 (9–10), 1275–1300.
Zhang, S., Gao, R., Li, H., Hou, H., Wu, H., Li, Q., Yang, K., Li, C., Li, W., Zhang, J., 2014c. Crustal structures revealed from a deep seismic reflection profile across the Solonker suture zone of the Central Asian Orogenic Belt, northern China: an integrated interpretation. Tectonophysics 612, 26–39.
Zhang, W., Jian, P., Kröner, A., Shi, Y., 2013c. Magmatic and metamorphic development of an early to mid-Paleozoic continental margin arc in the southernmost Central Asian Orogenic Belt, Inner Mongolia, China. Journal of Asian Earth Sciences 72, 63–74.
Zhang, X.Z., Dong, Y.S., Li, C., Deng, M.R., Zhang, L., Xu, W., 2014d. Silurian high-pressure granulites from Central Qiangtang, Tibet: constraints on early Paleozoic collision along the northeastern margin of Gondwana. Earth and Planetary Science Letters 405, 39–51.
Zhang, X., Zhao, G., Eizenhöfer, P.R., Sun, M., Han, Y., Hou, W., Liu, D., Wang, B., Liu, Q., Xu, B., 2015. Paleozoic magmatism and metamorphism in the Central Tianshan block revealed by U–Pb and Lu–Hf isotope studies of detrital zircons from the South Tianshan belt, NW China. Lithos 233, 193–208.
Zhang, X., Zhao, G., Eizenhöfer, P.R., Sun, M., Han, Y., Hou, W., Liu, D., Wang, B., Liu, Q., Xu, B., 2016c. Late Ordovician adakitic rocks in the Central Tianshan block, NW China: partial melting of lower continental arc crust during back-arc basin opening. Geological Society of America Bulletin 128 (9–10), 1367–1382.
Zhang, Y., Dostal, J., Zhao, Z., Liu, C., Guo, Z., 2011. Geochronology, geochemistry and petrogenesis of mafic and ultramafic rocks from Southern Beishan area, NW China: implications for crust–mantle interaction. Gondwana Research 20 (4), 816–830.

Zhang, Y., Wang, Y., Zhan, R., Fan, J., Zhou, Z., Fang, X., 2014e. Ordovician and Silurian Stratigraphy and Palaeontology of Yunnan, Southwest China. Science Press, Beijing, 138 pp.
Zhang, Z.M., Dong, X., Liu, F., Lin, Y.H., Yan, R., Santosh, M., 2012b. Tectonic evolution of the Amdo terrane, central tibet: petrochemistry and zircon U-Pb geochronology. The Journal of Geology 120 (4), 431–451.
Zhang, Z., Dong, X., Santosh, M., Zhao, G., 2014f. Metamorphism and tectonic evolution of the Lhasa terrane, Central Tibet. Gondwana Research 25 (1), 170–189.
Zhao, G., Cawood, P.A., 2012. Precambrian geology of China. Precambrian Research 222, 13–54.
Zhao, L., He, G., 2014. Geochronology and geochemistry of the Cambrian (~518 Ma) Chagantaolegai ophiolite in northern West Junggar (NW China): constraints on spatiotemporal characteristics of the Chingiz–Tarbagatai megazone. International Geology Review 56 (10), 1181–1196.
Zhao, P., Fang, J., Xu, B., Chen, Y., Faure, M., 2014a. Early Paleozoic tectonic evolution of the Xing-Meng Orogenic Belt: constraints from detrital zircon geochronology of western Erguna–Xing'an Block, North China. Journal of Asian Earth Sciences 95, 136–146.
Zhao, X., Coe, R.S., Liu, C., Zhou, Y., 1992. New Cambrian and Ordovician paleomagnetic poles for the North China Block and their paleogeographic implications. Journal of Geophysical Research: Solid Earth 97 (B2), 1767–1788.
Zhao, Y., Sun, Y., Diwu, C., Guo, A.L., Ao, W.H., Zhu, T., 2016. The Dunhuang block is a Paleozoic orogenic belt and part of the Central Asian Orogenic Belt (CAOB), NW China. Gondwana Research 30, 207–223.
Zhao, Y., Sun, Y., Yan, J., Diwu, C., 2015. The Archean-Paleoproterozoic crustal evolution in the Dunhuang region, NW China: constraints from zircon U–Pb geochronology and in situ Hf isotopes. Precambrian Research 271, 83–97.
Zhao, Z., 2015. Tectonic Evolution of the Qiangtang Terrane, Central Tibetan Plateau. Thesis. University of Tübingen, 172 pp.
Zhao, Z., Bons, P.D., Wang, G., Liu, Y., Zheng, Y., 2014b. Origin and pre-Cenozoic evolution of the south Qiangtang basement, Central Tibet. Tectonophysics 623, 52–66.
Zhdanova, A., Metelkin, D., Vernikovsky, V., Matushkin, N.Y., 2016. The First Paleomagnetic Data on Dolerites from Jeannette Island (New Siberian Islands, Arctic. Doklady Earth Sciences 468 (2), 580–583.
Zheng, R., Wu, T., Zhang, W., Xu, C., Meng, Q., 2013. Late Paleozoic subduction system in the southern Central Asian Orogenic Belt: evidences from geochronology and geochemistry of the Xiaohuangshan ophiolite in the Beishan orogenic belt. Journal of Asian Earth Sciences 62, 463–475.
Zhimulev, F., Buslov, M., Travin, A., Dmitrieva, N., De Grave, J., 2011. Early–Middle Ordovician nappe tectonics of the junction between the Kokchetav HP-UHP metamorphic belt and the Stepnyak paleoisland arc (northern Kazakhstan). Russian Geology and Geophysics 52 (1), 109–123.
Zhong, L., Wang, B., Shu, L., Liu, H., Mu, L., Ma, Y., Zhai, Y., 2015. Structural overprints of early Paleozoic arc-related intrusive rocks in the Chinese Central Tianshan: implications for Paleozoic accretionary tectonics in SW Central Asian Orogenic Belts. Journal of Asian Earth Sciences 113, 194–217.
Zhou, J.B., Wang, B., Wilde, S.A., Zhao, G.C., Cao, J.L., Zheng, C.Q., Zeng, W.S., 2015. Geochemistry and U–Pb zircon dating of the Toudaoqiao blueschists in the Great Xing'an Range, northeast China, and tectonic implications. Journal of Asian Earth Sciences 97, 197–210.
Zhou, J.B., Wilde, S.A., 2013. The crustal accretion history and tectonic evolution of the NE China segment of the Central Asian Orogenic Belt. Gondwana Research 23 (4), 1365–1377.
Zhou, J.B., Wilde, S.A., Zhang, X.Z., Ren, S.M., Zheng, C.Q., 2011. Early Paleozoic metamorphic rocks of the Erguna block in the Great Xing'an Range, NE China: evidence for the timing of magmatic and metamorphic events and their tectonic implications. Tectonophysics 499 (1), 105–117.
Zhou, X.C., Zhang, H.F., Luo, B.J., Pan, F.B., Zhang, S.S., Guo, L., 2016. Origin of high Sr/Y-type granitic magmatism in the southwestern of the Alxa Block, Northwest China. Lithos 256, 211–227.
Zhu, D.C., Zhao, Z.D., Niu, Y., Dilek, Y., Hou, Z.Q., Mo, X.X., 2013. The origin and pre-cenozoic evolution of the Tibetan Plateau. Gondwana Research 23 (4), 1429–1454.
Zhu, D.C., Zhao, Z.D., Niu, Y., Dilek, Y., Wang, Q., Ji, W.H., Dong, G.-C., Sui, Q.-L., Liu, Y.-S., Yuan, H.-L., 2012. Cambrian bimodal volcanism in the Lhasa Terrane, southern Tibet: record of an early Paleozoic Andean-type magmatic arc in the Australian proto-Tethyan margin. Chemical Geology 328, 290–308.
Zonenshain, L.P., Kuzmin, M.I., Natapov, L.M. (Eds.), 1990. Geology of the USSR: a plate-tectonic synthesis, vol. 21. American Geophysical Union Geodynamics Series, 227 pp.
Zong, K., Zhang, Z., He, Z., Hu, Z., Santosh, M., Liu, Y., Wang, W., 2012. Early Palaeozoic high-pressure granulites from the Dunhuang block, northeastern Tarim Craton: constraints on continental collision in the southern Central Asian Orogenic Belt. Journal of Metamorphic Geology 30 (8), 753–768.
Zorin, Y.A., Sklyarov, E., Belichenko, V., Mazukabzov, A., 2009. Island arc–back-arc basin evolution: implications for Late Riphean–Early Paleozoic geodynamic history of the Sayan–Baikal folded area. *Russian* Geology and Geophysics 50 (3), 149–161.

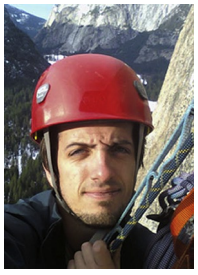

Mathew Domeier is a researcher at the Centre for Earth Evolution and Dynamics (CEED) at the University of Oslo, with research interests in tectonics, paleogeography and paleomagnetism. He received a B.Sc. (2006) from Slippery Rock University and a Ph.D. (2012) from the University of Michigan.